

**A SYSTEMATIC APPROACH TO THE MOLECULAR AND CELLULAR BASIS OF
BARTONELLA HENSELAE –TRIGGERED INVASOME FORMATION**

Inauguraldissertation

zur

Erlangung der Würde eines Doktors der Philosophie

vorgelegt der

Philosophisch-Naturwissenschaftlichen Fakultät

der Universität Basel

von

Matthias Christoph Truttmann

aus Seelisberg UR

Basel, 2011

Originaldokument gespeichert auf dem Dokumentenserver der Universität Basel
edoc.unibas.ch



Dieses Werk ist unter dem Vertrag „Creative Commons Namensnennung-Keine kommerzielle Nutzung-Keine Bearbeitung 2.5 Schweiz“ lizenziert. Die vollständige Lizenz kann unter creativecommons.org/licenses/by-nc-nd/2.5/ch eingesehen werden.



Namensnennung-Keine kommerzielle Nutzung-Keine Bearbeitung 2.5 Schweiz

Sie dürfen:



das Werk vervielfältigen, verbreiten und öffentlich zugänglich machen

Zu den folgenden Bedingungen:



Namensnennung. Sie müssen den Namen des Autors/Rechteinhabers in der von ihm festgelegten Weise nennen (wodurch aber nicht der Eindruck entstehen darf, Sie oder die Nutzung des Werkes durch Sie würden entlohnt).



Keine kommerzielle Nutzung. Dieses Werk darf nicht für kommerzielle Zwecke verwendet werden.



Keine Bearbeitung. Dieses Werk darf nicht bearbeitet oder in anderer Weise verändert werden.

- Im Falle einer Verbreitung müssen Sie anderen die Lizenzbedingungen, unter welche dieses Werk fällt, mitteilen. Am Einfachsten ist es, einen Link auf diese Seite einzubinden.
- Jede der vorgenannten Bedingungen kann aufgehoben werden, sofern Sie die Einwilligung des Rechteinhabers dazu erhalten.
- Diese Lizenz lässt die Urheberpersönlichkeitsrechte unberührt.

Die gesetzlichen Schranken des Urheberrechts bleiben hiervon unberührt.

Die Commons Deed ist eine Zusammenfassung des Lizenzvertrags in allgemeinverständlicher Sprache: <http://creativecommons.org/licenses/by-nc-nd/2.5/ch/legalcode.de>

Haftungsausschluss:

Die Commons Deed ist kein Lizenzvertrag. Sie ist lediglich ein Referenztext, der den zugrundeliegenden Lizenzvertrag übersichtlich und in allgemeinverständlicher Sprache wiedergibt. Die Deed selbst entfaltet keine juristische Wirkung und erscheint im eigentlichen Lizenzvertrag nicht. Creative Commons ist keine Rechtsanwalts-gesellschaft und leistet keine Rechtsberatung. Die Weitergabe und Verlinkung des Commons Deeds führt zu keinem Mandatsverhältnis.

Genehmigt von der Philosophisch-Naturwissenschaftlichen Fakultät
auf Antrag von

Prof. Dr. Christoph Dehio

Prof. Dr. Cécile Arrieumerlou

Basel, den 14.12.2010

Prof. Dr. Martin Spiess

(Dekan)

FÜR MEINE ELTERN UND CORINNE

Statement to my Thesis

This work was performed in the group of Prof. Christoph Dehio in the Focal area Infection Biology at the Biozentrum of the University of Basel, Switzerland. My PhD thesis committee consists of:

Prof. Christoph Dehio

Prof. Cécile Arrieumerlou

Prof. Dirk Bumann

My thesis is written in a cumulative format. It consists of a synopsis covering major aspects related to my work. This is followed by results chapters presenting my research consisting of two published research articles, one submitted manuscript and one manuscript in preparation. Finally, I resume the major findings of my thesis, discuss certain aspects and open questions of this work and provide suggestions for the future progression of the project.

Table of contents

| | | |
|----------|---|-----------|
| 1 | Introduction | 1 |
| 1.1 | Systems biology of host-pathogen interactions | 2 |
| 1.1.1 | The origin of molecular systems biology | 2 |
| 1.1.2 | Molecular systems biology of host-pathogen interactions | 3 |
| 1.1.3 | The mechanisms and applications of RNA interference (RNAi) | 4 |
| 1.1.4 | RNAi and its application in molecular systems biology | 6 |
| 1.2 | Invasion of host cells by bacterial pathogens | 7 |
| 1.2.1 | Bacterial invasion strategies | 8 |
| 1.2.2 | Integrins | 10 |
| 1.2.3 | Integrin activation | 11 |
| 1.2.4 | Integrin-mediated signaling | 12 |
| 1.2.5 | Integrin engagement as a cellular route of invasion by bacterial pathogens | 14 |
| 1.3 | The regulation of the actin cytoskeleton: How Rho GTPases shape cells | 17 |
| 1.3.1 | Dynamic regulation of the actin cytoskeleton: an overview | 17 |
| 1.3.2 | Rho GTPases and associated actin structures | 19 |
| 1.3.3 | Irreversible modification of Rho GTPase signaling by pathogenic bacteria | 21 |
| 1.3.4 | Reversible modification of Rho GTPases by bacterial factors | 22 |
| 1.3.5 | The WxxxE family of bacterial GEF proteins | 24 |
| 1.4 | The human pathogens <i>Bartonella</i> spp. | 25 |
| 1.4.1 | <i>Bartonella</i> spp. and associated disease patterns | 26 |
| 1.4.2 | <i>B. tribocorum</i> uptake into erythrocytes and endothelial cells | 27 |
| 1.4.3 | <i>B. henselae</i> entry into endothelial cells via the invasome | 28 |
| 1.5 | References | 30 |
| 2 | Aim of the thesis | 42 |
| 3 | Results | 44 |
| 3.1 | Research article I (published) | 44 |
| 3.1.1 | Summary | 45 |
| 3.1.2 | Statement of my own contribution | 46 |
| 3.1.3 | References | 46 |
| 3.1.4 | Manuscript: "A translocated protein of <i>Bartonella henselae</i> interferes with endocytic uptake of individual bacteria and triggers uptake of large bacterial aggregates via the invasome" | 47 |
| 3.2 | Research article II (published) | 66 |

Table of contents

| | | |
|------------|--|------------|
| 3.2.1 | Summary..... | 67 |
| 3.2.2 | Statement of my own contribution | 68 |
| 3.2.3 | References | 68 |
| 3.2.4 | Manuscript: "Combined action of the type IV secretion effector proteins BepC and BepF promotes invasome formation of <i>Bartonella henselae</i> on endothelial and epithelial cells" | 69 |
| 3.3 | Research article III (in preparation)..... | 85 |
| 3.3.1 | Summary..... | 86 |
| 3.3.2 | Statement of my own contribution | 87 |
| 3.3.3 | References | 87 |
| 3.3.4 | Manuscript: " <i>Bartonella henselae</i> effector protein BepF exhibits guanine nucleotide exchange factor activity against Cdc42" | 88 |
| 3.4 | Research article IV (submitted)..... | 131 |
| 3.4.1 | Summary..... | 132 |
| 3.4.2 | Statement of my own contribution | 133 |
| 3.4.3 | References | 133 |
| 3.4.4 | Manuscript: " <i>Bartonella henselae</i> engages inside-out and outside-in signaling via integrin β 1/talin1 during invasome formation" | 130 |
| 4 | Summary | 183 |
| 5 | Discussion | 187 |
| 5.1 | The effector proteins BepC, BepF and BepG and their roles in invasome formation | 187 |
| 5.2 | BepG vs. BepC/BepF triggered invasome formation: the benefit of degeneracy..... | 190 |
| 5.3 | The <i>in vivo</i> relevance of invasome formation..... | 192 |
| 5.4 | Integrin β 1-mediated transmembrane signaling during invasome formation | 193 |
| 5.5 | An automated setup to study invasome formation: towards genome-wide screening | 195 |
| 5.6 | References | 199 |
| 6 | Outlook..... | 203 |
| 6.1 | BepC/BepF and BepG-promoted invasome formation | 203 |
| 6.2 | The <i>in vivo</i> relevance and function of <i>Bhe</i> -mediated invasome formation | 205 |
| 6.3 | Establishment of initial contact between <i>Bhe</i> and the host cell..... | 207 |
| 6.4 | <i>Bhe</i> aggregation on the host cell surface..... | 208 |

Table of contents

| | | |
|-----|---|-----|
| 6.5 | The impact of <i>Bhe</i> research on general microbiology and cell biology..... | 209 |
| 6.6 | References | 210 |
| 7 | <i>Acknowledgements</i> | 213 |
| 8 | <i>Curriculum vitae</i> | 216 |

INTRODUCTION

1 INTRODUCTION

1.1 SYSTEMS BIOLOGY OF HOST-PATHOGEN INTERACTIONS

In the past century, molecular biologists tried to unravel the roles and functional properties of individual genes, RNAs and proteins to a tremendous extent. However, this reductionistic approach provided only limited understanding of the functions of individual units in their natural environment, e.g. RNAs and proteins in an intact cell, individual cells in a tissue, etc. The draw-backs of classical molecular biology are probably best described in an essay by Leland H. Hartwell, Nobel Prize winner in 2001: “Much of twentieth-century biology has been an attempt to reduce biological phenomena to the behavior of molecules. [...] Despite the enormous success of this approach, a discrete biological function can only rarely be attributed to an individual molecule.” [1]. In response to this obvious problem, the field of systems biology emerged, which tries to understand global properties of entire signaling networks and living organisms on an integrated level.

In the following chapter, I will briefly introduce the field of molecular systems biology and focus on its application in the research field of host-pathogen interactions. Further, I will explain the mechanism of RNA interference and discuss its application and associated problems with regard on molecular systems biology.

1.1.1 THE ORIGIN OF MOLECULAR SYSTEMS BIOLOGY

The routes of molecular systems biology date back to the early post-war years. In 1947, the mathematician Norbert Wiener, working on communication theory, defined the term cybernetics, which was meant to summarize all problems of communication control and the static mechanics behind it. In his famous book: “Cybernetics or Control and Communication in the Animal and the Machine”, published in 1948, he extended his idea to biological systems, referring to as biological cybernetics [2]. However, due to the limited knowledge of molecular biology and insufficient data quality and quantity as well as a lack of proper measurement techniques and equipment, Wiener's and others attempts on understanding biology on a systems level failed for a long time [3]. With the recent rise of the “-omics” era, those previously limiting shortcomings were solved to a great extent with the introduction of new methods and machines, such as RNA interference (RNAi) or high-throughput mass

spectrometry (MS). With this new equipment and techniques, it became possible to assess biological questions no longer focusing on a single unit, (e.g. a protein) but rather by following changes on the systems level (e.g. the entire proteome) simultaneously. The introduction of computers provided a tool to navigate through and deal with the enormous amount of generated quantitative data and further allowed to integrate individual data pieces into sophisticated, detailed models of entire biological processes. Further, the current and still increasing availability of sequenced genomes, transcriptomes and defined proteomes of different species even allow comparing different organisms on a systems level. Thus, compared to the early steps made by Wiener, today's technology and information accessibility offers a fair chance to seriously approach key questions of systems biology.

1.1.2 MOLECULAR SYSTEMS BIOLOGY OF HOST-PATHOGEN INTERACTIONS

The field of molecular systems biology of host pathogen interactions tries to understand how various bacterial, viral, protistic or fungal pathogens and parasites interact with and manipulate their target cells. The particular difficulty of this field is that it actually deals with two different biological systems, the pathogen and the host organism. While the isolated investigation of both the pathogens and the hosts yielded in interesting and important information on their respective biology, the question of how small changes and perturbations in one system, (e.g. bacteria) affect the second system (e.g. host cell) remains to be answered. Another prominent topic under investigation is how pathogens invade their host cells and multiply within. The major focus hereby lays on understanding which host cell units (e.g. proteins) and modules (signaling pathways) are abused by the pathogens to enable their internalization and intracellular replication [4,5,6]. A further aspect studied in depth is how the host cell proteome itself or post-translational proteome modifications such as phosphorylation, methylation, etc. are altered upon infection [7,8,9].

Besides the hunt for new cellular modules involved in pathogen uptake, the consequence of infections on a cell population and vice versa come more and more into focus. Already in 1940, the famous biologist Max Delbruck published a paper where he demonstrated that different physiological conditions of the host (bacteria) have an influence on the entry rate of the pathogen (bacteriophage) [10]. In 1960, Darnell showed that

different HeLa cell lines displayed different susceptibilities to poliovirus infection [11]. With the recent introduction of imaging-based high throughput screening, enormous amounts of data became available to analyze the effect of the cell context on infection. For example, by integrating single cell characteristics of millions of cells, it was shown that the population context accounted for 20-80% of the observed cell-to-cell variability in virus infections [12]. While the simian virus 40 (SV40) preferentially infected sparsely distributed cells, mouse hepatitis virus mainly invaded cells that were embedded in rather confluent cell layers. The combination of cell heterogeneity studies with the analysis of single gene contribution to the infection process offers a novel integrative method to investigate both aspects at the same time. Therefore, individual genes are specifically silenced in a given cell population and the cells are thereafter infected. Comparing the obtained results with uninfected-only, silenced-only, uninfected and not-silenced and infected-only controls allows determining the contribution of individual genes on i) the cell population context and ii) the infection process of a given pathogen. Due to the enormous relevance of gene silencing, predominantly achieved using RNA interference, I will introduce this technique in details below.

1.1.3 THE MECHANISMS AND APPLICATIONS OF RNA INTERFERENCE (RNAi)

For decades, the tools to silence individual genes in cultured mammalian cells have been missing. The standard approach to assess the role of proteins within cells was to over-express dominant-negative mutant versions, which were meant to lead to a functional shut-down of the assayed protein function [13]. However, this technique worked only for a limited number of proteins and was often accompanied by unwanted side effects due to the over-expression of the non-functional mutant construct. Shortly after the discovery of RNA interference (RNAi), for which Andrew Fire and Craig Mello were awarded the Nobel Prize in 2006, a new area started with the commercialized introduction of RNA silencing methods.

RNAi is an RNA-dependent gene-silencing process, which reduces the targeted mRNA of an introduced dsRNA in a sequence-specific manner [14]. The entire process is initiated by small interfering RNA (siRNA) molecules, that are generated through the cleavage of dsRNAs by the dicer enzyme and associated co-factors (Figure 1) [14,15]. The siRNAs are further delivered to the RNA-Induced Silencing Complex (RISC), which unwinds

the two siRNA strands, retaining the guide (anti-sense) strand to enable specific target mRNA recognition. Meanwhile, the second passenger (sense) strand is degraded [16]. Upon base-pairing of the RISC-siRNA complex with the complementary target mRNA, the RISC's endonuclease activity causes a single-site cleavage of the RNA transcript approximately in the middle of the siRNA binding region. The resulting fragments of target mRNA are thereby destabilized and subsequently fully degraded through additional cellular nucleases.

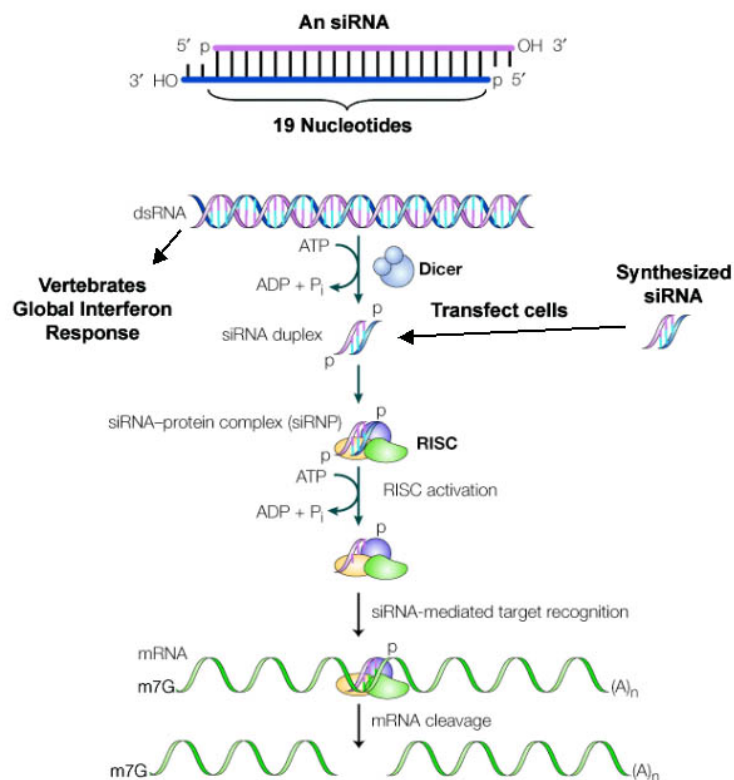


Figure 1: The principle of RNA interference. DsRNA is cleaved into siRNAs by the DICER enzyme. SiRNAs interact with the RISC complex, which leads to RISC activation, siRNA unwinding, and antisense strand binding to the RISC. Guided by the siRNA, the RISC-siRNA complex binds to target RNA transcripts and cleaves them. The resulting fragments are degraded by other cytosolic nucleases. Picture taken from [17].

By transfecting cells with artificially synthesized dsRNAs or pre-diced siRNAs, individual genes can be silenced (knocked-down). The knock-down efficiency depends on various factors and can reach 99%; yet, complete gene knock-down is never achieved [18]. Due to the ease of siRNA transfection into a wide variety of cell types, RNAi became the main technique to turn off individual genes in cell culture-based experiments. However, recent data shows that siRNAs can trigger so-called off-target effects. One of those site-effects to

account for is the dsRNA-dependent induction of the antiviral interferon pathway machinery [16], which can be prevented using commercially available pre-diced siRNAs. Next, sequence-dependent off-target effects can occur due to the binding of the first 2-8 bases of siRNAs (seed sequence) to unintended mRNA strands since mammalian cells have a high tolerance for mismatches between the siRNA and the complementary target mRNA outside of the seed sequence [19,20]. To minimize off-target effects, new generations of synthetic siRNAs are modified to prevent sense strand interaction with the RISC complex and to reduce seed-related off-targeting [21]. Although the modified siRNAs reduce off-target effects, the problem is not fully solved yet. Nevertheless, siRNA-dependent gene knock-down remains a well accepted and frequently applied tool to diminish protein levels of a target gene in eukaryotic cells.

1.1.4 RNAi AND ITS APPLICATION IN MOLECULAR SYSTEMS BIOLOGY

Using RNAi, researchers got a tool that allowed systematically studying the effects of any genes in the process of pathogen entry. In 2005, a first study addressing the effect of gene knock-down on *Listeria monocytogenes* and *Mycobacterium fortuitum* infections was published where 305 dsRNAs were used to knock-down genes representing various key units of several host signaling cascades [4]. Another lab interested in endocytic uptake of virus particles used high-throughput RNA interference and automated image analysis to explore the function of human kinases in clathrin- and caveolae/raft-mediated endocytosis, and therefore monitored the infection of vesicular stomatitis virus and simian virus 40 [22]. Since then, several commercial siRNA libraries targeting gene subsets or even the entire human genome have been used in screens to identify host factors involved in pathogen entry (*Mycobacterium tuberculosis*, HIV, *Pseudomonas aeruginosa*, *Chlamydia caviae*) [5,6,23,24] and intracellular replication (*M. tuberculosis*, HIV) [6,25,26,27]. Despite the identification of many new key signaling modules that mediate pathogen invasion and replication, the results of siRNA screens appear sometimes controversial. Probably the best example given to illustrate the problematic is the analysis and comparison of three independent full-genome RNAi screens to study HIV infection and replication [6,25,26]. Comparing the hit lists of these screens, the overlap between any pair of screens is less than 7% [28]. Further, while 1,254 genes were considered to be important for HIV infection in at

least one genome-wide screen, only 257 of them are listed in the HIV interaction database that contains 1434 genes previously identified in published peer-reviewed studies. Moreover, the three siRNA screens together named 842 genes (3.3% of all human protein-coding genes) implicated in decreasing HIV replication upon knock-down; only 34 of these genes were found in at least two screens. However, statistical comparisons of the screening data versus random gene picking showed that RNAi screening results are modestly but significantly enriched for proteins contributing to the HIV infection [28]. The discrepancies of the different screens may in part result from distinct celllines, viruses and siRNAs used in the screens as well as varying transfection and analysis methods. However, it remains puzzling that the overlap was only so little. Nevertheless, the increasing accessibility to RNAi screening facilities and the declining costs for genome-wide RNAi screens offers a suitable opportunity to generate a basis for future research by indentifying genes of interest for a given process.

1.2 INVASION OF HOST CELLS BY BACTERIAL PATHOGENS

Residing in the extracellular milieu, bacteria are subjected to a harsh environment. First, physical stresses such as the low pH in the gut or shear forces in blood vessels complicate the colonization of certain epithelial and endothelial tissues. Second, host defense mechanisms including complement deposition, antibody labeling and subsequent pathogen killing by macrophages or cyto-toxic T cells act against the invading bacteria [29]. To avoid clearance by host defense mechanisms, many pathogenic bacteria have evolved molecular strategies to actively invade host cells for replication, dissemination to other host tissues and/or persistence within the target tissue [30].

In the following section, I will briefly discuss general mechanisms of bacterial invasion and mention four typical examples. Further, I will introduce integrin receptors, briefly summarize their impact on bacterial internalization and focus on three illustrative representatives.

1.2.1 BACTERIAL INVASION STRATEGIES

Phagocytosis of bacteria by professional phagocytes is a process in which bacteria only play a passive role. In contrast, uptake of bacteria into non-phagocytic cells such as epithelial cells is dependent on an active contribution by the bacteria [31]. In general, bacterial invasion strategies can be divided into two major classes. The internalization via “zipper”-mechanism depends on the expression of a bacterial surface protein that is able to interact with eukaryotic surface receptors such as cadherins or integrins (Figure 2A). Host receptor binding leads to the formation of a vacuole that engulfs the bacterium through a "zippering" process. Moreover, the initial interaction between the bacteria and the host receptor initiates several signaling cascades that promote the activation of tyrosine kinases and the recruitment of cytoskeletal components eventually leading to vacuole closure and bacterial uptake. In contrast, bacterial internalization via “trigger”-mechanisms rely on the injection of bacterial effector proteins via specialized secretion systems into the host cell (Figure 2B). The effector proteins subvert host cell signaling cascades and trigger massive cytoskeletal rearrangements that lead to the formation of a macropinocytic pocket containing the loosely bound bacteria.

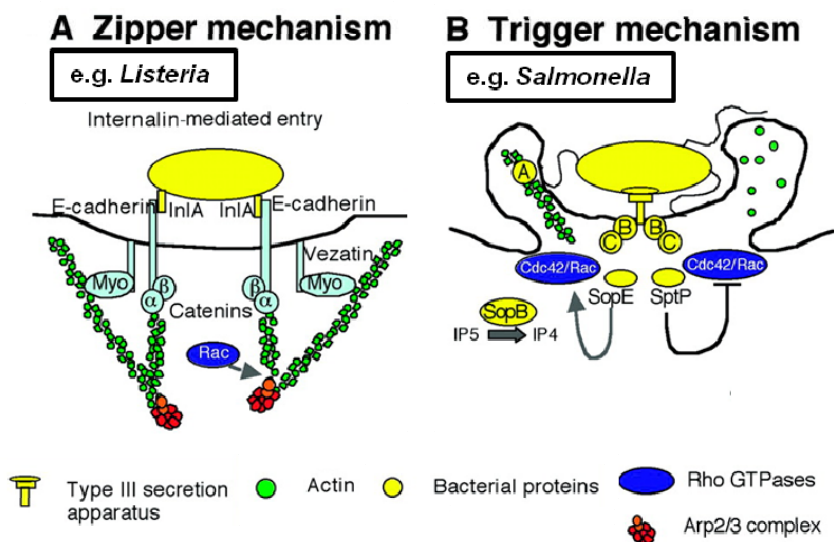


Figure 2: Zipper- and trigger-like uptake of bacterial pathogens. A) Zipper-like uptake of *Listeria* requires internalin A (inlA) that binds to E-cadherins. Subsequent actin rearrangements that are controlled by Rac1, WASP and Arp2/3 eventually lead to *Listeria* internalization. B) Trigger-like internalization of *Salmonella* employs the *Salmonella*-encoded type 3 secretion system and the translocated proteins SipB/SipC, which form the translocon pore, and effectors SopE, SptP and SopB that subvert GTPase signaling to promote *Salmonella* engulfment and internalization. Picture taken from [30] and adapted.

An illustrative example of zipper-like uptake is given by *L. monocytogenes* internalization into epithelial cells [32,33]. This food-borne pathogen that causes listeriosis expresses the surface proteins internalin A and B (InIA and InIB). InIA binds through its leucine-rich repeat (LRR) to E-cadherins triggering actin rearrangements in a catenin-, WASp- and Arp2/3-dependent manner [34]. In contrast, InIB mainly binds to Met, a transmembrane tyrosine kinase [35]. This interaction initiates actin nucleation and polymerization via Rac1, WAVE, and the Arp2/3 complex [36]. Cofilin, a regulatory protein that increases actin turnover and creates new free ends for polymerization by severing actin filaments as well as its upstream controller LIM kinase also play an important role in InIB-mediated entry [37,38].

As *Listeria*, *Yersinia spp.* employ zipper-like internalization mechanisms to invade their host cells. The two pathogens *Y. enterocolitica* and *Y. pseudotuberculosis*, which cause enterocolitis and gastroenteritis in infected humans, respectively, express the outer membrane protein invasin that directly interacts with integrin $\beta 1$ –containing heterodimeric receptors on the host cell surface. Receptor binding by invasin initiates signaling events that eventually lead to *Yersinia* uptake. Integrin-mediated *Yersinia* internalization is discussed in more details in section 1.2.5 on pages 14-17.

The two enteroinvasive pathogens *Salmonella enteritica* serovar *typhimorium* and *Shigella flexeneri* employ trigger-mechanisms to colonize their target cells. Both bacteria establish contact with their host cells via the pili of their type 3 secretion apparatus (T3SS). After initial contact of *Salmonella* with the host cell, the translocon pore is build by the insertion of SipB/SipC into the eukaryotic membrane [39]. SipC contains two functionally different cytoplasmic domains. The N-terminal domain binds to and bundles actin filaments and the C-terminal domain directly nucleates actin polymerization [40]. Subsequent translocation of effectors SopE1 and SopE2 that activate the small Rho GTPases Cdc42 and Rac1 increases actin nucleation and polymerization events promoted by SipC. Next, effector SopB/SigD, a phosphatidylinositol phosphatase, stimulates actin rearrangements while the translocated effector SipA decreases the critical concentration of actin required for actin polymerization and stabilizes existing actin filaments [41,42,43]. In a last step, the bi-functional effector SptP acting i) as a tyrosine phosphatase that regulates mitogen-activated protein kinase (MAPK) activity and ii) containing GAP functionalities to antagonize Cdc42

and Rac1 activities, mediates cup closure, actin depolymerization and *Salmonella* internalization [44].

Similar to *Salmonella* entry, *Shigella* forms a translocon pore with the SipB/SipC homologues IpaB/IpaC following initial contact with the host cell. In a next step, *Shigella* translocates effector protein VirA through its T3SS into the host cells, where the protein locally destabilizes and depolymerizes the microtubular network [45]. Whether or not the microtubuli depolymerization is directly mediated by VirA proteolytic activity or by an indirect mechanism remains controversial [46]. Microtubuli depolymerization leads to RhoA inactivation and consequent Rac1 activation. The C-terminal part of IpaC in addition acts as actin nuclator and is central to the activation of Cdc42 and Rac1 [47]. Activation of the tyrosine kinase c-Src upon contact to IpaC and recruitment of cortactin induce massive actin polymerization at the original site of the actin cup [48]. The *Shigella* effector IpgD, which harbors a phosphatidylinositol phosphatase activity, amplifies the process by disconnecting the actin cytoskeleton from the membrane [49]. In a last step, the effector IpaA, binding to vinculin, induces actin depolymerization and subsequent bacteria internalization [50].

1.2.2 INTEGRINS

Integrins represent a major class of cell adhesion receptors expressed throughout the mammalian kingdom. To date, 18 α and eight β subunits, which form 24 different non-covalently associated heterodimers, are reported [51,52]. Integrins interact with various extracellular Matrix (ECM) proteins that contain the RGD peptide motif [53]. They play an important role in mediating cell-matrix adhesion, contribute to tissue maintenance and are crucial during embryonic development [54]. Ligand binding to the extracellular domain of integrin receptors induces a signaling cascade that controls cell differentiation, motility, survival and migration [54]. In addition to this outside-in signal transmission, integrins regulate their own affinity for extracellular ligands by structural changes of the extracellular domains, modulated by proteins that interact with integrin C-tails. This process is called inside-out signaling [55].

1.2.3 INTEGRIN ACTIVATION

Integrin receptors exist in at least three distinct activation stages. In their closed (bent), conformation, integrin receptors possess low affinity for their ECM ligands and are found dispersed all over the cell [56]. In contrast, in their open (extended) conformation, integrins interact with high affinity with their ECM ligands and transmit signals across the membrane. The exact mechanism behind this process is still unclear [57]. The intermediate stage is only loosely defined and its physiological relevance as well as its appearance remains controversial. Two different models of integrin activation are currently proposed: The "switchblade" model suggests that only the extended conformation will bind ECM ligands [58] and the "deadbolt" model predicts that integrin extension takes place exclusively after ligand binding [59]. Outside-in signaling via integrins involves integrin clustering. Integrin clustering can be triggered i) by the binding of multivalent extracellular ligands to integrin ectodomains, ii) by the recruitment of multivalent proteins to activated integrin cytoplasmic tails or iii) by homo-dimerization of α/β tails belonging to two activated integrin heterodimeric receptors. However, the molecular details of how integrin clustering and ligand binding promotes signaling remains unclear [60].

Inside-out activation of integrins is mediated by the cytosolic protein talin1. This 270 kD protein exists in an auto-inhibited conformation that can be disrupted by calpain-mediated proteolysis or by binding of phosphatidylinositol (4,5)-bisphosphate (PtdIns(4,5)P₂) (Figure 3) [61]. Calpain-mediated talin1 cleavage releases a 47kDa talin head domain (TH), which binds to the WxxxNP(I/L)Y motif of β integrin C-tails via its FERM sub-domain (the FERM sub-domain is named in honor of the four proteins in which this domain was originally described: F for band Four-point-one, E for Ezrin, R for Radixin, M for Moesin) [62]. Upon integrin binding, the F3 domain of the TH disrupts the inhibitory salt bridge between the integrin α and β C-tails, which keeps the integrin receptors in an inactive state, thus inducing a conformational change that opens the integrin structure [63,64]. TH levels are controlled by the kinase Cdk5 and the ubiquitine ligase Smurf1. Cdk5 phosphorylates the TH at Ser-425, thereby inhibiting TH-Smurf1 interaction. In the unphosphorylated state, TH is ubiquitinated by Smurf1 and subsequently degraded by the cellular proteasome [65].

More recently, the family of kindlins has been identified and suggested to play a major role in activating integrins [66]. Kindlins contain a FERM domain that is split into two

parts by a pleckstrin homology (PH) domain [67]. Due to this interruption, kindlins and talin1 bind distinct regions of the β integrin tail. Although the action of kindlins may not shift integrins into a high-affinity state, they facilitate talin1 function.

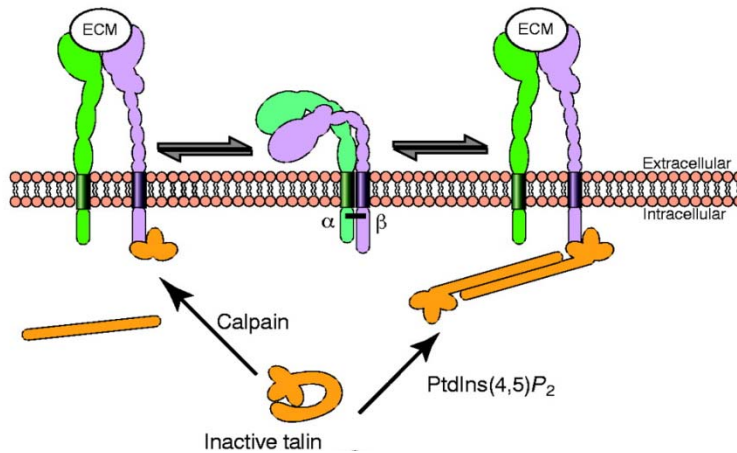


Figure 3: Inside-out activation of integrins. Release of the auto-inhibited form of talin1 by PtdIns(4,5)P₂ binding or Calpain-mediated proteolytic cleavage leads to inside-out activation of integrins. Picture taken from [55] and adapted.

1.2.4 INTEGRIN-MEDIATED SIGNALING

Integrin signaling engages several multi-protein complexes that assemble at the cytoplasmic surface of ligand-occupied integrin clusters [54]. Although the recruited signaling networks differ in response to various ligands and depending on the implicated integrin receptors, several key molecules that are involved in any outside-in signaling events have been characterized (Figure 4, upper part) [68]. In close proximity to the integrin C-tails, the kinases focal adhesion kinase (FAK), Src kinases (SFs) and integrin-linked kinase (ILK) integrate and amplify integrin signaling and promote its downstream transmission. FAK has a dominant role in integrin-mediated signaling as it acts as a phosphorylation-dependent signaling scaffold and is a major controller of adhesion turnover, cell migration and Rho GTPase activation [69]. Upon ligand engagement of integrins, the lipid kinase phosphatidylinositol-4-phosphate 5-kinase type-1 γ (PtdIns(4)P5KI γ) is recruited to the membrane and released from its auto-inhibited conformation, thereby generating locally high concentrations of PtdIns(4,5)P₂ (further referred to as PIP₂) [70,71,72]. As a consequence, PIP₂ interacts with the auto-inhibited form of FAK, triggering the dislocation of the FERM domain from the kinase domain and activating FAK. Upon activation, FAK gets auto-phosphorylated at tyrosine-397, thereby generating binding sites for SH2-domain

containing proteins. The SFK family member Src binds to FAK in a SH2-dependent manner, leading to Src activation, promoting Src-mediated phosphorylation of FAK-associated adaptor proteins. In addition to the displayed phosphotyrosine scaffold, the C-terminal focal-adhesion-targeting (FAT) domain of FAK interacts with paxillin and talin.

In addition to FAK-dependent activation of SFKs, these kinases bind directly to integrin β C-tails and are rapidly activated upon integrin-ligand interaction [73]. They transmit the signal to downstream kinases and adaptor proteins [55].

Similar to FAK, ILK carries an important role as a signaling scaffold at integrin clusters. Whether or not ILK is catalytically active is still controversial [74]. Nevertheless, ILK forms a heterotrimeric complex with the proteins PINCH and parvin that serves as a hub in integrin signaling networks, controlling the correct targeting of associated components to integrin-mediated adhesions. ILK also interacts with kindlins and may therefore play a role in integrin inside-out activation [75].

Besides the kinases, the adaptor proteins paxillin and vinculin have significant functions in integrin-mediated signal transduction. Paxillin is contributing to the control of adhesion turnover and migration [76]. It contains numerous protein-protein interaction domains and is phosphorylated at multiple tyrosines, thus offer SH2-binding sites. Paxillin directly interacts with kinases (FAK, Src, ILK), phosphatases (PTP-PEST), actin binding proteins (vinculin, parvin) and regulators of the Rho GTPases (Crk, Dock180/ELMO complex). The competition for the offered binding sites as well as the phosphorylation status of paxillin defines the dynamic regulatory function of this particular protein.

The multi-domain protein Vinculin does interact with many focal adhesion-associated proteins including paxillin, talin, F-actin, α -actinin and Arp2/3 and is essential for integrin-mediated cell adhesion [77]. The capacity of vinculin to stabilize existing F-actin filaments and to nucleate actin polymerization explains its critical role during cell spreading [78].

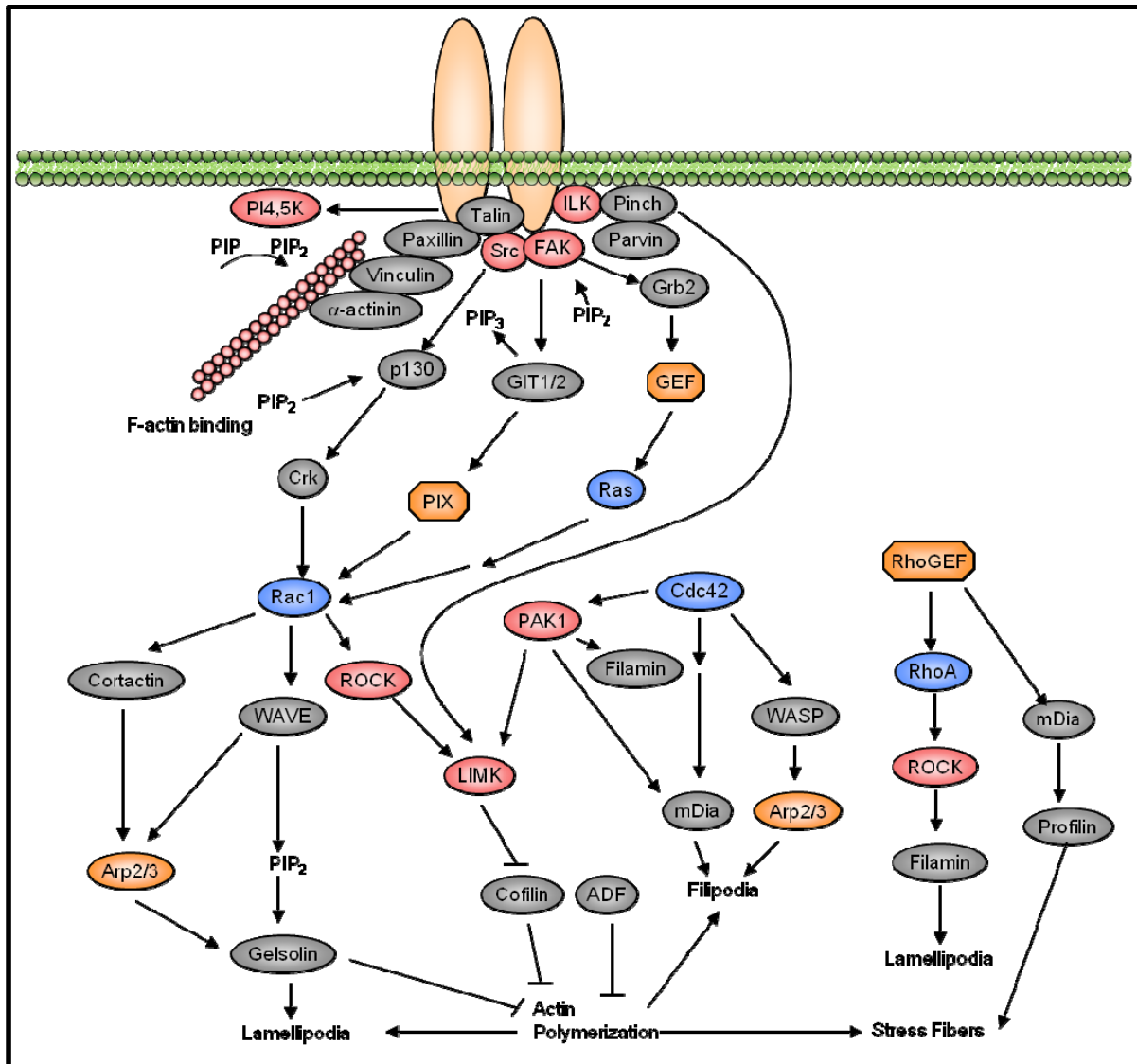


Figure 4: Integrin signaling and the control of the actin cytoskeleton. Integrin binding by extracellular ligands recruits kinases (Src, FAK, ILK, PI4,5K), scaffolding proteins (Paxillin, talin) and actin binding proteins (α -actinin, vinculin) to the cytoplasmic surface of integrin clusters. Downstream signaling via various pathways transmits the signal to Rho GTPases. Rho GTPases and associated factors control the actin cytoskeleton dynamics in an interlinked manner. Picture taken from [79] and adapted.

1.2.5 INTEGRIN ENGAGEMENT AS A CELLULAR ROUTE OF INVASION BY BACTERIAL PATHOGENS

Numerous bacterial pathogens bind to integrin receptors in order to mediate initial adherence to the cell membrane and/or to promote their internalization into the host cell in a zipper-like manner [80]. Integrin engagement by pathogenic bacteria can be mediated via the recruitment of ECM-derived integrin ligands to the bacterial cell surface (*Neisseria spp.*, *Staphylococcus aureus*) or by the direct interaction of fimbriae and/or dedicated adhesins

with integrins (*Escherichia coli*, *Yersinia spp.*). A comprehensive table listing the currently known bacterial pathogens interacting with integrins can be found in table I.

| Bacterium | Bacterial protein | Host cell | Reference |
|---------------------------------|----------------------------|--|---------------|
| <i>Bartonella bacilliformis</i> | ? | $\alpha_5\beta_1$ | [81] |
| <i>Bartonella henselae</i> | BadA | β_1 | [82,83,84] |
| <i>Bordetella parapertussis</i> | P.70 pertactin | β | [85] |
| <i>Bordetella pertussis</i> | P.69 pertactin | β | [85] |
| <i>Borrelia burgdorferi</i> | P66 | $\alpha_v\beta_3$ | [86] |
| <i>Campylobacter jejuni</i> | CadF | ? | [87,88] |
| <i>Escherichia coli</i> | EaeB | ? | [89] |
| <i>Escherichia coli</i> | Intimin | $\beta_1, \alpha_4, \alpha_5$ | [90] |
| <i>Mycobacterium</i> | FAP | $\alpha_5\beta_1$ | [91] |
| <i>Neisseria spp.</i> | Opa _{HS} , NadA | $\alpha_v\beta_3, \alpha_5\beta_1$ | [92,93,94] |
| <i>Orientia tsutsugamushi</i> | TSA56 | $\alpha_5\beta_1$ | [95] |
| <i>Porphyromonas gingivalis</i> | Fimbriae | $\alpha_5\beta_1, \alpha_v\beta_3$ | [96] |
| <i>Pseudomonas aeruginosa</i> | ? | $\alpha_v\beta_5, \alpha_5\beta_1$ | [97,98,99] |
| <i>Salmonella typhimurium</i> | Fimbriae, ShdA, MisL, Sips | ? | [42,100,101] |
| <i>Shigella spp.</i> | Ipas | $\alpha_5\beta_1$ | [102,103] |
| <i>Staphylococcus aureus</i> | FnbpA, FnbpB | $\alpha_5\beta_1$ | [104,105] |
| <i>Streptococcus spp.</i> | M proteins, FNZ, SFS | $\alpha_5\beta_1, \alpha_v\beta_3, \beta_2$ | [106,107,108] |
| <i>Yersinia spp.</i> | Invasin, YadA | $\alpha_3\beta_1, \alpha_4\beta_1, \alpha_5\beta_1,$ $\alpha_6\beta_1, \alpha_v\beta_1$ | [109,110] |

Table I: bacterial pathogens that interact with integrins. Table taken from [80] and adapted.

A well studied example of direct integrin engagement by pathogenic bacteria is the gram-negative enteropathogenic species *Y. enterocolitica* that initiates disease through the penetration of the intestinal mucosa, where it crosses the epithelial cell barrier and enters the Peyer's patches of the small intestine to multiply [111,112]. The pathogen expresses the outer-membrane protein invasin that binds to the integrin β_1 subunit [113]. Invasin has a higher affinity for integrin β_1 than its ECM-derived ligand, fibronectin, and can oligomerize, thereby inducing integrin clustering and efficient downstream signaling [114,115]. Integrin engagement by invasin leads to the activation of focal adhesion kinase (FAK), phosphoinositide 3-kinase (PI3K) and the small GTPase Rac1, which together orchestrate invasin-mediated *Yersinia* uptake by a zipper-mechanism [111].

Yersinia spp. also express the homotrimeric adhesin YadA, which indirectly binds to integrin β_1 by the recruitment of fibronectin and collagen [110]. While invasin appears to be essential for the crossing of the epithelial barrier, YadA is exposed in a later stage of infection and tissue penetration.

The gram-positive pathogen *S. aureus* causes septicemic and mucosal infections in humans and animals. *S. aureus* indirectly binds integrins to mediate its own internalization. The bacteria express two fibronectin-binding proteins, FnbpA and FnbpB that recruit fibronectin to the bacterial surface [104]. Fibronectin-mediated interactions with integrin $\alpha 5\beta 1$ receptors mediate *S. aureus* adhesion to the cell surface. Moreover, the activation of the integrin signaling machinery leads to a local recruitment and activation of FAK and Src, eventually promoting *S. aureus* uptake in a zipper-like manner [105,116].

Another interesting example of integrin engagement is *Helicobacter pylori*. This gram-negative bacterium is a major cause of duodenic,- gastric- and stomach ulcer [117]. *H. pylori* contains a Cag pathogenicity island (CagPAI) that encodes for the cag T4SS and its substrates CagA. In the host cell, CagA undergoes tyrosine phosphorylation by Src, inducing massive actin cytoskeletal rearrangements that resemble those of malignant cellular transformations. Several pilus proteins of the Cag T4SS interact with integrin $\alpha 5\beta 1$ receptors. The surface-exposed protein CagL binds to $\alpha 5\beta 1$ in a RGD-dependent-manner and triggers the activation of FAK and Src kinases [118]. Furthermore, the pilus-associated proteins CagY and CagI as well as the effector CagA have been reported to interact with integrin $\beta 1$ directly [119]. Interestingly, integrin binding and subsequent effector translocation does not lead to *H. pylori* internalization. However, integrin engagement still plays a major role during *H. pylori* infections: the interaction with integrin $\beta 1$ is required to enable CagA translocation into the host cell. The current model proposes that the cag T4SS pilus binds to integrin $\beta 1$ in its open, extended form. Upon receptor inactivation by an unknown process, integrins fold back into the closed conformation, thereby pulling the directly bound bacteria to the host cell membrane [119]. However, this model is under heavy debate.

While *Yersinia*, *Staphylococcus* and *Helicobacter* only interact with the extracellular domains of integrins, the *Shigella*-encoded Ipa proteins possess the ability to modulate integrin affinity for extracellular ligands. Besides building the translocation pore (*see section 2.1*), the IpaB/IpaC complex binds to integrins what is proposed to contribute to *Shigella* adhesion and entry [103]. IpaA interacts with vinculin and increases vinculin-mediated F-actin recruitment [50]. Furthermore, IpaA triggers the disassembly of focal adhesions and induces conformational changes of $\beta 1$ integrins from the open to the closed form, thus

reducing integrin affinity for extracellular ligands [120]. These processes are suggested to be a consequence of IpaA negatively interfering with talin recruitment to $\beta 1$ integrin C-tails, thereby destabilizing the extended integrin conformation. However, in detail investigation of that aspect is missing yet.

Since all here described integrin-dependent bacterial invasion mechanisms rely on massive actin cytoskeleton rearrangements, which are controlled by integrin-signaling cascades or injected bacterial effectors, the next section will introduce actin dynamics and the control thereof.

1.3 THE REGULATION OF THE ACTIN CYTOSKELETON: HOW RHO GTPASES SHAPE CELLS

In order to enable their own internalization, intracellular replication and survival within the host cells, bacteria have developed a variety of different mechanism that allow the pathogens to subvert host cell signaling pathways controlling the actin cytoskeleton dynamics and structure [121].

In the following section I will briefly talk about general properties of the actin cytoskeleton and introduce the Rho GTPases as one of the main regulators of actin dynamics. Further, I will describe in detail different mechanisms exploited by pathogenic bacteria to manipulate Rho GTPase signaling.

1.3.1 DYNAMIC REGULATION OF THE ACTIN CYTOSKELETON: AN OVERVIEW

The actin cytoskeleton of mammalian cells is a dynamic structure essential for a wide variety of cellular processes, including cytokinesis, cell shape and morphology regulation, adhesion, migration and the regulation of uptake mechanisms such as endo-/ and phagocytosis [122]. One of its major functions is the formation of lamellipodial and filopodial actin networks that enable the cell to migrate; however, the responsible machinery is also frequently abused by pathogenic bacteria during cell invasion.

The assembly and disassembly of actin filaments occur in a process called actin tread-milling [123]. Monomeric ATP-bound actin is added to the barbed end where ATP hydrolysis induces actin polymerization. On the opposite side of the strand at the pointed end, ADP-actin is depolymerized and released into the cytosol, where ADP is exchanged for

ATP to regenerate the cellular pool of ATP-actin available for polymerization (Figure 5). Thus, while the barbed end expands, the pointed end is shortened, and the filament length is kept constant resulting in a net forward movement of the actin structures [122]. The generated force creates the lamellipodium and drives the cell into directed movements.

Actin tread-milling is controlled by various proteins. Actin depolymerization factors (ADFs), also known as cofilins, binds to ADP-actin and increases pointed-end depolymerization enhancing the monomeric actin pool in the cytosol [124]. Furthermore, ADFs promote actin severing and are also implicated in the nucleation of actin filaments at high actin concentrations [125]. The highly abundant protein profilin enhances the exchange rate of ADP for ATP to recycle cytosolic actin monomers [126]. Finally, capping proteins bind to the majority of available barbed ends, thereby redirecting the addition of new actin monomers to the non-capped filaments [127].

To balance the effect of capping proteins in the tread-milling process that drives the formation of lamellipodia, cells continuously nucleate branched actin strands. This process is dependent on the Arp2/3 nucleation complex that acts at the leading edge of migrating cells [128]. The Arp2/3 multi-protein complex is itself activated by Wiskott-Aldrich syndrome proteins (WASP) that in turn are regulated by small Rho GTPases (Figure 4, lower part).

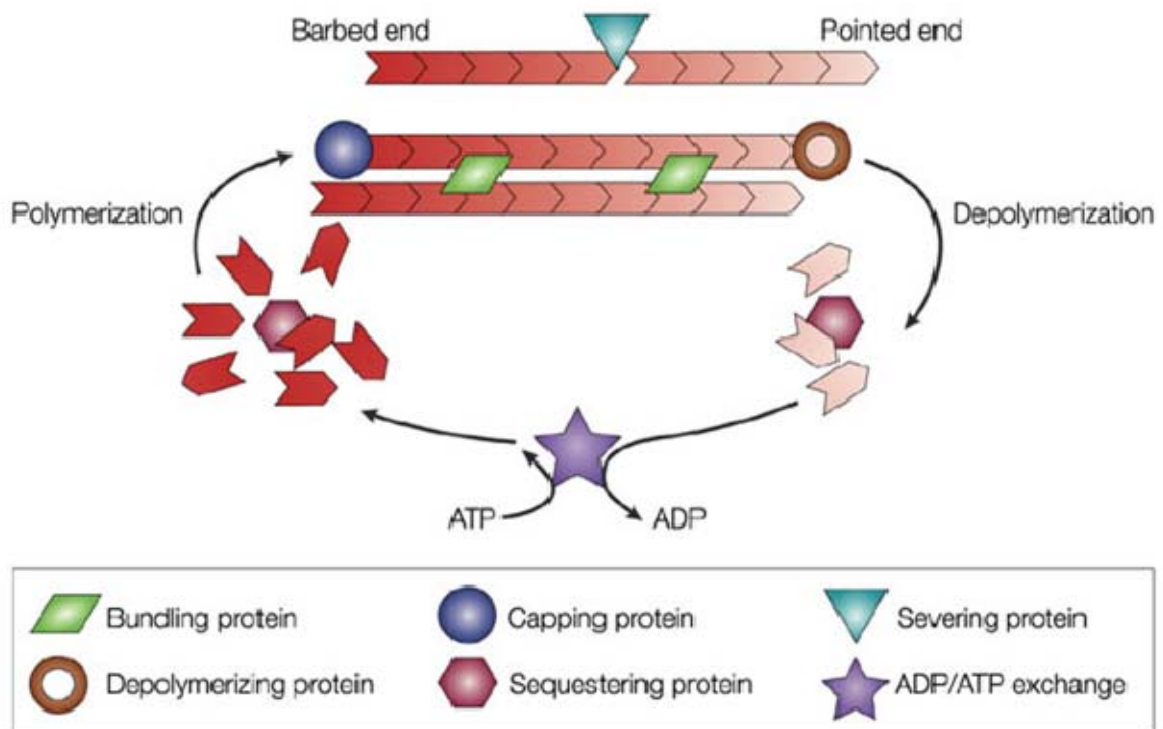


Figure 5: Actin tread-milling. ATP-actin binds to the barbed ends of actin strands. ATP hydrolysis induces polymerization. At the pointed end, ADP-actin is released. Severing proteins break existing actin strands. Capping proteins inhibit strand elongation by blocking the barbed ends. Depolymerizing proteins increase the depolymerization rate of ADP-actin at the pointed end. Bundling proteins enable the formation of thigh, parallel actin structures found in filopodia. Sequestering proteins decrease the available pool of monomeric G-actin. Picture taken from [129].

1.3.2 RHO GTPASES AND ASSOCIATED ACTIN STRUCTURES

The Rho-family of small GTPases consists of 22 members [130]. In cells, they maintain the actin cytoskeleton structure. The most prominent Rho GTPases are Cdc42, Rac1 and RhoA. Cdc42 conducts the formation of filopodial finger-like extensions of migrating cells, built to sense the environment (Figure 6) [131]. Filopodia formation includes the Cdc42-mediated activation of N-WASP that in turn stimulates Arp2/3-triggered actin nucleations [132]. In contrast, Rac1 orchestrates the establishment of lamellipodia that are flat, cellular protrusions shaped by a bidirectional dendritic actin assembly [133]. Here, the N-WASP isoform Scar/WAVE mainly responds to Rac1 activity and regulates lamellipodia formation [132]. The GTPase RhoA is involved in the assembly of parallel F-actin bundles, called actin stress fibers.

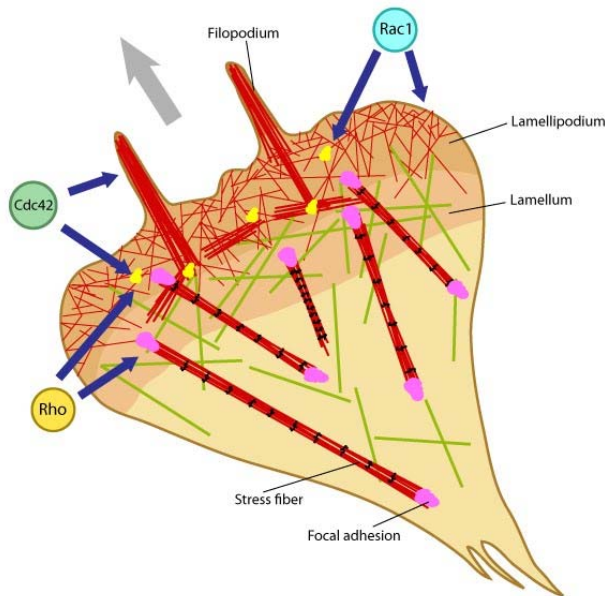


Figure 6: Rho GTPases regulate actin filaments and cytoskeletal organization. Cdc42 regulates the formation of finger-like filopodial extensions. Rac1 orchestrates the establishment of lamellipodia. RhoA controls the formation of actin stress fibers. Picture taken from [134].

All Rho GTPases share a conserved structure that is made of the two flexible domains, called switch I and switch II, and a phosphate binding loop (P-loop), which together build a Mg^{2+} - and nucleotide-binding pocket [135]. Rho GTPases are frequently post-translationally modified by the addition of prenyl, farnesyl or geranyl-geranyl moieties to their CAAX motif located near the C-terminus [136]. Depending on the lipid modification, the GTPases are targeted to various membranous compartments of the cells [136].

Rho GTPases act as molecular switches [137]. They transmit signals in the GTP-loaded conformation by recruiting and activating downstream effector proteins. To this end, the small GTPases cycle between a GTP-bound, active and a GDP-bound, inactive conformation [138]. The cycling between the GTP- and GDP-loaded form is a tightly controlled process. In order to promote signaling via small GTPases, guanine nucleotide exchange factors (GEFs) facilitate and increase the exchange of GDP with GTP, thus increasing GTPase-effector interactions. In contrast, GTPase activating proteins (GAPs) increase the intrinsic GTPase activity of the enzymes, thereby triggering the turnover of GTP to GDP and inhibiting the interaction of the small GTPases with their downstream partners. Another family of proteins, the so-called guanine nucleotide dissociation inhibitors (GDIs) interfere with small GTPase signaling by binding to the switch I and II regions and the lipid

moiety, thereby preventing membrane localization of the GTPases and sequestering them in an inactive state in the cytosol [139,140,141].

1.3.3 IRREVERSIBLE MODIFICATION OF RHO GTPASE SIGNALING BY PATHOGENIC BACTERIA

Most bacterial invasion mechanisms depend on F-actin rearrangements that enable pathogen internalization. In order to subvert Rho GTPase signaling and take over the control of the actin cytoskeleton, pathogenic bacteria developed a variety of different strategies of how to manipulate G proteins (Figure 7).

Clostridium difficile releases the pathogenicity factors toxin A (TcdA) and toxin B (TcdB). These typical AB toxins act as glucosyltransferases that mono-O-glucosylate RhoA, Cdc42 and Rac1 at threonine-7 (RhoA) or the equivalent threonine-35 (Cdc42, Rac1), respectively [142,143]. The additional glucosyl-modification renders the Rho GTPases inactive by inhibiting the recruitment of downstream binding partners [143]. In contrast, *Clostridium botulinum* secretes the exoenzyme C3 that ADP-ribosylates Rho GTPases what leads to a constant association of Rho with RhoGDI and probably blocks the activation of Rho by GEFs [144]. Thus, ADP-ribosylation interferes with GTPase cycling in a comparable manner to glucosylation. However, while glucosylated Rho G proteins are located at the cell membrane, ADP-ribosylated Rho GTPases are found in the cytosol, complexed with GDIs.

An alternative pathway is taken by the enteropathogenic bacteria *Y. enterocolitica*. These bacteria translocate the effector protein YopT, a cysteine protease, into the host cells where it proteolytically degrades the carboxyl-terminus of Cdc42, Rac1 and RhoA at the CAAX-box [145,146]. As a consequence, the GTPases dissolve from the membrane, the interaction with GDIs is inhibited and proper signaling through small GTPases is abrogated [147].

Pathogenic *E. coli* encode for the cytotoxic necrotizing factor 1 (CNF1). This classical AB toxin acts on Rho GTPases by deamidating a specific glutamine residue located in the switch II domain [148]. This glutamine residue is essential for the intrinsic as well as GAP-mediated GTPase activity of Rho proteins. By modifying glutamine into glutamic acid, CNF1 inhibits GTP hydrolysis, impairs the role of RhoGAPs and permanently keeps the GTPases in their activated, GTP-bound state [149].

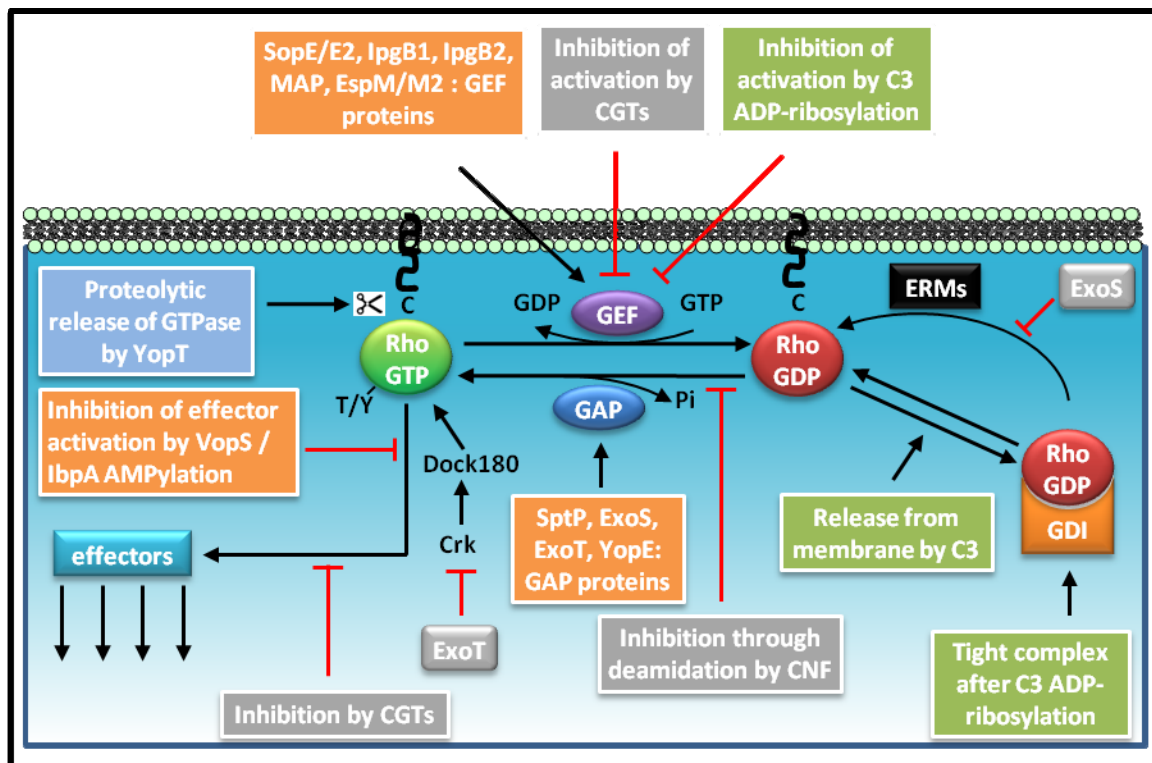


Figure 7: Subversion of GTPase signaling by bacterial pathogens. Proteolytic release of GTPases (yopT), AMPylation (VopS / IbpA) and O-glycosylation by cytotoxic glycosyl-transferases (CGTs) inhibits GTPase-effector interactions. CGTs and ADP-ribosylation of G proteins (C3) inhibits GTPase activation; ADP-ribosylation by C3 also blocks the release of GDI-complexed G proteins. GTPase deamination (CNF) renders G proteins constitutive active. GEFs (SopE, IpgB1, IpgB2, MAP, EspM) and GAPs (SptP, ExoS, ExoT, YopE) activate / inactivate Rho GTPases. Interferences with cellular Rho GTPase regulators (Crk, ERMs, etc.) abrogate G protein signaling (ExoS, ExoT). Figure summarizes data from [121,150]

1.3.4 REVERSIBLE MODIFICATION OF RHO GTPASES BY BACTERIAL FACTORS

In contrast to the previously mentioned mechanisms that irreversibly modify Rho G proteins, other translocated effectors interact in a reversible manner with Cdc42, Rac1 and RhoA. Furthermore, some bacterial effectors interfere in multiple ways with GTPase signaling. For example, the *Pseudomonas aeruginosa* effectors ExoS and ExoT, that share 75% amino acid identity, exhibit GAP and ADP-ribosyltransferase activities [151]. In both proteins, the carboxyl terminus contains a cytotoxic ADP-ribosyltransferase activity while the amino terminus stimulates the intrinsic GTPase activity of Cdc42, Rac1 and RhoA [152]. While ExoS ADP-ribosylates the early host proteins ezrin, radixin and moesin proteins (ERMs), ExoT acts on Crk proteins [153,154]. Thus, in contrast to the exoenzyme C3 from *C. botulinum*, ExoS

and ExoT ADP-ribosylate not the Rho GTPases themselves but indirect regulators of the G proteins.

AMPylation of Rho GTPases represents another modification promoted by bacterial factors. *Vibrio parahaemolyticus* translocates the effector VopS via its type III secretion system into the host cell [155]. VopS contains a C-terminal filamentation induced by cAMP (FIC) domain that is responsible for covalently attaching an AMP moiety to threonine-35 in the switch I region of Cdc42, Rac1 and threonine-37 in the corresponding domain of RhoA, respectively. This added AMP residue inhibits the binding of downstream interaction partners and abrogates GTPase-mediated signaling [156]. A similar mechanism is used by the *Histophilus somni*, an economically important pathogen that is frequently infecting cattle life-stocks [157]. *H. somni* expresses a surface antigen called immunoglobulin-binding protein A (IbpA), which harbors a direct repeat 2 / FIC domain (DR2/FIC). IbpA attaches to eukaryotic cells and is internalized. However, the mechanism of that process remains to be solved [158]. In the host cell, IbpA AMPylates Rho GTPases by covalently attaching an AMP residue to tyrosine-34 of RhoA and tyrosine-32 of Cdc42 and Rac, respectively, inhibiting downstream signaling and leading to the disruption of the actin cytoskeleton [159]. *In vitro* data suggests that AMPylation of Rho GTPases by either VopS or IbpA is reversible and can be removed by the action of phosphodiesterase (PDE). However, there is no *in vivo* data available yet to support that finding [156,159].

Various bacterial pathogens translocate GEF and GAP proteins into eukaryotic cells. A well-characterized example is *S. enterica* serovar *Typhimorium*, which injects the GEF-GAP pair SopE and SptP into host cells. There, SopE first activates Cdc42 and Rac1 which eventually leads to *Salmonella* entry [160,161]. Upon proteolytic degradation of SopE by the proteasome, the GAP protein SptP, which exhibits much slower degradation kinetics, helps the cell to recover from the SopE-promoted membrane ruffling [162]. Another bacterial GAP protein is YopE of *Y. pseudotuberculosis* that inactivates Cdc42, Rac1 and. YopE-associated cytotoxic effects include the disintegration of the actin cytoskeleton and cell rounding as well as detachment [163,164].

1.3.5 THE WXXXE FAMILY OF BACTERIAL GEF PROTEINS

Recently, a new family of bacterial proteins sharing a common Tryptophane-xxx-Glutamic acid motif (WxxxE) has been identified [165]. Although initially claimed to be GTPase mimics, biochemical and structural data strongly suggest that these proteins are GEFs of Rho GTPases [166]. The growing number of WxxxE family members, their cellular targets and the observed cellular phenotypes are summarized in table 2.

The bacterial WxxxE GEFs interact with different Rho GTPases and trigger various phenotypes [150]. The *EPEC* and *EHEC*- encoded protein MAP induces lamellipodia formation at sites of bacteria attachment by specifically activating Cdc42 [167,168]. Maintenance of MAP-induced filopodia is dependent on the PDZ-domain of MAP as well as ezrin and the RhoA/ROCK signaling pathway [168]. In contrast, EspM/EspM2 of pathogenic *E. coli* have been shown to bind to and activate RhoA, thus inducing stress fiber formation on infected cells [169]. Further, the WxxxE GEF EspT of *Citrobacter rodentium* acts on Cdc42 and Rac1, thus inducing membrane ruffling and lamellipodia formation [170]. Unusual representatives of the WxxxE-GEF family are the two *S. flexneri* proteins IpgB1 and IpgB2. While IpgB1 shows GEF activity on Rac1 and, to a lower extent on Cdc42, IpgB2 functions as a potent RhoA GEF with weak activity on Cdc42 and Rac1 [171]. Interestingly, both proteins also directly bind to additional proteins related to Rho GTPase signaling. So, IpgB1 binds to the DOCK180-ELMO complex by interacting with ELMO directly, what in turn activates Rac1 [172]. In contrast, IpgB2 interacts with the RhoA effectors ROCK and mDia [173].

The two *Salmonella* effectors SifA and SifB, which both contain a WxxxE-motif, are special since they consist of two domains and do not promote any actin-related phenotypes on infected cells. In fact, SifA is involved in the formation of *Salmonella*-induced filaments (Sifs) that play a major role in the maintenance of *Salmonella*-containing vacuoles (SCVs) [174]. Moreover, SifA binds to the cellular protein SKIP and Rab7, thus inhibiting the recruitment of kinesin and dynein to SCVs [175]. However, despite structural similarity to the potent non-WxxxE GEF SopE and the ability of SifA to interact with RhoA, no GEF function could yet be demonstrated [176]. Furthermore, the cellular targets of SifB remain unclear [177].

The WxxxE motif that is shared by all these translocated GEF proteins plays presumably rather a structural than a functional role. While replacement of tryptophane

with alanine (AxxxE) abolishes protein function, more conservative amino acid substitutions do not result in any significant loss of activity [165,169,178]. 3D structures of SifA, MAP and EspM2 indicated that the indicated tryptophane and glutamic acid residues are involved in maintaining the conformation of the putative catalytic loop through hydrophobic contacts [171,176].

The fact that IpgB1 and IpgB2 interact with additional cellular partners involved in GTPase signaling indicates that the intrinsic GEF activity of the bacterial effectors may be regulated by multi-protein signaling complexes, as it is described for several eukaryotic GEFs [150,179]. However, solid experimental evidence is lacking yet.

| Pathogen | GEF | Target | Cellular phenotype | reference |
|------------------------------|---------------|------------------------------------|---|-----------|
| <i>(EPEC/EHEC)</i> | MAP | Cdc42 | Lamelipodia formation | [167,168] |
| <i>(EPEC/EHEC)</i> | EspM EspM2 | RhoA | Induction of stress fibres | [169,178] |
| <i>Citrobacter rodentium</i> | EspT | Cdc42, Rac1 | Membrane ruffling; lamelipodia formation | [170] |
| <i>Shigella flexneri</i> | IpgB1 | Rac1, (Cdc42) Dock-ELMO complex | Membrane ruffling | [179] |
| <i>Shigella flexneri</i> | IpgB2 | RhoA, (Cdc42, Rac1) ROCK, mDia | Induction of stress fibres | [179] |
| <i>Salmonella spp.</i> | SifA | SKIP, Rab7 | Maintenance of SCVs | [174,177] |
| <i>Salmonella spp.</i> | SifB | ? | ? | [177] |

Table II: bacterial pathogens expressing WxxxE-family GEF proteins.

1.4 THE HUMAN PATHOGENS *BARTONELLA SPP.*

As many other bacterial pathogens, the gram-negative pathogens *Bartonella spp.* subvert the regulation of the actin cytoskeleton structure to promote cell invasion.

In this section, I will briefly introduce *Bartonella spp.* and mention their relevance as human pathogens. Further, I will focus on *Bartonella*-host cell interactions and explain the infection cycle of *B. tribocorum* and invasome-mediated *B. henselae* internalization into human umbilical vein endothelial cells (HUVECs).

1.4.1 *BARTONELLA SPP.* AND ASSOCIATED DISEASE PATTERNS

Bartonellae are facultative intracellular pathogens that are causing a characteristic intraerythrocytic infections in their mammalian reservoir hosts [180]. Transmission to humans occurs via arthropod vectors or by direct contact with infected host animals. While at least eight *Bartonella* species have been identified to cause diseases in humans, *B. bacilliformis* (*Bba*), *Bartonella quintana* (*Bqu*) and *Bartonella henselae* (*Bhe*) represent the major human pathogens. *Bba* infections are lethal in about 80% of the cases if the patients are not treated with antibiotics [181]. *Bba* causes the biphasic Carrion's disease; the acute phase, called Oroya fever, is frequently accompanied by hemolytic anemia caused by intraerythrocytic *Bba* infection. In contrast, the chronic phase, known as verruga peruana, is characterized by *Bba*-triggered vascular tumor formation due to the colonization of endothelial cells. *Bqu* is the causative agent of trench fever, an intraerythrocytic bacteraemia and colonizes the endothelium, too. In immuno-compromised hosts, such as AIDS patients, the colonization of endothelial cells manifests in bacillary angiomatosis *Bhe* accounts for the majority of human infections with bartonellae and promotes rather mild disease patterns such as cat-scratch disease or bacillary angiomatosis-pelosis. [182].

Bhe, *Bqu* and *Btr* all encode for a virB/D4 type IV secretion systems (T4SS) that translocate effector proteins into the host cells and a Trw T4SS that enables DNA transfer [183]. In contrast, *Bba* does not contain any T4SS. Sequence analysis of *Bhe*, *Bqu* and *Btr* T4SS showed that the virB/D4 systems are highly similar, suggesting an early acquisition of the virB/D4 T4SS in a common ancestor strain. Despite the similarities of the T4SS, the encoded Bep effectors are much less conserved. While *Bhe* expresses effector proteins BepA to BepG, *Btr* encodes for effectors BepC to BepE as well as BepH and BepI. *Bqu* only contains four Bep effector proteins that are BepC, BepE BepF1 and BepF2. BepC is well conserved among the three species, showing amino acid sequence similarities of 66% and 73%, respectively, using *Bhe* BepC as reference. However, most of the effector proteins display only moderate levels of sequence conservation, indicating a fast gene evolution due to positive selection [183]. The distinct functions of the individual effector proteins in bartonellae pathogenesis is to a large extent unclear.

1.4.2 *B. TRIBOCORUM* UPTAKE INTO ERYTHROCYTES AND ENDOTHELIAL CELLS

B. tribocorum (*Btr*) infects primarily rats, which serve as its reservoir host [184]. Work on the infection cycle of *Btr* in rats demonstrated that, immediately after inoculation, *Btr* colonizes the so-called primary niche, presumably represented by endothelial cells [184]. In five-day intervals, *Btr* are seeded from the primary niche into the blood stream in which they are attaching and colonizing mature erythrocytes. Once within erythrocytes, *Btr* replicates in membrane-bound compartments without lysing the cells. Due to the avoidance of haemolysis and the inaccessibility of erythrocytes to the host immune system, *Btr* can persist several weeks in the blood circulation of infected rats and is transmitted by blood-sucking arthropods to further animals (Figure 8) [185]. Similar results were observed for mice infected with *B. grahamii* or *B. birtlesii* and domestic cats infected with *Bhe* [186,187,188].

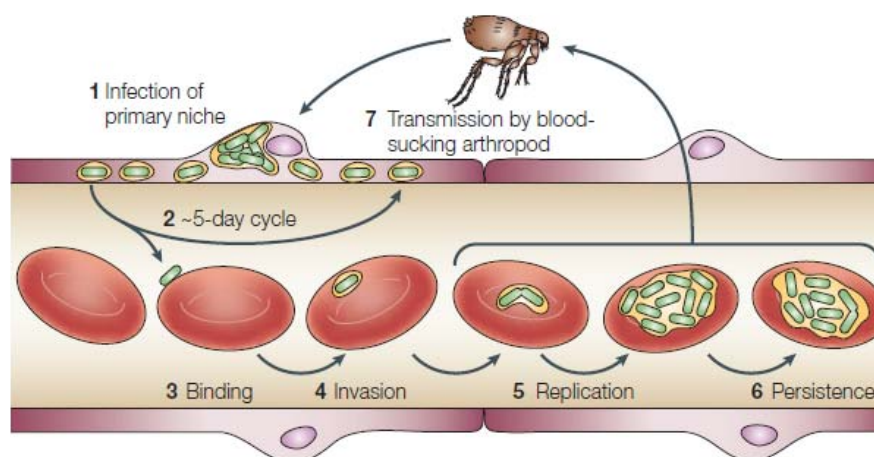


Figure 8: Infection cycle of Bartonella spp. in the reservoir host. Upon infection of the primary niche (1), bacteria are released in approximately five-day cycles into the blood stream (2) where they attach (3) and invade mature erythrocytes (4). Following intraerythrocytic replication (5), Bartonella persist (6) within the blood cells and are occasionally transmitted by blood-sucking arthropod vectors to other suspects (7) Picture taken from [180].

On the molecular level, the two type 4 secretion systems (T4SS) VirB/D4 and Trw are essential for the establishment of a complete infection cycle within in the reservoir host [185]. The Trw T4SS is highly similar to the conjugation machinery encoded on the broad-host range plasmid R388. However, no Trw substrate has been identified yet. Nevertheless,

the Trw system is required to mediate initial attachment to erythrocytes. Further, the two surface-located proteins TrwJ and TrwL are implicated in the determination of host specificity [188]. In contrast to the Trw system, the VirB/D4 T4SS is not directly involved in intraerythrocytic infection but rather contributes to the infection of the primary niche that is a prerequisite for the subsequent erythrocyte infection. The VirB/D4 T4SS is a protein secretion machine that translocates *Bartonella* effector proteins (Beps) from the bacterial cell into the host cell cytosol. There, the Beps are thought to interfere with various signaling cascades eventually resulting in *Btr* uptake into endothelial cells.

1.4.3 *B. HENSELAE* ENTRY INTO ENDOTHELIAL CELLS VIA THE INVASOME

The zoonotic pathogen *Bhe* accidentally infects humans through transmission from infected cats via cat scratches or bites. *Bhe* encodes for a VirB/D4 T4SS and seven Bep proteins that are translocated into the host cell cytosol [189]. Once in the host cell, the Bep proteins trigger various cellular phenotypes, including i) the activation of a pro-inflammatory response, (ii) inhibition of apoptosis and (iii) the capillary-like sprout formation of EC aggregates [190,191]. In addition, the Bep effectors promote the formation of a unique bacterial uptake structure, called the invasome [192].

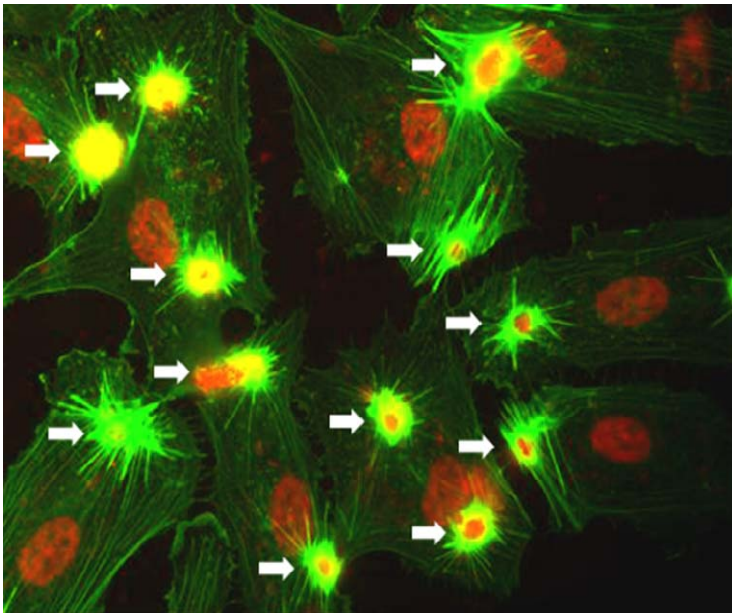


Figure 9: Bhe-triggered invasome formation on HUVEC cells. HUVEC cells infected with *Bhe* wild-type for 48 hours. F-actin is shown in green. Bacteria and cellular chromosomal DNA is stained in red. *Bhe*-triggered invasomes are marked with arrows.

Bhe enters endothelial cells by two distinct processes that exhibit different kinetics. First, within the first couple of hours, individual *Bhe* or small aggregates thereof enter HUVECs in an actin-dependent manner and assemble into small, *Bartonella*-containing vacuoles (BCVs) that localize into the peri-nuclear space [192]. Second, 24-48 hours after initial contact with cells, large *Bhe* aggregates invade HUVECs via invasome structures (Figure 9) [192]. *Bhe* internalization via the invasome route is a multi-step process (Figure 10). At its beginning, *Bhe* adhere to the cell surface and form big aggregates. Upon effector translocation into the host cell, *Bhe* are engulfed by plasma-membrane-derived membrane protrusions, eventually resulting in the complete internalization of the bacterial aggregates.

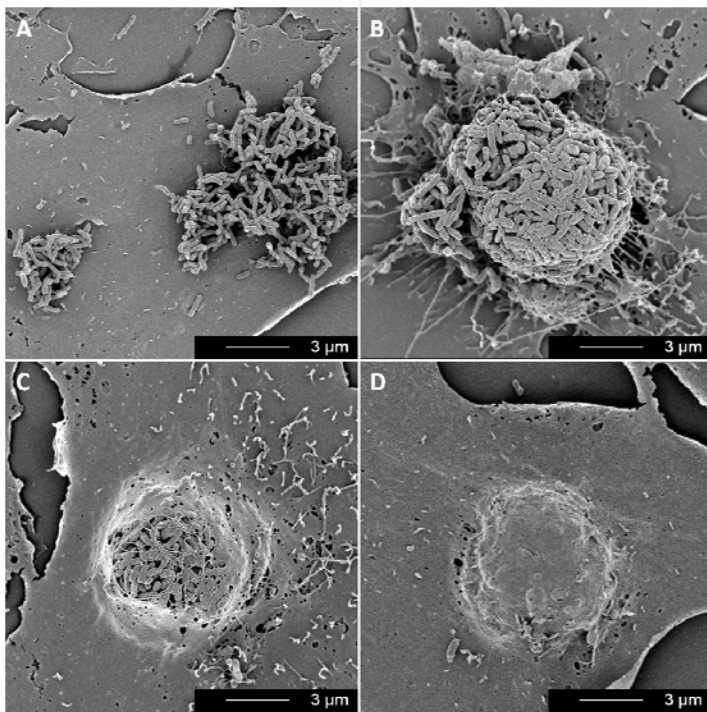


Figure 10: Individual steps of Bhe-triggered invasome formation on HUVEC cells. A) Initial adherence to the host cell (HUVEC). B) Bhe-clustering on the cell surface. C) Aggregate engulfment by membrane-derived protrusions from the host cell. D) Invasome closure and Bhe internalization.

Invasome formation depends on F-actin assembly/disassembly signaling via phosphotyrosine scaffolds [192]. However, the specific effector protein(s) required for invasome formation as well as the host cell signaling components contributing to invasome establishment remain to be identified.

1.5 REFERENCES

1. Hartwell LH, Hopfield JJ, Leibler S, Murray AW (1999) From molecular to modular cell biology. *Nature* 402: C47-52.
2. Wiener N (1948) *Cybernetics or Control and Communication in the Animal and the Machine*: Kessinger Publishing. 196 p.
3. Kitano H (2001) *Foundations of Systems Biology*, chapter Systems Biology: The MIT Press. 320 p.
4. Agaisse H, Burrack LS, Philips JA, Rubin EJ, Perrimon N, et al. (2005) Genome-wide RNAi screen for host factors required for intracellular bacterial infection. *Science* 309: 1248-1251.
5. Philips JA, Rubin EJ, Perrimon N (2005) *Drosophila* RNAi screen reveals CD36 family member required for mycobacterial infection. *Science* 309: 1251-1253.
6. Brass AL, Dykxhoorn DM, Benita Y, Yan N, Engelman A, et al. (2008) Identification of host proteins required for HIV infection through a functional genomic screen. *Science* 319: 921-926.
7. Pastorino B, Boucomont-Chapeaublanc E, Peyrefitte CN, Belghazi M, Fusai T, et al. (2009) Identification of cellular proteome modifications in response to West Nile virus infection. *Mol Cell Proteomics* 8: 1623-1637.
8. Pattanakitsakul SN, Rungrojcharoenkit K, Kanlaya R, Sinchaikul S, Noisakran S, et al. (2007) Proteomic analysis of host responses in HepG2 cells during dengue virus infection. *J Proteome Res* 6: 4592-4600.
9. Knauer O, Binai NA, Carra G, Beckhaus T, Hanschmann KM, et al. (2008) Differential phosphoproteome profiling reveals a functional role for VASP in *Helicobacter pylori*-induced cytoskeleton turnover in gastric epithelial cells. *Cell Microbiol* 10: 2285-2296.
10. Delbruck M (1940) Adsorption of Bacteriophage under Various Physiological Conditions of the Host. *J Gen Physiol* 23: 631-642.
11. Darnell JE, Jr., Sawyer TK (1960) The basis for variation in susceptibility to poliovirus in HeLa cells. *Virology* 11: 665-675.
12. Snijder B, Sacher R, Ramo P, Damm EM, Liberali P, et al. (2009) Population context determines cell-to-cell variability in endocytosis and virus infection. *Nature* 461: 520-523.
13. Sheppard D (1994) Dominant negative mutants: tools for the study of protein function in vitro and in vivo. *Am J Respir Cell Mol Biol* 11: 1-6.
14. Fire A, Xu S, Montgomery MK, Kostas SA, Driver SE, et al. (1998) Potent and specific genetic interference by double-stranded RNA in *Caenorhabditis elegans*. *Nature* 391: 806-811.
15. Zamore PD, Tuschl T, Sharp PA, Bartel DP (2000) RNAi: double-stranded RNA directs the ATP-dependent cleavage of mRNA at 21 to 23 nucleotide intervals. *Cell* 101: 25-33.
16. Tschuch C, Schulz A, Pscherer A, Werft W, Benner A, et al. (2008) Off-target effects of siRNA specific for GFP. *BMC Mol Biol* 9: 60.
17. Jobblogger B (2008) the demise of RNAi. *Bio JobBlog*.
18. Mohr S, Bakal C, Perrimon N (2010) Genomic screening with RNAi: results and challenges. *Annu Rev Biochem* 79: 37-64.

19. Jackson AL, Burchard J, Schelter J, Chau BN, Cleary M, et al. (2006) Widespread siRNA "off-target" transcript silencing mediated by seed region sequence complementarity. *Rna* 12: 1179-1187.
20. Echeverri CJ, Beachy PA, Baum B, Boutros M, Buchholz F, et al. (2006) Minimizing the risk of reporting false positives in large-scale RNAi screens. *Nat Methods* 3: 777-779.
21. Jackson AL, Burchard J, Leake D, Reynolds A, Schelter J, et al. (2006) Position-specific chemical modification of siRNAs reduces "off-target" transcript silencing. *Rna* 12: 1197-1205.
22. Pelkmans L, Fava E, Grabner H, Hannus M, Habermann B, et al. (2005) Genome-wide analysis of human kinases in clathrin- and caveolae/raft-mediated endocytosis. *Nature* 436: 78-86.
23. Pielage JF, Powell KR, Kalman D, Engel JN (2008) RNAi screen reveals an Abl kinase-dependent host cell pathway involved in *Pseudomonas aeruginosa* internalization. *PLoS Pathog* 4: e1000031.
24. Derre I, Pypaert M, Dautry-Varsat A, Agaisse H (2007) RNAi screen in *Drosophila* cells reveals the involvement of the Tom complex in *Chlamydia* infection. *PLoS Pathog* 3: 1446-1458.
25. Konig R, Zhou Y, Elleder D, Diamond TL, Bonamy GM, et al. (2008) Global analysis of host-pathogen interactions that regulate early-stage HIV-1 replication. *Cell* 135: 49-60.
26. Zhou H, Xu M, Huang Q, Gates AT, Zhang XD, et al. (2008) Genome-scale RNAi screen for host factors required for HIV replication. *Cell Host Microbe* 4: 495-504.
27. Jayaswal S, Kamal MA, Dua R, Gupta S, Majumdar T, et al. (2010) Identification of host-dependent survival factors for intracellular *Mycobacterium tuberculosis* through an siRNA screen. *PLoS Pathog* 6: e1000839.
28. Bushman FD, Malani N, Fernandes J, D'Orso I, Cagney G, et al. (2009) Host cell factors in HIV replication: meta-analysis of genome-wide studies. *PLoS Pathog* 5: e1000437.
29. Pizarro-Cerda J, Cossart P (2006) Bacterial adhesion and entry into host cells. *Cell* 124: 715-727.
30. Cossart P, Sansonetti PJ (2004) Bacterial invasion: the paradigms of enteroinvasive pathogens. *Science* 304: 242-248.
31. Finlay BB, Cossart P (1997) Exploitation of mammalian host cell functions by bacterial pathogens. *Science* 276: 718-725.
32. Isberg RR, Barnes P (2001) Subversion of integrins by enteropathogenic *Yersinia*. *J Cell Sci* 114: 21-28.
33. Cossart P, Pizarro-Cerda J, Lecuit M (2003) Invasion of mammalian cells by *Listeria monocytogenes*: functional mimicry to subvert cellular functions. *Trends Cell Biol* 13: 23-31.
34. Schubert WD, Urbanke C, Ziehm T, Beier V, Machner MP, et al. (2002) Structure of internalin, a major invasion protein of *Listeria monocytogenes*, in complex with its human receptor E-cadherin. *Cell* 111: 825-836.
35. Veiga E, Cossart P (2007) *Listeria* InlB takes a different route to met. *Cell* 130: 218-219.
36. Bierne H, Dramsi S, Gratacap MP, Randriamampita C, Carpenter G, et al. (2000) The invasion protein InlB from *Listeria monocytogenes* activates PLC-gamma1 downstream from PI 3-kinase. *Cell Microbiol* 2: 465-476.
37. Dussurget O, Pizarro-Cerda J, Cossart P (2004) Molecular determinants of *Listeria monocytogenes* virulence. *Annu Rev Microbiol* 58: 587-610.

38. Bierne H, Gouin E, Roux P, Caroni P, Yin HL, et al. (2001) A role for cofilin and LIM kinase in Listeria-induced phagocytosis. *J Cell Biol* 155: 101-112.
39. Blocker A, Komoriya K, Aizawa S (2003) Type III secretion systems and bacterial flagella: insights into their function from structural similarities. *Proc Natl Acad Sci U S A* 100: 3027-3030.
40. Hayward RD, Koronakis V (1999) Direct nucleation and bundling of actin by the SipC protein of invasive *Salmonella*. *Embo J* 18: 4926-4934.
41. Norris FA, Wilson MP, Wallis TS, Galyov EE, Majerus PW (1998) SopB, a protein required for virulence of *Salmonella* dublin, is an inositol phosphate phosphatase. *Proc Natl Acad Sci U S A* 95: 14057-14059.
42. Zhou D, Mooseker MS, Galan JE (1999) Role of the *S. typhimurium* actin-binding protein SipA in bacterial internalization. *Science* 283: 2092-2095.
43. McGhie EJ, Hayward RD, Koronakis V (2001) Cooperation between actin-binding proteins of invasive *Salmonella*: SipA potentiates SipC nucleation and bundling of actin. *Embo J* 20: 2131-2139.
44. Stebbins CE, Galan JE (2000) Modulation of host signaling by a bacterial mimic: structure of the *Salmonella* effector SptP bound to Rac1. *Mol Cell* 6: 1449-1460.
45. Yoshida S, Handa Y, Suzuki T, Ogawa M, Suzuki M, et al. (2006) Microtubule-severing activity of *Shigella* is pivotal for intercellular spreading. *Science* 314: 985-989.
46. Germane KL, Ohi R, Goldberg MB, Spiller BW (2008) Structural and functional studies indicate that *Shigella* VirA is not a protease and does not directly destabilize microtubules. *Biochemistry* 47: 10241-10243.
47. Tran Van Nhieu G, Caron E, Hall A, Sansonetti PJ (1999) IpaC induces actin polymerization and filopodia formation during *Shigella* entry into epithelial cells. *Embo J* 18: 3249-3262.
48. Tran Van Nhieu G, Bourdet-Sicard R, Dumenil G, Blocker A, Sansonetti PJ (2000) Bacterial signals and cell responses during *Shigella* entry into epithelial cells. *Cell Microbiol* 2: 187-193.
49. Picking WL, Nishioka H, Hearn PD, Baxter MA, Harrington AT, et al. (2005) IpaD of *Shigella flexneri* is independently required for regulation of Ipa protein secretion and efficient insertion of IpaB and IpaC into host membranes. *Infect Immun* 73: 1432-1440.
50. Bourdet-Sicard R, Rudiger M, Jockusch BM, Gounon P, Sansonetti PJ, et al. (1999) Binding of the *Shigella* protein IpaA to vinculin induces F-actin depolymerization. *Embo J* 18: 5853-5862.
51. Hynes RO (2002) Integrins: bidirectional, allosteric signaling machines. *Cell* 110: 673-687.
52. Humphries JD, Byron A, Humphries MJ (2006) Integrin ligands at a glance. *J Cell Sci* 119: 3901-3903.
53. Pierschbacher MD, Ruoslahti E (1984) Cell attachment activity of fibronectin can be duplicated by small synthetic fragments of the molecule. *Nature* 309: 30-33.
54. Harburger DS, Calderwood DA (2009) Integrin signalling at a glance. *J Cell Sci* 122: 159-163.
55. Calderwood DA (2004) Integrin activation. *J Cell Sci* 117: 657-666.
56. Takagi J, Petre BM, Walz T, Springer TA (2002) Global conformational rearrangements in integrin extracellular domains in outside-in and inside-out signaling. *Cell* 110: 599-511.
57. Moser M, Legate KR, Zent R, Fassler R (2009) The tail of integrins, talin, and kindlins. *Science* 324: 895-899.
58. Luo BH, Carman CV, Springer TA (2007) Structural basis of integrin regulation and signaling. *Annu Rev Immunol* 25: 619-647.

59. Xiong JP, Stehle T, Goodman SL, Arnaout MA (2003) New insights into the structural basis of integrin activation. *Blood* 102: 1155-1159.
60. Shattil SJ, Kim C, Ginsberg MH (2010) The final steps of integrin activation: the end game. *Nat Rev Mol Cell Biol* 11: 288-300.
61. Goksoy E, Ma YQ, Wang X, Kong X, Perera D, et al. (2008) Structural basis for the autoinhibition of talin in regulating integrin activation. *Mol Cell* 31: 124-133.
62. Franco SJ, Rodgers MA, Perrin BJ, Han J, Bennin DA, et al. (2004) Calpain-mediated proteolysis of talin regulates adhesion dynamics. *Nat Cell Biol* 6: 977-983.
63. Wegener KL, Partridge AW, Han J, Pickford AR, Liddington RC, et al. (2007) Structural basis of integrin activation by talin. *Cell* 128: 171-182.
64. Anthis NJ, Wegener KL, Ye F, Kim C, Goult BT, et al. (2009) The structure of an integrin/talin complex reveals the basis of inside-out signal transduction. *Embo J* 28: 3623-3632.
65. Huang C, Rajfur Z, Yousefi N, Chen Z, Jacobson K, et al. (2009) Talin phosphorylation by Cdk5 regulates Smurf1-mediated talin head ubiquitylation and cell migration. *Nat Cell Biol* 11: 624-630.
66. Calderwood DA, Yan B, de Pereda JM, Alvarez BG, Fujioka Y, et al. (2002) The phosphotyrosine binding-like domain of talin activates integrins. *J Biol Chem* 277: 21749-21758.
67. Calderwood DA, Zent R, Grant R, Rees DJ, Hynes RO, et al. (1999) The Talin head domain binds to integrin beta subunit cytoplasmic tails and regulates integrin activation. *J Biol Chem* 274: 28071-28074.
68. Ginsberg MH, Partridge A, Shattil SJ (2005) Integrin regulation. *Curr Opin Cell Biol* 17: 509-516.
69. Mitra SK, Hanson DA, Schlaepfer DD (2005) Focal adhesion kinase: in command and control of cell motility. *Nat Rev Mol Cell Biol* 6: 56-68.
70. Cai X, Lietha D, Ceccarelli DF, Karginov AV, Rajfur Z, et al. (2008) Spatial and temporal regulation of focal adhesion kinase activity in living cells. *Mol Cell Biol* 28: 201-214.
71. Papusheva E, Mello de Queiroz F, Dalous J, Han Y, Esposito A, et al. (2009) Dynamic conformational changes in the FERM domain of FAK are involved in focal-adhesion behavior during cell spreading and motility. *J Cell Sci* 122: 656-666.
72. Frame MC, Patel H, Serrels B, Lietha D, Eck MJ (2010) The FERM domain: organizing the structure and function of FAK. *Nat Rev Mol Cell Biol* 11: 802-814.
73. Arias-Salgado EG, Lizano S, Sarkar S, Brugge JS, Ginsberg MH, et al. (2003) Src kinase activation by direct interaction with the integrin beta cytoplasmic domain. *Proc Natl Acad Sci U S A* 100: 13298-13302.
74. Legate KR, Montanez E, Kudlacek O, Fassler R (2006) ILK, PINCH and parvin: the tIPP of integrin signalling. *Nat Rev Mol Cell Biol* 7: 20-31.
75. Tucker KL, Sage T, Stevens JM, Jordan PA, Jones S, et al. (2008) A dual role for integrin-linked kinase in platelets: regulating integrin function and alpha-granule secretion. *Blood* 112: 4523-4531.
76. Deakin NO, Turner CE (2008) Paxillin comes of age. *J Cell Sci* 121: 2435-2444.
77. Critchley DR (2004) Cytoskeletal proteins talin and vinculin in integrin-mediated adhesion. *Biochem Soc Trans* 32: 831-836.

78. Wen KK, Rubenstein PA, DeMali KA (2009) Vinculin nucleates actin polymerization and modifies actin filament structure. *J Biol Chem* 284: 30463-30473.
79. technology Cs (2009) Regulation of actin dynamics.
80. Scibelli A, Roperto S, Manna L, Pavone LM, Tafuri S, et al. (2007) Engagement of integrins as a cellular route of invasion by bacterial pathogens. *Vet J* 173: 482-491.
81. Williams-Bouyer NM, Hill EM (1999) Involvement of host cell tyrosine phosphorylation in the invasion of HEp-2 cells by *Bartonella bacilliformis*. *FEMS Microbiol Lett* 171: 191-201.
82. Burgess AW, Anderson BE (1998) Outer membrane proteins of *Bartonella henselae* and their interaction with human endothelial cells. *Microb Pathog* 25: 157-164.
83. Musso T, Badolato R, Ravarino D, Stornello S, Panzanelli P, et al. (2001) Interaction of *Bartonella henselae* with the murine macrophage cell line J774: infection and proinflammatory response. *Infect Immun* 69: 5974-5980.
84. Riess T, Andersson SG, Lupas A, Schaller M, Schafer A, et al. (2004) *Bartonella* adhesin a mediates a proangiogenic host cell response. *J Exp Med* 200: 1267-1278.
85. Everest P, Li J, Douce G, Charles I, De Azavedo J, et al. (1996) Role of the *Bordetella pertussis* P.69/pertactin protein and the P.69/pertactin RGD motif in the adherence to and invasion of mammalian cells. *Microbiology* 142 (Pt 11): 3261-3268.
86. Coburn J, Cugini C (2003) Targeted mutation of the outer membrane protein P66 disrupts attachment of the Lyme disease agent, *Borrelia burgdorferi*, to integrin alpha_vbeta₃. *Proc Natl Acad Sci U S A* 100: 7301-7306.
87. Konkel ME, Garvis SG, Tipton SL, Anderson DE, Jr., Cieplak W, Jr. (1997) Identification and molecular cloning of a gene encoding a fibronectin-binding protein (CadF) from *Campylobacter jejuni*. *Mol Microbiol* 24: 953-963.
88. Monteville MR, Yoon JE, Konkel ME (2003) Maximal adherence and invasion of INT 407 cells by *Campylobacter jejuni* requires the CadF outer-membrane protein and microfilament reorganization. *Microbiology* 149: 153-165.
89. Kenny B, Finlay BB (1995) Protein secretion by enteropathogenic *Escherichia coli* is essential for transducing signals to epithelial cells. *Proc Natl Acad Sci U S A* 92: 7991-7995.
90. Frankel G, Lider O, Hershkoviz R, Mould AP, Kachalsky SG, et al. (1996) The cell-binding domain of intimin from enteropathogenic *Escherichia coli* binds to beta₁ integrins. *J Biol Chem* 271: 20359-20364.
91. Middleton AM, Chadwick MV, Nicholson AG, Dewar A, Groger RK, et al. (2000) The role of *Mycobacterium avium* complex fibronectin attachment protein in adherence to the human respiratory mucosa. *Mol Microbiol* 38: 381-391.
92. Billker O, Popp A, Brinkmann V, Wenig G, Schneider J, et al. (2002) Distinct mechanisms of internalization of *Neisseria gonorrhoeae* by members of the CEACAM receptor family involving Rac1- and Cdc42-dependent and -independent pathways. *Embo J* 21: 560-571.
93. Dehio M, Gomez-Duarte OG, Dehio C, Meyer TF (1998) Vitronectin-dependent invasion of epithelial cells by *Neisseria gonorrhoeae* involves alpha_v integrin receptors. *FEBS Lett* 424: 84-88.

94. Dehio C, Gray-Owen SD, Meyer TF (1998) The role of neisserial Opa proteins in interactions with host cells. Trends Microbiol 6: 489-495.
95. Cho BA, Cho NH, Seong SY, Choi MS, Kim IS (2010) Intracellular invasion by *Orientia tsutsugamushi* is mediated by integrin signaling and actin cytoskeleton rearrangements. Infect Immun 78: 1915-1923.
96. Nakagawa I, Amano A, Inaba H, Kawai S, Hamada S (2005) Inhibitory effects of *Porphyromonas gingivalis* fimbriae on interactions between extracellular matrix proteins and cellular integrins. Microbes Infect 7: 157-163.
97. Esen M, Grassme H, Riethmuller J, Riehle A, Fassbender K, et al. (2001) Invasion of human epithelial cells by *Pseudomonas aeruginosa* involves src-like tyrosine kinases p60Src and p59Fyn. Infect Immun 69: 281-287.
98. Evans DJ, Maltseva IA, Wu J, Fleiszig SM (2002) *Pseudomonas aeruginosa* internalization by corneal epithelial cells involves MEK and ERK signal transduction proteins. FEMS Microbiol Lett 213: 73-79.
99. Leroy-Dudal J, Gagniere H, Cossard E, Carreiras F, Di Martino P (2004) Role of alphavbeta5 integrins and vitronectin in *Pseudomonas aeruginosa* PAK interaction with A549 respiratory cells. Microbes Infect 6: 875-881.
100. Collinson SK, Doig PC, Doran JL, Clouthier S, Trust TJ, et al. (1993) Thin, aggregative fimbriae mediate binding of *Salmonella enteritidis* to fibronectin. J Bacteriol 175: 12-18.
101. Kingsley RA, Keestra AM, de Zoete MR, Baumler AJ (2004) The ShdA adhesin binds to the cationic cradle of the fibronectin 13FnIII repeat module: evidence for molecular mimicry of heparin binding. Mol Microbiol 52: 345-355.
102. Sansonetti PJ (2001) Rupture, invasion and inflammatory destruction of the intestinal barrier by *Shigella*, making sense of prokaryote-eukaryote cross-talks. FEMS Microbiol Rev 25: 3-14.
103. Watarai M, Funato S, Sasakawa C (1996) Interaction of Ipa proteins of *Shigella flexneri* with alpha5beta1 integrin promotes entry of the bacteria into mammalian cells. J Exp Med 183: 991-999.
104. Jonsson K, Signas C, Muller HP, Lindberg M (1991) Two different genes encode fibronectin binding proteins in *Staphylococcus aureus*. The complete nucleotide sequence and characterization of the second gene. Eur J Biochem 202: 1041-1048.
105. Agerer F, Lux S, Michel A, Rohde M, Ohlsen K, et al. (2005) Cellular invasion by *Staphylococcus aureus* reveals a functional link between focal adhesion kinase and cortactin in integrin-mediated internalisation. J Cell Sci 118: 2189-2200.
106. Cue D, Southern SO, Southern PJ, Prabhakar J, Lorelli W, et al. (2000) A nonpeptide integrin antagonist can inhibit epithelial cell ingestion of *Streptococcus pyogenes* by blocking formation of integrin alpha 5beta 1-fibronectin-M1 protein complexes. Proc Natl Acad Sci U S A 97: 2858-2863.
107. Lindmark H, Guss B (1999) SFS, a novel fibronectin-binding protein from *Streptococcus equi*, inhibits the binding between fibronectin and collagen. Infect Immun 67: 2383-2388.
108. Rich M (2005) *Staphylococci* in animals: prevalence, identification and antimicrobial susceptibility, with an emphasis on methicillin-resistant *Staphylococcus aureus*. Br J Biomed Sci 62: 98-105.

109. Deleuil F, Mogemark L, Francis MS, Wolf-Watz H, Fallman M (2003) Interaction between the *Yersinia* protein tyrosine phosphatase YopH and eukaryotic Cas/Fyb is an important virulence mechanism. *Cell Microbiol* 5: 53-64.
110. El Tahir Y, Skurnik M (2001) YadA, the multifaceted *Yersinia* adhesin. *Int J Med Microbiol* 291: 209-218.
111. Cornelis GR (2002) *Yersinia* type III secretion: send in the effectors. *J Cell Biol* 158: 401-408.
112. Cornelis GR (2002) The *Yersinia* Ysc-Yop 'type III' weaponry. *Nat Rev Mol Cell Biol* 3: 742-752.
113. Isberg RR, Leong JM (1990) Multiple beta 1 chain integrins are receptors for invasin, a protein that promotes bacterial penetration into mammalian cells. *Cell* 60: 861-871.
114. Van Nhieu GT, Krukoni ES, Reszka AA, Horwitz AF, Isberg RR (1996) Mutations in the cytoplasmic domain of the integrin beta1 chain indicate a role for endocytosis factors in bacterial internalization. *J Biol Chem* 271: 7665-7672.
115. Dersch P, Isberg RR (1999) A region of the *Yersinia pseudotuberculosis* invasin protein enhances integrin-mediated uptake into mammalian cells and promotes self-association. *Embo J* 18: 1199-1213.
116. Agerer F, Michel A, Ohlsen K, Hauck CR (2003) Integrin-mediated invasion of *Staphylococcus aureus* into human cells requires Src family protein-tyrosine kinases. *J Biol Chem* 278: 42524-42531.
117. Polk DB, Peek RM, Jr. (2010) *Helicobacter pylori*: gastric cancer and beyond. *Nat Rev Cancer* 10: 403-414.
118. Kwok T, Zabler D, Urman S, Rohde M, Hartig R, et al. (2007) *Helicobacter* exploits integrin for type IV secretion and kinase activation. *Nature* 449: 862-866.
119. Jimenez-Soto LF, Kutter S, Sewald X, Ertl C, Weiss E, et al. (2009) *Helicobacter pylori* type IV secretion apparatus exploits beta1 integrin in a novel RGD-independent manner. *PLoS Pathog* 5: e1000684.
120. Demali KA, Jue AL, Burrige K (2006) IpaA targets beta1 integrins and rho to promote actin cytoskeleton rearrangements necessary for *Shigella* entry. *J Biol Chem* 281: 39534-39541.
121. Aktories K, Barbieri JT (2005) Bacterial cytotoxins: targeting eukaryotic switches. *Nat Rev Microbiol* 3: 397-410.
122. Le Clainche C, Carlier MF (2008) Regulation of actin assembly associated with protrusion and adhesion in cell migration. *Physiol Rev* 88: 489-513.
123. Theriot JA, Mitchison TJ (1991) Actin microfilament dynamics in locomoting cells. *Nature* 352: 126-131.
124. Carlier MF, Laurent V, Santolini J, Melki R, Didry D, et al. (1997) Actin depolymerizing factor (ADF/cofilin) enhances the rate of filament turnover: implication in actin-based motility. *J Cell Biol* 136: 1307-1322.
125. Carlier MF, Ressad F, Pantaloni D (1999) Control of actin dynamics in cell motility. Role of ADF/cofilin. *J Biol Chem* 274: 33827-33830.
126. Yarmola EG, Bubb MR (2006) Profilin: emerging concepts and lingering misconceptions. *Trends Biochem Sci* 31: 197-205.
127. Schafer DA, Jennings PB, Cooper JA (1996) Dynamics of capping protein and actin assembly in vitro: uncapping barbed ends by polyphosphoinositides. *J Cell Biol* 135: 169-179.
128. Svitkina TM, Borisy GG (1999) Arp2/3 complex and actin depolymerizing factor/cofilin in dendritic organization and treadmilling of actin filament array in lamellipodia. *J Cell Biol* 145: 1009-1026.

129. Revenu C, Athman R, Robine S, Louvard D (2004) The co-workers of actin filaments: from cell structures to signals. *Nat Rev Mol Cell Biol* 5: 635-646.
130. Ridley AJ (2006) Rho GTPases and actin dynamics in membrane protrusions and vesicle trafficking. *Trends Cell Biol* 16: 522-529.
131. Faix J, Rottner K (2006) The making of filopodia. *Curr Opin Cell Biol* 18: 18-25.
132. Nobes CD, Hall A (1995) Rho, rac, and cdc42 GTPases regulate the assembly of multimolecular focal complexes associated with actin stress fibers, lamellipodia, and filopodia. *Cell* 81: 53-62.
133. Hall A (1998) Rho GTPases and the actin cytoskeleton. *Science* 279: 509-514.
134. Thao PTP (2010) Rho GTPases regulate actin filaments and cytoskeletal organization. Singapore: Research Centre of Excellence in Mechanobiology, National University of Singapore, Republic of Singapore.
135. Dvorsky R, Ahmadian MR (2004) Always look on the bright side of Rho: structural implications for a conserved intermolecular interface. *EMBO Rep* 5: 1130-1136.
136. Roberts PJ, Mitin N, Keller PJ, Chenette EJ, Madigan JP, et al. (2008) Rho Family GTPase modification and dependence on CAAX motif-signaled posttranslational modification. *J Biol Chem* 283: 25150-25163.
137. Jaffe AB, Hall A (2005) Rho GTPases: biochemistry and biology. *Annu Rev Cell Dev Biol* 21: 247-269.
138. Bishop AL, Hall A (2000) Rho GTPases and their effector proteins. *Biochem J* 348 Pt 2: 241-255.
139. Fukazawa A, Alonso C, Kurachi K, Gupta S, Lesser CF, et al. (2008) GEF-H1 mediated control of NOD1 dependent NF-kappaB activation by *Shigella* effectors. *PLoS Pathog* 4: e1000228.
140. Scheffzek K, Stephan I, Jensen ON, Illenberger D, Gierschik P (2000) The Rac-RhoGDI complex and the structural basis for the regulation of Rho proteins by RhoGDI. *Nat Struct Biol* 7: 122-126.
141. Hoffman GR, Nassar N, Cerione RA (2000) Structure of the Rho family GTP-binding protein Cdc42 in complex with the multifunctional regulator RhoGDI. *Cell* 100: 345-356.
142. Just I, Wilm M, Selzer J, Rex G, von Eichel-Streiber C, et al. (1995) The enterotoxin from *Clostridium difficile* (ToxA) monoglucosylates the Rho proteins. *J Biol Chem* 270: 13932-13936.
143. Just I, Selzer J, Wilm M, von Eichel-Streiber C, Mann M, et al. (1995) Glucosylation of Rho proteins by *Clostridium difficile* toxin B. *Nature* 375: 500-503.
144. Sehr P, Joseph G, Genth H, Just I, Pick E, et al. (1998) Glucosylation and ADP ribosylation of rho proteins: effects on nucleotide binding, GTPase activity, and effector coupling. *Biochemistry* 37: 5296-5304.
145. Iriarte M, Cornelis GR (1998) YopT, a new *Yersinia* Yop effector protein, affects the cytoskeleton of host cells. *Mol Microbiol* 29: 915-929.
146. Shao F, Merritt PM, Bao Z, Innes RW, Dixon JE (2002) A *Yersinia* effector and a *Pseudomonas* avirulence protein define a family of cysteine proteases functioning in bacterial pathogenesis. *Cell* 109: 575-588.
147. Zumbihl R, Aepfelbacher M, Andor A, Jacobi CA, Ruckdeschel K, et al. (1999) The cytotoxin YopT of *Yersinia enterocolitica* induces modification and cellular redistribution of the small GTP-binding protein RhoA. *J Biol Chem* 274: 29289-29293.
148. Fiorentini C, Fabbri A, Flatau G, Donelli G, Matarrese P, et al. (1997) *Escherichia coli* cytotoxic necrotizing factor 1 (CNF1), a toxin that activates the Rho GTPase. *J Biol Chem* 272: 19532-19537.

149. Rittinger K, Walker PA, Eccleston JF, Nurmahomed K, Owen D, et al. (1997) Crystal structure of a small G protein in complex with the GTPase-activating protein rhoGAP. *Nature* 388: 693-697.
150. Bulgin R, Raymond B, Garnett JA, Frankel G, Crepin VF, et al. (2010) Bacterial guanine nucleotide exchange factors SopE-like and WxxxE effectors. *Infect Immun* 78: 1417-1425.
151. Geiser TK, Kazmierczak BI, Garrity-Ryan LK, Matthay MA, Engel JN (2001) *Pseudomonas aeruginosa* ExoT inhibits in vitro lung epithelial wound repair. *Cell Microbiol* 3: 223-236.
152. Knight DA, Finck-Barbancon V, Kulich SM, Barbieri JT (1995) Functional domains of *Pseudomonas aeruginosa* exoenzyme S. *Infect Immun* 63: 3182-3186.
153. Maresso AW, Baldwin MR, Barbieri JT (2004) Ezrin/radixin/moesin proteins are high affinity targets for ADP-ribosylation by *Pseudomonas aeruginosa* ExoS. *J Biol Chem* 279: 38402-38408.
154. Sun J, Barbieri JT (2003) *Pseudomonas aeruginosa* ExoT ADP-ribosylates CT10 regulator of kinase (Crk) proteins. *J Biol Chem* 278: 32794-32800.
155. Yarbrough ML, Li Y, Kinch LN, Grishin NV, Ball HL, et al. (2009) AMPylation of Rho GTPases by *Vibrio* VopS disrupts effector binding and downstream signaling. *Science* 323: 269-272.
156. Roy CR, Mukherjee S (2009) Bacterial FIC Proteins AMP Up Infection. *Sci Signal* 2: pe14.
157. Corbeil LB (2007) *Histophilus somni* host-parasite relationships. *Anim Health Res Rev* 8: 151-160.
158. Zekarias B, Mattoo S, Worby C, Lehmann J, Rosenbusch RF, et al. (2010) *Histophilus somni* lbpA DR2/Fic in virulence and immunoprotection at the natural host alveolar epithelial barrier. *Infect Immun* 78: 1850-1858.
159. Worby CA, Mattoo S, Kruger RP, Corbeil LB, Koller A, et al. (2009) The fic domain: regulation of cell signaling by adenylylation. *Mol Cell* 34: 93-103.
160. Hardt WD, Chen LM, Schuebel KE, Bustelo XR, Galan JE (1998) *S. typhimurium* encodes an activator of Rho GTPases that induces membrane ruffling and nuclear responses in host cells. *Cell* 93: 815-826.
161. Rudolph MG, Weise C, Miroid S, Hillenbrand B, Bader B, et al. (1999) Biochemical analysis of SopE from *Salmonella typhimurium*, a highly efficient guanosine nucleotide exchange factor for RhoGTPases. *J Biol Chem* 274: 30501-30509.
162. Kubori T, Galan JE (2003) Temporal regulation of *salmonella* virulence effector function by proteasome-dependent protein degradation. *Cell* 115: 333-342.
163. Black DS, Bliska JB (2000) The RhoGAP activity of the *Yersinia pseudotuberculosis* cytotoxin YopE is required for antiphagocytic function and virulence. *Mol Microbiol* 37: 515-527.
164. Von Pawel-Rammingen U, Telepnev MV, Schmidt G, Aktories K, Wolf-Watz H, et al. (2000) GAP activity of the *Yersinia* YopE cytotoxin specifically targets the Rho pathway: a mechanism for disruption of actin microfilament structure. *Mol Microbiol* 36: 737-748.
165. Alto NM, Shao F, Lazar CS, Brost RL, Chua G, et al. (2006) Identification of a bacterial type III effector family with G protein mimicry functions. *Cell* 124: 133-145.
166. Zhiwei Huang¹, Sarah E Sutton^{2,4}, Adam J Wallenfang², Robert C Orchard², Xiaojing Wu¹, Yingcai Feng¹, Jijie Chai^{1,3} & Neal M Alto² (2009) Structural insights into host GTPase isoform selection by a family of bacterial GEF mimics. *Nature Structural & Molecular Biology*: 8.

167. Kenny B, Ellis S, Leard AD, Warawa J, Mellor H, et al. (2002) Co-ordinate regulation of distinct host cell signalling pathways by multifunctional enteropathogenic *Escherichia coli* effector molecules. *Mol Microbiol* 44: 1095-1107.
168. Berger CN, Crepin VF, Jepson MA, Arbeloa A, Frankel G (2009) The mechanisms used by enteropathogenic *Escherichia coli* to control filopodia dynamics. *Cell Microbiol* 11: 309-322.
169. Arbeloa A, Garnett J, Lillington J, Bulgin RR, Berger CN, et al. (2010) EspM2 is a RhoA guanine nucleotide exchange factor. *Cell Microbiol* 12: 654-664.
170. Bulgin RR, Arbeloa A, Chung JC, Frankel G (2009) EspT triggers formation of lamellipodia and membrane ruffles through activation of Rac-1 and Cdc42. *Cell Microbiol* 11: 217-229.
171. Huang Z, Sutton SE, Wallenfang AJ, Orchard RC, Wu X, et al. (2009) Structural insights into host GTPase isoform selection by a family of bacterial GEF mimics. *Nat Struct Mol Biol* 16: 853-860.
172. Handa Y, Suzuki M, Ohya K, Iwai H, Ishijima N, et al. (2007) *Shigella* IpgB1 promotes bacterial entry through the ELMO-Dock180 machinery. *Nat Cell Biol* 9: 121-128.
173. Hussain NK, Jenna S, Glogauer M, Quinn CC, Wasiak S, et al. (2001) Endocytic protein intersectin-1 regulates actin assembly via Cdc42 and N-WASP. *Nat Cell Biol* 3: 927-932.
174. Beuzon CR, Meresse S, Unsworth KE, Ruiz-Albert J, Garvis S, et al. (2000) *Salmonella* maintains the integrity of its intracellular vacuole through the action of SifA. *Embo J* 19: 3235-3249.
175. Boucrot E, Henry T, Borg JP, Gorvel JP, Meresse S (2005) The intracellular fate of *Salmonella* depends on the recruitment of kinesin. *Science* 308: 1174-1178.
176. Ohlson MB, Huang Z, Alto NM, Blanc MP, Dixon JE, et al. (2008) Structure and function of *Salmonella* SifA indicate that its interactions with SKIP, SseJ, and RhoA family GTPases induce endosomal tubulation. *Cell Host Microbe* 4: 434-446.
177. Boucrot E, Beuzon CR, Holden DW, Gorvel JP, Meresse S (2003) *Salmonella typhimurium* SifA effector protein requires its membrane-anchoring C-terminal hexapeptide for its biological function. *J Biol Chem* 278: 14196-14202.
178. Arbeloa A, Bulgin RR, MacKenzie G, Shaw RK, Pallen MJ, et al. (2008) Subversion of actin dynamics by EspM effectors of attaching and effacing bacterial pathogens. *Cell Microbiol* 10: 1429-1441.
179. Bellanger JM, Astier C, Sardet C, Ohta Y, Stossel TP, et al. (2000) The Rac1- and RhoG-specific GEF domain of Trio targets filamin to remodel cytoskeletal actin. *Nat Cell Biol* 2: 888-892.
180. Dehio C (2005) *Bartonella*-host-cell interactions and vascular tumour formation. *Nat Rev Microbiol* 3: 621-631.
181. Maguina C, Gotuzzo E (2000) Bartonellosis. New and old. *Infect Dis Clin North Am* 14: 1-22, vii.
182. Dehio C (2004) Molecular and cellular basis of *bartonella* pathogenesis. *Annu Rev Microbiol* 58: 365-390.
183. Saenz HL, Engel P, Stoeckli MC, Lanz C, Raddatz G, et al. (2007) Genomic analysis of *Bartonella* identifies type IV secretion systems as host adaptability factors. *Nat Genet* 39: 1469-1476.
184. Schulein R, Seubert A, Gille C, Lanz C, Hansmann Y, et al. (2001) Invasion and persistent intracellular colonization of erythrocytes. A unique parasitic strategy of the emerging pathogen *Bartonella*. *J Exp Med* 193: 1077-1086.

185. Schulein R, Dehio C (2002) The VirB/VirD4 type IV secretion system of *Bartonella* is essential for establishing intraerythrocytic infection. *Mol Microbiol* 46: 1053-1067.
186. Abbott RC, Chomel BB, Kasten RW, Floyd-Hawkins KA, Kikuchi Y, et al. (1997) Experimental and natural infection with *Bartonella henselae* in domestic cats. *Comp Immunol Microbiol Infect Dis* 20: 41-51.
187. Koesling J, Aebischer T, Falch C, Schulein R, Dehio C (2001) Cutting edge: antibody-mediated cessation of hemotropic infection by the intraerythrocytic mouse pathogen *Bartonella grahamii*. *J Immunol* 167: 11-14.
188. Vayssier-Taussat M, Le Rhun D, Deng HK, Biville F, Cescau S, et al. (2010) The Trw type IV secretion system of *Bartonella* mediates host-specific adhesion to erythrocytes. *PLoS Pathog* 6: e1000946.
189. Schulein R, Guye P, Rhomberg TA, Schmid MC, Schroder G, et al. (2005) A bipartite signal mediates the transfer of type IV secretion substrates of *Bartonella henselae* into human cells. *Proc Natl Acad Sci U S A* 102: 856-861.
190. Schmid MC, Schulein R, Dehio M, Denecker G, Carena I, et al. (2004) The VirB type IV secretion system of *Bartonella henselae* mediates invasion, proinflammatory activation and antiapoptotic protection of endothelial cells. *Mol Microbiol* 52: 81-92.
191. Scheidegger F, Ellner Y, Guye P, Rhomberg TA, Weber H, et al. (2009) Distinct activities of *Bartonella henselae* type IV secretion effector proteins modulate capillary-like sprout formation. *Cell Microbiol* 11: 1088-1101.
192. Dehio C, Meyer M, Berger J, Schwarz H, Lanz C (1997) Interaction of *Bartonella henselae* with endothelial cells results in bacterial aggregation on the cell surface and the subsequent engulfment and internalisation of the bacterial aggregate by a unique structure, the invasome. *J Cell Sci* 110 (Pt 18): 2141-2154.

AIM OF THE THESIS

2 AIM OF THE THESIS

Started in November 2006, the aim of my thesis was to systematically identify and characterize host cell factors required for *Bartonella henselae*-triggered invasome formation and to analyze how the *Bartonella* effector proteins (Beps) manipulate host cell signaling in order to provoke invasome assembly. To this end, I applied modern methods of molecular systems biology and bioinformatics, including imaging-based high-throughput RNAi screening, subsequent automated image analysis and computer-based exploration of signaling networks. Moreover, I used methods of classical molecular and infections biology as well as biochemistry to work on BepC/BepF-triggered invasome formation and the molecular function of the effector protein BepF.

RESULTS

3 RESULTS

3.1 RESEARCH ARTICLE I

A translocated protein of *Bartonella henselae* interferes with endocytic uptake of individual bacteria and triggers uptake of large bacterial aggregates via the invasome

Thomas A. Rhomberg, Matthias C. Truttmann, Patrick Guye, Yvonne Ellner, Christoph Dehio

Cellular Microbiology, Volume 11, Issue 6, pages 927–945, June 2009

3.1.1 SUMMARY

Invasion of host cells is an often employed strategy of pathogenic bacteria to avoid clearance by the host immune system and to enable replication, persistence and dissemination. *Bartonella henselae* (*Bhe*) Houston-1 mediates its internalization by promoting the formation of a unique uptake structure on the host cell, which is named the invasome. This process is dependent on a functional VirD/B4 type 4 secretion system (T4SS) and T4SS-translocated *Bartonella* effector proteins (Beps) [1,2].

Infection experiments on HUVECs demonstrated that invasome-mediated internalization of *Bhe* counteracts individual *Bhe* uptake into *Bartonella* containing vacuoles (BCVs). To identify the accountable T4SS-translocated effector(s), epitope-tagged versions of BepA to BepG were expressed *in trans* in the effector-deficient *Bhe* mutant $\Delta bepA-G$ and tested for phenotypic complementation. The obtained results showed that only effector BepG is sufficient to i) trigger wild-type-like invasomes as characterized by massive rearrangements of the actin cytoskeleton and ii) to negatively interfere with the formation of BCVs. As shown for wild-type bacteria, BepG-dependent invasome formation was sensitive to cytochalasin D. Ectopic expression of GFP-tagged BepG in Ea.hy926 cells showed its co-localization with the actin cytoskeleton such as stress fibers or F-actin clusters in filopodial cell extensions. Surprisingly, neither ectopic expression of GFP- nor FLAG-tagged BepG in Ea.hy926 cells did promote any obvious actin rearrangements. Nevertheless, BepG restored invasome establishment by the effector-deficient mutant $\Delta bepA-G$ while at the same time inhibiting the individual uptake of *Bhe* into BCVs. Moreover, BepG was shown to reduce the zipper-like internalization of invasin-expressing *Yersinia enterocolitica* and BSA-coated small microspheres. These results suggested that BepG may regulate/inhibit key protein(s) playing a central role of various internalization processes in Ea.hy926 cells.

To assess the host cell site of invasome establishment, we used dominant-negative constructs of the Rho GTPases Cdc42, Rac1 and RhoA, all of which are major controllers of the actin cytoskeleton. Over-expressing N17-Cdc42, N17-Rac1 and N19-RhoA showed that Cdc42 and Rac1, but not RhoA are essential for *Bhe*-triggered invasome formation on Ea.hy926 cells. Furthermore, over-expression of the constitutive-active L61-Cdc42 and L61-Rac1 constructs also resulted in a significant reduction of invasome formation on Ea.hy926 cells. Ectopically expressed eGFP-tagged Cdc42 and Rac1 (both wild-type) were found to co-localize to a great extent with invasome structures of *Bhe*-infected Ea.hy926 cells.

Moreover, over-expressing the dominant negative constructs of Scar/WAVE and WASp in *Bhe*-infected Ea.hy926 cells, their involvement in invasome formation was demonstrated. Finally, co-localization of the Arp2/3 complex with invasome structures, as assessed by immuno-fluorescence microscopy, indicated its contribution to invasome establishment. Supporting evidence for the role of Rac1, Cdc42, Scar/WAVE, WASp and Arp2/3 in the process of BepG-triggered invasome formation resulted from RNAi knock-down experiments. All together, the cellular data suggested that positive as well as negative downstream signaling via the small GTPases Cdc42 and Rac1, but not RhoA, is required for invasome formation.

3.1.2 STATEMENT OF MY OWN CONTRIBUTION

I performed the experimental part of the paper revision. This included microsphere uptake assays (Fig. 6C) as well as siRNA-mediated knock-down experiments (Fig. S4). In addition, I extended the materials & methods section. The other data showed in the manuscript were obtained by Thomas A. Rhomberg and the manuscript was written by Thomas A. Rhomberg and Christoph Dehio.

3.1.3 REFERENCES

1. Schulein R, Guye P, Rhomberg TA, Schmid MC, Schroder G, et al. (2005) A bipartite signal mediates the transfer of type IV secretion substrates of *Bartonella henselae* into human cells. *Proc Natl Acad Sci U S A* 102: 856-861.
2. Schmid MC, Schulein R, Dehio M, Denecker G, Carena I, et al. (2004) The VirB type IV secretion system of *Bartonella henselae* mediates invasion, proinflammatory activation and antiapoptotic protection of endothelial cells. *Mol Microbiol* 52: 81-92.

A translocated protein of *Bartonella henselae* interferes with endocytic uptake of individual bacteria and triggers uptake of large bacterial aggregates via the invasome

Thomas A. Rhomberg, Matthias C. Truttmann, Patrick Guye, Yvonne Ellner and Christoph Dehio*
Focal Area Infection Biology, Biozentrum of the University of Basel, Klingelbergstrasse 70, CH-4056 Basel, Switzerland.

Summary

Bartonella henselae enters human endothelial cells (ECs) by two alternative routes: either by endocytosis, giving rise to *Bartonella*-containing vacuoles or by invasome-mediated internalization. Only the latter process depends on the type IV secretion system VirB/VirD4 and involves the formation of cell surface-associated bacterial aggregates, which get engulfed by EC membranes in an F-actin-dependent manner, eventually resulting in their complete internalization. Here, we report that among the VirB/VirD4-translocated effector proteins BepA-BepG only BepG is required for triggering invasome-mediated internalization. Expression of BepG in the Bep-deficient $\Delta bepA-G$ mutant restored invasome-mediated internalization. Likewise, ectopic expression of BepG in ECs also restored invasome-mediated internalization of the $\Delta bepA-G$ mutant, while no discernable cytoskeletal rearrangements were triggered in uninfected cells. Rather, BepG inhibited endocytic uptake of *B. henselae* into *Bartonella*-containing vacuoles and other endocytic processes, that is, invasin-mediated uptake of *Yersinia enterocolitica* and uptake of inert microspheres. BepG thus triggers invasome-mediated internalization primarily by inhibiting bacterial endocytosis. Bacteria accumulating on the cell surface then induce locally the F-actin rearrangements characteristic for the invasome. These cytoskeletal changes encompass both the rearrangement of pre-existing F-actin

fibres and the *de novo* polymerization of cortical F-actin in the periphery of the invasome by Rac1/Scar1/WAVE- and Cdc42/WASP-dependent pathways that involve the recruitment of the Arp2/3 complex.

Introduction

Bartonella henselae (*Bh*) is a worldwide distributed zoonotic pathogen. This facultative intracellular bacterium causes long-lasting intraerythrocytic infections in the cat reservoir host. Transmission from cat to cat occurs predominantly via infected cat fleas, while transmission to the incidental human host typically results from cat scratches or bites (Dehio, 2004). Human infection by *Bh* can result in a wide range of clinical symptoms. In immunocompetent patients, the most frequent manifestation is cat-scratch disease, a typically self-limiting disease resulting in local swelling of lymph nodes and fever (Florin *et al.*, 2008). Immuno-compromised patients commonly develop bacillary angiomatosis-peliosis, a clinical condition characterized by the formation of vasoproliferative lesions in skin and liver. These tumour-like lesions arise from bacterial colonization of the vasculature, which results in the activation, migration and proliferation of vascular endothelial cells (ECs) (Dehio, 2005).

Vascular colonization by *Bh in vivo* can be mimicked *in vitro* by infection of cultured ECs, that is, primary human umbilical vein endothelial cells (HUVECs) or the Ea.hy926 cell line originating from the fusion of HUVECs with the lung carcinoma cell line A549 (Dehio *et al.*, 1997; Dehio, 2005; Kyme *et al.*, 2005; Scheidegger *et al.*, 2009). Many of the distinct cell biological outcomes of EC infection by *Bh* are dependent on a functional VirB/VirD4 type IV secretion (T4S) system (Schmid *et al.*, 2004). This macromolecular transporter ancestrally related to bacterial conjugation systems (Saenz *et al.*, 2007; Dehio, 2008; Pulliainen and Dehio, 2009) is known to translocate seven effector proteins, BepA to BepG (*Bartonella*-translocated effector proteins), into infected ECs. The Beps display a modular domain structure, which is characterized by putative N-terminal effector domains and a C-terminal export

Received 24 November, 2008; revised 17 February, 2009; accepted 18 February, 2009. *For correspondence. E-mail christoph.dehio@unibas.ch; Tel. (+41) 61 267 2140; Fax (+41) 61 267 2118.

signal. This signal for T4S-dependent protein translocation is bi-partite, comprising at least one copy of the approximately 140-aa-large BID domain (*Bartonella* Intracellular Delivery) and an adjacent non-conserved C-terminal tail sequence carrying a net positive charge (Schulein *et al.*, 2005). BepA to BepG mediate all known VirB/VirD4-dependent cellular phenotypes of ECs, namely: (i) activation of the transcription factor NF- κ B and stimulation of a pro-inflammatory response, (ii) protection from apoptosis and (iii) cell invasion by a unique cellular structure termed the invasome (Schmid *et al.*, 2004; 2006; Schulein *et al.*, 2005).

Invasome-mediated internalization is a multi-step process, which is characterized by an initial accumulation and aggregation of bacteria on the cell surface, followed by the successive engulfment of the bacterial aggregate by EC-derived membrane protrusions, which eventually result in its complete internalization. The membrane protrusions engulfing the bacterial aggregate are enriched for cortical F-actin, intercellular adhesion molecule-1 and phosphotyrosine. Underneath the engulfed bacterial aggregate, the invasome characteristically comprises stress fibres that are wound up to a dense ring-shaped F-actin structure. Invasome-mediated internalization of *Bh* by ECs occurs with slow kinetics and requires at least 16 h for completion in individual ECs (Dehio *et al.*, 1997). With a much faster kinetics, lasting minutes to hours, *Bh* can alternatively enter ECs as individual bacteria or small aggregates by a VirB/VirD4-independent endocytic route resembling phagocytosis. The nature of the *Bartonella*-containing vacuoles (BCVs) formed by this process in a perinuclear localization is not well defined. BCVs display delayed lysosomal fusion as up to 24 h post infection they are not acidified and lack typical endocytic markers such as LAMP1 (Kyme *et al.*, 2005). BCVs harbouring multiple bacteria can be observed, but it remains unclear whether these originate from the internalization of small bacterial aggregates into BCVs, intracellular replication or fusion of multiple BCVs harbouring single bacteria (Dehio *et al.*, 1997).

In the present study, we have investigated the molecular and cellular basis of invasome-mediated internalization of *Bh* into ECs. Based on the expression of individual Bep effectors in the effector-deficient mutant Δ bepA-G, which is impaired for invasome formation, we genetically defined BepG as the VirB/VirD4 effector triggering invasome-mediated internalization of bacterial aggregates. Moreover, we show that invasome formation is associated with an inhibition of the endocytic uptake of single *Bh* into BCVs. Finally, we show that F-actin polymerization associated with invasome formation occurs in a Rac1/Scar/WAVE- and Cdc42/WASP-dependent manner and involves the recruitment of the Arp2/3 complex.

Results

VirB/VirD4 effector proteins trigger invasome-mediated internalization of bacterial aggregates and interfere with bacterial uptake into BCVs

Bh ATCC49882^T wild-type bacteria were previously shown to enter HUVECs predominately as large bacterial aggregates by the VirB/VirD4-dependent process of invasome-mediated internalization (Dehio *et al.*, 1997; Schmid *et al.*, 2004; Schulein *et al.*, 2005). With an multiplicity of infection (moi) = 100, > 80% of HUVECs form at least one invasome structure specified by confocal laser scanning microscopy as characteristic F-actin rearrangement in association with the bacterial aggregate (Fig. 1A and C). Under these conditions, only few bacteria enter individually or as small aggregates via a VirB/VirD4-independent endocytic process resulting in the formation of perinuclear-localizing BCVs (Fig. 1A and D). As reported previously (Schulein *et al.*, 2005), deletion of the genes *bepA-bepG* encoding all seven VirB/VirD4-translocated effector proteins (Δ bepA-G) resulted in the complete abrogation of invasome-mediated uptake (Fig. 1B and C). Instead, uptake of this mutant into HUVECs is rerouted to VirB/VirD4-independent endocytosis, resulting in a vastly increased number of BCVs (Fig. 1B and D).

The endocytic process resulting in the formation of BCVs is not yet well characterized (Dehio *et al.*, 1997; Kyme *et al.*, 2005). However, acquisition of the lysosomal marker protein LAMP-1 within 48 h of infection indicates that BCVs represent fusigenic compartments of the endosomal-lysosomal pathway in HUVECs (Fig. S1), even so this fusion event may occur with delay (Kyme *et al.*, 2005). In the same period, the membranes engulfing the bacterial aggregate of the invasome structure do not acquire any detectable LAMP-1 staining, indicating that they constitute a unique membrane compartment that is strictly separated from the endosomal-lysosomal network (Fig. S1).

*BepG translocation triggers invasome-mediated internalization of *Bh* into ECs*

To identify the VirB/VirD4-translocated effector(s) that trigger invasome-mediated internalization, we individually expressed FLAG-epitope-tagged versions of BepA to BepG *in trans* in the effector-deficient mutant Δ bepA-G and assayed for phenotypic complementation. By Western blot analysis using anti-FLAG antibodies, all strains used in this analysis were found to stably express the respective Flag-tagged Bep effector (Fig. 2B). We tested the capacity of these strains to promote the characteristic F-actin rearrangements of the invasome that colocalize with bacterial aggregates, and to interfere with

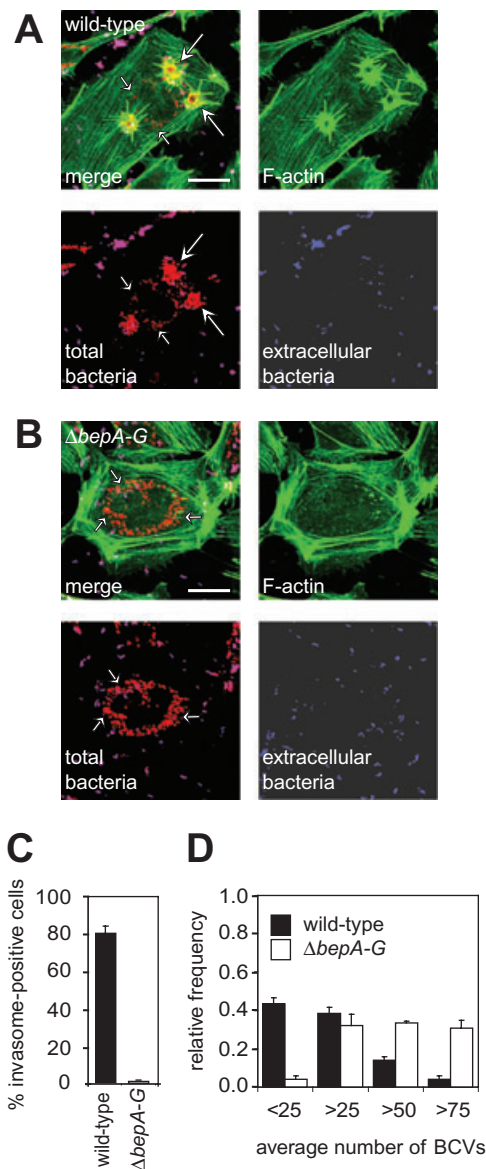


Fig. 1. Invasome-mediated uptake of *Bh* aggregates into ECs interferes with endocytic uptake of individual bacteria into BCVs. HUVECs were infected for 48 h with an moi = 100 of *Bh* (A) wild-type or (B) the effector-deficient mutant $\Delta bepA-G$, followed by fixation, immunocytochemical staining and confocal laser scanning microscopy. Extracellular bacteria are represented in purple, intracellular bacteria in red and the F-actin cytoskeleton in green. The scale bar corresponds to 20 μ m. Large arrows point towards the invasome structure, small arrows point towards perinuclear BCVs. Quantification of (C) formed invasomes ($n = 50$ cells) and (D) BCVs ($n = 50$ cells). Results of three independent experiments \pm standard deviation are depicted.

the formation of BCVs (Fig. 2A and B) by means of immunocytochemical staining and confocal laser scanning microscopy. Strikingly, the expression of BepG alone was sufficient to trigger invasome-mediated internalization and to reduce BCV formation. In contrast, none of the other effectors, that is, BepA to BepF, displayed this wild

type-like phenotype. However, the strain expressing BepF ($\Delta bepA-G/pbepF$) fostered the formation of small F-actin foci at the cell cortex, but these structures were not reminiscent of invasomes. Single bacteria or bacterial aggregates adhering to the cell surface were observed with all strains, but only the BepG-expressing strain ($\Delta bepA-G/pbepG$) promoted the complete internalization of these bacterial aggregates in concert with rearrangement of the underlying F-actin (Fig. 2A and B). A low number of BCVs comparable to infection with wild-type bacteria was observed exclusively for the BepG-expressing strain $\Delta bepA-G/pbepG$ (Fig. 2A and B). Thus, it appears that among the seven Bep effectors encoded by *Bh* only BepG is required to promote the cellular changes characteristic for invasome-mediated internalization.

Analysis of the BepG protein sequence revealed a modular architecture with four individual BID domains and a series of shorter repeat sequences (Fig. S2A). A BlastP query of full-length BepG against the nr database of non-redundant protein sequences did not identify significant hits except for BID domains of other Bep effectors. Although all seven Bep proteins of *Bh* are considered to represent effector proteins translocated into ECs in a VirB/VirD4-dependent manner (Dehio, 2008), this was experimentally shown so far only for BepA, BepC, BepD and BepF (Schulein *et al.*, 2005; Schmid *et al.*, 2006). To test whether BepG is as well a canonical VirB/VirD4 effector, we fused amino acids 715–1009 corresponding to the most C-terminal BID domain and the adjacent C-terminal tail sequence to the Cre recombinase and tested this reporter construct in the previously described Cre recombinase assay for translocation (CRAFT) (Schulein *et al.*, 2005). By this approach, we were able to demonstrate that BepG is a *bona fide* VirB/VirD4 effector protein of *Bh* as postulated earlier (Fig. S2B and C).

Bh wild-type and the BepG-expressing strain $\Delta bepA-G/pbepG$ induce similar invasome structures

Invasome structures elicited by *Bh* wild type and the effector-less mutant expressing BepG ($\Delta bepA-G/pbepG$) were found to be very similar in appearance (Fig. 3A). Both strains were shown to induce extensive rearrangements of the F-actin cytoskeleton in association with bacterial aggregates, giving rise to the described basal ring-like structures (Fig. 3A). The $\Delta bepA-G/pbepG$ strain restored the ability to induce at least one invasome per EC in approximately 50% of cells, compared with > 85% cells for the wild-type strain (Fig. 3B), indicating that BepG as sole effector could restore invasome formation almost to wild-type levels. Furthermore, inhibition of invasome formation by the F-actin-destabilizing drug cytochalasin D occurred for both strains with a similar dose dependency (Fig. 3B).

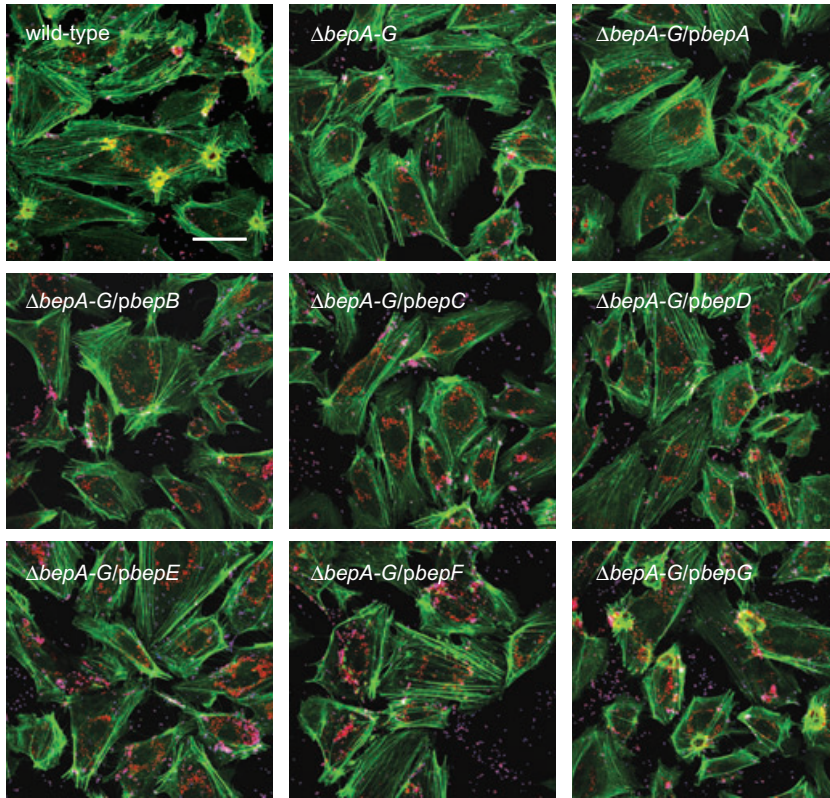
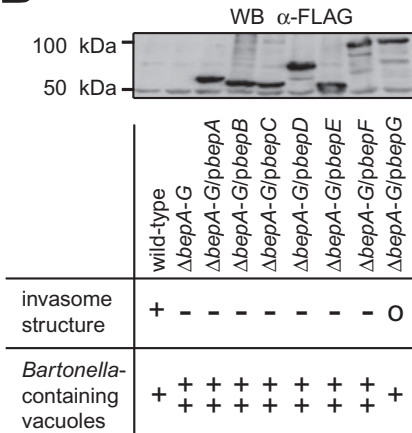
A

Fig. 2. Expression of BepG in an effector-deficient mutant background of *Bh* is sufficient to trigger invasome-mediated uptake by EC.

A. HUVECs were infected for 48 h with an moi = 100 of *Bh* wild type, the effector-deficient mutant $\Delta b e p A - G$ or isogenic strains expressing individual Bep proteins ($\Delta b e p A - G / p b e p A$ to $\Delta b e p A - G / p b e p G$), followed by fixation, immunocytochemical staining and confocal laser scanning microscopy. Extracellular bacteria are represented in purple, intracellular bacteria in red and the F-actin cytoskeleton in green. The scale bar corresponds to 50 μm .

B. Semi-quantitative evaluation of the abundance of invasome structures and BCVs. ++ = higher abundance than wild type; + = abundance like wild type; o = abundance lower than wild type; - = absent. The upper panel shows an immunoblot analysis of the steady-state protein levels of Flag-tagged Beps of bacterial cultures used for infection of HUVECs.

B

BepG-triggered invasome-mediated internalization of bacterial aggregates into ECs inhibits endocytic uptake of individual bacteria into BCVs

Next, we used confocal laser scanning microscopy to quantify the endocytic uptake of *Bh* into BCVs in HUVECs in dependency of BepG translocation (Fig. 3C). To better understand the influence of invasome formation on endocytic uptake into BCVs, we categorized cells

infected with wild-type bacteria or the BepG-expressing strain $\Delta b e p A - G / p b e p G$ with respect to the presence or absence of invasome structures, while cells infected with the effector-deficient strain $\Delta b e p A - G$ displayed a uniformly invasome-negative phenotype. The invasome-negative populations of cells infected either with wild type (< 15%), $\Delta b e p A - G$ (100%) or $\Delta b e p A - G / p b e p G$ (approximately 50%) displayed a high number of BCVs (Fig. 3C). In contrast, the invasome-positive populations

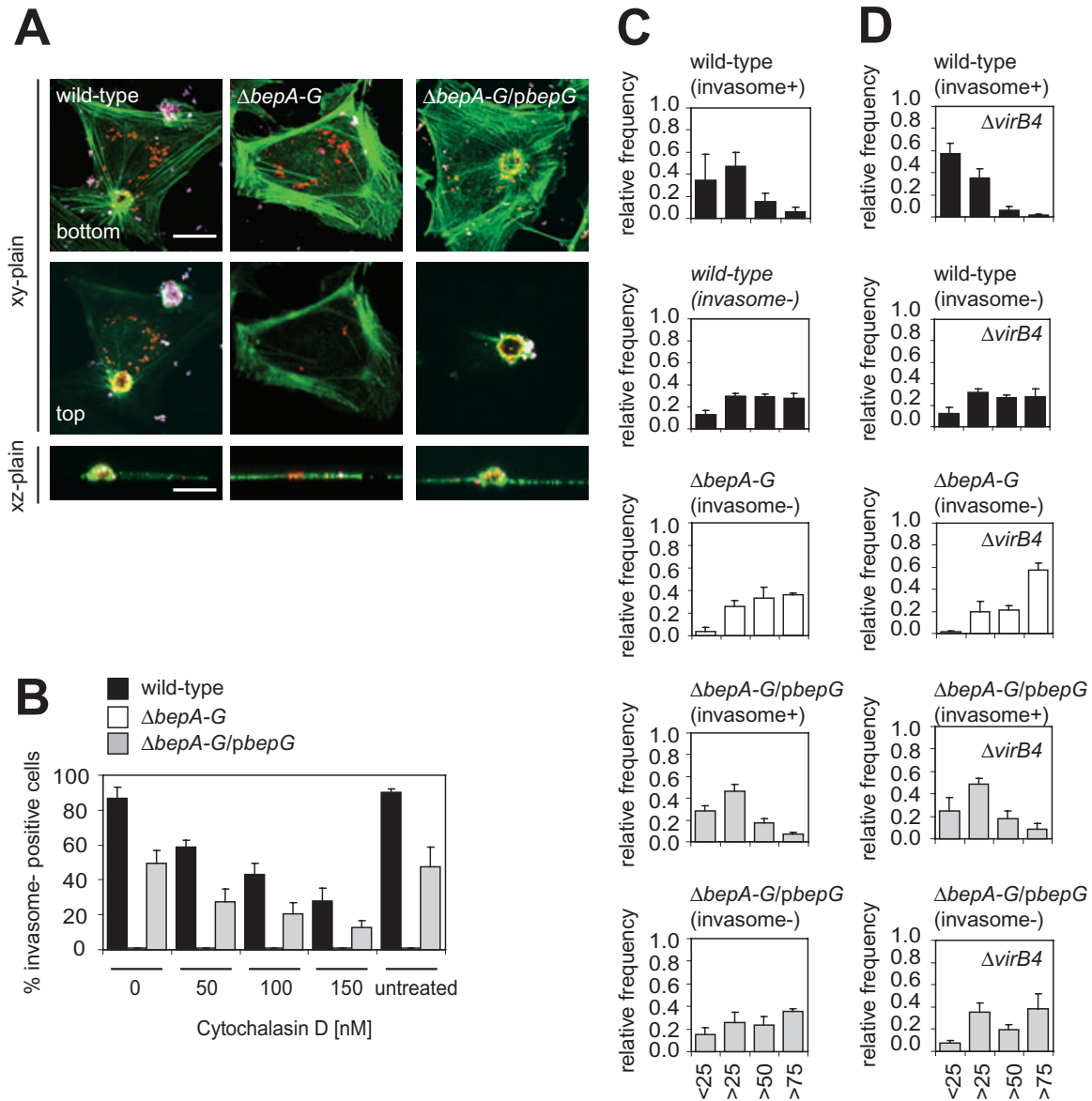


Fig. 3. Invasomes triggered by *Bh* wild-type and a strain expressing BepG in an effector-deficient mutant background display similar actin-dependent cytoskeletal rearrangements.

A. HUVECs were infected for 48 h with an moi = 100 of *Bh* wild type, the effector-deficient mutant $\Delta b e p A - G$ or the isogenic BepG-expressing derivative $\Delta b e p A - G / p b e p G$, followed by fixation, immunocytochemical staining and confocal laser scanning microscopy. Extracellular bacteria are represented in purple, intracellular bacteria in red and the F-actin cytoskeleton in green. Representative images of invasome formation acquired in xy-plains at bottom and top levels and in an xz-plain on the single cell level. The scale bar corresponds to 20 μ m.

B. HUVECs were infected for 48 h with an moi = 100 of *Bh* wild type, the effector-deficient mutant strain ($\Delta b e p A - G$) or the BepG-expressing derivative ($\Delta b e p A - G / p b e p G$) in the presence of different concentration of cytochalasin D. Cells were fixed, stained and analysed for the presence of invasome structures by epifluorescence microscopy. Frequencies of invasome formation ($n = 50$ cells) illustrated as bar graphs. Results of three independent experiments \pm standard deviation are depicted.

C. HUVECs were infected for 48 h with the indicated strains (moi = 100), followed by fixation, immunocytochemical staining and confocal laser scanning microscopy. BCVs were then quantified separately for cells that either formed invasomes (invasome+) or did not form invasomes (invasome-) ($n = 50$ cells). Results of three independent experiments \pm standard deviation are depicted.

D. Similarly, HUVECs were preinfected for 12 h with the indicated strain (moi = 100), followed by super-infection with GFP-expressing strain $\Delta v i r B 4 / p C D 3 5 4$ (moi = 100), followed by 36 h incubation before fixation, immunocytochemical staining and confocal laser scanning microscopy. BCVs were then quantified separately for cells that formed invasomes (invasome+) or did not form invasomes (invasome-) ($n = 50$ cells). Results of three independent experiments \pm standard deviation are depicted.

of cells infected either with wild type (> 85%) or $\Delta bepA-G/pbepG$ (approximately 50%) displayed a strongly reduced number of BCVs, indicating that BepG-triggered invasome-mediated internalization interferes with endocytic uptake into BCVs (Fig. 3C). To rule out the possibility that the number of bacteria used in this assays is too low for allowing both entry modes to occur in parallel, we set up a series of super-infection experiments (Fig. 3D). For this purpose, we infected Ea.hy926 cells for 12 h with the same set of strains as before. Then, cells were super-infected for an additional 36 h with the isogenic VirB/VirD4-defective $\Delta virB4$ strain, which by itself does not induce invasome formation, but uniformly enters ECs by the endocytic route resulting in BCV formation (Schmid *et al.*, 2004). To allow discrimination of this entry reporter strain used for super-infection from the strains used for initial infection, we introduced plasmid pCD354 into the $\Delta virB4$ mutant resulting in constitutive GFP expression (Dehio *et al.*, 1998). Using confocal laser scanning microscopy, we were able to demonstrate that BepG-dependent, invasome-mediated internalization not only interferes with, but actively inhibits the endocytic process leading to BCV formation (Fig. 3D). Interestingly, the reporter strain $\Delta virB4/pCD354$ was not only internalized less efficiently into BCVs in a BepG-dependent and invasome-mediated manner, but was even redirected into the invasome structure triggered by these strains (data not shown).

Ectopic expression of BepG in ECs restores invasome formation by the effector-deficient strain ($\Delta bepA-G$) and inhibits bacterial uptake into BCVs

Next, we tested BepG for its capacity to promote cytoskeletal rearrangements by means of cotransfection of Ea.hy926 cells with eukaryotic expression plasmids encoding FLAG-epitope-tagged BepG (pFLAG-BepG) and eGFP (pWay19), the latter allowing the identification of transfected cells based on GFP-fluorescence. Surprisingly, no apparent changes on the integrity of the F-actin cytoskeleton were observed, in particular no invasome-like structures were detected (Fig. 4A). However, upon infection with the effector-deficient strain $\Delta bepA-G$, invasome structures were detected at a frequency of approximately 30% per transfected cell (Fig. 4B). This finding indicated that ectopically expressed BepG promotes invasome-mediated uptake of cell surface-associated aggregates of a *Bh* mutant impaired in triggering invasome formation. To test whether BepG inhibits endocytic uptake of *Bh* into BCVs in an invasome-dependent manner, the number of BCVs was determined. An inhibition of endocytic uptake into BCVs occurred indeed in a BepG-dependent manner in cells displaying concomitant invasome structures (Fig. 4C).

Taken together, the ectopic expression of BepG restores the invasome-mediated uptake of a *Bh* mutants that by itself is incapable of triggering invasome formation. This finding raises the question whether the local F-actin rearrangements associated with invasome formation are a direct consequence of the BepG-dependent inhibition of endocytosis, or rather represent an indirect cellular response to the accumulation of cell surface-associated bacteria.

BepG inhibits invasin-mediated uptake of Yersinia enterocolitica and the internalization of inert microspheres

Adhesion to and invasion of non-phagocytic host cells by the bacterial pathogen *Y. enterocolitica* is a well-defined process employing the $\beta 1$ -integrin-binding bacterial surface protein invasin (Dersch and Isberg, 1999). During zipper-mediated internalization, the membrane of the host cells wraps up intimately around the adhering bacterium leading to subsequent internalization of the bacterium in conjunction with transient actin cytoskeletal rearrangements (Young *et al.*, 1992). To better understand the mechanism of BepG inhibition of endocytosis, we tested whether internalization of *Y. enterocolitica* expressing invasion (inv+) can be inhibited in a BepG-dependent manner. For this purpose, we preinfected Ea.hy926 cells with different isogenic strains of *Bh* for 48 h, followed by a super-infection with *Y. enterocolitica* (inv+) for 90 min. To assess the frequency of invasion of *Y. enterocolitica* (inv+), extracellular bacteria were killed by gentamicin treatment, host cells were lysed, viable intracellular bacteria were plated in serial dilutions and the number of colony forming units was determined after incubation. Thus, we were able to show that internalization of *Y. enterocolitica* (inv+) by ECs is inhibited in a BepG-dependent manner (Fig. 5A). In cases of preinfection with *Bh* wild type and the BepG-expressing strain $\Delta bepA-G/pbepG$, the number of intracellular *Y. enterocolitica* (inv+) was significantly reduced, whereas preinfection with the effector-less mutant $\Delta bepA-G$ did not affect invasion of *Y. enterocolitica* (inv+) (Fig. 5A). Non-invasive *Y. enterocolitica* (inv-) served as negative control and did not invade host cells at significant levels regardless of the *Bh* strain used for preinfection (Fig. 5A).

To confirm these findings by an independent experimental approach, we cotransfected HeLa cells with pWay19 (encoding eGFP) and with either pFLAG-BepG or the control vector pFLAG-CMV2 for 48 h and infected these transfected cell populations either with invading (inv+) or non-invading (inv-) strains of *Y. enterocolitica* for 90 min. After fixation and staining for intra- and extracellular bacteria, invasion of *Y. enterocolitica* was assessed by counting intracellular bacteria in GFP-positive cells by

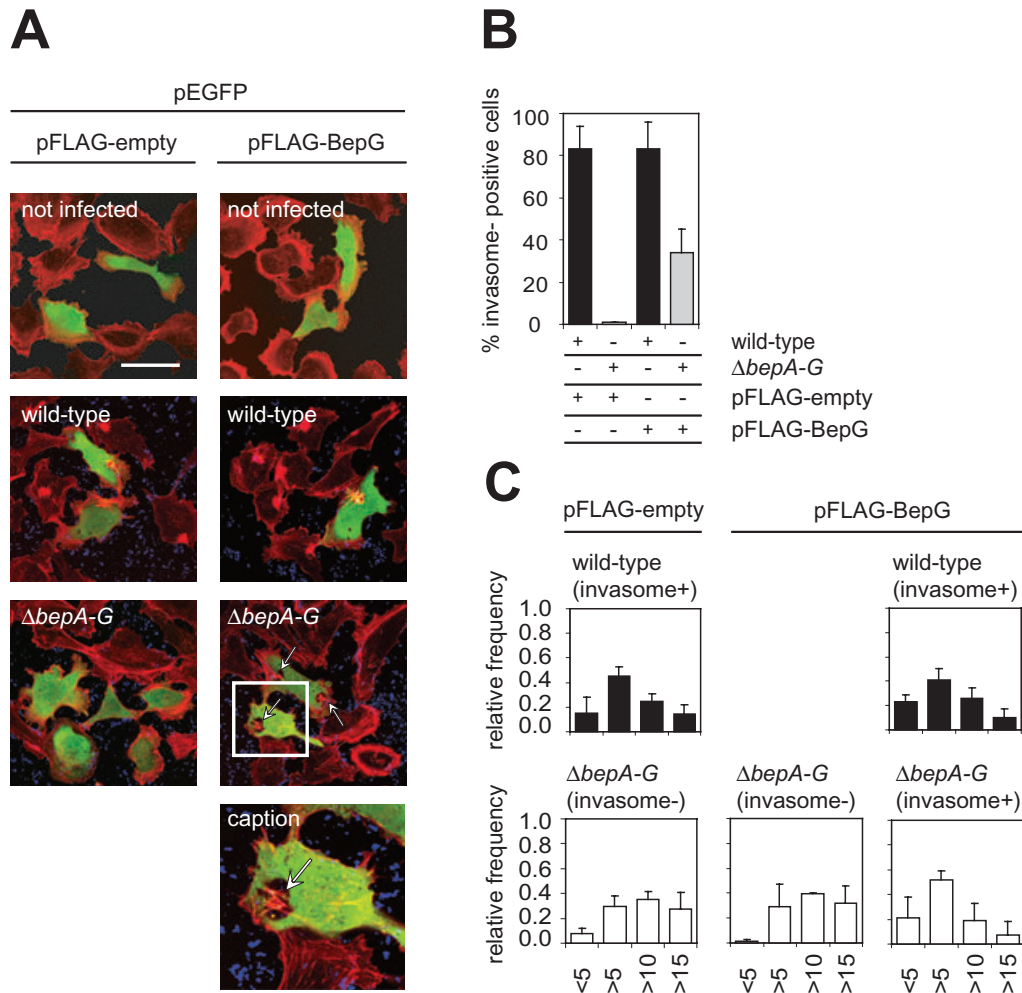
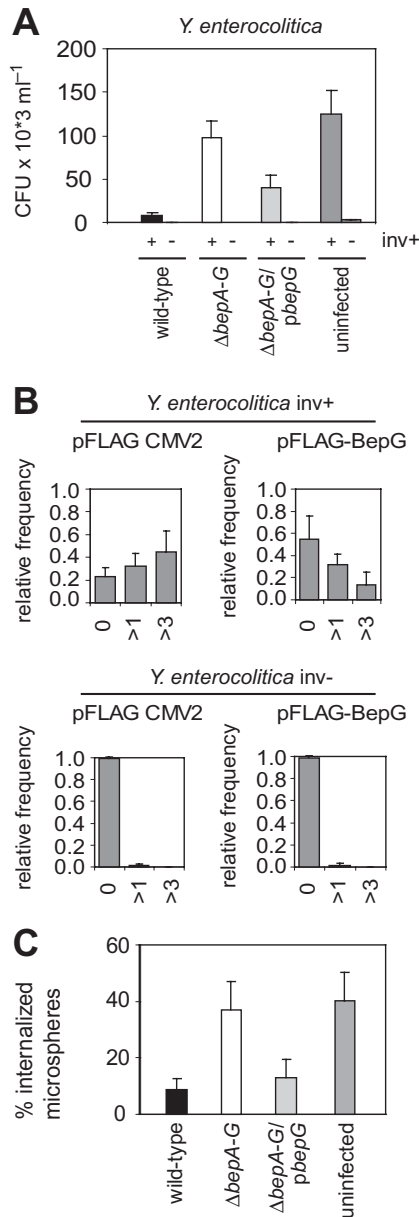


Fig. 4. Ectopic expression of BepG in ECs is sufficient to trigger invasome-mediated uptake of the effector-deficient mutant $\Delta bepA-G$. Ea.hy926 cells were cotransfected with the GFP expression plasmid pWay19 (to identify transfected cells) and either the BepG-expression plasmid pFLAG-BepG, or the control vector pFLAG-empty. Six hours later cells were infected for 48 h with an moi = 100 of *Bh* wild-type or the effector-deficient mutant $\Delta bepA-G$, or left uninfected (control), followed by fixation, cytochemical staining of F-actin and confocal laser scanning microscopy.

A. Representative confocal images. The GFP signal of transfected cells is shown in green, and F-actin in red. The scale bar corresponds to 50 μ m. Quantification of (B) invasome formation ($n = 50$ cells) and (C) BCVs ($n = 50$ cells) with respect to ectopic expression to BepG. BCVs were quantified separately for cells that formed invasomes (invasome+) or did not form invasomes (invasome-) ($n = 50$ cells). Results of three independent experiments \pm standard deviation are depicted.

means of confocal laser scanning microscopy. The invasive *Y. enterocolitica* strain (inv+) was found to be less frequent in an intracellular location in cells transfected with pFLAG-BepG than cells transfected with the control plasmid pFLAG-CMV2. The non-invasive (inv-) strain used as negative control remained mostly extracellular (Fig. 5B). Taken together, we conclude that the presence of BepG in the host cell cytoplasm is sufficient to block zipper-mediated internalization of individual *Y. enterocolitica* bacteria (Fig. 5B). Moreover, ectopic expression of BepG did not trigger discernable actin cytoskeletal rearrangements. The BepG-dependent, invasome-mediated internalization of *Bh* thus appears to be an indirect consequence of the inhibition of endocytic uptake.

To further corroborate these findings, we analysed whether BepG may also inhibit other uptake processes in ECs. ECs were shown to internalize inert microspheres efficiently (Yao *et al.*, 1995). Ea.hy926 cells were thus preinfected for 24 h with *Bh* wild type, the effector-deficient mutant $\Delta bepA-G$ and its BepG-expressing derivative $\Delta bepA-G/pbepG$, followed by antibiotic killing of bacteria and incubation of cells with BSA-saturated carboxylate-modified polystyrene microspheres for an additional 24 h. Confocal laser scanning microscopy analysis of fixed and stained samples revealed that infection with the effector-deficient mutant $\Delta bepA-G$ did not affect microsphere uptake, while both the BepG-expressing derivative $\Delta bepA-G/pbepG$ and *Bh* wild type



efficiently inhibited microsphere uptake (Fig. 5C). BepG thus appears to inhibit various uptake processes in ECs.

Taken together, the engulfment of cell surface-associated bacterial aggregates by membrane protrusions formed in association with major rearrangements of the cortical F-actin might be regarded as cellular response to the accumulation of extracellular bacteria on the cell surface that occur in consequence to the BepG-mediated inhibition of endocytic uptake of *Bh* into BCVs. This cellular response leading to invasome formation may engage locally a yet unknown and possibly VirB/VirD4-independent bacterial factor.

Fig. 5. BepG inhibits invasive-mediated uptake of *Yersinia enterocolitica*.

A. EA.hy926 cells were preinfected with an moi = 200 of *Bh* wild type, the effector-deficient mutant $\Delta b e p A - G$ or the isogenic BepG-expressing derivative $\Delta b e p A - G / p b e p G$, or left uninfected (control) for 48 h. Subsequently, the infected cell monolayers were super-infected with *Y. enterocolitica* strains (pYV-) expressing invasion (inv+) or a respective mutant (inv-) for 90 min with an moi = 10. After fixation, immunocytochemical staining and confocal laser scanning microscopy, the number of intracellular *Y. enterocolitica* was quantified. Results of three independent experiments \pm standard deviation are depicted.

B. Ea.hy926 cells were cotransfected with the GFP expression plasmid pWay19 and either the BepG-expression plasmid pFLAG-BepG or the control vector pFLAG-empty. Six hours later cells were washed and incubated for an additional 48 h before super-infecting the samples with *Y. enterocolitica* strains (pYV-) expressing invasion (inv+) or a respective mutant (inv-) for 90 min with an moi = 10. After fixation, immunocytochemical staining and confocal laser scanning microscopy, the number of intracellular *Y. enterocolitica* was quantified. Results of three independent experiments \pm standard deviation are depicted.

C. EA.hy926 cells were preinfected with an moi = 100 of *Bh* wild type, the effector-deficient mutant $\Delta b e p A - G$ or the isogenic BepG-expressing derivative $\Delta b e p A - G / p b e p G$, or left uninfected (control) for 24 h. Thereafter, bacteria were killed by antibiotic treatment and fluorescent microspheres were added to the infected cells for another 24 h. After fixation, staining and confocal laser scanning microscopy the number of intracellular versus total microspheres was quantified in at least nine randomly chosen microscopic fields. Results of three independent experiments \pm standard deviation are depicted.

BepG colocalizes to components of the F-actin cytoskeleton

To analyse the subcellular localization of BepG within ECs, we transfected Ea.hy926 cells with an eukaryotic expression plasmid encoding an eGFP-BepG fusion protein (peGFP-BepG). Co-staining of F-actin by tetramethyl rhodamine isothiocyanate (TRITC)-phalloidine and inspection by confocal laser scanning microscopy unexpectedly revealed a colocalization of eGFP-BepG with distinct components of the actin cytoskeleton. In detail, colocalization was observed with: (i) F-actin stress fibres, (ii) F-actin clusters in filopodial cell extensions and (iii) patches of cortical F-actin underneath the apical plasma membrane (Fig. 6B). eGFP serving as control displayed a homogenous distribution in the cytoplasm of transfected cells (Fig. 6A). Next, we assessed the subcellular location of eGFP-BepG upon infection. For this purpose, Ea.hy926 cells transfected with the same vectors as before were infected with *Bh* wild type and the pattern of eGFP-BepG localization was analysed by confocal laser scanning microscopy. We observed that F-actin structures localizing to its periphery of the invasome were highly enriched for eGFP-BepG (Fig. 6D), whereas canonical eGFP (Fig. 6C) did not display increased straining of these structures.

Taken together, the ectopically expressed GFP-BepG fusion colocalizes with F-actin structures, but does not appear to trigger F-actin rearrangements by itself.

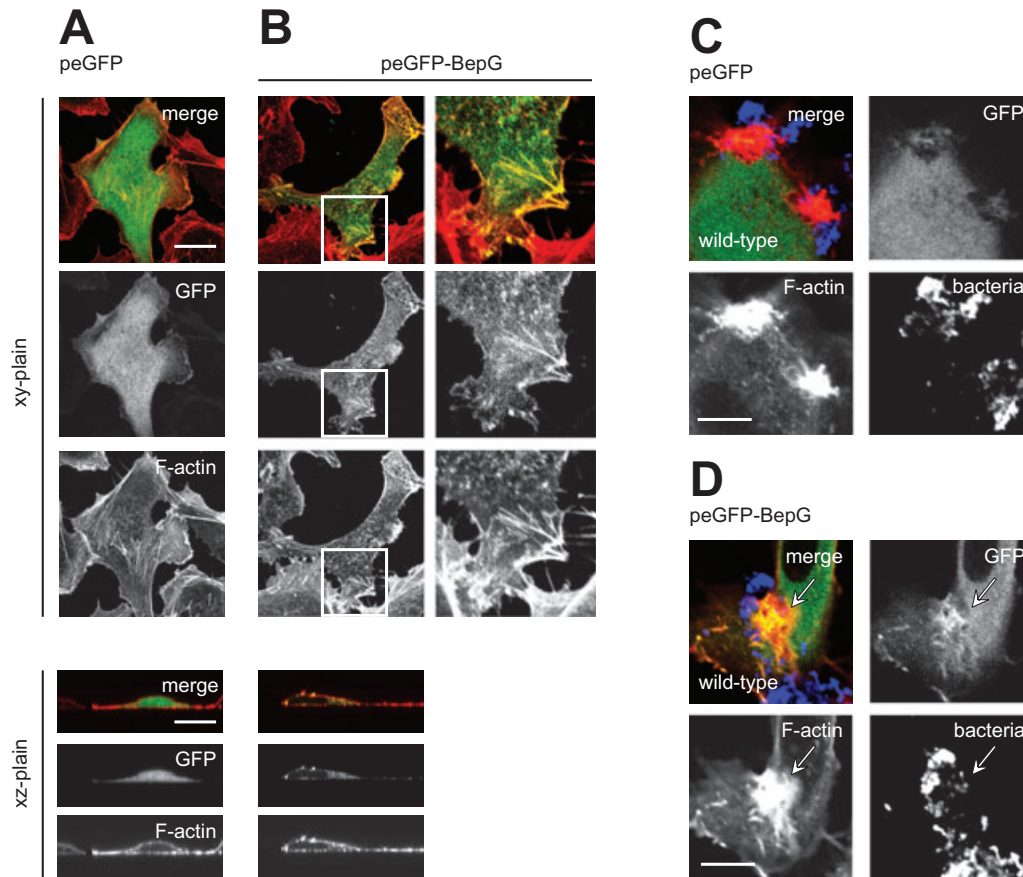


Fig. 6. Ectopic expression of an eGFP–BepG fusion in ECs results in colocalization of the fusion protein with components of the actin cytoskeleton. Ea.hy926 cells transfected with plasmids encoding either (A) eGFP alone (pWAY21) or (B) an N-terminal fusion of eGFP to BepG (eGFP–BepG). Six hours after transfection cells were washed and incubated for additional 48 h, followed by fixation, staining for F-actin and analysis by confocal laser scanning microscopy in the xy-plane or xz-plane (in merged pictures GFP signal is shown in green, and F-actin staining in red). Colocalization of the eGFP–BepG fusion protein is shown for stress fibres (B, boxed close-up) or cortical F-actin (B, xz-plane). The scale bar corresponds to 20 μm (C and D). Ea.hy 926 cells were transfected with plasmids encoding (C) eGFP alone (pWAY21) or (D) the eGFP–BepG fusion (peGFP–BepG). After 6 h cells were washed and infected with an moi = 100 of *Bh* wild type for 48 h. Thereafter, cells were fixed, stained for F-actin and bacteria and analysed by confocal laser scanning microscopy in the xy-plane (in merged pictures GFP signal is shown in green, F-actin staining in red, and bacteria stained in blue). The scale bar corresponds to 10 μm .

Invasome formation is dependent on the small GTPases Rac1 and Cdc42, which are recruited to the sites of invasome formation

To characterize the cell biological basis of invasome formation, we next analysed which host cell signalling proteins control the dynamics of the F-actin cytoskeleton in the course of invasome formation. RhoA, Rac1 and Cdc42 are key regulators of the actin cytoskeleton, triggering the formation of stress fibres anchored by focal adhesions, lamellipodia at the leading edge of cells along with membrane ruffles and filopodial cell extensions respectively (Jaffe and Hall, 2005). These Rho-family GTPases have also been shown to be involved in the cellular invasion process of several bacterial pathogens (Finlay, 2005). To assess their putative involvement in invasome formation, we transfected Ea.hy926 cells with

eGFP (as transfection marker) together with dominant-negative versions of RhoA (N19), Rac1 (N17) and Cdc42 (N17). Six hours later, cells were infected for 48 h with either *Bh* wild-type strain, the effector-deficient mutant $\Delta\text{bepA-G}$ or its BepG-expressing derivative $\Delta\text{bepA-G}/\text{pbepG}$. Finally, the frequency of invasome formation was determined in GFP-positive cells (Fig. 7A). Invasome formation decreased modestly (> 25%) in ECs transfected with dominant-negative Cdc42, and strongly (> 50%) in ECs transfected with dominant-negative Rac1. No significant change in frequency could be observed in ECs transfected with dominant-negative RhoA compared with empty vector or non-transfected ECs (Fig. 7A).

Sphingosine-1-phosphate is a potent activator of Rac1, which induces the formation of lamellipodia and membrane ruffles. Badykinin is an activator of Cdc42, which induces filopodial cell structures. In a control experiment,

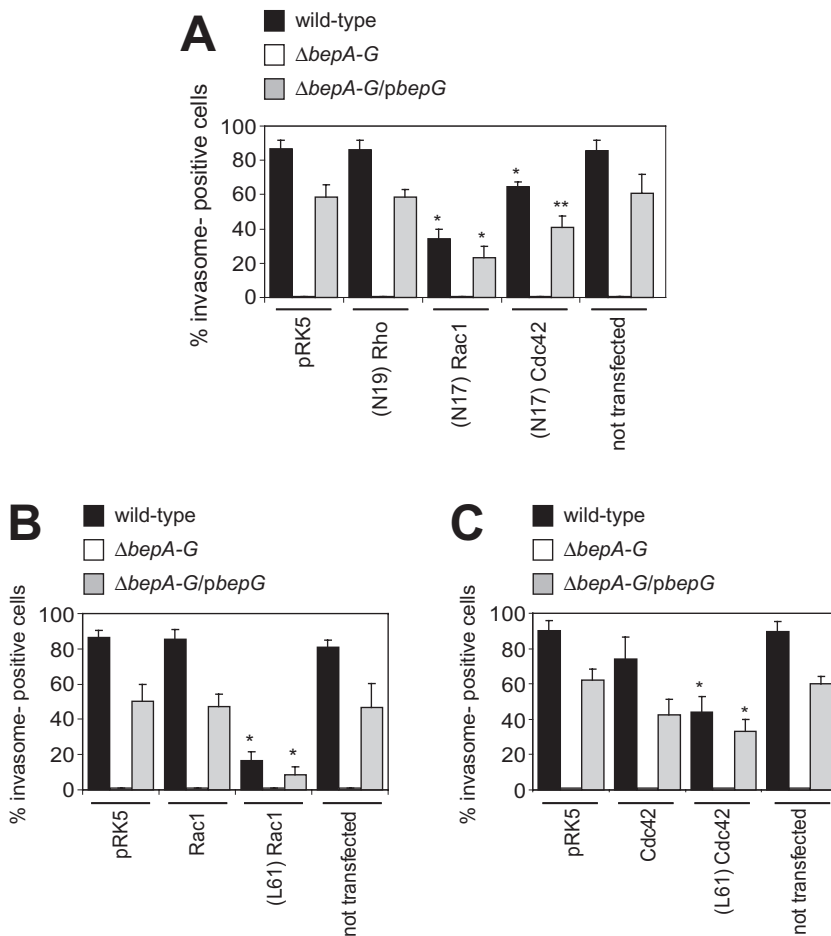


Fig. 7. Invasome formation is dependent on Rac1 and Cdc42. Ea.hy926 cells were cotransfected with a plasmid encoding eGFP (pWay19) and a second plasmid encoding (A) dominant-negative RhoA [(N19) Rho], dominant-negative Rac1 [(N17) Rac1] or dominant-negative Cdc42 [(N17) Cdc42], (B) Rac1 (wild type) or constitutively active Rac1 [(L61)Rac1] or (C) Cdc42 (wild type) and constitutively active Cdc42 [(L61)Cdc42]. In all experiments, non-transfected cells or cells transfected with the empty expression plasmid pRK5 served as controls. Six hours post transfection, cells were washed and infected with *Bh* wild type, the effector-deficient mutant $\Delta bepA-G$ or the isogenic BepG-expressing derivative $\Delta bepA-G/pbepG$ (moi = 100) for 48 h. The frequency of invasome formation was determined in cells expressing visible amounts of eGFP. Results of four independent experiments \pm standard deviation are depicted ($n = 50$).

sphingosine-1-phosphate and bradykinin were used to test for suppression of these structures in Ea.hy926 cells cotransfected with either the dominant-negative versions of Rac1 or Cdc42 together with eGFP as a reporter (Fig. S3A and B). In the case of Rac1 (N17) the formation of membrane ruffles and lamellipodia was indeed strongly reduced in transfected cells, while these structures were formed with normal frequencies in non-transfected cells (Fig. S3A). In the case of Cdc42 (N17) filopodial structures in transfected cells were reduced respectively (Fig. S3B). Thus, in the EC system used in this study, endogenous Rac1 and Cdc42 activity can be effectively suppressed by overexpression of the corresponding dominant-negative versions of these small GTPases.

In parallel, we tested whether ectopic expression of a constitutive form of Rac1, Rac1 (L61), influences invasome-mediated internalization. Upon cotransfection of Ea.hy926 cells with eGFP (as transfection marker) and (L61) Rac1, the constitutively active Rac1 elicited the formation of lamellipodial structures (Fig. S3C) and of subcortical membrane ruffles (Fig. S3D). Likewise, we assayed the constitutive active form of Cdc42 (L61) Cdc42, obtaining comparable results for its respective

capacity to induce the formation of filopodia (Fig. S3F). Furthermore, an increase of stress fibres was observed in these cells (Fig. S3E). Following infection of the transfected Ea.hy926 cells with *Bh* wild type, the effector-deficient mutant $\Delta bepA-G$ and its BepG-expressing derivative $\Delta bepA-G/pbepG$, the frequencies of invasome formation were determined for cells transfected with either Rac1 (L61) (Fig. 7B) or Cdc42 (L61) (Fig. 7C). The empty vector pRK5myc, the wild-type versions of Rac1 and Cdc42, and non-transfected cells served as controls. Again, we found that Rac1 and Cdc42 play a pivotal role for invasome-mediated internalization. In the case of Rac1, overexpression of the constitutively active version reduced the rate of invasome formation dramatically (more than 70%); in the case of Cdc42, the respective overexpression reduced the rate of invasome formation significantly (approximately 40%), but not as strong as compared with the corresponding assay with Rac1. No significant change in frequency was observed in ECs transfected with empty vector or wild-type Rac1, and only a mild effect was detected for wild-type Cdc42.

Corroborative evidence supporting a prominent role of Rac1 in BepG-triggered invasome formation and a

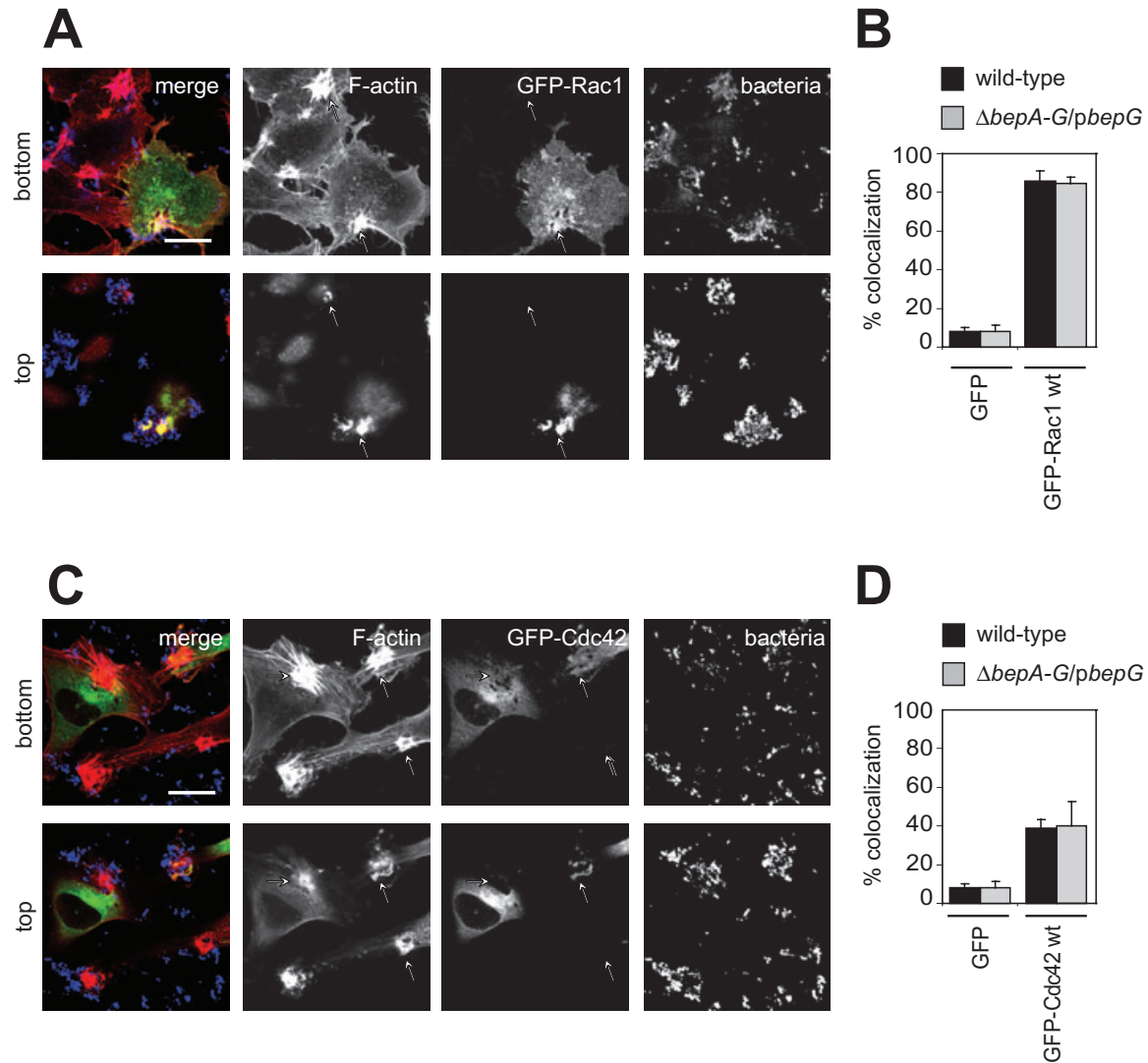


Fig. 8. Rac1 and Cdc42 are recruited to the invasome structure. Ea.hy926 cells were transfected with plasmids encoding (A and B) GFP-Rac1 (C and D) GFP-Cdc42 or (B and D) eGFP (pWay19). Six hours post transfection, cells were infected with *Bh* wild type or the BepG-expressing derivative of the effector-deficient mutant ($\Delta b e p A - G / p b e p G$) with an moi = 100 for 48 h, followed by fixation, immunocytochemical staining of F-actin and bacteria. Confocal images are illustrated for three xy sections (bottom, middle, top) with an approximate spacing of 2–5 μ m. The scale bar corresponds to 20 μ m (B and D). The frequency of colocalization of invasome structures and GFP signal was determined in cells expressing visible amounts of eGFP. Results of three independent experiments \pm standard deviation are depicted ($n = 50$).

contribution of Cdc42 to this bacterial uptake process resulted from RNAi knock-down experiments in Ea.hy926 cells presented in Fig. S4.

To localize Rac1 and Cdc42 during infection we transfected Ea.hy926 cells with expression plasmids for eGFP–Rac1 and eGFP–Cdc42 (both wild-type versions). Strikingly, both eGFP–Rac1 (Fig. 8A) and eGFP–Cdc42 (Fig. 8C) were found to be enriched at sites of invasome formation. However, the frequencies of colocalization with the invasome structure varied (Fig. 8B and D). eGFP–Rac1 was found to be enriched in approximately 90% of invasomes, whereas eGFP–Cdc42 was enriched in only

40% of invasome structures respectively. The enrichment of the GFP signal was observed predominantly in the core of the invasome structure where the highly compacted membranes engulf the bacterial aggregate. Canonical eGFP used as a cytoplasmic control protein was found to be enriched in less than 10% of invasome structures, which may reflect that some cytoplasmic content is trapped in between the membrane protrusions established in the process of invasome formation.

We conclude that BepG-dependent and invasome-mediated internalization of *Bh* into vascular EC requires both active and negative signals generated by the small

GTPases Rac1 and Cdc42, whereas RhoA seems not to be involved in this process. Furthermore, the enrichment of both Rac1 and Cdc42 in membranes surrounding the bacterial aggregate residing in the core of the invasome structure suggests that the actin machinery is specifically triggered at sites of invasome formation to promote changes in the host cell actin cytoskeleton.

Downstream of Rac1 and Cdc42, the adaptor proteins Scar/WAVE and WASP are required for Arp2/3 complex-dependent actin polymerization during invasome formation

Scar/WAVE and WASP adaptor proteins are involved in the formation of lamellipodia/membrane ruffles and filopodia downstream of Rac1 and Cdc42 respectively. Scar/WAVE and WASP are able to bind and activate the Arp2/3 complex, which in turn nucleates F-actin at barbed ends and branching filaments. To test for the involvement of Scar/WAVE and WASP adaptor proteins in invasome formation, we overexpressed truncated derivatives of Scar1 (Scar-WA) and WASP (WASP-WA) that bind the Arp2/3 complex but interfere with actin polymerization and thus display a dominant-negative effect (Machesky and Insall, 1998). Ea.hy926 cells were transfected for 48 h with eGFP (as transfection marker) together with Scar-WA (Fig. S5A) or WASP-WA (Fig. S5B). Phalloidin staining revealed the deleterious effect of these constructs on the integrity of the actin cytoskeleton. Compared with non-transfected cells, only few F-actin stress fibres were visible. Next, we quantified the ability of *Bh* wild-type strain, the effector-deficient mutant $\Delta bepA-G$ and its BepG-expressing derivative $\Delta bepA-G/pbepG$ to induce invasomes after infection of the transfected Ea.hy926 cells with these constructs (Fig. 9A). Cells transfected with the empty vector pRK5myc and non-transfected cells served as controls. We found that overexpression of both Scar-WA and WASP-WA negatively affected the frequency of invasome-mediated internalization as indicated by a significant decrease in the number of invasomes detected per cell, clearly indicating their importance in mediating signals to the actin machinery downstream of Rac1 and Cdc42.

Corroborative evidence supporting a role of Scar and WASP in the process of BepG-triggered invasome formation resulted from RNAi knock-down experiments presented in Fig. S4.

Finally, we tested whether the Arp2/3 complex is recruited to the sites of F-actin polymerization in invasome structures (Fig. 9B). Therefore, we stained Ea.hy926 cells infected for 48 h with *Bh* by immunocytochemical means for Arp3 and analysed samples by confocal laser scanning microscopy. Arp3 was indeed found to be enriched in the cortical F-actin of membrane protrusion engulfing the bacterial aggregates within inva-

somes (Fig. 9B), suggesting that *de novo* F-actin polymerization occurs in these membrane protrusions of the invasome structure. Moreover, RNAi knock-down experiments indicated that Arp3 plays a role in BepG-triggered invasome formation (Fig. S4). Thus, not only rearrangements of the pre-existing actin cytoskeletal structures, but also active actin polymerization events mediated by the Arp2/3 complex are required for the successful internalization of *Bh* by invasomes into vascular ECs.

Discussion

Bacterial pathogens have evolved numerous strategies to corrupt, hijack or mimic cellular processes involved in the modulation of the host cell actin cytoskeleton (Steele-Mortimer *et al.*, 2000). In particular, intracellular pathogens subvert host cell cytoskeletal functions to trigger their internalization into non-professional phagocytes, such as epithelial cells or ECs (Pizarro-Cerda and Cossart, 2006). In this study we investigated the molecular and cellular basis of invasome-mediated internalization of *Bh* into ECs, which is an actin-dependent process associated with extensive rearrangements of the F-actin cytoskeleton (Dehio *et al.*, 1997). The Rho-family GTPases RhoA, Rac1 and Cdc42 are key regulators of the actin cytoskeleton, which regulate the formation of stress fibres, lamellipodia and filopodia respectively (Jaffe and Hall, 2005). These Rho-family GTPases have been reported to play specific roles in host cell invasion by several intracellular bacteria (Finlay, 2005) and we have thus accessed their role in invasome-mediated internalization of *Bh*. Despite of the massive rearrangements of F-actin stress fibres occurring during invasome formation, we found RhoA to be dispensable for this process, indicating that a *de novo* formation of stress fibres is not required. Instead, the characteristic ring-shaped bundle of stress fibres localizing to the basis of the invasome appears to be formed by wrapping pre-existing stress fibres around this structure, probably as the result of a rotational movement of the cell relative to the invasome. Consistent with this assumption, time-lapse video microscopy has indicated that the invasome is partially impaired in migratory movements initiated by the leading edge (Dehio *et al.*, 1997). The molecular mechanism of how invasome formation interferes with cellular migration is unknown; however, circumstantial evidence suggests that the invasome locally interferes with focal adhesion turnover (Dehio *et al.*, 1997). Other than RhoA, the small GTPases Rac1 and to a lesser extent also Cdc42 are required for invasome-mediated invasion. These GTPases appear to be required for the formation of membrane protrusions engulfing the bacterial aggregates that are formed on the cell surface rather early during invasome formation (Dehio *et al.*, 1997). We have further

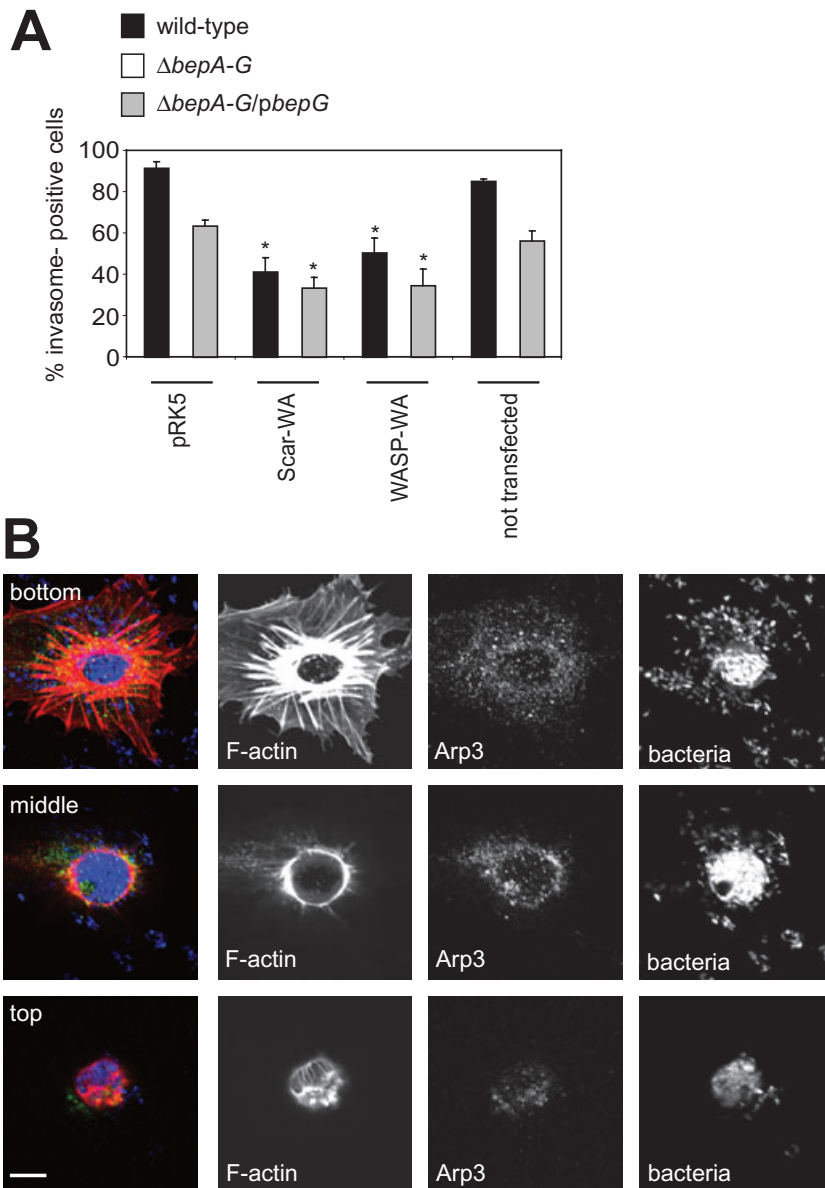


Fig. 9. Cytoskeletal remodelling during invasome formation depends on Scar and WASP and involves the Arp2/3 complex. **A.** Ea.hy926 cells were cotransfected with a plasmid encoding eGFP (pWay19, to identify transfected cells) and a second plasmid encoding either the Scar WA domain (Scar-WA), the WASP WA domain (WASP-WA) or the empty vector pRK5. After 6 h, cells were washed and infected with *Bh* wild type for 48 h, followed by cell fixation, staining for F-actin with TRITC-phalloidin and analysis by confocal laser scanning microscopy. The frequency of invasome formation was determined in cells expressing visible amounts of eGFP. Results of three independent experiments \pm standard deviation are depicted ($n = 50$). **B.** HUVEC infected with *Bh* wild type ($moi = 100$) for 48 h, followed by cell fixation, staining for F-actin and Arp3 and analysis by confocal laser scanning microscopy. The scale bar corresponds to 10 μm .

shown that the Rac1 effector Scar/WAVE and the Cdc42 effector WASP are involved in the invasome-mediated uptake process, and that their target Arp2/3 is recruited to the dense cortical actin network formed in membrane protrusions at sites of invasome formation. We conclude that the rearrangements of the F-actin cytoskeleton involved in invasome-mediated invasion depend on Rac1/Scar1/WAVE and Cdc42/WASP signalling pathways that converge at the F-actin nucleating and branching complex Arp2/3.

Invasome-mediated uptake was previously shown to depend on a functional T4S system, the VirB/VirD4 system (Schmid *et al.*, 2004), and the presence of a genomic region encoding seven VirB/VirD4-translocated *Bartonella* effector proteins (BepA to BepG) (Schulein

et al., 2005). Here we demonstrate that the translocation of a single effector, BepG, is sufficient to trigger invasome-mediated internalization. BepG is a multi-domain protein displaying four copies of the BID domain, which together with a non-conserved, positively charged C-terminal tail sequence was originally described as a bi-partite signal for VirB/VirD4-dependent translocation (Schulein *et al.*, 2005). Using the CRAfT reporter assay for protein translocation (Schulein *et al.*, 2005) we have shown that the C-terminal BID domain and the proximal C-terminal tail are sufficient to mediate VirB/VirD4-dependent translocation. The other three BID domains of BepG are thus dispensable for VirB/VirD4-dependent protein translocation into host cells, but could instead play structural or functional roles in the effector functions of

BepG within the host cell, particularly given that no other known protein domain has been identified in BepG. Multiple BID domains are also present in the VirB/VirD4 effectors BepE and BepF, indicating that the BID represents a modular domain fold that following duplication and diversification allows fast evolution of effector proteins by adopting novel functions within host cells (Saenz *et al.*, 2007; Dehio, 2008). The adoption of effector functions within host cells has even been described for the single BID domain of BepA, which further to mediating VirB/VirD4-dependent protein transfer also mediates protection of ECs from apoptosis by a mechanisms involving plasma membrane targeting and an increase in the cyclic AMP level (Schmid *et al.*, 2006).

Ectopic expression of a GFP–BepG fusion construct in ECs demonstrated colocalization of the fusion protein with F-actin structures such as stress fibres and cortical actin, which are distinctly enriched in the invasome structure, but unexpectedly did not result in any detectable rearrangement of the F-actin cytoskeleton in uninfected cells. Ectopic expression of epitope-tagged BepG did also not alter the F-actin cytoskeleton in uninfected cells, but fully restored the capacity of the effector-deficient *Bh* mutant (Δ bepA–G) to form invasomes. These findings suggest that BepG is recruited – either directly or indirectly – to F-actin structures; however, without affecting the dynamics of the F-actin cytoskeleton itself. Thus BepG does not appear to represent an effector protein subverting host cellular functions controlling actin dynamics as previously reported for other translocated bacterial effector proteins, such as diverse type III secreted effectors that target or mimic the activity small Rho-family GTPases (Finlay, 2005; Alto *et al.*, 2006). Instead, we observed that the VirB/VirD4-dependent translocation or the ectopic expression of BepG equally resulted in a marked inhibition of the endocytic uptake of individual *Bh* bacteria into BCVs, thereby resulting in the accumulation of bacteria on the cell surface. We assume that the resulting formation of cell surface-associated bacterial aggregates then triggers the characteristic F-actin rearrangements leading to invasome formation, possibly via the clustering of a yet unknown host cell receptor by surface-expressed bacterial ligand(s). The available data do not allow concluding whether or not BepG may contribute to this specific invasion process of a large bacterial aggregate further to the inhibition of endocytic uptake of individual bacteria into BCVs that occurs with a much faster kinetics (Dehio *et al.*, 1997). Importantly, the inhibition of endocytic uptake of individual bacteria by BepG is not limited to *Bh* as the well-studied zipper-like internalization of *Y. enterocolitica* mediated by an high-affinity interaction of the bacterial surface ligand invasin with β 1-integrins (Alrutz *et al.*, 2001) was inhibited by BepG as well. Moreover, we could demonstrate that BepG inhibits

also the uptake of inert microspheres by ECs (Yao *et al.*, 1995). Several translocated bacterial effector proteins have been reported to interfere with bacterial uptake, for example, the *Y. pseudotuberculosis* effectors YopE, YopH, YopT and YpkA block phagocytic uptake of bacteria into macrophages (Fallman and Gustavsson, 2005). However, for all these effectors the capacity to block bacterial uptake was shown to depend on known enzymatic activities targeting basic cellular signalling processes that eventually block essential actin cytoskeletal functions, often resulting in a complete paralysis of the cell (Fallman and Gustavsson, 2005). In contrast, BepG is composed of multiple copies of the relatively short BID domain and thus probably does not bear any enzymatic activity. Moreover, while BepG effectively blocks uptake of *Bh* into BCVs, invasin-mediated uptake of *Y. enterocolitica* and uptake of inert microspheres, it cannot mediate these anti-endocytic activities by simply blocking basic actin cytoskeletal functions as invasome-mediated internalization triggered as an alternative route of *Bh* entry also occurs in a strictly F-actin-dependent manner. BepG thus represents a novel type of an anti-endocytic bacterial effector protein. Future studies on BepG should focus on identifying the molecular basis of the inhibition of endocytic uptake of individual bacteria and the link to invasome-mediated internalization.

Experimental procedures

Bacterial strains, growth conditions, conjugations

Bacterial strains were cultured following standard procedures on solid agar (Columbia base agar supplemented with 5% sheep blood) or in liquid broth (Luria Bertani broth, Bovine Heart infusion) with appropriate antibiotics. Triparental matings between *E. coli* and *Bh* and strains were performed as described (Dehio and Meyer, 1997). The bacterial strains used in this study are listed in Table 1.

Plasmid construction

DNA manipulations were carried out following standard protocols. Oligonucleotide primers used in this study are listed in Table 2. All parts of DNA constructs generated by the polymerase chain reaction (PCR) were confirmed by sequencing. Shuttle vector pPG100 and derivatives encoding full-length *bepA* (pPG101), *bepB* (pMS006), *bepC* (pMS007) and *bepD* (pPG104) have been described. Accordingly, the coding regions of full-length *bepE*, *bepF* and *bepG* were amplified by PCR with primer pairs prPG100/prPG101, prPG102/prPG103 and prPG131/prPG105 respectively, and cloned into pPG100 via NdeI or AseI giving rise to plasmids pPG105, pPG106 and pPG107 respectively. pTR1703 was obtained by PCR-amplifying the C-terminal part of *bepG* (corresponding to amino acids 715–1009) by primer pairs prTR078/prTR076. The resulting 0.9 kb fragment was cleaved with Sall/XmaI and ligated into the plasmid backbone of pRS51 cleaved accordingly. pTR1778 (eGFP–BepG) was obtained by

Table 1. Bacterial strains and plasmids used in this study.

| Strain/plasmid | Genotype or relevant characteristics | Reference/Source |
|----------------------------------|--|---------------------------------|
| <i>Bh</i> strains | | |
| ATCC 49882 ^T | 'Houston-1', isolated from a bacteremic HIV-patient, U.S. | Regnery <i>et al.</i> (1992) |
| RSE247 | spontaneous Sm ^r strain of ATCC 49882 ^T | Schmid <i>et al.</i> (2004) |
| RSE242 | $\Delta virB4$ mutant of RSE247 | Schmid <i>et al.</i> (2004) |
| MSE150 | $\Delta bepA-G$ mutant of RSE247 | Schulein <i>et al.</i> (2005) |
| MSE156 | MSE150 containing pPG101 ($\Delta bepA-G/pbepA$) | Schmid <i>et al.</i> (2006) |
| MSE167 | MSE150 containing pMS006 ($\Delta bepA-G/pbepB$) | Schmid <i>et al.</i> (2006) |
| MSE159 | MSE150 containing pMS007 ($\Delta bepA-G/pbepC$) | Schmid <i>et al.</i> (2006) |
| PGD03 | MSE150 containing pPG104 ($\Delta bepA-G/pbepD$) | Schulein <i>et al.</i> (2005) |
| PGD10 | MSE150 containing pPG105 ($\Delta bepA-G/pbepE$) | This study |
| TRB171 | MSE150 containing pPG106 ($\Delta bepA-G/pbepF$) | This study |
| TRB169 | MSE150 containing pPG107 ($\Delta bepA-G/pbepG$) | This study |
| RSE308 | RSE247 containing pRS51 | Schulein <i>et al.</i> (2005) |
| TRB265 | RSE247 containing pTR1703 | This study |
| TRB295 | RSE242 containing pTR1703 | This study |
| TRB247 | RSE242 containing pCD354 | This study |
| <i>Y. enterocolitica</i> strains | | |
| BK009 | pYV ⁻ , inv ⁺ | Sory <i>et al.</i> (1995) |
| BK010 | pYV ⁻ , inv::pMS154 | Sory <i>et al.</i> (1995) |
| <i>E. coli</i> strains | | |
| β 2150 | <i>F lacZDM15 lacI^rtraD36 proA+B+ thrB1004 pro thi strA hsdS lacZΔM15 ΔdapA::erm (Erm^R) pir endA1 hsdR17(r K12-m K12+) supE44 thi-1 recA1 gyrA96 relA1 lacI^r proA+B+ lacI^rZΔM15::Tn10 (Tc^R)</i> | Schulein and Dehio (2002) |
| NovaBlue | | Novagen, Madison |
| Plasmids | | |
| pCD354 | <i>Bartonella</i> spp. vector, expressing GFP | Dehio <i>et al.</i> (1998) |
| peGFP-Cdc42 | Mammalian expression vector for eGFP-Cdc42 fusion | del Pozo <i>et al.</i> (1999) |
| peGFP-Rac1 | Mammalian expression vector for eGFP-Rac1 fusion | del Pozo <i>et al.</i> (1999) |
| pFLAG CMV2 | For transient expression of N-terminal FLAG fusion proteins in mammalian cells | Invitrogen, California |
| pMS006 | Derivative of pPG100, encoding FLAG-BepB | Schmid <i>et al.</i> (2006) |
| pMS007 | Derivative of pPG100, encoding FLAG-BepC | Schmid <i>et al.</i> (2006) |
| pPG100 | <i>E. coli-Bartonella</i> spp. shuttle vector | Schulein <i>et al.</i> (2005) |
| pPG101 | Derivative of pPG100, encoding FLAG-BepA | Schmid <i>et al.</i> (2006) |
| pPG104 | Derivative of pPG100, encoding FLAG-BepD | Schulein <i>et al.</i> (2005) |
| pPG105 | Derivative of pPG100, encoding FLAG-BepE | This study |
| pPG106 | Derivative of pPG100, encoding FLAG-BepF | This study |
| pPG107 | Derivative of pPG100, encoding FLAG-BepG | This study |
| pRK5myc Cdc42 wt | Mammalian expression vector for Cdc42 | Olson <i>et al.</i> (1995) |
| pRK5myc L61 Cdc42 | Mammalian expression vector for L61 Cdc42 | Ridley and Hall (1992) |
| pRK5myc L61 Rac1 | Mammalian expression vector for L61 Rac1 | Ridley and Hall (1992) |
| pRK5myc N17 Cdc42 | Mammalian expression vector for N17 Cdc42 | Olson <i>et al.</i> (1995) |
| pRK5myc N17 Rac1 | Mammalian expression vector for N17 Rac1 | Ridley and Hall (1992) |
| pRK5myc N17 RhoA | Mammalian expression vector for N17 RhoA | Ridley and Hall (1992) |
| pRK5myc Rac1 wt | Mammalian expression vector for Rac1 | Ridley and Hall (1992) |
| pRK5myc-SCAR-WA | Mammalian expression vector for SCAR-WA | Machesky and Insall (1998) |
| pRK5myc-WASP-WA | Mammalian expression vector for WASP-WA | Machesky and Insall (1998) |
| pRS51 | Cre-vector, encoding NLS-Cre-BepD-BID (aa 352-534) | Schulein <i>et al.</i> (2005) |
| pTR1178 | Derivative of pFLAG CMV2, encoding FLAG-BepG | This study |
| pTR1703 | Cre-vector, encoding NLS-Cre-BepG-BID#4 (aa 715-1009) | This study |
| pTR1778 | Derivative of pWAY21, encoding eGFP-BepG | This study |
| pWAY19 | Mammalian expression vector for eGFP | Molecular Motion Lab Montana |
| pWAY21 | Mammalian expression vector for N-terminal eGFP fusions | Molecular Motion Lab Montana |

PCR amplification of full-length *bepG* by primer pair prTR079/prTR076, cutting the resulting 3.05 kb fragment with XmaI and by its ligation into pWAY21 (eGFP, Molecular Motion, Montana Laboratories) cut accordingly. pTR1778 (eGFP-BepG) was obtained similarly by primer pair prTR079/prTR076, restriction by XmaI and by ligation into pWAY21 (eGFP, Molecular Motion, Montana Laboratories) cut accordingly.

Cell lines and cell culture

The HUVECs were isolated and cultivated as described (Dehio *et al.*, 1997). Ea.hy296 cells and the stably transfected cell line Ea.hy296/pRS56-clone B1 were cultivated in DMEM/10% FCS as described (Schulein *et al.*, 2005). HeLa cells were cultivated in DMEM/10% FCS.

Table 2. Oligonucleotide primers used in this study.

| Name | Sequence ^a | Restriction site |
|---------|--|------------------|
| prPG100 | GGAATTCCAT ATG AAAAAGAAATCAACCACCC | NdeI |
| prPG101 | GGAATTCCATATGTTAGATGGCGAAAGCTATTG | NdeI |
| prPG102 | GGAATTCCAT ATG AAAAAAAACCAACCATCCT | NdeI |
| prPG103 | GGAATTCCATATGTTAGAGTGCCAGCACCATT | NdeI |
| prPG131 | CGCGCTTATTAAT ATG AAAAAAAACAACCAGCCC | AseI |
| prPG105 | CGCGCTTATTAATTTATCTACTCATAGAACTACTT | AseI |
| prTR044 | ATAAGAATGCGGCCGG ATG AAAAAAAACAACCAGCCC | NotI |
| prTR020 | CGGGATCCTTATCTACTCATAGAACTACTTT | BamHI |
| prTR048 | ATAAGAATGCGGCCGG ATG AAAAAAAACAACCAGCCC | NotI |
| prTR020 | CGGGATCCTTATCTACTCATAGAACTACTTT | BamHI |
| prTR078 | ACGCGTCGACTCTTCACTCAAGAAACGCAAAAAAT | Sall |
| prTR076 | CCCCCGGGTTATCTACTCATAGAACTACTTT | XmaI |
| prTR079 | TCCCCCGGG ATG AAAAAAAACAACCAGCCC | XmaI |

a. Restriction endonuclease cleavage sites are underlined; the ATG start codon is highlighted in bold.

Infection and transfection assays

The day before infection, HUVEC (passage 3–9) were seeded onto gelatine-coated coverslips into 24-well plates. Fresh medium was supplemented 4–6 h post seeding. Approximately 30 000 cells were infected at an moi = 100 in medium M199/10%FCS supplemented with 500 μ M IPTG (Promega) and incubated for 48 h. Cytochalasin D (Sigma) was dissolved in DMSO (Fluka) and added to the final concentrations indicated. For transfection, Ea.hy926 and HeLa cells were seeded onto coverslips into 24-well plates at cell densities of 50 000 cells per well. Cells were transfected with Effectene (Qiagen) and 200 ng of endotoxin-free high-purity DNA (Endotoxin Free Plasmid Maxi Prep, QIAGEN or Macherey Nagel) according to the manufacturer's protocol at a ratio of 1:3 for reporter versus tester plasmid. pRK5 encoding myc-tagged versions of Rho-family small GTPases RhoA, Rac1 and Cdc42 as well as pRK5 encoding myc-tagged Scar1 and WASP derivatives have been described (see Table 1). Six hours post transfection, cells were washed once with phosphate-buffered saline (PBS) and fresh medium M199/10% FCS supplemented with 500 μ M IPTG was added. Bacteria were then added at an moi = 100. To test functionality of dominant-negative version of Rac1, Ea.hy926 cells were washed 30 h post transfection once with PBS and supplemented with fresh serum-free DMEM including D-erythro sphingosine-1-phosphate (Calbiochem, 1 μ M) and stimulated for 2 min as described or including bradykinin (Calbiochem, 2 μ M) and stimulated for 15 min respectively. At the time points indicated, cells were washed once with PBS and fixed in 3.7% paraformaldehyde (Sigma). For superinfections, cells were preinfected with the indicated strain of *Bh* for 12 or 48 h with an moi = 100 or 200 respectively, followed superinfection with the Δ virB4 strain of *Bh* expressing GFP (pCD354) or *Y. enterocolitica* for 90 min, respectively, before fixation or cell lysis with saponin respectively.

For microsphere uptake assays, Ea.hy926 cells were preinfected with the indicated strain of *Bh* for 24 h with an moi of 100, followed by 1 h treatment with amikacin (40 mg ml⁻¹) to kill bacteria. Thereafter, cells were washed twice with M199/10%FCS and fresh M199/10%FCS containing BSA-saturated, carboxylate-modified fluorescent (535/575 nm) microspheres (1 μ m Nile red FluoSpheres, Molecular Probes) was added to the cells (100 microspheres/cell). Following 24 h of incubation, cells

were fixed with paraformaldehyde, stained for F-actin and DNA and analysed by confocal laser scanning microscopy.

Immunofluorescent labelling

Indirect immunofluorescent (IF) labelling was performed as described (Dehio *et al.*, 1997). For staining of F-actin, TRITC-phalloidin (Sigma, 100 μ g ml⁻¹ stock solution, final concentration 1:400) was used. Primary antibodies for IF used in this study are: (i) serum 2037 (polyclonal rabbit anti-*Bh* total bacteria, 1:100), (ii) anti-Arp3 (monoclonal mouse clone 4, BD Biosciences Pharmingen, 1:50) and (iii) anti-LAMP-1 (monoclonal mouse clone H4A3, Developmental Studies Hybridoma Bank, University of Iowa, Iowa City, IA, US, 1:100). Secondary antibodies for IF used in this study are: (i) Cy5-conjugated goat anti-rabbit Ig antibodies and (ii) Cy2-conjugated goat anti-rabbit Ig antibodies (both Dianova, Hamburg, Germany, 1:100). For triple staining of bacteria, F-actin and a third probe the secondary antibody was goat anti-mouse IgG (H + L) Alexa Fluor 488 (Molecular Probes, 1:100). For cells incubated with fluorescent microspheres, Cy5-phalloidine (Sigma, 100 μ g ml⁻¹ stock solution, final concentration 1:400) was used for staining of F-actin and DAPI (Roche, 0.1 mg ml⁻¹) for staining of nuclei.

Epi-fluorescence and confocal laser scanning microscopy

For visualization and quantification of invasome structures, specimens were examined with a Leica DM-IRBE inverted epi-fluorescence microscope at a magnification of 40 \times in immersion. Assessment of successive invasome stages was performed as described (Dehio *et al.*, 1997). For confocal laser scanning microscopy, a Leica TCS SP was used. Recordings were made in one focal plane at 40 \times or 63 \times magnification in immersion in the xyz or xz λ mode with image size of 512 \times 512 pixels. Channels were assembled and adjusted using Metamorph and Adobe Photoshop, and pictures were arranged and labelled in Adobe CS Illustrator.

To quantify intra- versus extracellular microspheres, the stained cells samples were analysed by confocal laser scanning

microscopy using an IQ iXON spinning disc system from Andor in combination with an Olympus IX2-UCB microscope. Z-stacks with 30 focal planes with a spacing of 0.2 μm were recorded and intra- and extracellular beads were counted using x-z reconstructions of the recorded z-stacks. Planes and channels were adjusted using Andor IQ software.

CRAFT

CRAFT was used to monitor translocation of NLS-Cre-BepG fusion proteins from *Bh* into the stably transfected reporter cell line Ea.hy296/pRS56 clone B1 as described (Schulein *et al.*, 2005). Approximately 50 000 cells seeded in individual wells of a 24-well plate were infected with an moi = 150 for 5 days and the percentage of GFP-positive cells was measured with a FACS Calibur flow cytometer (Becton Dickinson).

Immunoblot analysis

Expression of N-terminal FLAG-tagged Bep fusion proteins was verified by analysis of total cell lysates obtained from Ea.hy926 cells infected with *Bh* for 48 h. Proteins were separated by SDS-PAGE, transferred onto nitrocellulose membranes (Hybond, Amersham Biosciences), and examined for the presence of the FLAG epitope using mouse monoclonal anti-FLAG antibody M2 (Sigma, 1:1000). Steady-state levels of NLS-Cre-Bep fusion proteins were analysed by separation of bacterial cell lysates by SDS-PAGE, transferred onto PVDF membranes (Hybond-P, Amersham Biosciences), and examined for the presence of the Cre fusion protein using polyclonal anti-Cre antibody (EMD Biosciences, Novagen, 1:10000). In both experiments, the secondary horseradish peroxidase-conjugated antibody (Amersham, 1:2000) was visualized by enhanced chemiluminescence (PerkinElmer).

siRNA-mediated gene silencing

Ea.hy926 cells were seeded into dark, clear-bottom 96-well plates (Costar, no. 3904) at a density of 2000 cells per well. Following overnight incubation, cells were transfected with HiPerFect (Qiagen) and siRNA pools targeting Rac1, Cdc42, Scar/WAVE, WASP or Arp3 (Dharmacon/Thermo Fisher Scientific; ON-TARGETplus SMARTpool siRNAs, see Table S1) as described in the HiPerFect manual. Final siRNA concentration was set to 20 nM. Cells were incubated for 36 h and infected subsequently at an moi = 75. Following an incubation period of 48 h, cells were fixed, stained with DAPI (Roche, 0.1 mg ml⁻¹) and TRITC-phalloidin (Sigma, 100 μg ml⁻¹ stock solution, final concentration 1:400) and images were acquired using an MDC IXM automated microscope. Ten images were taken per well and images were quantified semiautomatically using MetaExpress.

Acknowledgements

We would like to thank Arto Pulliainen for critical reading of the manuscript and Ilaria Carena and Nadège Devaux for excellent technical assistance. The Kantonspital Bruderholz and University Women's Hospital Basel are acknowledged for providing human umbilical cords. We are indebted to Anja Schmidt and Alan Hall

(MRC Cell Biology, University College London, London, UK), Edith Gouin and Pascale Cossart (Unité des Interactions Bactéries \times Cellules, Institut Pasteur, Paris, France), Francisco García-del Portillo (Departamento de Biotecnología Microbiana, Centro Nacional de Biotecnología, Madrid, Spain) and Laura Machesky (Department of Biochemistry, University of Birmingham, UK) for the kind gift of plasmids encoding different versions of small GTPases and their effectors Scar1 and WASP respectively. Furthermore, we would like to thank G. R. Cornelis for providing *Y. enterocolitica* strains. This work was supported by Grant 3100-061777 from the Swiss National Science Foundation and Grant 55005501 from the Howard Hughes Medical Institute.

References

- Alrutz, M.A., Srivastava, A., Wong, K.W., D'Souza-Schorey, C., Tang, M., Ch'Ng, L.E., *et al.* (2001) Efficient uptake of *Yersinia pseudotuberculosis* via integrin receptors involves a Rac1-Arp 2/3 pathway that bypasses N-WASP function. *Mol Microbiol* **42**: 689–703.
- Alto, N.M., Shao, F., Lazar, C.S., Brost, R.L., Chua, G., Mattoo, S., *et al.* (2006) Identification of a bacterial type III effector family with G protein mimicry functions. *Cell* **124**: 133–145.
- Dehio, C. (2004) Molecular and cellular basis of bartonella pathogenesis. *Annu Rev Microbiol* **58**: 365–390.
- Dehio, C. (2005) Bartonella–host–cell interactions and vascular tumour formation. *Nat Rev Microbiol* **3**: 621–631.
- Dehio, C. (2008) Infection-associated type IV secretion systems of Bartonella and their diverse roles in host cell interaction. *Cell Microbiol* **10**: 1591–1598.
- Dehio, C., and Meyer, M. (1997) Maintenance of broad-host-range incompatibility group P and group Q plasmids and transposition of Tn5 in *Bartonella henselae* following conjugal plasmid transfer from *Escherichia coli*. *J Bacteriol* **179**: 538–540.
- Dehio, C., Meyer, M., Berger, J., Schwarz, H., and Lanz, C. (1997) Interaction of *Bartonella henselae* with endothelial cells results in bacterial aggregation on the cell surface and the subsequent engulfment and internalisation of the bacterial aggregate by a unique structure, the invasome. *J Cell Sci* **110**: 2141–2154.
- Dehio, M., Knorre, A., Lanz, C., and Dehio, C. (1998) Construction of versatile high-level expression vectors for *Bartonella henselae* and the use of green fluorescent protein as a new expression marker. *Gene* **215**: 223–229.
- Dersch, P., and Isberg, R.R. (1999) A region of the *Yersinia pseudotuberculosis* invasin protein enhances integrin-mediated uptake into mammalian cells and promotes self association. *EMBO J* **18**: 1199–1213.
- Fallman, M., and Gustavsson, A. (2005) Cellular mechanisms of bacterial internalization counteracted by *Yersinia*. *Int Rev Cytol* **246**: 135–188.
- Finlay, B.B. (2005) Bacterial virulence strategies that utilize Rho GTPases. *Curr Top Microbiol Immunol* **291**: 1–10.
- Florin, T.A., Zaoutis, T.E., and Zaoutis, L.B. (2008) Beyond cat scratch disease: widening spectrum of *Bartonella henselae* infection. *Pediatrics* **121**: e1413–e1425.
- Jaffe, A.B., and Hall, A. (2005) Rho GTPases: biochemistry and biology. *Annu Rev Cell Dev Biol* **21**: 247–269.
- Kyme, P.A., Haas, A., Schaller, M., Peschel, A., Iredell, J., and Kempf, V.A. (2005) Unusual trafficking pattern of

- Bartonella henselae*-containing vacuoles in macrophages and endothelial cells. *Cell Microbiol* **7**: 1019–1034.
- Machesky, L.M., and Insall, R.H. (1998) Scar1 and the related Wiskott–Aldrich syndrome protein, WASP, regulate the actin cytoskeleton through the Arp2/3 complex. *Curr Biol* **8**: 1347–1356.
- Olson, M.F., Ashworth, A., and Hall, A. (1995) An essential role for Rho, Rac, and Cdc42 GTPases in cell cycle progression through G1. *Science* **269**: 1270–1272.
- Pizarro-Cerda, J., and Cossart, P. (2006) Bacterial adhesion and entry into host cells. *Cell* **124**: 715–727.
- del Pozo, M.A., Vicente-Manzanares, M., Tejedor, R., Serrador, J.M., and Sanchez-Madrid, F. (1999) Rho GTPases control migration and polarization of adhesion molecules and cytoskeletal ERM components in T lymphocytes. *Eur J Immunol* **29**: 3609–3620.
- Pulliaainen, A., and Dehio, C. (2009) *Bartonella henselae*: subversion of vascular endothelial cell functions by translocated bacterial effector proteins. *Int J Biochem Cell Biol* **41**: 507–510.
- Regnery, R.L., Anderson, B.E., Claridge, J.E., 3rd, Rodriguez-Barradas, M.C., Jones, D.C., and Carr, J.H. (1992) Characterization of a novel Rochalimaea species, *R. henselae* sp. nov., isolated from blood of a febrile, human immunodeficiency virus-positive patient. *J Clin Microbiol* **30**: 265–274.
- Ridley, A.J., and Hall, A. (1992) The small GTP-binding protein rho regulates the assembly of focal adhesions and actin stress fibres in response to growth factors. *Cell* **70**: 389–399.
- Saenz, H.L., Engel, P., Stoeckli, M.C., Lanz, C., Raddatz, G., Vayssier-Taussat, M., et al. (2007) Genomic analysis of *Bartonella* identifies type IV secretion systems as host adaptability factors. *Nat Genet* **39**: 1469–1476.
- Scheidegger, F., Ellner, Y., Guye, P., Rhomberg, T.A., Weber, H., Augustin, H.G., and Dehio, C. (2009) Distinct activities of *Bartonella henselae* type IV secretion effector proteins modulate capillary-like sprout formation. *Cell Microbiol* (in press) Doi: 10.1111/j.1462-5822.2009.01313.x
- Schmid, M.C., Schulein, R., Dehio, M., Denecker, G., Carena, I., and Dehio, C. (2004) The VirB type IV secretion system of *Bartonella henselae* mediates invasion, proinflammatory activation and antiapoptotic protection of endothelial cells. *Mol Microbiol* **52**: 81–92.
- Schmid, M.C., Dehio, M., Balmelle-Devaux, N., Scheidegger, F., Biedermann, B., and Dehio, C. (2006) A translocated bacterial protein protects vascular endothelial cells from apoptosis.
- Schulein, R., and Dehio, C. (2002) The VirB/VirD4 type IV secretion system of *Bartonella* is essential for establishing intraerythrocytic infection. *Mol Microbiol* **46**: 1053–1067.
- Schulein, R., Guye, P., Rhomberg, T.A., Schmid, M.C., Schroder, G., Vergunst, A.C., et al. (2005) A bipartite signal mediates the transfer of type IV secretion substrates of *Bartonella henselae* into human cells. *Proc Natl Acad Sci USA* **102**: 856–861.
- Sory, M.P., Boland, A., Lambermont, I., and Cornelis, G.R. (1995) Identification of the YopE and YopH domains required for secretion and internalization into the cytosol of macrophages, using the *cyaA* gene fusion approach. *Proc Natl Acad Sci USA* **92**: 11998–12002.
- Steele-Mortimer, O., Knodler, L.A., and Finlay, B.B. (2000) Poisons, ruffles and rockets: bacterial pathogens and the host cell cytoskeleton. *Traffic* **1**: 107–118.
- Yao, L., Bengualid, V., Lowy, F.D., Gibbons, J.J., Hatcher, V.B., and Berman, J.W. (1995) Internalization of *Staphylococcus aureus* by endothelial cells induces cytokine gene expression. *Infect Immun* **63**: 1835–1839.
- Young, V.B., Falkow, S., and Schoolnik, G.K. (1992) The invasins protein of *Yersinia enterocolitica*: internalization of invasins-bearing bacteria by eukaryotic cells is associated with reorganization of the cytoskeleton. *J Cell Biol* **116**: 197–207.

Supporting information

Additional Supporting Information may be found in the online version of this article:

Fig. S1. Bacteria entering ECs by endocytosis or invasome-mediated uptake have different intracellular fates. HUVECs were infected with *Bh* wild type (moi = 100) for 48 h, followed by fixation and immunocytochemical staining for F-actin (represented in green), bacteria (represented in red) and the lysosomal marker protein LAMP-1 (represented in blue), followed by laser scanning microscopy. The scale bar corresponds to 20 μ m.

Fig. S2. The C-terminal part of BepG mediates VirB/VirD4-dependent translocation into ECs.

A. Modular domain organization of BepG. BepG harbours four BID domains (BID-G1 to G4) and two sets of repeated domains of unknown function (DUF1a, 1b, 1c and DUF2a and DUF2b).

B. For the CRAfT, the Cre-reporter cell line Ea.hy296/pRS56-clone B1 was infected for 5 days with an moi = 100 of *Bh* strains harbouring plasmid pRS51 [encoding NLS-Cre-BepD (aa 352–534)] in the wild-type background, and plasmid pTR1703 [encoding NLS-Cre-BepG (aa 716–1009)] in the wild-type or Δ virB4 mutant background. Then, the percentage of GFP-positive cells was determined by flow cytometric analysis.

C. Steady-state levels of expression of NLS-Cre reporter fusion proteins in plate-grown bacteria of the different strains used for CRAfT. Total cell lysates were separated by SDS-PAGE, transferred to nitrocellulose and probed with anti-Cre antibodies.

Fig. S3. Effects of dominant-negative and constitutive active forms of Rac1 and Cdc42 on the F-actin cytoskeleton of ECs. Ea.hy926 cells were cotransfected with a plasmid encoding eGFP (pWay19, to identify transfected cells) and a second plasmid encoding (A) dominant-negative Rac1 [(N17) Rac1], (B) dominant-negative Cdc42 [(N17) Cdc42], (C,D) constitutively active Rac1 [(L61)Rac1] and (E,F) constitutively active Cdc42 [(L61)Cdc42]. Forty-eight hours post transfection, (A) endogenous Rac1 was activated for 2 min by 1 μ M sphingosine-1-phosphate and (B) endogenous Cdc42 was activated for 15 min by 2 μ M bradykinin. Samples were then fixed, followed by staining for F-actin and laser scanning microscopy in (A–D) the xy-plane or (C–F) xz-plane (right). The scale bar corresponds to 10 μ m.

Fig. S4. RNAi knock-down of Rac1, Cdc42, Scar/Wave, WASP or Arp3 inhibits invasome formation. Ea.hy926 cells were transfected with siRNA pools targeting Rac1, Cdc42, Scar/Wave, WASP, Arp3, mock-transfected (control) or left untransfected for 36 h. Subsequently, cells were infected with an moi = 75 of *Bh* wild-type, or the isogenic BepG-expressing derivative Δ bepA–G/pbepG for 48 h. Following fixation, staining and automated

microscopy, the frequency of invasome formation was determined semiautomatically. One representative out of three independent experiments is depicted. Data points represent the mean of quadruplicate samples \pm standard deviation.

Fig. S5. Effects of dominant-negative forms of Scar and WASP on the F-actin cytoskeleton of EC. Ea.hy926 cells were cotransfected with a plasmid encoding eGFP (pWay19, to identify transfected cells) and a second plasmid encoding either (A) Scar WA domain only (Scar-WA) or (B) WASP-WA domain only (WASP-

WA). After 48 h, cells were fixed, stained for F-actin with TRITC-phalloidine and analysed by confocal laser scanning microscopy. The scale bar corresponds to 10 μ m.

Table S1. siRNA pools used in this study.

Please note: Wiley-Blackwell are not responsible for the content or functionality of any supporting materials supplied by the authors. Any queries (other than missing material) should be directed to the corresponding author for the article.

3.2 RESEARCH ARTICLE II

Combined action of the type IV secretion effector proteins BepC and BepF promotes invasome formation of *Bartonella henselae* on endothelial and epithelial cells

Matthias C. Truttmann, Thomas A. Rhomberg and Christoph Dehio

Cellular Microbiology, published online 22. October 2010, j.1462-5822.2010.01529.x

3.2.1 SUMMARY

Invasome- mediated internalization of *Bartonella henselae* (*Bhe*) Houston-1 into endothelial cells (ECs) is dependent on a functional VirB/D4 type 4 secretion system (T4SS) and the subsequent effector translocation into the host cell [1,2]. Further, previous work has implicated that the effector BepG is sufficient to trigger invasome formation on endothelial cells [3].

Infections of ECs with the in-frame deletion mutant *Bhe* Δ bepG resulted in frequent invasome formation. To determine the accountable alternative mechanism, we infected ECs with all possible dual combinations of the *Bhe* mutant Δ bepA-G that expressed *in trans* epitope-tagged versions of BepA to BepG and tested for phenotypic complementation. The obtained results showed that besides BepG, the combined function of effectors BepC and BepF promote the establishment of invasome structures that are morphologically indistinguishable from those triggered by *Bhe* wild-type. To exclude the existence of additional effector combinations competent to provoke invasome formation, a Δ bepCG mutant was constructed and was shown in infection experiment on ECs to be unable to stimulate invasome formation. Thus, we conclusively demonstrate that *Bhe* encodes for two different mechanisms that are potent to trigger invasome formation on ECs.

Next, we introduced a new HeLa cell-based model that allows studying invasome formation in full details. *Bhe*-triggered invasomes on HeLa cells were similar to those observed on ECs. Using this new cellular system, we showed that ectopically expressed eGFP-tagged BepC as well as BepF reduced cell fitness dramatically. Nevertheless, infections of eGFP-BepC & eGFP-BepF co-expressing cells with the effector-deficient Δ bepA-G strain promoted invasome establishment, while the effectors alone in the absence of any bacteria did not. Characterization of BepC & BepF-induced invasome formation showed that i) it is sensitive to Cytochalasin D treatment, ii) is accompanied by the inhibition of individual *Bhe* uptake into BCVs and iii) requires the small GTPases Cdc42, Rac1 and their downstream effectors Scar/WAVE and WASp as well as the nucleation complex Arp2/3, as previously shown for BepG-triggered invasome formation [3]. However, assessments of the role of the actin dynamics-regulating protein cofilin1 showed that cofilin1 is essential for BepC/BepF-triggered invasome establishment while it is dispensable for BepG-promoted invasomes. Over-expression of constitutive active cofilin1 S3A mutant and constitutive active LIM kinase

(LIMK) in HeLa cells lead to a significant decrease in BepC/BepF-triggered invasome formation while BepG-promoted invasome establishment was only slightly affected. Infection of siRNA-transfected human umbilical vein endothelial cells (HUVECs) with different *Bhe* strains showed the same pattern as observed on HeLa cells: while BepG-promoted invasome formation was not affected by the cofilin1 knock-down, BepC/BepF-triggered invasome formation was significantly reduced. These results suggest that cofilin1 is central for BepC/BepF-triggered invasome establishment on epithelial and endothelial cells and validate the HeLa cell-based model as suitable to study *Bhe*-promoted invasome formation.

3.2.2 STATEMENT OF MY OWN CONTRIBUTION

The data presented in that manuscript was obtained by me. Exceptions are data relevant for figures 1A and S2B that were generated by Thomas A. Rhomberg. He also created plasmids as well as *Bhe* knock-out strains and originally discovered the BepC & BepF-dependent invasome formation. All experiments performed were designed by me, Thomas A. Rhomberg and Christoph Dehio. The manuscript was written by me and Christoph Dehio.

3.2.3 REFERENCES

1. Schmid MC, Schulein R, Dehio M, Denecker G, Carena I, et al. (2004) The VirB type IV secretion system of *Bartonella henselae* mediates invasion, proinflammatory activation and antiapoptotic protection of endothelial cells. *Mol Microbiol* 52: 81-92.
2. Schulein R, Guye P, Rhomberg TA, Schmid MC, Schroder G, et al. (2005) A bipartite signal mediates the transfer of type IV secretion substrates of *Bartonella henselae* into human cells. *Proc Natl Acad Sci U S A* 102: 856-861.
3. Rhomberg TA, Truttmann MC, Guye P, Ellner Y, Dehio C (2009) A translocated protein of *Bartonella henselae* interferes with endocytic uptake of individual bacteria and triggers uptake of large bacterial aggregates via the invasome. *Cell Microbiol* 11: 927-945.

Combined action of the type IV secretion effector proteins BepC and BepF promotes invasome formation of *Bartonella henselae* on endothelial and epithelial cells

Matthias C. Truttmann, Thomas A. Rhomberg and Christoph Dehio*

Focal Area Infection Biology, Biozentrum of the University of Basel, Klingelbergstrasse 70, CH-4056 Basel, Switzerland.

Summary

Bartonella henselae (*Bhe*) can invade human endothelial cells (ECs) by two distinguishable entry routes: either individually by endocytosis or as large bacterial aggregates by invasome-mediated internalization. Only the latter process is dependent on a functional VirB/VirD4 type IV secretion system (T4SS) and the thereby translocated Bep effector proteins. Here, we introduce HeLa cells as a new cell system suitable to study invasome formation. We describe a novel route to trigger invasome formation by the combined action of the effectors BepC and BepF. Co-infections of either HUVEC or HeLa cells with the Bep-deficient $\Delta b e p A - G$ mutant expressing either BepC or BepF restores invasome formation. Likewise, ectopic expression of a combination of BepC and BepF in HeLa cells enables invasome-mediated uptake of the *Bhe* $\Delta b e p A - G$ mutant strain. Further, eGFP-BepC and eGFP-BepF fusion proteins localize to the cell membrane and, upon invasome formation, to the invasome. Furthermore, the combined action of BepC and BepF inhibits endocytic uptake of inert microspheres. Finally, we show that BepC and BepF-triggered invasome formation differs from BepG-triggered invasome formation in its requirement for cofilin1, while the Rac1/Scar1/WAVE/Arp2/3 and Cdc42/WASP/Arp2/3 signalling pathways are required in both cases.

Introduction

Bartonella henselae (*Bhe*) is a worldwide distributed, Gram-negative, zoonotic pathogen. Cats serve as reservoir hosts and transmission of *Bhe* from cat to cat mostly occurs by cat fleas. In contrast, incidental transmission of *Bhe* from cats to humans typically results from cat scratches or bites (Dehio, 2004). Human infections with *Bhe* can manifest in a broad spectrum of clinical symptoms. Immuno-competent patients typically develop cat-scratch disease, characterized by local lymph node swelling and fever (Florin *et al.*, 2008). In contrast, immuno-compromised patients often develop bacillary angiomatosis or peliosis, which manifest as vasoproliferative lesions in skin or liver respectively. These tumour-like lesions arise from bacterial infection of vascular endothelial cells (ECs) leading to enhanced ECs migration and proliferation (Dehio, 2005).

Colonization of vascular ECs by *Bhe* can be studied *in vitro* by infection of cultured primary human umbilical vein endothelial cells (HUVECs) or endothel-derived hybridoma Ea.hy926 cells (Kyme *et al.*, 2005; Rhomberg *et al.*, 2009; Scheidegger *et al.*, 2009). Most of the cellular phenotypes of EC infection by *Bhe* depend on the VirB/VirD4 system (Schmid *et al.*, 2004), a type IV secretion system (T4SS) ancestrally related to bacterial conjugation machineries (Schroder and Dehio, 2005). The VirB/VirD4 T4SS was shown to translocate seven distinct effector proteins, namely BepA to BepG (*Bartonella*-translocated effector proteins) into infected ECs (Schulein *et al.*, 2005; Dehio, 2008). The Bep proteins share a modular domain structure with at least one BID domain (*Bartonella* intracellular delivery) present near the C-terminus of each effector. Together with a positively charged C-terminal tail sequence, the BID domain serves as a bi-partite translocation signal for the Beps (Schulein *et al.*, 2005; Dehio, 2008). In contrast, the N-terminal Bep architecture is less conserved. BepA, BepB and BepC all contain a single FIC domain, while BepD, BepE and BepF display tyrosine repeat motifs in their N-terminal portion that have been demonstrated to recruit host proteins upon tyrosine phosphorylation (Schulein *et al.*, 2005; Dehio, 2008; Selbach *et al.*, 2009). In contrast, BepG consists of four BID

Received 7 June, 2010; revised 20 September, 2010; accepted 22 September, 2010. *For correspondence. E-mail christoph.dehio@unibas.ch; Tel. (+41) 61 267 2140; Fax (+41) 61 267 2118.

domains flanked by small linker regions (Schulein *et al.*, 2005; Pulliainen and Dehio, 2009; Rhomberg *et al.*, 2009). BepA to BepG promote all so far described VirB/VirD4-dependent cellular phenotypes resulting from *Bhe* infection of ECs: (i) activation of the pro-inflammatory response, (ii) inhibition of apoptosis, (iii) capillary-like sprout formation of EC aggregates and (iv) uptake of large *Bhe* aggregates by a unique cellular process termed invasome-mediated internalization (Schulein *et al.*, 2005; Schmid *et al.*, 2006; Rhomberg *et al.*, 2009; Scheidegger *et al.*, 2009; Selbach *et al.*, 2009). *Bhe* internalization via the invasome route is a tightly controlled multi-step process (Dehio *et al.*, 1997). At its initiation, bacteria accumulate on the EC cell surface and form aggregates consisting of hundreds of bacteria. These bacterial aggregates are successively engulfed by plasma membrane-derived membrane protrusions, eventually resulting in their complete internalization. The kinetics of invasome-mediated *Bhe* uptake is slow, taking at least 16 h to completion. In contrast, individual bacteria or small clusters can invade ECs via a VirB/VirD4-independent endocytic route within minutes, resulting in the formation of *Bartonella*-containing vacuoles (BCVs) that localize to the perinuclear space (Dehio *et al.*, 1997; Rhomberg *et al.*, 2009). Interestingly, invasome formation is accompanied by the inhibition of endocytic uptake of individual bacteria into BCVs. In previous work, we demonstrated that BepG is the only *Bartonella* effector required for triggering invasome formation on ECs. Moreover, we could show that BepG inhibits uptake of *Bhe*, *Y. enterocolitica* or inert fluorescent microspheres into Ea.hy926 cells. Although primary ECs or Ea.hy926 cells represent good models to study the cellular processes underlying *Bhe* uptake, there are several limitations of ECs as cellular models compared with other well-established laboratory cell lines. Primary ECs cannot be grown to high passage numbers without losing endothelial characteristics and show donor variability in cell growth and behaviour in infection assays. In addition, siRNA or DNA transfection of Ea.hy926 cells and especially primary ECs with standard methods is inefficient compared with other cell types. The human cervix carcinoma cell line HeLa (Gey *et al.*, 1952) is an epithelial cell line that is widely used to study cell invasion by both viral and bacterial pathogens (Jones *et al.*, 1981; Goodwin *et al.*, 2009; Snijder *et al.*, 2009). Due to the ease to transfect HeLa cells, they have been utilized in several RNAi-based studies focusing on pathogen internalization (Goodwin *et al.*, 2009). Here, we introduce a HeLa cell-based *in vitro* system that allows studying invasome formation. Using the new HeLa cell system, in parallel with the well-established HUVEC/Ea.hy926 EC models, we characterized a new route of invasome formation that is based on the combined action of the effector protein BepC and BepF. We show that

BepC- and BepF-triggered invasome formation is sensitive to cytochalasin D, a potent inhibitor of F-actin polymerization and depends on Rac1/Scar1/WAVE/Arp2/3 and Cdc42/WASP/Arp2/3 signalling pathways. Finally, we demonstrate that BepC/BepF-triggered invasome formation differs from BepG-promoted invasome formation in its requirement for cofilin1.

Results

B. henselae Δ bepG strain triggers invasome formation

Recently, we reported that in the effector-free Δ bepA-G mutant background deficient for invasome-mediated internalization BepG is the only individual Bep that restores the formation of invasomes, yet with lower abundance compared with wild-type (Rhomberg *et al.*, 2009). Based on this result we tested whether BepG is required for invasome formation in a wild-type background. To this end, we constructed a Δ bepG mutant strain carrying an in-frame deletion of *bepG*. The Δ bepG strain was tested by infecting HUVECs with a multiplicity of infection (moi) of 100 for 48 h. Upon fixation and staining of F-actin cells were analysed by epifluorescence microscopy. Unexpectedly, infection of ECs with Δ bepG still gave rise to invasomes, even so at a slightly lower abundance than *Bhe* wild-type. Complementation of the Δ bepG mutant strain with plasmid pPG107 encoding FLAG-BepG restored invasome abundance back to wild-type level (Fig. 1A). The invasome structures induced by the mutant strain Δ bepG showed the characteristic F-actin rearrangements surrounding a bacterial aggregate and were indistinguishable from invasomes triggered by wild-type (Fig. S1). These results demonstrate that invasome formation must be promoted by redundant Bep-dependent mechanisms.

Systematic screen for dual effector combinations promoting invasome formation reveals BepC and BepF

To investigate BepG-independent invasome formation, we systematically tested all possible dual combinations of Bep proteins in a standard infection assay on HUVECs. To this end, HUVECs were co-infected with two *Bhe* Δ bepA-G strains expressing individual FLAG-tagged Bep-proteins *in trans* (Δ bepA-G/*pbepA* to Δ bepA-G/*pbepG*). We previously showed that the tested strains stably express the respective FLAG-tagged Bep fusion proteins (Rhomberg *et al.*, 2009). Control infections with individual strains resulted in invasome formation only in case of the BepG-expressing strain, albeit with lower frequency than wild-type (Fig. 1B), thus confirming our published results (Rhomberg *et al.*, 2009). Importantly, in double infection experiments the combination of Δ bepA-G/*pbepC* and Δ bepA-G/*pbepF* turned out to promote the

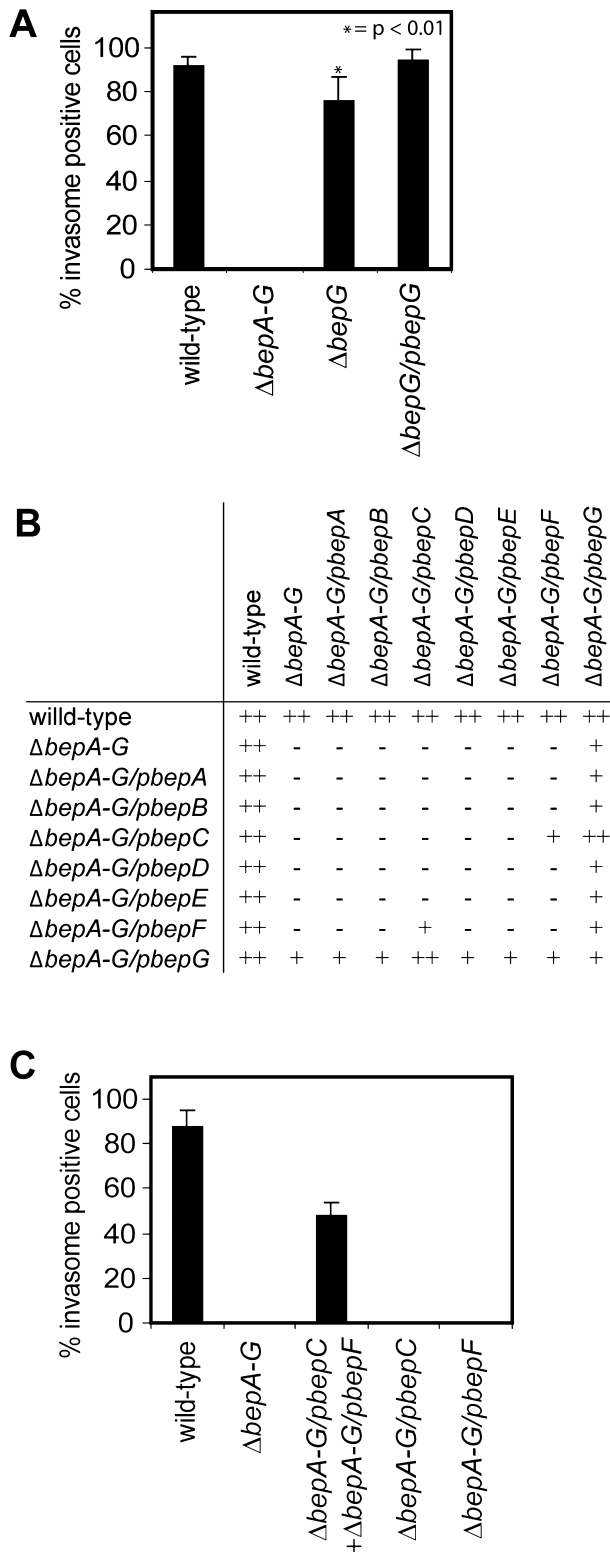


Fig. 1. The combined action of *Bartonella* effector proteins BepC and BepF triggers invasome formation.

A. HUVECs were infected with *Bhe* wild-type, the effector-deficient mutant $\Delta bepA-G$, the *bepG*-deletion mutant $\Delta bepG$, and the isogenic *bepG*-expressing strain $\Delta bepG/pbepG$ at moi = 100 for 48 h. Following fixation, staining with TRITC-phalloidin and DAPI and image acquisition by automated epifluorescence microscopy, invasomes were quantified ($n > 1000$ cells). Using Student's t-test the data marked by an asterisk differ statistically significantly ($P < 0.01$) from wild-type infected control.

B. For evaluation of invasome formation upon double infections, HUVECs were infected for 48 h with a combination of two indicated *Bhe* strains at moi = 100, followed by staining with TRITC-phalloidin and DAPI. Strains tested were wild-type, the effector-deficient mutant $\Delta bepA-G$, or isogenic strains expressing individual Bep proteins ($\Delta bepA-G/pbepA$ to $\Delta bepA-G/pbepG$). The abundance of invasome formation was semi-quantitatively assessed by confocal laser scanning microscopy using the following scoring scheme: ++ = invasome abundance like wild-type; + = invasome abundance lower than wild-type; - = no invasomes. For quantification of BepC and BepF induced invasome formation (C), HUVEC cells were infected for 48 h with indicated strains at moi = 100 per strain, fixed, stained with TRITC-phalloidin and DAPI and imaged by automated epifluorescence microscopy. Invasome formation was quantified semi-automatically ($n > 1000$ cells). Results of at least three independent experiments \pm standard deviation are depicted.

morphological level based on scanning electron and confocal microscopy, there was no obvious difference between invasome structures triggered by wild-type or the combination of $\Delta bepA-G/pbepC$ and $\Delta bepA-G/pbepF$ (Fig. 2A and B). Further to this novel invasome formation route triggered by BepC and BepF, we observed that co-infection of HUVECs with the $\Delta bepA-G/pbepC$ and $\Delta bepA-G/pbepG$ restored invasome formation approximately to wild-type level (Figs 1B and S2), thus indicating a synergistic activity of BepC on BepG-triggered invasome formation. To test whether both *Bhe* strains used in co-infection experiments are internalized together in individual invasome structures, we infected HUVEC cells with GFP- or dsRed-expressing combinations of $\Delta bepA-G/pbepC$ and $\Delta bepA-G/pbepF$ or $\Delta bepA-G/pbepC$ and $\Delta bepA-G/pbepG$ for 48 h. Following fixation and staining, the localization of the different *Bhe* strains expressing either GFP or dsRed was analysed by confocal microscopy (Fig. S3). The results clearly showed that bacteria of both strains mixed inside invasomes without displaying any specific localization within the invasome structures.

In a next step, we constructed single in-frame deletion mutants of *bepC* ($\Delta bepC$) and *bepF* ($\Delta bepF$) and tested them together with the isogenic $\Delta bepG$ mutant for invasome formation on HUVECs. The results showed that the deletion of either *bepC* or *bepG* resulted in a moderate but significant decrease in invasome formation, whereas deletion of *bepF* had no significant effect (Fig. S4A). Complementation of each in-frame deletion mutant *in trans* from a plasmid (strains $\Delta bepC/pbepC$, $\Delta bepF/pbepF$ and $\Delta bepG/pbepG$) restored invasome formation to wild-type levels. These observations indicate that under

establishment of invasome structures on HUVECs (Fig. 1B). Compared with wild-type infected cells, invasome abundance was 35% reduced for the combination of $\Delta bepA-G/pbepC$ and $\Delta bepA-G/pbepF$ (Fig. 1C). On the

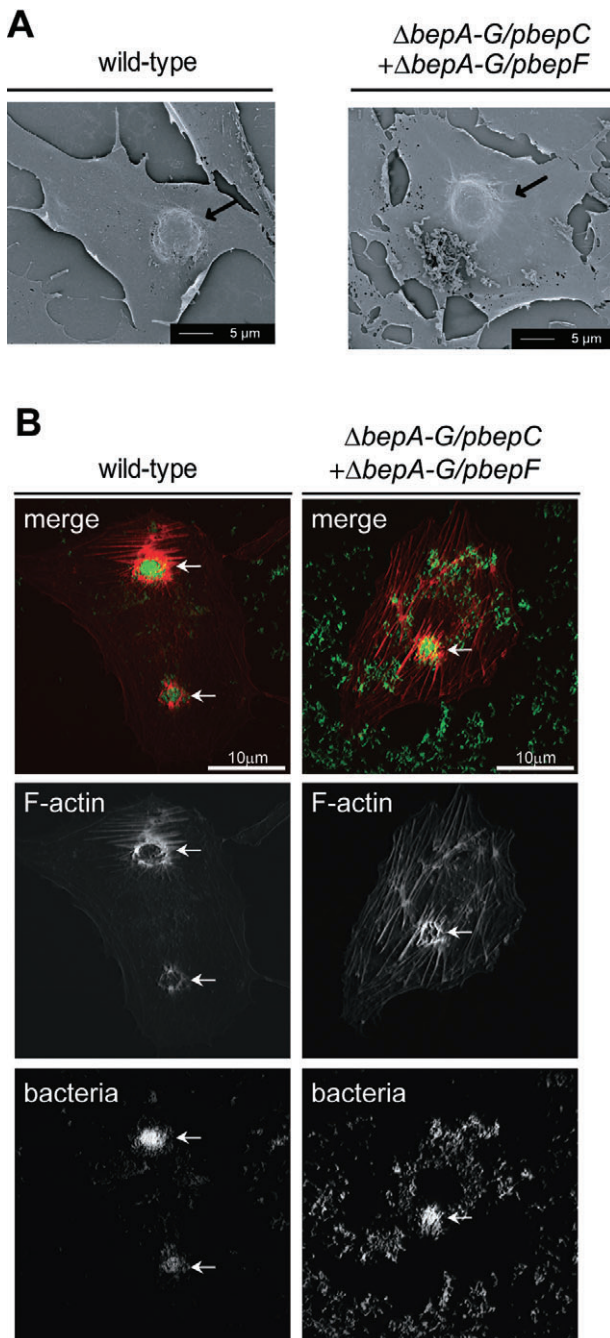


Fig. 2. Microscopic characterization of invasomes induced by BepC and BepF. To compare invasome structures, HUVEC cells were infected for 48 h with *Bhe* wild-type or a 1:1 mixture of $\Delta b e p A - G / p b e p C$ and $\Delta b e p A - G / p b e p F$ at $m o i = 100$, fixed, and (A) processed and analysed by scanning electron microscopy or (B) stained with Cy5-phalloidin and DAPI and visualized by means of confocal microscopy. Invasome structures are marked with an arrow. Scale bars are indicated.

the conditions tested the BepC/BepG pathway is quantitatively the prominent pathway of invasomes formation; however, the difference to the BepC/BepF pathway is only marginal. To test whether the two redundant invasome

formation pathways display different kinetics, HUVECs were co-infected with the above-described strain combinations and samples were fixed at various time points between 12 and 60 h, stained for F-actin and invasome structures were quantified based on confocal laser scanning microscopy. The data demonstrate that BepC/BepF and BepC/BepG combinations trigger invasome structures with indistinguishable kinetics (Fig. S4B). To exclude alternative Bep-dependent invasome formation routes to BepG or BepC/BepF, we constructed the *Bhe* mutant $\Delta b e p C G$ carrying in-frame deletions in *bepC* and *bepG*. Infection assays clearly showed that $\Delta b e p C G$ has lost its capacity to trigger invasome formation on HUVECs (Fig. S4C). Complementation of the $\Delta b e p C G$ mutant with either FLAG-BepC or FLAG-BepG *in trans* restored invasome formation. Taken together, the results highlight that invasome formation on HUVECs is triggered either by BepG alone – with synergistic enhancement by BepC – or by the combined activity of BepC and BepF.

Invasome formation is not unique to endothelial cells

Up to date, invasome formation has been exclusively studied using primary ECs (i.e. HUVECs) or the endothelial-like hybridoma cell line Ea.hy926 (Edgell *et al.*, 1983; Schmid *et al.*, 2004; Rhomberg *et al.*, 2009). Due to their limited transfectability and robustness these cell lines are difficult to use in combined transfection–infection experiments to further study the molecular and cellular basis of invasome formation. In order to define a more robust model system to study invasome formation, we infected HeLa cells, HEK293 cells, and for control HUVECs and Ea.hy926 cells with *Bhe* wild-type, $\Delta b e p A - G$, $\Delta b e p A - G / p b e p G$, or combinations of either $\Delta b e p A - G / p b e p C$ and $\Delta b e p A - G / p b e p F$ or $\Delta b e p A - G / p b e p C$ and $\Delta b e p A - G / p b e p G$ with three different infection doses ($m o i = 100, 300$ or 1000) (Fig. S5A–C). The cervix carcinoma cell line HeLa as well as the embryonic kidney-derived cell line HEK293 (Graham *et al.*, 1977) are both immortalized cell lines of epithelial origin that are widely used to study pathogen entry (Jones *et al.*, 1981; Li *et al.*, 2001; Goodwin *et al.*, 2009; Snijder *et al.*, 2009). As expected, HUVECs and Ea.hy926 cells formed invasomes upon infection with all strains/strain combinations, except for the negative control $\Delta b e p A - G$, at $m o i$ of 100 and 300 while infections at $m o i$ of 1000 were not tolerated by the cells and lead to cell death. In contrast, HeLa cells did not show any invasome formation at the $m o i$ of 100. However, at the higher $m o i$ of 300 and 1000, invasome structures were frequently present on HeLa cells. In contrast, invasome structures were completely absent from HEK293 cells at all tested conditions. To quantify invasome formation on HeLa cells, infections were repeated with the same *Bhe* strain set at the elevated $m o i$ of 500.

After fixation and staining of cells with DAPI and TRITC-phalloidin, invasome formation was determined by automated epifluorescence microscopy. Compared with HUVEC infection, invasome formation on HeLa cells was less prominent with wild-type yielding only ~50% invasome-positive cells (Fig. 3A). Infections with combinations of $\Delta bepA$ -G/*pbepC* and $\Delta bepA$ -G/*pbepF* or $\Delta bepA$ -G/*pbepC* and $\Delta bepA$ -G/*pbepG* resulted in approximately 25% of invasome positive cells, while only 5% of cells infected with $\Delta bepA$ -G/*pbepG* showed invasome formation. Analysis of similar samples by scanning electron or confocal microscopy showed that invasomes on HeLa cells were similar in appearance to invasome structures on HUVECs (Fig. S6A and B). Co-infections with dsRed- or GFP-expressing $\Delta bepA$ -G/*pbepC*, $\Delta bepA$ -G/*pbepF* and $\Delta bepA$ -G/*pbepG* strains showed that, as seen for HUVECs, both strains mixed in invasomes (Fig. S7A). Further, quantification of invasome structures demonstrated that GFP or dsRed expression did not affect *Bhe* infectivity (Fig. S7B).

Taken together, invasome structures on HeLa cells show the typical characteristics described for invasomes on HUVECs, thereby qualifying HeLa as an appropriate model cell line to study the cellular processes underlying invasome formation.

Infection of HeLa cells expressing eGFP-BepC and eGFP-BepF with the effector-deficient strain $\Delta bepA$ -G leads to invasome formation

As a next step, we explored the new HeLa cell model to test whether ectopically expressed *Bhe* effectors can trigger invasome formation. Therefore, HeLa cells were transfected with eukaryotic expression plasmids encoding eGFP-tagged fusions of either BepC or BepF. After 24 h, cells were infected at the moi of 500 with *Bhe* wild-type, $\Delta bepA$ -G/*pbepC*, $\Delta bepA$ -G/*pbepF*, a 1:1 mixture of the latter two strains, $\Delta bepA$ -G/*pbepG* or left uninfected. Following 48 h incubation, cells were fixed, stained and analysed by epifluorescence microscopy. As a first finding, both ectopically expressed eGFP-BepC or eGFP-BepF fusion proteins affected HeLa cell fitness and morphology (Fig. S8A). Expression of eGFP-BepC resulted in frequent cell rounding and detachment within 24 h of incubation, while cells expressing eGFP-BepF regularly showed small actin rearrangements and had in general an elongated appearance. Despite of these phenotypes, invasomes were clearly formed by HeLa cells expressing either eGFP-BepC and being infected with $\Delta bepA$ -G/*pbepF* (approximately 5% invasome-positive cells), or expressing eGFP-BepF and being infected with $\Delta bepA$ -G/*pbepC* (approximately 10% invasome-positive cells) (Figs 3B and S6C). Thus, both eGFP-tagged fusion constructs are functional and contribute to invasome for-

mation upon ectopic expression in HeLa cells. Notably, confocal laser scanning microscopic analysis of GFP localization showed that both fusion proteins were clearly enriched at the site of invasome formation triggered by either BepC/BepF or BepG (Figs 3C and S7B). Next, we determined invasome formation on HeLa cells co-transfected with a combination of plasmids encoding for eGFP-BepC and eGFP-BepF and infected with *Bhe* $\Delta bepA$ -G. Although individual eGFP-tagged effectors were shown to be active upon ectopic expression, co-transfected cells showed invasome formation only at an extremely low frequency (approximately 1%). Nevertheless, the observed invasome structures were indistinguishable from *Bhe* wild-type promoted invasomes (Fig. 4B). Interestingly, ectopic expression of either eGFP-BepC, eGFP-BepF or coexpression of eGFP-BepC + eGFP-BepF significantly decreased invasome formation triggered by *Bhe* wild-type infection. This finding suggests that effector quantities as well as the temporal-spatial distribution in the host cell are critical for invasome formation.

BepC- and BepF-triggered invasome formation is sensitive to the F-actin polymerization inhibitor cytochalasin D

Invasome formation by *Bhe* wild-type or $\Delta bepA$ -G/*pbepG* has previously been shown to be sensitive to cytochalasin D (Dehio *et al.*, 1997; Rhomberg *et al.*, 2009), a drug that caps barbed ends of F-actin filaments, thereby inhibiting actin polymerization (Brown and Spudich, 1979). We tested if this is also the case for invasomes triggered by the combination of strains $\Delta bepA$ -G/*pbepC* and $\Delta bepA$ -G/*pbepF*. To this end, HeLa and HUVECs were infected with *Bhe* wild-type, $\Delta bepA$ -G or a 1:1 mixture of strains $\Delta bepA$ -G/*pbepC* and $\Delta bepA$ -G/*pbepF* for 48 h in the presence of different concentrations of cytochalasin D. Following fixation and staining, invasome formation was quantified. The results showed that invasome formation triggered by wild-type and the combination of $\Delta bepA$ -G/*pbepC* and $\Delta bepA$ -G/*pbepF* display a similar dose-dependent inhibition by cytochalasin D in both endothelial and epithelial cells (Fig. 4A and B).

The combined activity of BepC and BepF inhibits uptake of fluorescent microspheres via an endocytic process

Previously, we have shown using Ea.hy926 cells that invasome formation interferes with the uptake of individual *Bhe* by an endocytic process resulting in the formation of BCVs (Rhomberg *et al.*, 2009). Further, we demonstrated that the effector BepG inhibits internalization of inert microspheres into Ea.hy926 (Rhomberg *et al.*, 2009). To test if this holds true as well for

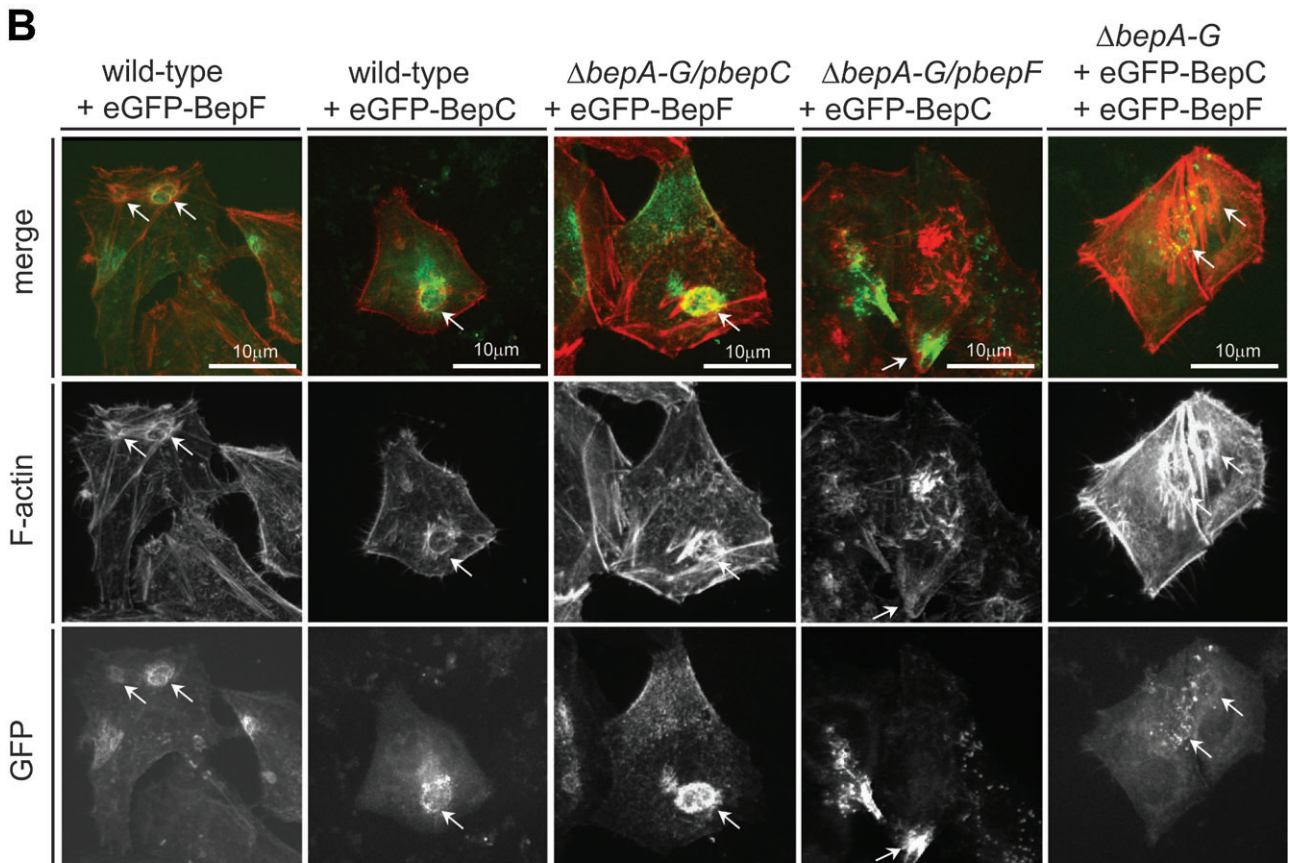
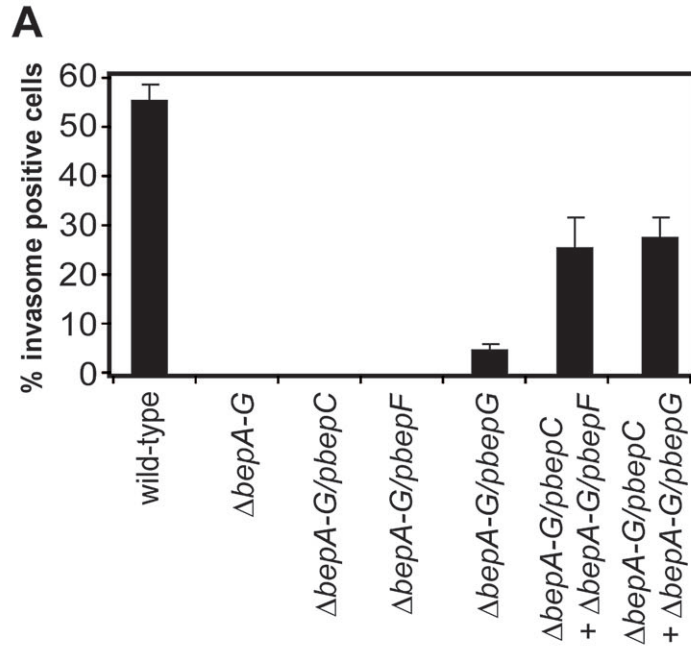


Fig. 3. Invasome formation on HeLa cells.

A. HeLa cells were infected with indicated strains at moi = 500 for 48 h. Cells were fixed, stained with TRITC-phalloidin and DAPI, imaged by automated epifluorescence microscopy and invasomes were quantified ($n > 1000$ cells). Results of at least three independent experiments \pm standard deviation are depicted.

B. HeLa cells were transfected with plasmids encoding for eGFP-BepC (pTR1769), eGFP-BepF (pMT563) or a 1:1 mixture of eGFP-BepC and eGFP-BepF. After 24 h incubation, cells were infected with *Bhe* wild-type, Δ bepA-G, Δ bepA-G/pBepC, Δ bepA-G/pBepF or a 1:1 mixture of Δ bepA-G/pBepC and Δ bepA-G/pBepF at moi = 500 for 48 h, followed by fixation and staining with TRITC-phalloidin and DAPI. Stained cells were analysed by confocal laser scanning microscopy. Invasome structures are marked with an arrow. Scale bars are indicated.

BepC/BepF-induced invasome formation, Ea.hy926 cells were infected at moi of 100 with wild-type, Δ bepA-G, Δ bepA-G/pbepC, Δ bepA-G/pbepF, a combination of Δ bepA-G/pbepC and Δ bepA-G/pbepF, or left uninfected. Twenty-four hours later, bacteria were killed by antibiotic treatment and cells were incubated with BSA-saturated carboxylate-modified polystyrene microspheres for an additional 24 h. Analysis of fixed and stained samples by confocal microscopy revealed that infections with the effector-deficient mutant Δ bepA-G and the BepC- or BepF-expressing derivatives Δ bepA-G/pbepC and Δ bepA-G/pbepF did not affect microspheres internalization, while a co-infection with Δ bepA-G/pbepC and Δ bepA-G/pbepF or infection with wild-type efficiently inhibited microspheres uptake (Fig. 5). These results demonstrate that the combined action of both BepC and BepF effectively inhibits microsphere uptake, similar as we have previously shown for BepG (Rhomberg *et al.*, 2009). Inhibition of endocytic internalization of *Bhe* may contribute to the accumulation of bacteria on the cell surface that eventually get engulfed to form an invasome structure.

BepC/BepF-triggered invasome formation is dependent on the small GTPases Rac1 and Cdc42, the adaptor proteins Scar/WAVE and WASP and the nucleation factor Arp2/3

To test whether BepC/BepF requires the same host cell proteins for invasome formation as we previously reported for BepG (Rhomberg *et al.*, 2009), we performed RNAi knock-down experiments targeting this set of proteins. Therefore, HeLa cells were reverse transfected with siRNA targeting Rac1, Cdc42, WASP, Scar/WAVE, Arp3 or non-targeting control siRNA and incubated for 32 h. Cells were then infected with either *Bhe* wild-type or a combination of strains Δ bepA-G/pbepC and Δ bepA-G/pbepF, and incubated for 48 h. Following fixation and staining of F-actin and nuclei with TRITC-phalloidin and DAPI, respectively, cells were imaged using an automated microscope and invasome formation was semi-automatically quantified. As previously reported for Ea.hy926, the results clearly showed that all five tested proteins play a role in invasome formation on HeLa cells triggered by *Bhe* wild-type, thereby validating the HeLa cell system as a suitable model to study invasome

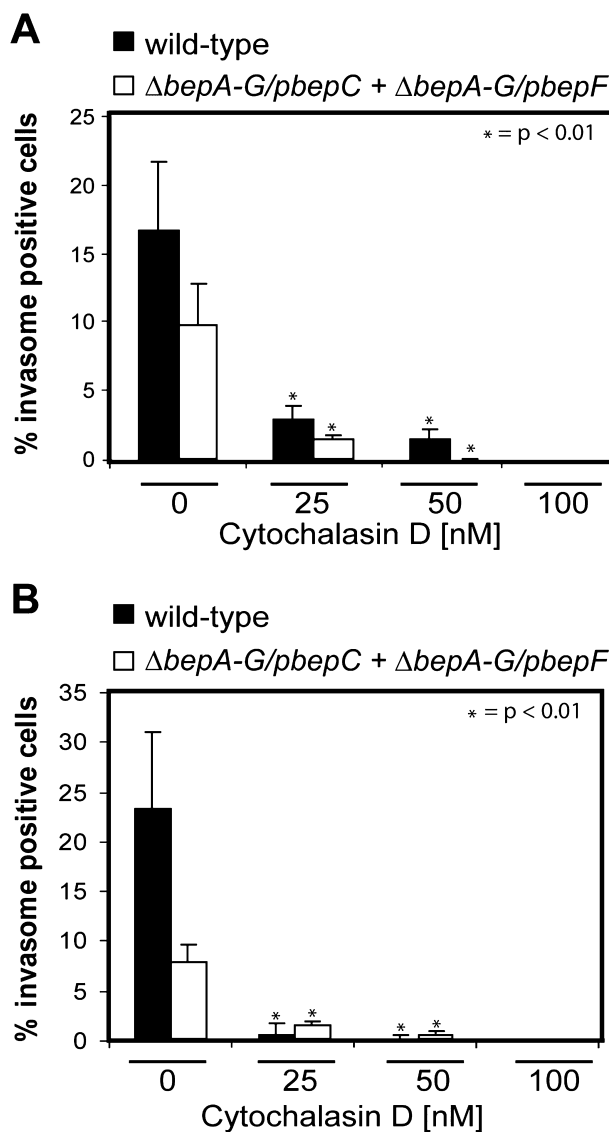


Fig. 4. Invasome formation triggered by BepC and BepF is sensitive to the F-actin polymerization inhibitor cytochalasin D. HeLa (A) or HUVEC (B) cells were infected for 48 h with an moi of 500 or 100, respectively, of *Bhe* wild-type or a 1:1 mixture of Δ bepA-G/pbepC and Δ bepA-G/pbepF in the presence of different concentrations of cytochalasin D. Cells were fixed, stained with TRITC-phalloidin and DAPI, imaged by automated epifluorescence microscopy and semi-automatically quantified ($n > 1000$ cells). Results of at least three independent experiments \pm standard deviation are depicted. Using Student's *t*-test the data marked by an asterisk differ statistically significantly ($P < 0.01$) from untreated control.

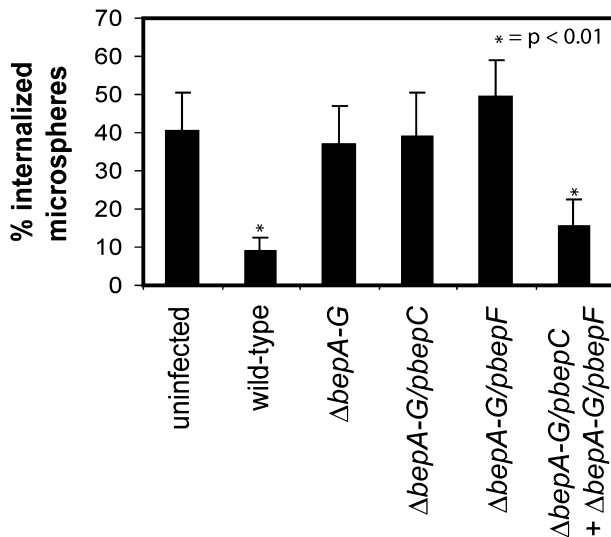


Fig. 5. The combined activity of BepC and BepF inhibits phagocytic uptake of inert microspheres. Ea.hy926 cells were infected with *Bhe* wild-type, $\Delta b e p A - G$, $\Delta b e p A - G / p b e p C$, $\Delta b e p A - G / p b e p F$ or a 1:1 mixture of $\Delta b e p A - G / p b e p C$ and $\Delta b e p A - G / p b e p F$ at $m o i = 100$ and incubated for 24 h. Afterwards, bacteria were killed by the addition of amikacin to reach a final concentration of 40 mg l^{-1} and incubated for 1 h. Following incubation, cells were washed once and M199/10% FCS containing 50 microspheres per cell was added. Cells were incubated for 24 h, fixed, stained with Cy5-phalloidin and DAPI and analysed by confocal laser scanning microscopy. Cells of at least 10 randomly chosen fields of vision were analysed and beads uptake was quantified. Results of at least three independent experiments \pm standard deviation are depicted. Using Student's *t*-test the data marked by an asterisk differ statistically significantly ($P < 0.01$) from uninfected control.

formation (Fig. 6). Importantly, HeLa cells infected with a combination of $\Delta b e p A - G / p b e p C$ and $\Delta b e p A - G / p b e p F$ displayed a similar dependence on the tested host cell proteins as wild-type-infected cells. However, for both tested infection conditions, the siRNA targeting Rac1 displayed the most prominent knock-down phenotype ($> 90\%$ compared with mock control), while also the siRNAs targeting Cdc42, WASP, Scar/WAVE and Arp3 resulted in significant reductions of the frequency of invasome formation.

Cofilin1 is essential for BepC/BepF-mediated invasome formation, but not for BepC/BepG-mediated invasome formation

Since invasome-mediated invasion depends on F-actin remodelling, we wanted to test whether the family of the actin-dynamizing proteins (ADFs), known to control F-actin turnover rates, may play a role in that process. Of special interest was cofilin1 that was previously implicated in contributing to *Listeria monocytogenes* entry into epithelial cells (Bierne *et al.*, 2001). To this end, HeLa cells were transfected with siRNA targeting cofilin1 and incubated for 32 h. Following incubation, cells were infected

with either *Bhe* wild-type, or a combination of either $\Delta b e p A - G / p b e p C$ and $\Delta b e p A - G / p b e p F$ or $\Delta b e p A - G / p b e p C$ and $\Delta b e p A - G / p b e p G$, followed by incubation for another 48 h. After fixation and staining, cells were imaged and invasome formation was quantified. The results showed that cofilin1 knock-down cells infected with either *Bhe* wild-type or $\Delta b e p A - G / p b e p C$ and $\Delta b e p A - G / p b e p G$ displayed no significant reduction in invasome formation compared with mock-transfected cells. In contrast, cells infected with $\Delta b e p A - G / p b e p C$ and $\Delta b e p A - G / p b e p F$ displayed an approximately 70% reduction in invasome positive cells compared with the mock control (Fig. 7A). To validate the specific requirement of cofilin1 for BepC/BepF-mediated invasome formation, we transfected HeLa cells with plasmids encoding for eGFP, cofilin1 wild-type, the cofilin1 S3A mutant or the constitutive active mutant of the Lim kinase (LIMK+). LIM kinases are known to phosphorylate cofilin1 at serine-3, thereby leading to its inactivation. In contrast, the cofilin1 S3A mutant cannot be phosphorylated at Serine-3 and is therefore constitutive active (Bierne *et al.*, 2001; Scott and Olson, 2007). Twenty-four hours after transfection, HeLa cells were infected for 48 h with either *Bhe* wild-type, $\Delta b e p A - G$, or combinations of strains $\Delta b e p A - G / p b e p C$ and $\Delta b e p A - G /$

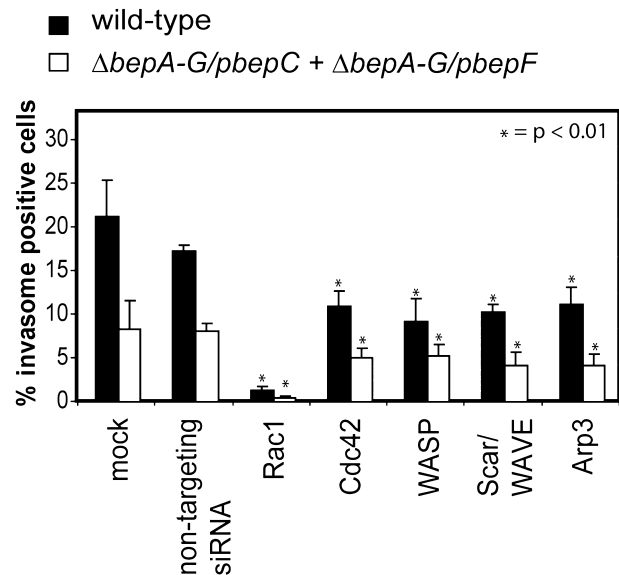
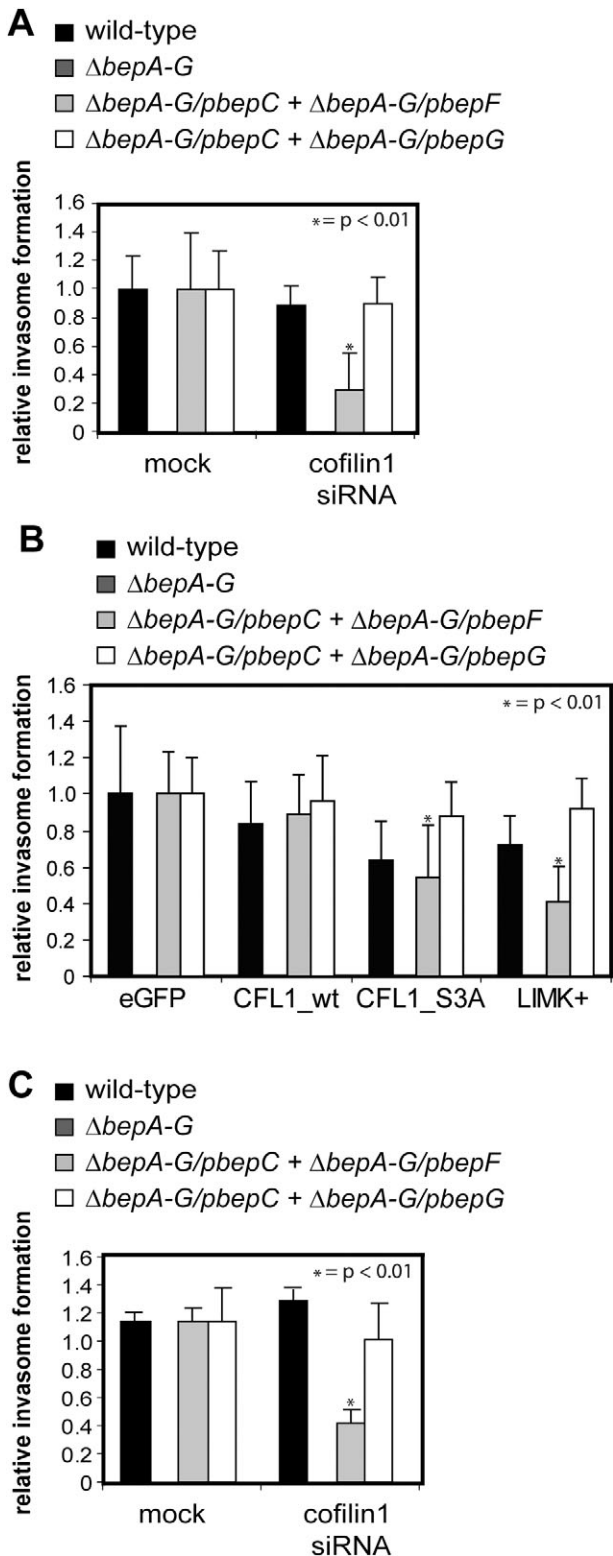


Fig. 6. Invasome formation triggered by BepC and BepF is dependent on the small GTPases Rac1 and Cdc42, the adaptor proteins Scar/WAVE and WASP and the nucleation factor Arp2/3. HeLa cells were transfected with smart-pool siRNA targeting Rac1, Cdc42, Scar/WAVE, WASP, Arp2/3 or non-targeting control siRNA for 36 h and subsequently infected for 48 h at $m o i = 300$ (wild-type) or $m o i = 500$ ($\Delta b e p A - G / p b e p C + \Delta b e p A - G / p b e p F$). Cells were fixed, stained with TRITC-phalloidin and DAPI, imaged by automated epifluorescence microscopy and semi-automatically quantified ($n > 1000$ cells). Results of at least three independent experiments \pm standard deviation are depicted. Using Student's *t*-test the data marked by an asterisk differ statistically significantly ($P < 0.01$) from mock-transfected control.



pbepF or $\Delta bepA-G/pbepC$ and $\Delta bepA-G/pbepG$. Following fixation and staining of F-actin and nuclei with TRITC-phalloidin and DAPI, respectively, cells were imaged and semi-automatically analysed (Fig. 7B). Infection of cells

Fig. 7. Cofilin1 is essential for invasome formation triggered by the combined activity of BepC and BepF, but not by BepG.

A. HeLa cells were transfected with siRNA targeting cofilin1 for 32 h and subsequently infected for 48 h at moi = 500. Cells were fixed, stained with TRITC-phalloidin and DAPI, imaged by automated epifluorescence microscopy and semi-automatically quantified using MetaExpress software ($n > 1000$ cells). Results of at least three independent experiments \pm standard deviation are depicted. Using Student's *t*-test the data marked by an asterisk differ statistically significantly ($P < 0.01$) from mock-transfected control samples.

B. HeLa cells were transfected with plasmids encoding eGFP, cofilin1, cofilin1 S3A or a constitutive active mutant of the LIM kinase. Following 24 h incubation, cells were infected with *Bhe* wild-type, 1:1 mixtures of $\Delta bepA-G/pbepC$ and $\Delta bepA-G/pbepF$ or $\Delta bepA-G/pbepC$ and $\Delta bepA-G/pbepG$ for 48 h at moi = 500, followed by fixation, staining with Cy3-phalloidin and DAPI imaged by automated epifluorescence microscopy and semi-automatically analysed. Normalized results of three independent experiments \pm standard deviation are depicted ($n > 1000$ cells). Using Student's *t*-test the data marked by an asterisk differ statistically significantly ($P < 0.01$) from eGFP-transfected control.

C. HUVEC cells were transfected with siRNA targeting cofilin1 for 32 h and subsequently infected with the indicated strains for 48 h at moi = 100. Cells were fixed, stained, imaged by automated epifluorescence microscopy and semi-automatically quantified ($n > 500$ cells). Mock-transfection normalized results of three independent experiments \pm standard deviation are depicted. Using Student's *t*-test the data marked by an asterisk differ statistically significantly ($P < 0.01$) from mock-transfected control.

ectopically expressing any of the constructs with either *Bhe* wild-type or $\Delta bepA-G/pbepC$ and $\Delta bepA-G/pbepG$ did not significantly decrease invasome formation compared with the control level. However, cells infected with $\Delta bepA-G/pbepC$ and $\Delta bepA-G/pbepF$ showed in comparison to mock transfection a significant decrease in invasome formation of approximately 60% on cells expressing the constitutive active cofilin1 S3A mutant and approximately 50% on cells expressing the constitutive active LIMK+ protein. These results strongly indicate that cofilin1 is indeed a critical factor for BepC/BepF-dependent invasome formation, but not for BepC/BepG-dependent invasome formation.

To test whether cofilin1 is also required for BepC/BepF-dependent invasome formation in cells other than HeLa, we performed similar RNAi knock-down experiments using HUVECs. Therefore, using the Amaxa nucleofection system, HUVECs were transfected with siRNAs targeting cofilin1. Following 32 h incubation, cells were infected with *Bhe* wild-type or a combination of strains $\Delta bepA-G/pbepC$ and $\Delta bepA-G/pbepF$ or $\Delta bepA-G/pbepC$ and $\Delta bepA-G/pbepG$ and incubated for 48 h. After fixation and staining, invasome formation was quantified. The results confirmed the importance of cofilin1 for BepC/BepF-triggered invasome formation (Fig. 7C). Cofilin1 knock-down reduced invasome formation on HUVECs infected with a combination of $\Delta bepA-G/pbepC$ and $\Delta bepA-G/pbepF$ strains by approximately 60%, while wild-type or the combination of $\Delta bepA-G/pbepC$ and $\Delta bepA-G/pbepG$

did not display a decrease in invasome count. To analyse whether cofilin1 might be differentially recruited to the invasome structure by the two distinct pathways for invasome formation, we have infected HUVEC as well as HeLa cells for 48 h with the same strains as described above. After fixation and staining for cofilin1 and F-actin, samples were analysed by confocal laser microscopy. The obtained results illustrate that cofilin1 is enriched in the cortical F-actin ring of approximately 71% and 72% of HUVEC cells infected with wild-type bacteria or the mixed infection with BepC/BepF-expressing strains respectively (Fig. 8A and B). Furthermore, cells infected with BepC/BepG-expressing strains showed significantly less cofilin1 recruitment (38%) to the characteristic F-actin rings of the invasomes on HUVECs. In contrast, there was no cofilin1 recruitment to invasomes detectable in correspondingly infected HeLa cells. In summary, we show that BepC/BepF-dependent invasome formation requires cofilin1, while this major controller of F-actin turnover is not required for BepC/BepG-dependent invasome formation.

Discussion

Bhe-triggered invasome formation is a unique bacterial entry process dependent on the translocation of *Bartonella* effector proteins by the VirB/VirD4 T4SS into ECs that was previously studied exclusively in ECs (Schulein *et al.*, 2005; Schmid *et al.*, 2006). In the present study, we report that HeLa cells infected with *Bhe* wild-type establish well defined invasome structures, albeit at least a three-time-higher moi is required. This observation may result from reduced effector translocation efficiency, arising from a weaker interaction of *Bhe* with the HeLa cell surface, as reported elsewhere (Kaiser *et al.*, 2008). Despite of this, the new HeLa system has proven to be suitable to study *Bhe*-triggered invasome establishment.

In previous work, we demonstrated that the effector protein BepG is sufficient to trigger the formation of invasomes on Ea.hy926 cells (Rhomberg *et al.*, 2009). Here, we characterize a novel Bep-dependent route of invasome formation. We show that independently from BepG, the combined action of BepC and BepF promotes invasome formation on both HeLa and HUVEC cells. In addition, we demonstrated that BepC acts synergistically with BepG by enhancing BepG-triggered invasome formation.

BepC is composed of an N-terminal FIC domain (Kinch *et al.*, 2009) and a single BID domain close to its C-terminus. In contrast, BepF harbours a tyrosine-repeat motif near its N-terminus and contains an array of three BID domains in the C-terminal part. Selbach *et al.* (2009) demonstrated that phosphorylated peptides displaying the tyrosine-repeat motif of BepF interact with the SH2-domain containing signalling and adaptor proteins Grb2, RasGAP and Crk. However, there is yet no direct evi-

dence of the involvement of one of those proteins in the process of invasome formation. Interestingly, the domain structure of BepG consists exclusively of an array of four BID domains (Rhomberg *et al.*, 2009). Earlier work on Bep translocation emphasized that only the most C-terminal BID domain is required for effector translocation (Schulein *et al.*, 2005). It is thus conceivable to assume that the additional BID domains of BepF and BepG may have evolved effector functions crucial for the process of invasome formation (Saenz *et al.*, 2007; Dehio, 2008). However, sequence comparisons of *Bhe* BID domains showed that the BID domains of BepF and BepG are poorly conserved and are not closer related to each other than to the BID domains of the other Bep effectors that are not involved in invasome formation (Schulein *et al.*, 2005). The lack of domain and sequence conservation between BepF and BepG suggests that these effectors may trigger invasome formation via independent rather than by shared host targets. It will be an interesting subject for future studies to elucidate which domains of the structurally distinct effectors BepC, BepF and BepG are functionally involved in triggering invasome formation.

The ability of elements that are structurally different to perform the same function is termed degeneracy, also often referred to as functional redundancy (Edelman and Gally, 2001). It was demonstrated that *S. enterica* serovar Typhimurium double mutants disrupting *sopB* and *sopE* gene function had a more pronounced virulence defect in bacterial entry than either of the single mutants, indicating considerable functional redundancy between several translocated effector proteins (Miroid *et al.*, 2001). Moreover, *Salmonella* actin-binding proteins SipA and SipC were demonstrated to directly modulate host actin dynamics in a redundant manner to facilitate bacterial uptake (Zhou and Galan, 2001). In the case of *Bhe*-promoted invasome formation both BepC/BepF and BepG-triggered routes depend on drastic actin cytoskeleton rearrangements and inhibit the uptake of inert microspheres into Ea.hy926 cells. We assume that the BepC/BepF- or BepG-dependent inhibition of endocytic uptake of individual *Bhe* is a prerequisite to allow bacteria to aggregate on the cellular surface. Since *Bhe* are tightly anchored by surface-expressed bacterial ligand(s) to the cell surface, it is likely that bacterial aggregation relies on the clustering of yet not identified host cell receptors. This receptor clustering may activate cellular signalling cascades eventually leading to the engulfment of the *Bartonella* aggregates resulting in invasome formation. The observed recruitment of BepC and BepF to the site of invasome formation is probably an indirect event, either by binding of the effectors to the cytoplasmic tails of transmembrane receptors that do cluster due to invasome formation or by the recruitment of cellular signalling components that act locally beneath the

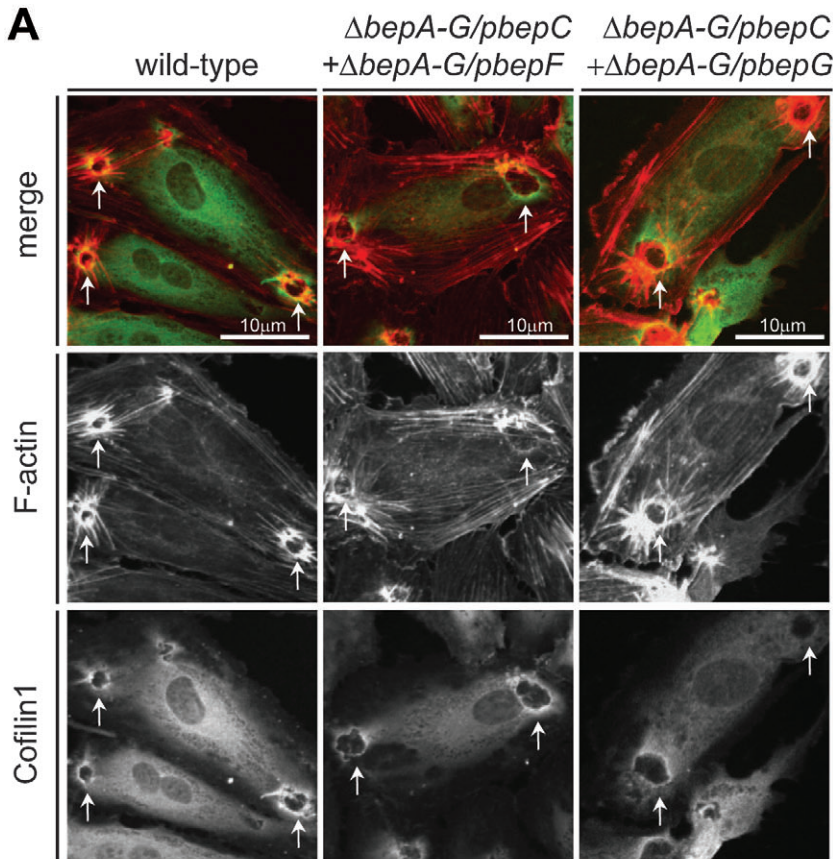
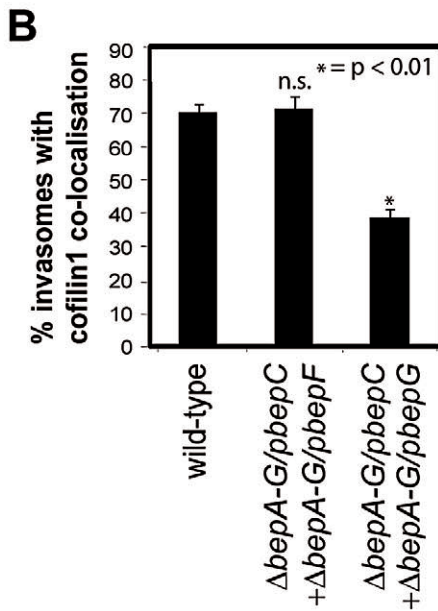


Fig. 8. BepC/BepF- and wild-type-triggered invasomes on HUVEC cells display increased cofilin1 recruitment. HUVEC cells were infected with *Bhe* wild-type, a 1:1 mixture of $\Delta bepA-G/pbepC$ and $\Delta bepA-G/pbepF$, or $\Delta bepA-G/pbepG$ with an moi of 100 for 48 h. A. Following incubation, cells were fixed, stained with Cy3-phalloidin, DAPI and anti-cofilin1 antibody and imaged using a confocal laser scanning microscope. Invasomes are marked with white arrows. Scale bars are indicated.

B. Cofilin1 colocalization with invasomes on cells of at least 10 randomly chosen fields of vision was quantified. Results of at least three independent experiments \pm standard deviation are depicted. Using Student's *t*-test the data marked with an asterisk ($P < 0.01$) differ statistically significantly from wild-type control.



forming invasome structure. However, the available data do not allow concluding whether or not BepC together with BepF contribute to invasome formation further than to the inhibition of endocytic uptake of individual bacteria or

smaller aggregates. As previously shown for BepG-triggered invasome formation, BepC/BepF-dependent invasome establishment involves Rac1/Scar1/WAVE/Arp2/3- and Cdc42/WASP/Arp2/3-dependent F-actin

modulations. In addition, cofilin1, an actin-modulating protein, was identified to be essential for BepC/BepF-triggered invasome formation, whereas BepG-promoted invasome formation does not depend on cofilin1. Cofilin1 controls F-actin turnover rates by both increasing F-actin depolymerization and severing actin filaments (Van Troys *et al.*, 2008). It is known to be essential for InIB-induced phagocytosis of *L. monocytogenes* and its involvement in *L. monocytogenes* actin-based motility (Bierne *et al.*, 2001). Interestingly, both constitutive active cofilin1 S3A and overexpression of constitutive-active LIMK1, which leads to phosphorylation-dependent inactivation of cofilin1, significantly decreased invasome formation. These results indicate that invasome formation may depend on both F-actin filament elongation as well as F-actin depolymerization. Our results do not elucidate why cofilin1 is important only for BepC/BepF-promoted invasome formation. Nevertheless, the gathered findings indicate that BepC and BepF may act at an intermediate level of the signalling cascade controlling invasome formation, e.g. by controlling GTPase-mediated signalling, while BepG could play its role further downstream in the regulatory network controlling cellular actin dynamics, maybe by direct interaction with actin itself. A direct interaction of BepG with actin could neglect the need for cofilin1. This hypothesis gets supported by the findings that BepC boosts BepG-mediated invasome formation back to almost wild-type levels, that BepC/BepG-dependent invasome formation is not dependent on cofilin1 and that cofilin1 does not localize to BepC/BepG-triggered invasomes on HUVEC cells.

Our current results do not allow explaining why *Bhe* encodes for a redundant system capable to trigger invasome formation on epithelial and ECs. However, degeneracy is a general principle in biology, contributing to an increase in the robustness of relevant biological systems. In cell metabolism, multiple parallel biosynthetic pathways exist to guarantee constant supply of key molecules even upon inhibition of one supplying branch (Becker *et al.*, 2006; Boyd *et al.*, 2008). The fact that invasome formation can be triggered by two functional redundant pathways supports the relevance of the invasome structure to contribute to *Bartonella* host cell entry. However, further investigation of the process of invasome formation is needed to determine the biological role of the here described functional redundancy.

Experimental procedures

Bacterial strains, growth conditions and conjugations

Bartonella henselae strains were cultured following previously described procedures on solid agar plates (Columbia base agar supplemented with 5% sheep blood and appropriate antibiotics). *Escherichia coli* strains were grown in liquid broth or solid agar

plates (Luria–Bertani broth) supplemented with appropriate antibiotics. Triparental matings between *E. coli* and *Bhe* and strains were performed as described (Dehio and Meyer, 1997). Table S1 lists all bacteria strains used in this study.

Construction of in-frame deletion mutants

In-frame deletion mutants were generated as described previously by a two-step gene replacement procedure (Schulein *et al.*, 2005). The basic mutagenesis vector pTR1000 was generated by BamHI digestion of pRS14 (Schulein and Dehio, 2002) and self-ligation of the vector backbone. All mutagenesis plasmids harbour a cassette with the flanking regions of the in-frame deletion in the gene of interest. pTR1069, pTR1075 and pTR1078 used for generating non-polar Δ bepC, Δ bepF, Δ bepG and Δ bepCG in-frame mutants were constructed as follows: oligonucleotide primer pairs prTR057/prTR058, prTR53/54 and prTR082/prTR083 amplified fragments 1 and prTR059/prTR060, prTR55/prTR56 and prTR084/prTR085, amplified fragments 2, which were fused by megaprimer PCR with oligonucleotide primers prTR057/prTR060, prTR053/prTR056 and prTR082/prTR085, resulting in a DNA fragments carrying an in-frame deletion of 1575 bp in bepC, 1382 bp in bepF and 2934 bp in bepG respectively. Using flanking XbaI or BamHI sites the fragments were inserted into the corresponding site of pTR1000, cut accordingly. The use of pTR1069 for gene replacement in RSE247 resulted in the Δ bepC mutant TRB288. The use of pTR1075 in RSE247 resulted in the Δ bepF mutant TRB222. The use of pTR1078 for gene replacement in RSE247 and in TRB288 resulted in the Δ bepG mutant TRB223 and the Δ bepCG mutant TRB286 respectively.

Plasmid construction

DNA manipulations were carried out following standard protocols. Shuttle vector pPG100 and derivatives encoding full-length single Beps (bepA – bepG) have been described (Schulein *et al.*, 2005; Rhomberg *et al.*, 2009). pTR1769 (eGFP–BepC) and pMT563 (eGFP–BepF) were obtained similarly by PCR amplification of full-length bepC or bepF by primer pairs prTR109/prTR112 or prMT67/prMT68, cutting the purified PCR products with XmaI and XbaI and their ligation into pWAY21 (eGFP, Molecular Motion, Montana Laboratories) cut accordingly. Plasmid pTR1169 and pTR1175 were constructed by PCR amplification of full-length bepC or bepF by primer pairs prTR047/prTR019 or prTR017/prTR018, cutting the purified PCR fragments with BamHI and NotI and by their ligation into pFLAG-CMV2 (Invitrogen, CA, USA) cut accordingly. Plasmid pMT353 was constructed by PCR amplification of dsRed by primer pairs prMT156/prMT157, cutting the purified PCR fragments with XbaI and HindIII and by their ligation into pCD353 cut accordingly. All constructs were sequence confirmed. Plasmids pcDNA3-LIMK+, pcDNA3-cofilin1 and pcDNA3-cofilin1_S3A were kindly provided by P. Cossart, Institut Pasteur, Paris, FR (Arber *et al.*, 1998). Table S1 and Table S2 list all plasmids and primers constructed or used or in this study respectively.

Cell lines and cell culture

HeLa Kyoto β cells (Snijder *et al.*, 2009), Ea.hy926 cells (Edgell *et al.*, 1983) and HEK293 cells (Graham *et al.*, 1977) were kept in

DMEM (Gifco, invitrogen) supplemented with 10% FCS. HUVECs were isolated and cultivated as described (Dehio *et al.*, 1997).

Infection and transfection assays

The HUVEC infection assays using glass slides were performed as described (Rhombert *et al.*, 2009). For a standard 96-well plate assay, HUVEC cells (passages 3–6) were seeded at a density of 3000 cells per well the day before infection into gelatine-coated wells of a 96-well plate. Following over-night incubation, cells were washed once with 50 μ l M199/10% FCS and infected with eGFP-expressing *Bhe* at moi of 100 per strain in 100 μ l medium M199/10% FCS supplemented with 500 μ M IPTG (Promega) to induce GFP expression and incubated for 48 h. Cytochalasin D (Sigma) was dissolved in DMSO (Fluka) and added to the final concentrations indicated. Transfection of HUVEC was performed using the Amaxa nucleofection kit (Lonza) according to manufacturer's instructions. Following nucleofection, 5000 cells were seeded per well of a 96-well plate and incubated for 32 h. Infection of transfected cells was performed as mentioned above.

Transfection of HeLa cells was initiated by seeding 15 000 or 4500 onto glass slides into 24-well plates or into wells of a 96-well plate, respectively. Cells were transfected with Lipofectamine2000 (invitrogen) following manufacturer's instructions. In brief, Lipofectamine2000 was diluted 1:100 in optimem (Invitrogen) and put aside for 5 min (mixA). In the meantime, highly pure DNA or siRNA pools targeting Rac1, Cdc42, Scar/WAVE, WASP, Arp3 (all On-TARGETplus SMART-pool siRNAs from Dharmacon/Thermo Fisher Scientific) or cofilin1 (1:1 pool of experimentally validated siRNAs CFL1-3 and CFL1-6, Qiagen) was diluted at appropriate concentrations in an equivalent volume of optimem (mixB). Next, mixA and mixB were combined, vortexed briefly and incubated for 20–30 min at room temperature. Following incubation, cell medium was exchanged with fresh DMEM/10% FCS and optimem containing the transfection complexes in a 1:1 ratio. In case of DNA transfection, cells were washed once with phosphate-buffered saline (PBS) and supplemented with fresh DMEM/10% FCS medium 6–8 h post transfection. Cells were incubated for 24 h (DNA transfection) or 36 h (siRNA transfection) at 35°C, 5% CO₂.

HeLa infections were basically carried out as described for HUVEC infection assays. Thereby, HeLa cells were washed once with 50 μ l M199/10% FCS and infected with GFP-expressing *Bhe* at moi of 500 per strain in 100 μ l medium M199/10% FCS supplemented with 500 μ M IPTG (Promega). Following 48 h incubation cells were fixed with Para-formaldehyde (PFA).

Microspheres uptake assay was performed strictly following the previously described procedure (Rhombert *et al.*, 2009).

Immunofluorescent labelling

Indirect immunofluorescent labelling was performed as described (Dehio *et al.*, 1997). Standard 96-well plate assays were stained with TRITC-phalloidin (Sigma, 100 μ g ml⁻¹ stock solution, final concentration 1:400), and DAPI (Roche, 0.1 mg ml⁻¹) using a Tecan Eoware freedom pipeting robot. Glassslides for confocal microscopy were stained with Cy3- or Cy5-phalloidine (Sigma, 100 μ g ml⁻¹ stock solution, final concentration 1:100), DAPI and in

some cases a third probe using serum 2037 (polyclonal rabbit anti-*Bhe* total bacteria, 1:100). or cofilin1 antibody (abcam, ab11062). Secondary antibodies for Immunofluorescent used in this study were Cy5-conjugated goat anti-rabbit Ig antibodies (Dianova, Hamburg, Germany, 1:100). For cells incubated with fluorescent microspheres, Cy5-phalloidine was used for staining of F-actin and DAPI for staining of nuclei.

Semi-automatic image analysis and invasome quantification

Experiments performed in 96-well plates were subjected to automated microscopy, using MD ImageXpress Micro automated microscopes. In every well, 10 sites were imaged in up to three different wavelengths depending on the applied cell staining. Images were visualized using MetaExpress software (MDC) and the number of cells per image was determined automatically by MetaExpress in-build analysis modules (CountNuclei). Invasomes on the very same images were defined and counted by eye. Using the automatically determined cell number and the manual invasome count, the percentage of invasome positive cells was calculated using Microsoft Office Excel. In every experiment, at least 500 cells were analysed per condition.

Epi-fluorescence and confocal laser scanning microscopy

For visualization and quantification of cellular structures, specimens in a 96-well plate format were imaged with an MD ImageXpress Micro automated microscope from Molecular devices. In general, 10 images were taken per well. Images were further processed semi-automatically using MetaExpress or CellProfiler; for each quantification, at least 500 cells were analysed. For confocal laser microscopy, the stained samples were analysed using an IQ iXON spinning disc system from Andor in combination with an Olympus IX2-UCB microscope. Z-stacks with 20–30 focal planes with a spacing of 0.1–0.2 μ m were recorded and Xz- and yz-planes were reconstructed using Andor IQ software. Images were exported and finalized using Metamorph, ImageJ and Adobe photoshop.

Scanning electron microscopy

Cells were seeded onto glass slides in a 24-well plate and transfected/infected as described above (infection and transfection assays). After incubation, cells were washed once with cold PBS and fixed with 250 μ l of 2.5% glutaraldehyde in 1 \times PBS for 30 min at room temperature. Afterwards, glutaraldehyde fixative was washed out twice with cold PBS and once with cold ddH₂O and the samples were subsequent dehydrated with either an acetone or Ethanol step gradient (30%, 50%, 70%, 90%, 100%; 15 min each). Dehydration was carried out at 4°C. Following dehydration, samples were critical point-dried and sputter-coated with a 3 nm thick Platin layer. Micrographs were taken on a Hitachi S-4800 field emission scanning electron microscope, using an acceleration voltage of 2 kV.

Acknowledgements

We would like to thank Dr A. Pulliainen for critical reading of the manuscript and Y. Ellner as well as C. Mistl for technical assis-

tance. We are grateful to M. Düggelin and M. Dürrenberger for their excellent SEM service. The University Women's Hospital Basel is acknowledged for providing human umbilical cords. This work was supported by grant 31003A-109925 from the Swiss National Science Foundation, grant 55005501 from the Howard Hughes Medical Institute and grant 51RT-0-126008 (InfectX) from SystemsX.ch, the Swiss Initiative for Systems Biology.

References

- Arber, S., Barbayannis, F.A., Hanser, H., Schneider, C., Stanyon, C.A., Bernard, O., and Caroni, P. (1998) Regulation of actin dynamics through phosphorylation of cofilin by LIM-kinase. *Nature* **393**: 805–809.
- Becker, D., Selbach, M., Rollenhagen, C., Ballmaier, M., Meyer, T.F., Mann, M., and Bumann, D. (2006) Robust *Salmonella* metabolism limits possibilities for new antimicrobials. *Nature* **440**: 303–307.
- Bierne, H., Gouin, E., Roux, P., Caroni, P., Yin, H.L., and Cossart, P. (2001) A role for cofilin and LIM kinase in *Listeria*-induced phagocytosis. *J Cell Biol* **155**: 101–112.
- Boyd, J.M., Lewis, J.A., Escalante-Semerena, J.C., and Downs, D.M. (2008) *Salmonella enterica* requires ApbC function for growth on tricarballoylate: evidence of functional redundancy between ApbC and IscU. *J Bacteriol* **190**: 4596–4602.
- Brown, S.S., and Spudich, J.A. (1979) Cytochalasin inhibits the rate of elongation of actin filament fragments. *J Cell Biol* **83**: 657–662.
- Dehio, C. (2004) Molecular and cellular basis of *Bartonella* pathogenesis. *Annu Rev Microbiol* **58**: 365–390.
- Dehio, C. (2005) *Bartonella*-host-cell interactions and vascular tumour formation. *Nat Rev Microbiol* **3**: 621–631.
- Dehio, C. (2008) Infection-associated type IV secretion systems of *Bartonella* and their diverse roles in host cell interaction. *Cell Microbiol* **10**: 1591–1598.
- Dehio, C., and Meyer, M. (1997) Maintenance of broad-host-range incompatibility group P and group Q plasmids and transposition of Tn5 in *Bartonella henselae* following conjugal plasmid transfer from *Escherichia coli*. *J Bacteriol* **179**: 538–540.
- Dehio, C., Meyer, M., Berger, J., Schwarz, H., and Lanz, C. (1997) Interaction of *Bartonella henselae* with endothelial cells results in bacterial aggregation on the cell surface and the subsequent engulfment and internalisation of the bacterial aggregate by a unique structure, the invasome. *J Cell Sci* **110**: 2141–2154.
- Edelman, G.M., and Gally, J.A. (2001) Degeneracy and complexity in biological systems. *Proc Natl Acad Sci USA* **98**: 13763–13768.
- Edgell, C.J., McDonald, C.C., and Graham, J.B. (1983) Permanent cell line expressing human factor VIII-related antigen established by hybridization. *Proc Natl Acad Sci USA* **80**: 3734–3737.
- Florin, T.A., Zautis, T.E., and Zautis, L.B. (2008) Beyond cat scratch disease: widening spectrum of *Bartonella henselae* infection. *Pediatrics* **121**: e1413–e1425.
- Gey, G.O., Coffman, W.D., C.W., and Kubicek, M.T. (1952) Tissue culture studies of the proliferative capacity of cervical carcinoma and normal epithelium. *Cancer Res* **12**: 264–265.
- Goodwin, E.C., Atwood, W.J., and DiMaio, D. (2009) High-throughput cell-based screen for chemicals that inhibit infection by simian virus 40 and human polyomaviruses. *J Virol* **83**: 5630–5639.
- Graham, F.L., Smiley, J., Russell, W.C., and Nairn, R. (1977) Characteristics of a human cell line transformed by DNA from human adenovirus type 5. *J Gen Virol* **36**: 59–74.
- Jones, G.W., Richardson, L.A., and Uhlman, D. (1981) The invasion of HeLa cells by *Salmonella typhimurium*: reversible and irreversible bacterial attachment and the role of bacterial motility. *J Gen Microbiol* **127**: 351–360.
- Kaiser, P.O., Riess, T., Wagner, C.L., Linke, D., Lupas, A.N., Schwarz, H., et al. (2008) The head of *Bartonella* adhesin A is crucial for host cell interaction of *Bartonella henselae*. *Cell Microbiol* **10**: 2223–2234.
- Kinch, L.N., Yarbrough, M.L., Orth, K., and Grishin, N.V. (2009) Fido, a novel AMPylation domain common to fic, doc, and AvrB. *PLoS ONE* **4**: e5818.
- Kyme, P.A., Haas, A., Schaller, M., Peschel, A., Iredell, J., and Kempf, V.A. (2005) Unusual trafficking pattern of *Bartonella henselae*-containing vacuoles in macrophages and endothelial cells. *Cell Microbiol* **7**: 1019–1034.
- Li, E., Brown, S.L., Stupack, D.G., Puente, X.S., Cheresh, D.A., and Nemerow, G.R. (2001) Integrin alpha(v)beta1 is an adenovirus coreceptor. *J Virol* **75**: 5405–5409.
- Miold, S., Ehrbar, K., Weissmuller, A., Prager, R., Tschape, H., Russmann, H., and Hardt, W.D. (2001) *Salmonella* host cell invasion emerged by acquisition of a mosaic of separate genetic elements, including *Salmonella* pathogenicity island 1 (SPI1), SPI5, and sopE2. *J Bacteriol* **183**: 2348–2358.
- Pulliaainen, A.T., and Dehio, C. (2009) *Bartonella henselae*: subversion of vascular endothelial cell functions by translocated bacterial effector proteins. *Int J Biochem Cell Biol* **41**: 507–510.
- Rhomberg, T.A., Truttmann, M.C., Guye, P., Ellner, Y., and Dehio, C. (2009) A translocated protein of *Bartonella henselae* interferes with endocytic uptake of individual bacteria and triggers uptake of large bacterial aggregates via the invasome. *Cell Microbiol* **11**: 927–945.
- Saenz, H.L., Engel, P., Stoeckli, M.C., Lanz, C., Raddatz, G., Vayssier-Taussat, M., et al. (2007) Genomic analysis of *Bartonella* identifies type IV secretion systems as host adaptability factors. *Nat Genet* **39**: 1469–1476.
- Scheidegger, F., Ellner, Y., Guye, P., Rhomberg, T.A., Weber, H., Augustin, H.G., and Dehio, C. (2009) Distinct activities of *Bartonella henselae* type IV secretion effector proteins modulate capillary-like sprout formation. *Cell Microbiol* **11**: 1088–1101.
- Schmid, M.C., Schulein, R., Dehio, M., Denecker, G., Carena, I., and Dehio, C. (2004) The VirB type IV secretion system of *Bartonella henselae* mediates invasion, proinflammatory activation and antiapoptotic protection of endothelial cells. *Mol Microbiol* **52**: 81–92.
- Schmid, M.C., Scheidegger, F., Dehio, M., Balmelle-Devaux, N., Schulein, R., Guye, P., et al. (2006) A translocated bacterial protein protects vascular endothelial cells from apoptosis. *PLoS Pathog* **2**: e115.
- Schroder, G., and Dehio, C. (2005) Virulence-associated type IV secretion systems of *Bartonella*. *Trends Microbiol* **13**: 336–342.

- Schulein, R., and Dehio, C. (2002) The VirB/VirD4 type IV secretion system of *Bartonella* is essential for establishing intraerythrocytic infection. *Mol Microbiol* **46**: 1053–1067.
- Schulein, R., Guye, P., Rhombert, T.A., Schmid, M.C., Schroder, G., Vergunst, A.C., *et al.* (2005) A bipartite signal mediates the transfer of type IV secretion substrates of *Bartonella henselae* into human cells. *Proc Natl Acad Sci USA* **102**: 856–861.
- Scott, R.W., and Olson, M.F. (2007) LIM kinases: function, regulation and association with human disease. *J Mol Med* **85**: 555–568.
- Selbach, M., Paul, F.E., Brandt, S., Guye, P., Daumke, O., Backert, S., *et al.* (2009) Host cell interactome of tyrosine-phosphorylated bacterial proteins. *Cell Host Microbe* **5**: 397–403.
- Snijder, B., Sacher, R., Ramo, P., Damm, E.M., Liberali, P., and Pelkmans, L. (2009) Population context determines cell-to-cell variability in endocytosis and virus infection. *Nature* **461**: 520–523.
- Van Troys, M., Huyck, L., Leyman, S., Dhaese, S., Vandekerckhove, J., and Ampe, C. (2008) Ins and outs of ADF/cofilin activity and regulation. *Eur J Cell Biol* **87**: 649–667.
- Zhou, D., and Galan, J. (2001) *Salmonella* entry into host cells: the work in concert of type III secreted effector proteins. *Microbes Infect* **3**: 1293–1298.

Supporting information

Additional Supporting Information may be found in the online version of this article:

Fig. S1. The BepG deletion mutant is not impaired in invasome formation. HUVECs were infected for 48 h at moi = 100 with *Bhe* wild-type, the effector-deficient mutant Δ bepA-G, Δ bepG or Δ bepG/pbepG. Cells were fixed, stained with TRITC-phalloidin and DAPI analysed by confocal laser scanning microscopy. Invasome structures are marked with an arrow. Scale bars are indicated.

Fig. S2. BepC boosts BepG-promoted invasome formation. HUVECs were infected for 48 h at moi = 100 with *Bhe* wild-type, the effector-deficient mutant Δ bepA-G, isogenic strains Δ bepA-G/pbepC, Δ bepA-G/pbepG or a 1:1 mixture of Δ bepA-G/pbepC and Δ bepA-G/pbepG. Cells were fixed, stained with TRITC-phalloidin and DAPI and analysed by confocal laser scanning microscopy. Cells of at least 10 randomly chosen fields of vision were quantified. Results of at least three independent experiments \pm standard deviation are depicted. Using Student's *t*-test the data marked with an asterisk ($P < 0.01$) differ statistically significantly from wild-type control.

Fig. S3. *Bhe* strains used in co-infections are both engulfed by invasome structures. HUVECs were infected for 48 h at moi = 100 with a 1:1 mixture of Δ bepA-G/pbepC and Δ bepA-G/pbepF or Δ bepA-G/pbepC and Δ bepA-G/pbepG, expressing either GFP or dsRed. Cells were fixed, stained with Cy5-phalloidin and DAPI and analysed by confocal laser scanning microscopy. Invasome structures are marked with an arrow. Scale bars are indicated.

Fig. S4. *Bhe* Δ bepCG is unable to trigger invasome formation. A. HUVECs were infected with wild-type, Δ bepA-G, Δ bepC, Δ bepF, Δ bepG, Δ bepC/pbepC, Δ bepF/pbepF and Δ bepG/pbepG, at moi = 100 for 48 h. Cells were fixed, stained and analysed by

confocal laser scanning microscopy. Cells of at least 10 randomly chosen fields of vision were quantified. Results of at least three independent experiments \pm standard deviation are depicted. Using Student's *t*-test the data marked with an asterisk ($P < 0.01$) differ statistically significantly from wild-type control.

B. HUVECs were infected with *Bhe* wild-type, Δ bepA-G, a 1:1 mixture of Δ bepA-G/pbepC and Δ bepA-G/pbepF, or Δ bepA-G/pbepG, at moi = 100 for indicated time points. Cells were fixed, stained and analysed by confocal laser scanning microscopy. Results of at least three independent experiments \pm standard deviation are depicted; n.s. indicates not-significant differences ($P > 0.5$) between the indicated conditions based on Student's *t*-test.

C. HUVECs were infected with wild-type, Δ bepA-G, Δ bepG, Δ bepG/pbepG, Δ bepCG, Δ bepCG/pbepC or Δ bepCG, Δ bepCG/pbepG at moi = 100 for 48 h. Cells were fixed, stained and analysed by confocal laser scanning microscopy. Cells of at least 10 randomly chosen fields of vision were quantified. Results of at least three independent experiments \pm standard deviation are depicted. Using Student's *t*-test the data marked by an asterisk differ statistically significantly ($P < 0.01$) from wild-type control. Scale bars are indicated.

Fig. S5. Invasome formation is not restricted to ECs. HUVECs, Ea.hy926, HeLa and HEK293 cells were infected for 48 h at moi of 100 (A), 300 (B) and 1000 (C), respectively, of *Bhe* wild-type, Δ bepA-G, Δ bepA-G/pbepG, or combinations of either Δ bepA-G/pbepC and Δ bepA-G/pbepF or Δ bepA-G/pbepC and Δ bepA-G/pbepG. Following fixation, staining with TRITC-phalloidin and DAPI and automated epifluorescence microscopy, invasome formation was evaluated semi-quantitatively. ++ = reference: HUVEC infected with *Bhe* wild-type; + = invasome abundance comparable to reference; = = invasome abundance lower than reference; – = invasomes absent; CD implicates host cell death due to bacterial overgrowth.

Fig. S6. Invasome formation on HeLa cells. Invasome formation on HeLa cells was analysed after infection for 48 h with an moi of 500 of *Bhe* wild-type or a 1:1 mixture of Δ bepA-G/pbepC and Δ bepA-G/pbepF.

A and B. Cells were fixed and (A) processed and analysed by scanning electron microscopy, or (B) stained with Cy5-phalloidin and DAPI and visualized by confocal microscopy. Invasome structures are marked with an arrow. Scale bars are indicated.

C. HeLa cells were transfected with plasmids encoding for eGFP–BepC (pTR1769), eGFP–BepF (pMT563) or a 1:1 mixture of eGFP–BepC and eGFP–BepF. After 24 h incubation, cells were infected with *Bhe* wild-type, Δ bepA-G, Δ bepA-G/pbepC, Δ bepA-G/pbepF or a 1:1 mixture of Δ bepA-G/pbepC and Δ bepA-G/pbepF at moi = 500 for 48 h, followed by fixation and staining with TRITC-phalloidin and DAPI. Stained cells were imaged by automated epifluorescence microscopy and invasome formation was semi-automatically quantified ($n > 500$ cells). Results of at least three independent experiments \pm standard deviation are depicted here. Using Student's *t*-test the data marked by an asterisk differ statistically significantly ($P < 0.05$) from wild-type-infected control.

Fig. S7. GFP or dsRed expression in *Bhe* does not affect infectivity.

A. HeLa cells were infected with indicated *Bhe* strains containing either pCD353 encoding GFP or pMT353 encoding dsRed under control of the *tac-lac* promoter (Dehio and Meyer, 1997; this study) at moi = 500. After 48 h of infection, cells were fixed,

stained with Cy5-phalloidin and DAPI and analysed by confocal microscopy. Invasomes are indicated with arrows. Scale bars are indicated.

B. HeLa cells were infected with indicated *Bhe* strains containing either pCD353 (encoding GFP) or pMT353 (encoding dsRed), or without additional plasmid (Dehio and Meyer, 1997; this study) at moi = 500. After 48 h of infection, cells were fixed, stained with Cy5-phalloidin and DAPI and imaged by automated epifluorescence microscopy. Invasomes were quantified in a semi-automated manner ($n > 1000$ cells). Using Student's *t*-test the data marked with n.s. did not differ in a statistically significant manner ($P > 0.05$).

Fig. S8. Effects of ectopic expression of BepC and BepF in HeLa cells.

A. HeLa cells were transfected with pWay19 (eGFP), pTR1769 (eGFP–BepC) or pMT563 (eGFP–BepF) and incubated for 72 h.

Following incubation, cells were fixed, stained with Cy5-phalloidin and DAPI and visualized by confocal laser scanning microscopy. Scale bars are indicated.

B. HeLa cells were transfected with pTR1769 (eGFP–BepC) or pMT563 (eGFP–BepF) incubated for 24 h and infected with $\Delta bepA-G/pbepG$ for 48 h with an moi of 500. Following incubation, cells were fixed, stained with Cy5-phalloidin and DAPI and visualized by confocal laser scanning microscopy. Invasomes are marked with white arrows. Scale bars are indicated.

Table S1. Bacterial strains and plasmids used in this study.

Table S2. Oligonucleotide primers used in this study.

Please note: Wiley-Blackwell are not responsible for the content or functionality of any supporting materials supplied by the authors. Any queries (other than missing material) should be directed to the corresponding author for the article.

3.3 RESEARCH ARTICLE III

***Bartonella henselae* effector protein BepF exhibits guanine nucleotide exchange factor activity against Cdc42**

Matthias C. Truttmann, Arnaud Goepfert, Shyan H. Low and Christoph Dehio

In preparation for Cellular Microbiology

3.3.1 SUMMARY

Bartonella henselae (*Bhe*) Houston-1 can trigger bacterial uptake via the invasome route by two distinct mechanisms: either by the action of effector protein BepG alone [1] or by the combined action of effectors BepC and BepF [1].

To define the minimal portion of BepF required for BepC/BepF-triggered invasome formation, we tested different *Bhe* strains expressing BepF mutant constructs in standard co-infection experiments with *Bhe* Δ bepA-G/*pbepC*. The results showed that i) the three BidF domains together with the positively charged C-tail are sufficient to contribute to invasome formation and that ii) the N-terminal portion of BepF, although phosphorylated in the host cell, is dispensable for this process. Further, ectopic expression of individual GFP-tagged BidF domains in HeLa cells and subsequent infection of these cells with *Bhe* Δ bepA-G/*pbepC* demonstrated that the domains BidF1 as well as BidF2, but not BidF3 are sufficient to trigger invasome formation together with BepC. Moreover, the disruption of a bacterial GEF-associated WxxxE motif in the BidF1 domain significantly reduced the capacity of BepF to contribute to invasome formation.

Next, we investigated the effect of BepF and individual BepF-derived protein domains on cell morphology. Microscopic analysis of HeLa and NIH 3T3 cells infected with Δ bepA-G/*pbepF* or expressing GFP-tagged individual BidF domains showed that BepF triggers the formation of filopodia-like structures. In contrast, infections with *Bhe* Δ bepA-G/*pbepC* or Δ bepA-G/*pbepG* did not trigger any obvious changes in cell morphology. Interestingly, the ectopic expression of constitutive-active Cdc42 (L61-Cdc42) or Rac1 (L61-Rac1) could substitute for BepF in the process of invasome formation, indicating that BepF may activate Cdc42 and Rac1. To investigate whether BidF1 and BidF2 domains act as GEF for Cdc42 and Rac1, we purified His-tagged BidF1 and BidF2 and tested the domains in guanine nucleotide exchange assays with Cdc42 and Rac1. The obtained data showed that the BidF1 and BidF2 domains possess moderate GEF functionalities against Cdc42 but not Rac1. Concluding, we demonstrate that BepF contributes to invasome formation by activating Cdc42.

3.3.2 STATEMENT OF MY OWN CONTRIBUTION

The data discussed in this manuscript was obtained by me. Arnaud Goepfert contributed by purifying His-tagged BidF1, BidF2, Cdc42 and Rac1. Further, he edited the materials & methods part concerning the protein purification section. Shyan Low performed experiments shown in Figure S6. All experiments performed were designed by me and Christoph Dehio. The manuscript was written by me, Arnaud Gopfert and Christoph Dehio.

3.3.3 REFERENCES

1. Truttmann MC, Rhomberg, T.R., Dehio, C. (In Press) Combined action of the type IV secretion effector proteins BepC and BepF promotes invasome formation of *Bartonella henselae* on endothelial and epithelial cells. Cell Microbiol in press.

***Bartonella henselae* effector protein BepF exhibits guanine nucleotide exchange factor activity against Cdc42**

Matthias C. Truttmann, Arnaud Goepfert, Shyan H. Low and Christoph Dehio*

Focal Area Infection Biology, Biozentrum of the University of Basel,
Klingelbergstrasse 70, CH-4056 Basel, Switzerland

*Corresponding author: Prof. Christoph Dehio
Focal Area Infection Biology
Biozentrum, University of Basel
Klingelberstrasse 70
CH-4056 Basel, Switzerland
Tel. +41-61-267-2140
Fax: +41-61-267-2118
E-mail: Christoph.dehio@unibas.ch

Condensed title: BepF acts as a Cdc42-GEF

Word count: 8765

Summary

The zoonotic pathogen *Bartonella henselae* (*Bhe*) can trigger its own internalization into endothelial or epithelial cells (EnCs / EpCs) either by an endocytosis-like process, giving rise to *Bartonella*-containing vacuoles (BCVs), or by invasome-mediated internalization (Schmid *et al.*, 2004; Dehio *et al.*, 1997). The latter process is strictly dependent on the translocation of *Bartonella* effector proteins (Beps) via the VirB/VirD4 type IV secretion system into human cells (Rhomberg *et al.*, 2009; Schmid *et al.*, 2004). In particular, effector BepG alone or the combination of BepC and BepF subvert the regulation of the host actin cytoskeleton and trigger massive actin rearrangements that lead to the establishment of invasome structures (Truttmann *et al.*, 2010; Rhomberg *et al.*, 2009). In this report, we investigate the molecular function of the effector protein BepF. First, we show that, although phosphorylated in the host cell, the tyrosine-rich repeats of BepF do not contribute to invasome-mediated *Bhe* uptake. Next, we demonstrate that the first two Bids of BepF, BidF1 and BidF2, are sufficient to trigger invasome formation together with BepC. Further, we show that mutating W367 of the WxxxE motif of BidF1 inhibits its ability to contribute to invasome formation. Over-expression of constitutive-active Rho GTPases Rac1 or Cdc42 is shown to pheno-copy BepF in the process of invasome establishment. Next, we demonstrate that BidF1 and BidF2 promote filopodial cell extensions on NIH 3T3 and HeLa cells. Finally, we show that BidF1 and BidF2 trigger nucleotide exchange on Cdc42 but not Rac1, demonstrating a direct activation of Cdc42 by BepF during invasome formation.

Introduction

Bartonella henselae (*Bhe*) is a worldwide distributed, zoonotic pathogen. In its feline reservoir host (cats), it causes intraerythrocytic bacteraemia. Accidental transmission of *Bhe* from cats to humans typically occurs by cat bites or scratches (Dehio, 2004). Human infections with *Bhe* can manifest in a variety of clinical symptoms. They range from the so-called cat-scratch disease in immuno-competent patients to bacillary angiomatosis or peliosis in immuno-compromised persons, respectively (Florin *et al.*, 2008).

Bhe expresses a VirB/VirD4 type IV secretion system (T4SS) that is used to translocate *Bartonella* effector proteins (Beps) BepA to BepG into the host cell cytosol (Schmid *et al.*, 2006; Schmid *et al.*, 2004). The Bep effectors share a common basal architecture, consisting of at least one Bid domain (*Bartonella* intracellular delivery) close to their respective C-terminus and a variable N-terminal part (Schulein *et al.*, 2005). This single Bid domain, together with a positively charged C-tail, acts as a bi-partite translocation signal for the Bep translocation (Dehio, 2008; Schulein *et al.*, 2005). Furthermore, effectors BepA, BepB and BepC all contain a single FIC domain in proximity to their respective N-terminus, while BepD, BepE and BepF display tyrosine/proline-rich repeats in their N-terminal portion (Dehio, 2008; Schulein *et al.*, 2005). Interestingly, effectors BepE, BepF and BepG all contain multiple Bid domains while BepG consists exclusively of four Bid domains flanked by short linker regions (Pulliainen and Dehio, 2009; Rhomberg *et al.*, 2009; Schulein *et al.*, 2005).

Bep translocation into the host cell promotes a variety of distinct phenotypes that include: (i) inhibition of apoptosis, (ii) activation of the pro-inflammatory response, (iii) capillary-like sprout formation of EC aggregates and (iv) EnC as well as EpC invasion by a cellular structure named the invasome (Rhomberg *et al.*, 2009; Scheidegger *et al.*, 2009; Selbach *et al.*, 2009; Schmid *et al.*, 2006; Schulein *et al.*, 2005). *Bhe* internalization via the invasome route is a well controlled multi-step process, consisting of *Bhe* adherence to the cell surface, *Bhe* aggregation, *Bhe* engulfment by plasma-membrane-derived membrane protrusions and eventually *Bhe* internalization (Dehio *et al.*, 1997). Invasome formation can be triggered in a redundant manner, either by BepG alone or by the combined action of effectors BepC and BepF (Truttmann *et al.*, 2010; Rhomberg *et al.*, 2009).

Various pathogenic bacteria translocate effector proteins into their respective host cells that interfere with Rho GTPase signaling events (Bulgin *et al.*, 2010; Litvak and Selinger, 2003). Rho GTPases interact in their GTP-bound form with multiple downstream proteins,

thereby transmitting incoming signals to basal levels. In contrast, GDP-bound GTPases are not able to bind to and activate their interaction partners (Tybulewicz and Henderson, 2009). GTPase signaling is in general controlled by GAP, GEF and GDI proteins. While GAPs (GTPase-activating proteins) stimulate the turn-over of the GTP to GDP, GEF (guanine nucleotide exchange factor) increase the exchange rate of GDP with GTP. GDI (guanine nucleotide dissociation inhibitor) bind to the C-terminal lipid group of GTPases, thereby preventing membrane binding and stabilizing them in the inactive state in the cytosol (Tybulewicz and Henderson, 2009; Hoffman *et al.*, 2000). Pathogenic bacteria translocate various GAPs or GEFs into the host cell in order to subvert Rho GTPase signaling: In example, *Salmonella enterica* effector SptP or *Yersinia enterocolitica* effector YopE act as GAPs of Rho GTPases, while the *S. enterica* protein, SopE as well as *Escherichia coli* effector MAP possess GEF functionality on Rho-family G proteins (Bulgin *et al.* 2010; Litvak and Selinger, 2003). Recently, it was shown that many of the translocated bacterial GEF proteins, including SifA and SifB from *Salmonella*, MAP and EspM/M2 from *E.coli* as well as IpgB2 and IpgB1 from *Shigella* share a common Trp-xxx-Glu motif (WxxxE motif) (Bulgin *et al.*, 2010 ; Alto *et al.*, 2006). The WxxxE motif was shown to be essential for GEF function although it is not directly involved in establishing contact with the target Rho GTPases (Huang *et al.*, 2009).

In this study, we characterize the effector protein BepF on molecular level. We investigate the function of the first two Bid domains BidF1 and BidF2 during invasome formation and the promotion of filopodia-like structures. We show that, although phosphorylated in the host cell, the tyrosine-rich repeat motif of BepF does not contribute to BepC/BepF-triggered invasome establishment. Further, we demonstrate that BepF can be pheno-copied with constitutive-active Cdc42 or Rac1. Finally, we demonstrate that BidF1 and BidF2 act as GEF proteins for Cdc42 but not Rac1, thus suggesting a direct regulatory role of BepF on the small Rho GTPases during the process of invasome formation.

Results

BepF tyrosine phosphorylation is not required for invasome formation. In previous work, we have shown that BepC together with BepF can trigger invasome mediated uptake of Bhe into EnCs and EpCs (Truttmann *et al.*, 2010). However, the molecular details of the function of either of the two proteins remained to be determined. *In silico* analysis of the sequence of BepF revealed that BepF contains a tyrosine-rich repeat motif close to its N-terminus

linked to three Bid domains, of which the first and the second Bid domain, BidF1 and BidF2, respectively, are fused together while the third Bid domain, BidF3, is linked via a short spacer sequence to BidF2 (Fig. 1A). Web-based sequence analysis of BepF using NetPhos and Scansite yielded in high probability predictions of multiple tyrosine phosphorylations of the tyrosine-rich motifs [E/T]PLYAT (fig, S1A, B, C). Furthermore, Selbach *et al.* (2009) could demonstrated that short, synthesized peptide fragments containing the [E/T]PLYAT motif of BepF are *in vitro* phosphorylated and interact with Crk, RasGAP and Grb2. To check whether the tyrosine-rich repeats of BepF are indeed phosphorylated upon host cell entry and contribute to invasome formation, we generated two BepF mutants, one having all seven tyrosine replaced with phenylalanine (further referred to as BepF-YF) and one mutant consisting only of the three BidF domains and the positively charged C-tail (further referred to as BidF1-3) (Fig. 1A). HeLa cells were thereafter co-infected with the effector-deficient *Bhe* strain Δ bepA-G expressing FLAG-tagged BepC and *Bhe* Δ bepA-G strains expressing BepF or mutant BepF constructs BepF-YF, BidF1-3 or *in trans* with an MOI = 500 per strain for 48 h. The stability of FLAG-tagged mutant constructs of BepF was verified by Western blotting (Fig. S2A). Following immunoprecipitation using anti-FLAG agarose beads, tyrosine phosphorylation was analyzed by Western blotting. The results clearly showed that wild-type BepF is tyrosine phosphorylated in the host cell, while neither of the two mutants showed any detectable tyrosine phosphorylation signal (Fig. 1B). These results clearly show that the N-terminal tyrosine-containing repeat motifs are indeed phosphorylated in the host cell. Next, we investigated if the tyrosine-rich repeat is required for BepF to contribute to invasome-mediated *Bhe* internalization. Therefore, we infected HeLa cells with *Bhe* Δ bepA-G/pBepC and *Bhe* Δ bepA-G/pbepF, Δ bepA-G/pbepF-YF or Δ bepA-G/pBidF1-3 (Fig. 1C). Quantification of invasome formation of fixed, stained and microscopically imaged cells demonstrated that BidF1-3 was sufficient to trigger invasome formation together with BepC to the same level as wild-type BepF or BepF-YF. To further strengthen that point, we generated eGFP-tagged fusion proteins containing either only the N-terminal part of BepF (NterF) or the BidF1-3 region (Fig. 1D). HeLa cells were thereafter transfected with plasmids encoding for eGFP-BepF, eGFP-NterF and eGFP-BidF1-3 and, after 24 h incubation, infected with *Bhe* Δ bepA-G/pbepC at an MOI = 500 for another 48h. Stable expression of the eGFP-fusion was verified by Western blot (Fig. S2B). The obtained data were in line with our

previous finding: HeLa cells expressing either eGFP-BepF or eGFP-BidF1-3 and infected with *Bhe ΔbepA-G/pbepC* showed invasome formation at a frequency of about 10%, while HeLa cells expressing GFP-NterF and infected with the same strain did not show any invasomes. Taken together, we show that the Bid domains BidF1-3 are sufficient to trigger invasome formation together with BepC. Further, we show that, although tyrosine-phosphorylated in the host cell, the N-terminal tyrosine-containing repeat motif of BepF does not contribute to BepC/BepF-dependent invasome formation.

The Bid domains BidF1 and BidF2 of BepF are sufficient to promote invasome formation together with BepC.

In a next step, we tested whether individual BidF domains could contribute to invasome formation in combination with BepC. Therefore, we first cloned FLAG-tagged BepF mutant constructs that consist of BidF2-3 or BidF3 only and transformed the plasmids into *Bhe ΔbepA-G* (Fig. 1A). Fusion construct expression and stability was tested by Western blot. (Fig. S2A). The new *Bhe* mutant strains *ΔbepA-G/pBidF2-3* and *ΔbepA-G/pBidF3* were tested in co-infection experiments with BepC according to the standard protocol. Quantification of invasome formation on fixed, stained and imaged cells indicated that the removal of the first Bid domain (BidF1) reduced invasome formation by about 70% compared to BidF1-3, while the removal of both BidF1 and BidF2 together lead to a complete abolishment of invasome formation (Fig. 2A). To investigate the capacity of BidF1 and BidF2 to contribute to invasome formation in more details, we generated plasmids encoding for eGFP-tagged constructs eGFP-BidF1, eGFP-BidF2, eGFP-BidF3 and eGFP-BidF1-2. Fusion protein stability was verified by Western blotting (Fig. S2B). Following transfection of HeLa cells with the indicated constructs, cells were infected with *Bhe ΔbepA-G/pbepC* for 48 h. The results showed that both BidF1 and BidF2 together with BepC are able to promote invasome formation while it was absent from cells expressing eGFP-BidF3 and infected with *Bhe ΔbepA-G/pbepC* (Fig. 2B). Interestingly, eGFP-BidF2 was significantly more potent than eGFP-BidF1 to promote invasome establishment and eGFP-BidF1-F2 was promoting invasome formation to the same extent than BidF1-3 in combination with BepC.

Bid domains were initially identified to be required for *Bhe* effector recruitment to the T4SS and the subsequent effector translocation into the recipient cell (Schulein *et al.*, 2005). In previous work, we showed that a fusion of the BidF2 domain with the positively

charged C-tail of BepD was translocated into host cells in a VirB/D4-dependent manner (Schulein *et al.*, 2005). In order to test whether the BidF1 and BidF3 domains are capable to serve as translocation signal, too, we performed Cre Recombinase Reporter Assays for Translocation (CRAFT), in which NLS-Cre-Bid fusion protein transfer into recipient cells triggers a Cre-recombinase-dependent recombination event in the nucleus that eventually initiates GFP expression (Schulein *et al.*, 2005). To this end, Ea.hy926/pRS56-c#B1 cells were infected for 96 h with an MOI = 400 of *Bhe* Δ bepA-G expressing the plasmid-encoded NLS-Cre-BidF1 construct fused to the positively charged C-tail of BepD or the NLS-Cre-BidF3 together with its native C-tail. Following fixation and staining for cell nuclei, GFP-positive cells were automatically counted. NLS-Cre-Bid fusion proteins expression was validated by Westernblotting (S2C). The results demonstrated that both fusion proteins were recognized and translocated in a VirB/D4-dependent manner (Fig. 2C). These findings indicate that the BidF1 and BidF2 function required for invasome formation was acquired in a later stage of effector evolution while the translocation functionality was conserved.

In summary, our results show that BidF1 and BidF2, but not BidF3 domains are individually sufficient to mediate invasome formation in combination with BepC and that BidF1 or BidF3 fused to a positively charged C-tail are translocated in a virB/D4-dependent manner into the host cell.

Disruption of the WxxxE motif in BidF1 interferes with BidF1 function. In 2008, Alto *et al* claimed a newly defined family of bacterial effector proteins, all containing the so-called WxxxE motif, to be mimics of host cell GTPases (Alto *et al.*, 2006). This statement was later revised and it was shown for multiple instances that translocated bacterial proteins containing a WxxxE motif act as GEFs for Rho family GTPases (Arbeloa *et al.*, 2010). Sequence analysis of the BidF domains showed that BidF1 contains a WxxxE motif as well, while BidF2 and BidF3 harbor a closely related motif at the same position, WxxxN. However, amino acid sequence alignments of BidF1, BidF2 and BidF3 with known WxxxE-family GEFs showed low sequence homology besides the motif itself (Fig. 3A). Nevertheless, we decided to further focus on BidF1, since it contains an intact WxxxE motif, and mutated tryptophan-362 into alanine in various BepF-related constructs to disrupt the WxxxE motif (AxxxE). Thereafter, we co-infected HeLa cells according to the standard protocol with *Bhe* Δ bepA-G/pbepC and Δ bepA-G/pbepF W362A, Δ bepA-G /pBidF1-3 W362A or Δ bepA-G /pBidF2-3

and checked for invasome formation. Mutant protein stability was tested by Western blot (Fig. S2A). The obtained results demonstrate that, upon changing the WxxxE motif to AxxxE, the capacity of BepF as well as BidF1-3 to contribute to invasome formation decreased to the level obtained for co-infections with $\Delta bepA$ -G/p**bepC** and $\Delta bepA$ -G/p**BidF2-3**, thus basically eradicating the contribution of BidF1 to the process of invasome formation (Fig. 3B). Next, we introduced the mutation into our eGFP-fusion constructs and quantified invasome formation on HeLa cells expressing eGFP-fusion proteins and infected with *Bhe* $\Delta bepA$ -G /p**BepC** following standard protocols. GFP-fusion protein stability was tested by Western blot (Fig. S2B). These results were in line with our previous findings: the introduced W362A mutation in eGFP-BidF1-F2 decreased invasome formation down to the level found for eGFP-BidF2 alone in combination with BepC. Furthermore, mutating the WxxxE motif in eGFP-BidF1 significantly decreased invasome formation compared to wild-type eGFP-BidF1. Comparing the amino acid sequences of BidF domains with characterized WxxxE-family GEF proteins, we identified a conserved serine residue located six amino acids downstream of the glutamic acid of the WxxxE motif (Fig. 3A). This serine was present in all WxxxE-family proteins except for SifA, while being present in BidF2 but absent in BidF3. To test whether this serine residue may play a role in BidF1 and BDF2 functionality during invasome formation, we constructed mutant constructs encoding for GFP-BidF1 S372A, GFP-BidF1 W362A / S372A and GFP-BidF2 S508A. The constructs were tested in standard transfection-infection assays and invasome formation was quantified after 48 h of infection with *Bhe* $\Delta bepA$ -G/p**BepC**. The results showed that mutation of serines 372 and 508 did not affect invasome formation, implying that the indicated residue is not critical to maintain BidF1 and BidF2 domain function and structure (Fig. S3).

Concluding, our results indicate that the WxxxE motif found in BidF1 is essential for the function of the BidF1 domain and that the conserved serine residue downstream of the WxxxE motif is not critical to maintain BidF1 and BidF2 functionality.

BepF can be substituted by *in trans* expression of constitutive active Cdc42 or Rac1 during BepC/BepF-mediated invasome formation. Several bacterial effectors containing the WxxxE motif were shown to act as GEFs for the small GTPases RhoA, Rac1 and Cdc42 (Bulgin *et al.*, 2010). Previous work on *Bhe*-triggered invasome formation has further demonstrated that Cdc42 and Rac1, but not RhoA, are required for invasome formation (Truttmann *et al.*,

2010; Rhomberg *et al.*, 2009). To test whether BepF interferes with Rac1- or Cdc42-mediated signaling, we transfected HeLa cells with plasmids encoding for myc-tagged constitutive active (c-a) Cdc42 (L61-Cdc42) and Rac1 (L61-Rac1). After 24 h of incubation, cells were infected with *Bhe* Δ bepA-G/pBepC at an MOI = 500 and incubated for another 48 h. Following fixation and staining, invasome formation was quantified (Fig. 4). Our results showed that *Bhe* Δ bepA-G/pBepC could indeed promote invasome formation on HeLa cells expressing either L61-Rac1 or L61-Cdc42. Further, we also observed a more than 50% increase in invasome formation on HeLa cells expressing either c-a GTPase and infected with *Bhe* Δ bepA-G/pBepC and Δ bepA-G /pbepF compared to empty vector transfected cells. Interestingly, invasome formation on HeLa cells expressing the c-a GTPases and infected with *Bhe* wild-type decreased compared to the empty vector control, thereby confirming previous published results (Rhomberg *et al.*, 2009).

Taken together, we show that BepF can be replaced by c-a GTPases during the process of invasome formation. The fact that artificial substitution of BepF with Cdc42, or Rac1 leads to significantly less invasome formation as the combined action of BepC/BepF indicates that the activity of Cdc42 and Rac1 is essential for certain steps of invasome establishment but may act rather inhibitory on other aspects of the entire process.

BepF triggers the formation of filapodia-like extension on HeLa and Swiss 3T3 cells.

Although BepF has been shown to infrequently trigger the formation of small actin foci, the function of BepF has mainly been investigated in the context of invasome formation (Truttmann *et al.*, 2010). However, the finding that the c-a GTPases Cdc42 and Rac1 can substitute for BepF function suggested checking for a BepF-specific phenotype on the actin cytoskeleton level that is comparable to the effect of c-a Cdc42 or Rac1. To this end, we infected HeLa cells with various *Bhe* strains at a high MOI (1000) for 48 h to trigger maximal phenotypic penetrance. After cell fixation, we analyzed the cells transmission electron microscopy (TEM). Uninfected as well as *Bhe* Δ bepA-G, Δ bepA-G/pBepC or Δ bepA-G/pbepG infected HeLa cells showed low levels of filapodia-like structures. (Fig. 5A). In contrast, infection of the HeLa cells with *Bhe* wild-type or *Bhe* Δ bepA-G/pBepF induced a drastic change in cell morphology: cells showed massive formation of filopodia-like structures. In addition, there were also dominant structures interconnecting the individual cells with each

other. The previously reported small actin foci promoted by BepF on HUVECs were completely absent on HeLa cells.

In a next step, we tested our eGFP-BidF fusion constructs in the same TEM-based assay. We found that BidF1 as well as BidF2, but not BidF3 or BidF1 AxxxE induced the massive formation of filopodial extensions (Fig. S4). To strengthen our findings, we repeated the experiments with the eGFP-fusion constructs in NIH 3T3 cells, a cellline well known for a highly responsive actin cytoskeleton that is often used to study stress fibers, lamellipodia and filopodia formation upon system perturbation (Guillou *et al.*, 2008). To this end, we transfected serum-starved NIH 3T3 cells with indicated plasmids encoding for eGFP-fusion constructs as well as proper controls. After fixation and staining, cells we analyzed the actin cytoskeleton phenotype of GFP-positive cells. The results showed that eGFP-tagged full-length BepF, BidF1 and BidF2 induced a change in actin cytoskeleton morphology that is phenotypically identical to the expression of c-a Rac1 or c-a Cdc42 in these cells while neither eGFP control, eGFP-tagged BidF3 nor eGFP-tagged BidF1 AxxxE fusion proteins affected the F-actin organization of NIH 3T3 cells (Fig. 5B, S5). In summary, our data strongly suggest that BepF and in particular BidF1 is involved in the activation of Rac1 and Cdc42 in a WxxxE-dependent manner.

BidF1 and BidF2 harbor GEF activity against Cdc42. In order to test whether BidF1 and BidF2 directly interact and regulate the Rho GTPases Cdc42 and Rac1, we constructed expression plasmids encoding BidF1 or BidF2 fused to a C-terminal hexa-his tag. When ectopically expressed in cells, HIS-BidF1 was shown to promote invasome formation together with BepC (Fig. S6). The protein domains were over-expressed in *E. coli* and purified as described in the materials and methods section. The purified proteins were used in guanine nucleotide exchange assays to check for the capacity of BidF constructs to trigger nucleotide exchange on recombinant Cdc42 and Rac1. Purified SopE and plain assay buffer served as assay controls. The results from the in vitro GEF assay demonstrated that BidF1 as well as BidF2 exhibit GEF activity against Cdc42 but not Rac1 (Fig. 6A, B). Compared to SopE, an extremely potent GEF protein that activates Cdc42 and Rac1 in seconds, BidF1 and BidF2 displayed delayed and only moderate GEF activities. Nevertheless, the measured counts per minute (cpm) were significantly higher for BidF1 and BidF2 compared to buffer only. Interestingly, while SopE activity decreased over 60 minutes from approximately 40 000

cpm (1 minute) to 16 000 (60 minutes), BidF1 and BidF2 activities steadily increased from approximately 3500 cpm (1 minute) to more than 25 000 cpm (60 minutes). Taken together, our results indicate that BepF may act as a specific GEF protein against Cdc42 but not Rac1, however, with slower kinetics than SopE.

Discussion

The *Bartonella henselae* effector protein BepF has previously been implicated in triggering invasome formation together with BepC in a cofilin1-dependent manner (Truttmann *et al.*, 2010). Here, we show that the individual Bid domains BidF1 and BidF2, but not BidF3 are sufficient to promote invasome formation together with BepC. Sequence analysis of the three BidF domains implies that BidF2 and BidF3 are more homologue to each other than to BidF1; however, the general level of sequence homology is low. Thus, from sequence comparison it is not evident why BidF1 and BidF2 can contribute to invasome formation while BidF3 cannot. Moreover, there is also no indication for a common host target of BidF1 and BidF2 on sequence level. Interestingly, all three BidF domains, when fused to a positively charged C-tail, enable fusion protein translocation into the host cell. Whether or not this original Bid function is still required in all three domains is unclear. However, it could be speculated that the multiple Bid domains prime BepF and also BepG to be translocated as early substrates while Beps containing a single Bid domain such as BepA-BepD align further down in the translocation hierarchy. However, our data do not allow concluding on that aspect. Nevertheless, the fact that all three BidF domains still possess the ability to act as a translocation signal indicates that they may have emerged due to partial gene duplications of an ancestral Bep protein containing a single Bid domain and fusions thereof. The additional functionality required for invasome formation probably evolved as a secondary event upon the accumulation of mutations in the BidF1 and BidF2 domains (Saenz *et al.*, 2007).

Besides the three BidF domains, BepF contains a tyrosine-rich repeat motif that is phosphorylated in the host cell upon effector translocation. Interestingly, the replacement of all tyrosine residues as well as the complete removal of that protein portion did not interfere with BepC/BepF-mediated invasome formation, nor with BepF triggered formation of filopodial cell extensions. It is tempting to assume that BepF may interact with multiple SH2-domain containing proteins that can bind to the phosphor-tyrosine scaffold of BepF.

However, we were so far unable to identify a cellular phenotype that is linked to the N-terminal portion of this translocated effector protein.

The interference with Rho GTPases to subvert host signaling cascades is a frequent function associated with translocated bacterial effector proteins. Several distinct mechanisms have been reported yet, including bacterial GEF and GAP proteins (SopE, SptP) (Bulgin *et al.*, 2010), covalent modification of the target GTPases by AMPylation (VopS, IbpA) (Roy and Mukherjee, 2009), glucosylation (TcdA/B) (Just *et al.*, 1995) or ADP-rybosylation (C3) (Sehr *et al.*, 1998) as well as the deamidation (CNF1) (Fiorentini *et al.*, 1997) and partial proteolytic degradation (YopT) (Iriarte and Cornelis, 1998) of Rho-family G proteins. In this report, we show that BepF can be replaced by constitutive-active CDC42 or Rac1 in the process of invasome formation. The findings that neither c-a GTPase was as potent as BepF to contribute to invasome formation and that over-expression of both c-a GTPases interfered with BepC/BepF- or *Bhe* wild-type promoted invasome assembly suggests that the tempo-spatial control of Cdc42 and Rac1 activity is important for the establishment of invasome structures. This hypothesis is in accordance with the published data on invasome formation, which showed that the assembly of the massive actin structure is followed by the eventual retraction of the actin arrangement that leads to the release of the bacteria into the host cell (Dehio *et al.*, 1997). The constitutive activation of Cdc42 and Rac1 that both control processes associated with F-actin filament elongation and cell protrusion formation may be central for the assembly of the invasome structure but rather disadvantageous for the retraction and the disassembly thereof. Next, we demonstrate that BidF1 and BidF2, but not BidF3 domains trigger the formation of filopodial cell extensions on HeLa and NIH 3T3 cells. Filopodia formation is a well characterized process controlled by Cdc42 activity, while the formation of lamellipodia is controlled by Rac1 (Nobes and Hall, 1995). Several bacterial pathogens abuse the cellular machineries controlling filopodia and lamellipodia formation to enable their own internalization. For example, *S. enteritica* serovar *typhimorium* injected effector proteins SopE1 / SopE2 activate Cdc42 and Rac1 simultaneously, promoting *Salmonella* entry, associated with characteristic membrane ruffling (Hardt *et al.*, 1998). The fact that we did not observe increased lamellipodia formation in cells expression BidF1 or BidF2 suggests that Rac1 is not targeted by these two protein domains, as indicated by the finding that BidF1 and BidF2 exhibit GEF functionality on Cdc42 but not Rac1. Compared to SopE, BidF1 and BidF2 domains contain moderate GEF activities with slow kinetics.

However, the *Shigella* WxxxE effector protein IpgB2 shows also only limited GEF activity on RhoA at equal GEF:GTPase ratios as used in this study and does not reach full RhoA activation in 30 minutes (Klink *et al.*, 2010). Moreover, the measured GEF activity of BidF1, BidF2 and IpgB2 is comparable to the activity of the RhoA-GEF protein EspM2 on Cdc42 (Arbeloa *et al.*, 2010). For multiple reasons, there is no comparable quantitative data published on the GEF activity of the WxxxE-effector proteins SifA, SifB, IpgB1 and MAP (Ohya *et al.*, 2005; Dean and Kenny, 2004). Thus, with respect to published data on WxxxE-GEF proteins, the GEF activity kinetics of BidF1 and BidF2 are in the range of IpgB2 and are substantially slower than the potent non-WxxxE GEF protein SopE. Recent work on bacterial GEF proteins suggested that they may act in a multi-protein complex rather than in a GEF-GTPase interaction (Bulgin *et al.*, 2010). This could explain why bacterial WxxxE GEF proteins performed rather poorly in *in vitro* nucleotide exchange assays that lack any potential additional cellular interaction partner and why we were unable to detect any evidence for direct interaction of BidF1 / BidF2 with Cdc42.

As BidF1 contains an intact WxxxE motif, it is tempting to speculate that BepF is a further WxxxE-family bacterial GEF protein. Mutation of the motif abolished BidF1 function on invasome formation and the promotion of filopodial structures. Recent work on the WxxxE GEF proteins suggested that the motif itself may have mainly structural roles, in particular by maintaining the conformation of the putative catalytic loop through hydrophobic contacts with surrounding residues (Huang *et al.*, 2009). BidF2 contains a WxxxN motif at the respective position, that has comparable electro-chemical properties and may stabilize a similar structural conformation as WxxxE. However, sequence alignments of the distinct WxxxE-GEF proteins together with the comparison of available GEF-GTPase co-structures indicate that the WxxxE-GEF protein share more than only the common WxxxE-motif (Bulgin *et al.*, 2010 ; Huang *et al.*, 2009). They display several key residues that directly contact the GTPase interface and are important for GEF function. In contrast, alignments of BidF1 and BidF2 showed that both domains lack all of these described critical residues besides the central WxxxE motif. Thus, BepF may not represent a classical WxxxE-family GEF protein.

We previously showed that BepC and BepF together mediate invasome formation on various cell types (Truttmann *et al.*, 2010). Further, we showed that this process depends on Cdc42, Rac1 and their subsequent downstream signaling partners (Truttmann *et al.*, 2010;

Rhomberg *et al.*, 2009). With respect to the results presented on this work, the function of BepF in the process of invasome formation is presumably the activation of Cdc42. Thus, BepC may act in a process that is involved in the control of Rac1. BepC consists of a FIC domain and a single c-terminal Bid domain. Recently, FIC domains have been demonstrated to reversibly modify Rho GTPases by AMPylation, thereby inhibiting their interaction with downstream partners (Roy and Mukherjee, 2009). Thus, it is tempting to speculate that i) BepC may negatively regulate Rac1 by AMPylation or ii) BepC may down-regulate the constitutive-active GTPase RhoH, which antagonizes Rac1 activity. However, further work on BepC and the function of its FIC domain is required to answer that question.

In summary, we show that the *Bartonella* effector protein BepF acts as a GEF protein of Cdc42 and that the GEF functionality is contained in the two Bid domains BidF1 and BidF2.

Material and Methods

Bacterial Strains, Growth Conditions, Conjugations. *B. henselae* strains were cultured as previously described on solid agar plates (Columbia base agar supplemented with 5% sheep blood and appropriate antibiotics). *E. coli* strains were grown on solid agar plates (Luria Bertani broth) supplemented with appropriate antibiotics. Triparental matings between *E. coli* and *Bhe* strains were performed as described (Dehio and Meyer, 1997). Supplementary table S1 lists all bacteria strains used in this study.

Plasmid Construction. DNA manipulations were carried out following standard protocols. Vectors pCD353, pMS007, pPG100 and derivatives, pRS79, pMT563 and pTR1769 as well as peGFP-Cdc42, peGFP-Cdc42, pRK5mycL61-Cdc42, pRK5mycL61-Rac1 have been described (see table S1 for plasmid origins). eGFP-Bep fusion plasmids pMT560, pMT562, pMT567, pMT591, pMT592, pMT593, pMT597. pMT612, pMT613 and pMT614 were obtained by PCR amplification of the respective insert with the corresponding primers, cutting the purified PCR products with XmaI and XbaI and their ligation into pWAY21 (eGFP, Molecular Motion, Montana Labs) cut accordingly. pMT001, pMT004, pMT005, pMT030, pMT031 and pMT52 were generated by PCR amplification of the respective insert with the corresponding primers, cutting the purified PCR products with NdeI and their ligation into NdeI-digested pPG100. pMT041 and pMT043 were constructed by PCR amplification of the respective

inserts with the corresponding primers, cutting the purified PCR products with Sall and XmaI and their ligation into pRS79, cut accordingly. Plasmids pMT573, pMT574, pMT575 and pMT579 were cloned by PCR amplification of the respective inserts using corresponding primers, cutting the purified PCR products with NdeI and NcoI and their ligation into pET15b, cut accordingly. All constructs were sequence confirmed. Supplementary tables S1 and S2 list all plasmids and primers constructed or used in this study.

Cell Lines and Cell Culture. HeLa Kyoto β cells (Snijder *et al.*, 2009), NIH3T3 cells (Todaro and Green, 1963) and Ea.hy926/pRS56-c#B1 cells used for CRAfT assay were cultured in DMEM (Gifco, invitrogen) supplemented with 10%FCS.

Infection and Transfection Assays. Transfection and infection of HeLa cells was performed as described (Truttmann *et al.*, 2010). In brief, cells were seeded out, incubated o/n and transfected with DNA using Lipofectamine2000 (invitrogen), following manufacturer's instructions. Cells were washed once with phosphate-buffered saline (PBS) and supplemented with fresh DMEM/10%FCS medium 6-8 h hours post transfection. Cells were further incubated for 24 h at 35°C, 5% CO₂ before continuing with the respective assays.

HeLa infections were carried out as described (Truttmann *et al.*, 2010). In brief, HeLa cells were infected with *Bhe* at a multiplicity of infection (MOI) = 500 in 100 μ l medium M199/10%FCS supplemented with 500 μ M IPTG (Promega). Following 48 h incubation cells were fixed with Para-formaldehyde (PFA).

Transfection of NIH 3T3 cells was performed following manufacturer's instructions. Briefly, cells were seeded out at a density of 30000 / well of a 24 well plate and incubated o/n in serum-free DMEM. The next day, 200 μ l opti-mem was mixed with 2 μ g of plasmid DNA and 6 μ l of lipofectamine2000 and incubated for 30min. Afterwards, 100 μ l of the transfection mix was added to the cells together with 400ul of fresh DMEM10%FCS and incubated for 4 h. Then, medium was exchanged with 500 μ l fresh DMEM10%FCS and cells were incubated for 48 h at 35°C, 5% CO₂.

Immunoprecipitation (IP) and Immunoblot analysis. IP was performed as described elsewhere (Selbach *et al.*, 2009). Expression of novel N-terminal FLAG-tagged and NLS-Cre-Bep fusion proteins was verified by analysis of total *Bhe* lysates obtained from *Bhe* grown on

CBA plates contained 500 μ M IPTG. Proteins were run on a SDS-PAGE gel for separation and transferred onto nitrocellulose membranes (Hybond, Amersham Biosciences) and probed either against the FLAG epitope using mouse monoclonal anti-FLAG antibody M2 (Sigma, 1:1000) or against the Cre epitope using polyclonal anti-Cre antibody (EMD Biosciences, Novagen, 1:10000). Novel eGFP-Bep fusion proteins were assessed for their stability by analysis of total cell lysates obtained from HeLa cells transfected with plasmids encoding the respective constructs and incubated for 24 h. After protein separation by SDS-PAGE and transfer onto nitrocellulose, membranes were examined for the presence of eGFP using rabbit monoclonal anti-GFP antibody (Molecular Probes, 1:5000). In all experiments, secondary horseradish peroxidase-conjugated antibody (Amersham, 1:10000) was visualized by enhanced chemiluminescence (PerkinElmer).

Immunofluorescent (IF) labeling. Indirect IF labeling was performed as described (Dehio *et al.*, 1997). Standard 96-well plate assays were stained with TRITC-phalloidin (Sigma, 100 μ g/ml stock solution, final concentration 1:400), and DAPI (Roche, 0.1 mg/ml) using a Tecan Eoware freedom pipeting robot. Glassslides for confocal microscopy were stained with Cy5-phalloidine (Sigma, 100 μ g/ml stock solution, final concentration 1:100), and DAPI.

Cre Recombinase Reporter Assay For Translocation (CRAFT). CRAFT to monitor Bep translocation into the human endothelial cells has previously been described in full details (Schulein *et al.*, 2005). Briefly, 2000 Ea.hy926/pRS56-c#B1 cells were seeded into each well of a 96 well plate. The next day, cells were infected with indicated *Bhe* strains containing plasmids pRS79, pMT041 or pMT043, respectively, at an MOI = 400 in 100 μ l medium M199/10%FCS supplemented with 500 μ M IPTG (Promega). Afterwards, cells were incubated for 96 h, fixed, stained, imaged and analysed as described in the “*Semi-automatic image analysis, invasome quantification and microscopy*” section”.

Protein purification. GST-tagged Cdc42, Rac1 and SopE were expressed and purified according to published protocols: (Hardt *et al.*, 1998; Self and Hall, 1995) for expression and (Smith and Rittinger, 2002) for purification. BidF1, BidF2 and BidF1-2 were expressed as C-terminal hexa-histidine fusion proteins in *E. coli* strain BL21 (DE3) pLysS. *E. coli* Cultures were grown at 37°C in LB medium to an OD₆₀₀ of 0.7 and afterwards induced with 0.1 mM

IPTG for 3 h at room temperature (23°C). Cells were then harvested by centrifugation and resuspended in 50 mM Tris pH8, 500 mM NaCl, 50 mM L-Arg, 50 mM L-Glu, 10 mM imidazole and 1 EDTA-free protease inhibitor cocktail tablet (Roche Diagnostics) and disrupted using French press (40K French pressure cell, Thermo Electron Corporation). Insoluble cell debris was pelleted by ultracentrifugation (45000 rpm, 4°C, 45 minutes). Supernatant was loaded on a 1 mL HisTrap HP column (GE healthcare) pre-equilibrated with 50mM Tris pH8, 500 mM NaCl, 50 mM L-Arg, 50 mM L-Glu, 10 mM Imidazole. Proteins were eluted on FPLC system (Akta purifier, Amersham Biosciences), using different gradients of elution buffer (50 mM Tris pH8, 500 mM NaCl, 50 mM L-Arg, 50 mM L-Glu, 500 mM Imidazole). The eluted proteins were concentrated via an Amicon Ultra device (Millipore) and loaded on a Hiloal Superdex 75 prep grade 16/60 gel filtration column (GE Healthcare), which was pre-equilibrated with 10 mM Tris pH8, 150 mM NaCl, 1 mM DTT. Purified proteins were concentrated and further used for In vitro GEF assays.

In vitro GEF assay. GEF assay was adapted from previously described protocols (Hardt *et al.*, 1998). In brief, 5-10 µg of GTPase were incubated in 100 µl loading buffer (50 mM Tris-HCl pH 7.5, 10 µM GDP, 50 mM NaCl, 3 mM MgCl₂, 0.1 mM DTT) for 90 min at 25°C. Thereafter, GTPase loading was stopped by adding 300 µl ice-cold buffer X (50 mM Tris-HCl pH 7.5, 50 mM NaCl, 5 mM MgCl₂, 0.5 mM DTT) and chilling the samples for 10 min on ice. Afterwards, the GTPase-mix was distributed in equal amounts into 4-8 eppendorf tubes containing 220 µl exchange buffer (50 mM Tris-HCl pH 7.5, 50 mM NaCl, 10 mM MgCl₂, 0.5 mM DTT, 0.1 .mg/ml BSA, 5 µM [H]³-GTP) and i) 0.1 mM EDTA, ii) 1-10 µg SopE or ii) 1-100 µg BidF1, BidF1-F2, BidF2 or BidF3. The reaction mix was further mixed and incubated at 25°C. Samples were withdrawn at indicated time-points, immediately mixed with 800 µl ice-cold buffer X and transferred onto nitrocellulose membranes (Sartorius stedim biotech). Membranes were washed five times with 5 ml of ice-cold wash buffer (50 mM Tris-HCl pH 7.5, 100 mM NaCl, 10 mM MgCl₂) using an active-pressure vacuum device and thereafter air-dried for 60 min. GTP-loading of GTPases was determined by scintillation counting, measuring each sample for two minutes and calculating the counts per minute (cpm). Experiments were repeated with different batches of enzyme & BepF-derived constructs and performed at least in triplicate.

Semi-automatic image analysis, invasome quantification and microscopy. Image analysis and invasome quantification was performed as described (Truttmann *et al.*, 2010). In brief, cells were automatically imaged in up to three different wavelengths depending on the applied cell staining. The number of cells per image was determined by MetaExpress in-build analysis modules (CountNuclei) and invasomes on the very same images were defined and counted by eye. In every experiment, at least 500 cells were analyzed per condition.

For processing of CRAFT experiments, images were analyzed using CellProfiler (Carpenter *et al.*, 2006). In a first step, cell nuclei were identified and subsequently filtered against several shape- and intensity-related parameters to exclude artifacts. Next, the corresponding GFP-signal intensity of each filtered nucleus was calculated from the GFP-image. Finally, the number of GFP-positive nuclei was determined and the percentage of GFP-positive nuclei was calculated. The used CellProfiler pipeline can be found in the online supplementary materials and methods.

Epi-fluorescence, confocal Laser Scanning and scanning electron Microscopy was performed as described earlier (Truttmann *et al.*, 2010).

Acknowledgements

We would like to thank C. Mistl for technical assistance and Phillipp Engel for help with figure 3A. Furthermore we are grateful to M. Düggelein, E. Bieler and M. Dürrenberger from the ZMB for their great SEM service. This work was supported by grant 31003A-132979 from the Swiss National Science Foundation, grant 55005501 from the Howard Hughes Medical Institute and grant 51RT-0_126008 (InfectX) from SystemsX.ch, the Swiss Initiative for Systems Biology.

References

- Alto, N.M., Shao, F., Lazar, C.S., Brost, R.L., Chua, G., Mattoo, S., *et al* (2006) Identification of a bacterial type III effector family with G protein mimicry functions. *Cell*. **124**: 133-145.
- Arbeloa, A., Garnett, J., Lillington, J., Bulgin, R.R., Berger, C.N., Lea, S.M., *et al* (2010) EspM2 is a RhoA guanine nucleotide exchange factor. *Cell Microbiol*. **12**: 654-664.
- Bulgin, R., Raymond, B., Garnett, J.A., Frankel, G., Crepin, V.F., Berger, C.N. and Arbeloa, A. (2010) Bacterial guanine nucleotide exchange factors SopE-like and WxxxE effectors. *Infect Immun*. **78**: 1417-1425.
- Carpenter, A.E., Jones, T.R., Lamprecht, M.R., Clarke, C., Kang, I.H., Friman, O., *et al* (2006) CellProfiler: image analysis software for identifying and quantifying cell phenotypes. *Genome Biol*. **7**: R100.
- Dean, P. and Kenny, B. (2004) Intestinal barrier dysfunction by enteropathogenic *Escherichia coli* is mediated by two effector molecules and a bacterial surface protein. *Mol Microbiol*. **54**: 665-675.
- Dehio, C. (2004) Molecular and cellular basis of bartonella pathogenesis. *Annu Rev Microbiol*. **58**: 365-390.
- Dehio, C. (2008) Infection-associated type IV secretion systems of Bartonella and their diverse roles in host cell interaction. *Cell Microbiol*. **10**: 1591-1598.
- Dehio, C. and Meyer, M. (1997) Maintenance of broad-host-range incompatibility group P and group Q plasmids and transposition of Tn5 in Bartonella henselae following conjugal plasmid transfer from Escherichia coli. *J Bacteriol*. **179**: 538-540.
- Dehio, C., Meyer, M., Berger, J., Schwarz, H. and Lanz, C. (1997) Interaction of Bartonella henselae with endothelial cells results in bacterial aggregation on the cell surface and the subsequent engulfment and internalisation of the bacterial aggregate by a unique structure, the invasome. *J Cell Sci*. **110 (Pt 18)**: 2141-2154.
- Fiorentini, C., Fabbri, A., Flatau, G., Donelli, G., Matarrese, P., Lemichez, E., *et al* (1997) *Escherichia coli* cytotoxic necrotizing factor 1 (CNF1), a toxin that activates the Rho GTPase. *J Biol Chem*. **272**: 19532-19537.
- Florin, T.A., Zaoutis, T.E. and Zaoutis, L.B. (2008) Beyond cat scratch disease: widening spectrum of Bartonella henselae infection. *Pediatrics*. **121**: e1413-1425.
- Guillou, H., Depraz-Depland, A., Planus, E., Vianay, B., Chaussy, J., Grichine, A., *et al* (2008) Lamellipodia nucleation by filopodia depends on integrin occupancy and downstream Rac1 signaling. *Exp Cell Res*. **314**: 478-488.
- Hardt, W.D., Chen, L.M., Schuebel, K.E., Bustelo, X.R. and Galan, J.E. (1998) *S. typhimurium* encodes an activator of Rho GTPases that induces membrane ruffling and nuclear responses in host cells. *Cell*. **93**: 815-826.
- Hoffman, G.R., Nassar, N. and Cerione, R.A. (2000) Structure of the Rho family GTP-binding protein Cdc42 in complex with the multifunctional regulator RhoGDI. *Cell*. **100**: 345-356.
- Huang, Z., Sutton, S.E., Wallenfang, A.J., Orchard, R.C., Wu, X., Feng, Y., *et al* (2009) Structural insights into host GTPase isoform selection by a family of bacterial GEF mimics. *Nat Struct Mol Biol*. **16**: 853-860.
- Iriarte, M. and Cornelis, G.R. (1998) YopT, a new *Yersinia* Yop effector protein, affects the cytoskeleton of host cells. *Mol Microbiol*. **29**: 915-929.
- Just, I., Selzer, J., Wilm, M., von Eichel-Streiber, C., Mann, M. and Aktories, K. (1995) Glucosylation of Rho proteins by *Clostridium difficile* toxin B. *Nature*. **375**: 500-503.

- Klink, B.U., Barden, S., Heidler, T.V., Borchers, C., Ladwein, M., Stradal, T.E., *et al* (2010) Structure of *Shigella* IpgB2 in complex with human RhoA: implications for the mechanism of bacterial guanine nucleotide exchange factor mimicry. *J Biol Chem.* **285**: 17197-17208.
- Litvak, Y. and Selinger, Z. (2003) Bacterial mimics of eukaryotic GTPase-activating proteins (GAPs). *Trends Biochem Sci.* **28**: 628-631.
- Nobes, C.D. and Hall, A. (1995) Rho, rac, and cdc42 GTPases regulate the assembly of multimolecular focal complexes associated with actin stress fibers, lamellipodia, and filopodia. *Cell.* **81**: 53-62.
- Ohya, K., Handa, Y., Ogawa, M., Suzuki, M. and Sasakawa, C. (2005) IpgB1 is a novel *Shigella* effector protein involved in bacterial invasion of host cells. Its activity to promote membrane ruffling via Rac1 and Cdc42 activation. *J Biol Chem.* **280**: 24022-24034.
- Pulliainen, A.T. and Dehio, C. (2009) Bartonella henselae: subversion of vascular endothelial cell functions by translocated bacterial effector proteins. *Int J Biochem Cell Biol.* **41**: 507-510.
- Rhomberg, T.A., Truttmann, M.C., Guye, P., Ellner, Y. and Dehio, C. (2009) A translocated protein of Bartonella henselae interferes with endocytic uptake of individual bacteria and triggers uptake of large bacterial aggregates via the invasome. *Cell Microbiol.* **11**: 927-945.
- Roy, C.R. and Mukherjee, S. (2009) Bacterial FIC Proteins AMP Up Infection. *Sci Signal.* **2**: pe14.
- Saenz, H.L., Engel, P., Stoeckli, M.C., Lanz, C., Raddatz, G., Vayssier-Taussat, M., *et al* (2007) Genomic analysis of Bartonella identifies type IV secretion systems as host adaptability factors. *Nat Genet.* **39**: 1469-1476.
- Scheidegger, F., Ellner, Y., Guye, P., Rhomberg, T.A., Weber, H., Augustin, H.G. and Dehio, C. (2009) Distinct activities of Bartonella henselae type IV secretion effector proteins modulate capillary-like sprout formation. *Cell Microbiol.* **11**: 1088-1101.
- Schmid, M.C., Schulein, R., Dehio, M., Denecker, G., Carena, I. and Dehio, C. (2004) The VirB type IV secretion system of Bartonella henselae mediates invasion, proinflammatory activation and antiapoptotic protection of endothelial cells. *Mol Microbiol.* **52**: 81-92.
- Schmid, M.C., Dehio, M., Balmelle-Devauux, N., Scheidegger, F., Biedermann, B. and Dehio, C. (2006) A translocated bacterial protein protects vascular endothelial cells from apoptosis.
- Schulein, R., Guye, P., Rhomberg, T.A., Schmid, M.C., Schroder, G., Vergunst, A.C., *et al* (2005) A bipartite signal mediates the transfer of type IV secretion substrates of Bartonella henselae into human cells. *Proc Natl Acad Sci U S A.* **102**: 856-861.
- Sehr, P., Joseph, G., Genth, H., Just, I., Pick, E. and Aktories, K. (1998) Glucosylation and ADP ribosylation of rho proteins: effects on nucleotide binding, GTPase activity, and effector coupling. *Biochemistry.* **37**: 5296-5304.
- Selbach, M., Paul, F.E., Brandt, S., Guye, P., Daumke, O., Backert, S., *et al* (2009) Host cell interactome of tyrosine-phosphorylated bacterial proteins. *Cell Host Microbe.* **5**: 397-403.
- Self, A.J. and Hall, A. (1995) Purification of recombinant Rho/Rac/G25K from *Escherichia coli*. *Methods Enzymol.* **256**: 3-10.
- Smith, S.J. and Rittinger, K. (2002) Preparation of GTPases for structural and biophysical analysis. *Methods Mol Biol.* **189**: 13-24.

Snijder, B., Sacher, R., Ramo, P., Damm, E.M., Liberali, P. and Pelkmans, L. (2009) Population context determines cell-to-cell variability in endocytosis and virus infection. *Nature*. **461**: 520-523.

Todaro, G.J. and Green, H. (1963) Quantitative studies of the growth of mouse embryo cells in culture and their development into established lines. *J Cell Biol.* **17**: 299-313.

Truttmann, M.C., Rhomberg, T.A. and Dehio, C. (2010) Combined action of the type IV secretion effector proteins BepC and BepF promotes invasome formation of *Bartonella henselae* on endothelial and epithelial cells. *Cell Microbiol.*

Tybulewicz, V.L. and Henderson, R.B. (2009) Rho family GTPases and their regulators in lymphocytes. *Nat Rev Immunol.* **9**: 630-644.

Figure legends and Tables**Figure 1. Tyrosine phosphorylation of BepF is not essential for invasome formation. (A)**

Schematic representation of BepF, the tyrosine phosphorylation sites and the individual domains. The black bars indicate the corresponding size of GFP- or FLAG-tagged BepF truncated constructs used in this study. **(B)** HeLa cells were infected with indicated *Bhe* strains at an MOI = 500 for 48 h. Following anti FLAG-IP, samples were subjected to SDS-PAGE, transferred onto a nitrocellulose membrane and probed using anti-FLAG antibodies (left panel). Upon stripping, membranes were re-probed using anti-phosphotyrosine antibodies (right panel). **(C)** HeLa cells were infected with indicated *Bhe* strains at an MOI = 500 for 48 h. Following fixation, staining with TRITC-Phalloidin and DAPI and image acquisition by automated epifluorescence microscopy, invasomes were quantified (n>500 cells). Results of at least 3 independent experiments +/- standard deviation are depicted. Student's t-test was performed as indicated. **(D)** HeLa cells were transfected with indicated plasmids for 24 h and thereafter infected with *Bhe* Δ bepA-G/pBepC at an MOI = 500 for 48 h. Following fixation, staining with TRITC-Phalloidin and DAPI and image acquisition by automated epifluorescence microscopy, invasomes were quantified (n>500 cells). Results of at least 3 independent experiments +/- standard deviation are depicted. Student's t-test was performed as indicated.

Figure 2. Individual BidF domains BidF1 and BidF2 are sufficient to trigger invasome formation together with BepC. (A) HeLa cells were infected with indicated *Bhe* strains at an MOI = 500 for 48 h. Following fixation, staining with TRITC-Phalloidin and DAPI and image acquisition by automated epifluorescence microscopy, invasomes were quantified (n>500 cells). Results of at least 3 independent experiments +/- standard deviation are depicted. Student's t-test was performed as indicated. **(B)** HeLa cells were transfected with indicated plasmids for 24 h and thereafter infected with *Bhe* Δ bepA-G/pBepC at an MOI = 500 for 48 h. Following fixation, staining with TRITC-Phalloidin and DAPI and image acquisition by automated epifluorescence microscopy, invasomes were quantified (n>500 cells). Results of at least 3 independent experiments +/- standard deviation are depicted. **(C)** Ea.hy926/pRS56-c#B1 cells were infected with indicated *Bhe* strains at an MOI = 400 for 96 h. Following fixation, staining with DAPI and image acquisition by automated epifluorescence microscopy, GFP-positive cells were quantified (n>500 cells). Results of at least 3 independent experiments +/- standard deviation are depicted.

Figure 3. Disruption of the WxxxE motif in BidF1 interferes with BidF1 function during invasome formation. (A) Amino acid sequence alignment of so-far described WxxxE effectors and BepF domains BidF1, BidF2 and BidF3. Homologue amino acids are highlighted in grey to dark depending on the conservation level. **(B)** HeLa cells were infected with indicated *Bhe* strains at an MOI = 500 for 48 h. Following fixation, staining with TRITC-Phalloidin and DAPI and image acquisition by automated epifluorescence microscopy, invasomes were quantified (n>500 cells). Results of at least 3 independent experiments +/- standard deviation are depicted. Student's t-test was performed as indicated. **(C)** HeLa cells were transfected with indicated plasmids for 24 h and thereafter infected with *Bhe* Δ bepA-G/pBepC at an MOI = 500 for 48 h. Following fixation, staining with TRITC-Phalloidin and DAPI and image acquisition by automated epifluorescence microscopy, invasomes were quantified (n>500 cells). Results of at least 3 independent experiments +/- standard deviation are depicted. Student's t-test was performed as indicated.

Figure 4. L61-Cdc42 and L61-Rac1 can substitute for BepF in the process of invasome formation. HeLa cells were transfected with indicated plasmids for 24 h and thereafter infected with *Bhe* Δ *bepA-G/pBepC* at an MOI = 500 for 48 h. Following fixation, staining with TRITC-Phalloidin and DAPI and image acquisition by automated epifluorescence microscopy, invasomes were quantified (n>500 cells). Results of at least 3 independent experiments +/- standard deviation are depicted. Student's t-test was performed as indicated.

Figure 5. BepF triggers the formation of filopodia-like structures. (A) HeLa cells were infected with indicated *Bhe* strains at an MOI = 500 for 48 h. Following fixation, and critical-point drying, cells were visualized by TEM microscopy. Representative images of parallel infections are depicted. Scale bare is indicated. **(B)** Swiss 3T3 cells were serum-starved for 48 h and thereafter transfected with indicated plasmids for 24 h. Following fixation, and staining with TRITC-Phalloidin and DAPI, cells were visualized by confocal microscopy. Representative images of parallel transfections are depicted. Scale bars are indicated.

Figure 6. BidF1 exhibits GEF functionalities against Cdc42 but not Rac1. GEF activity kinetics of BidF1 and BidF2 against **(A)** Cdc42 and **(B)** Rac1 at two different concentrations. SopE and plain assay buffer were used as controls. Time-points and protein concentrations are indicated. Results of at least 3 independent experiments +/- standard deviation are depicted. Using student's t-test the data marked by an asterisk differ statistically significantly ($p < 0.05$) from buffer controls.

Figure S1. In silico analysis of BepF. (A) BepF amino acid sequence. Predicted tyrosine phosphorylation motifs (violet) as well as individual Bid domains BidF1 (red), BidF2 (green) and BidF3 (blue). are highlighted. **(B)** NetPhos tyrosine phosphorylation prediction. **(C)** ScanSite tyrosine phosphorylation predictions.

Figure S2. Stability test of FLAG-, NLS-Cre-, and GFP-tagged fusion constructs. (A) HeLa cells were transfected with indicated plasmids and incubated for 48 h. Following cell lysis, total cell extract was separated by SDS-PAGE, transferred onto a nitrocellulose membrane and probed using anti-GFP antibodies. **(B)** Indicated *Bhe* strains were induced for 48 h on CBA-blood plates and thereafter lysed. Total *Bhe* lysates were separated by SDS-PAGE, transferred onto a nitrocellulose membrane and probed using anti-FLAG antibodies. **(C)** Indicated *Bhe* strains were induced for 48 h on CBA-blood plates and thereafter lysed. Total *Bhe* lysates were separated by SDS-PAGE, transferred onto a nitrocellulose membrane and probed using anti-Cre-recombinase antibodies.

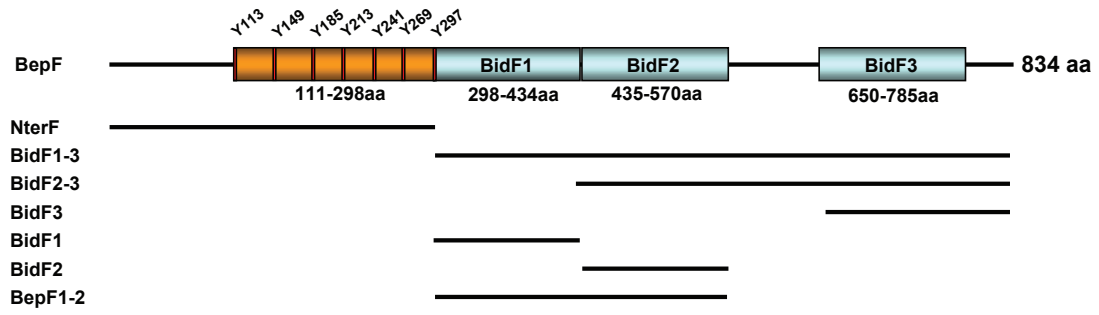
Figure S3. Serine 372 (BidF1) and 508 (BidF2) are not essential for Bid domain function. HeLa cells were transfected with indicated plasmids for 24 h and thereafter infected with *Bhe* Δ *bepA-G/pBepC* at an MOI = 500 for 48 h. Following fixation, staining with TRITC-Phalloidin and DAPI and image acquisition by automated epifluorescence microscopy, invasomes were quantified ($n > 500$ cells). Results of at least 3 independent experiments \pm standard deviation are depicted. Student's t-test was performed as indicated.

Figure S4. BepF triggers the formation of filopodia-like structures on HeLa cells. HeLa cells were transfected with indicated plasmids for 48 h. Following fixation, and critical-point drying, cells were visualized by TEM microscopy. Representative images of parallel infections are depicted. Scale bars are indicated.

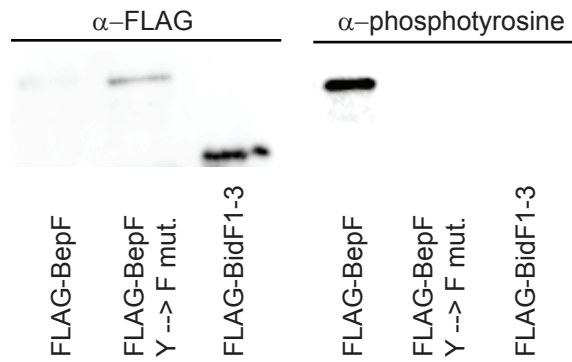
Figure S5. BepF triggers the formation of filopodia-like structures on NIH 3T3 cells. Swiss 3T3 cells were serum-starved for 48 h and thereafter transfected with indicated plasmids for 24 h. Following fixation, and staining with TRITC-Phalloidin and DAPI, cells were visualized by confocal microscopy. Representative images of parallel transfections are depicted. Scale bars are indicated.

Figure S6. Hexa-HIS-tagged BidF1 is functional in invasome formation. HeLa cells were transfected with indicated plasmids for 24 h and thereafter infected with *Bhe ΔbepA-G/pBepC* at an MOI = 500 for 48 h. Following fixation, staining with TRITC-Phalloidin and DAPI and image acquisition by automated epifluorescence microscopy, invasomes were quantified (n>500 cells). Results of at least 3 independent experiments +/- standard deviation are depicted. Student's t-test was performed as indicated.

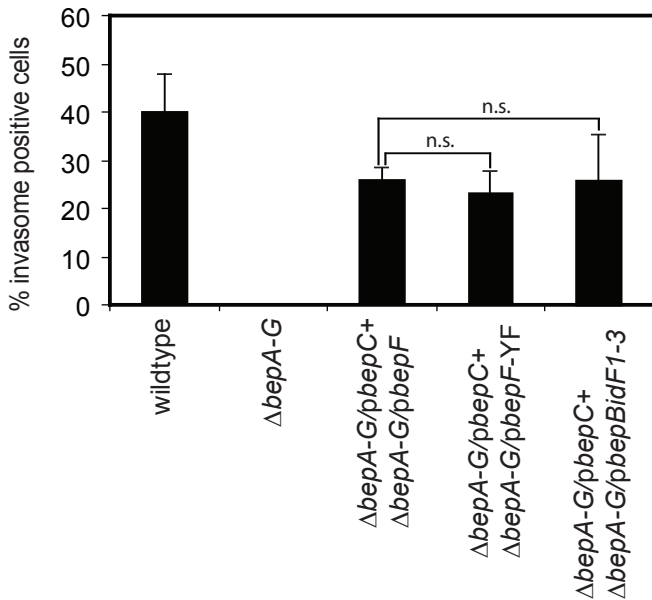
A



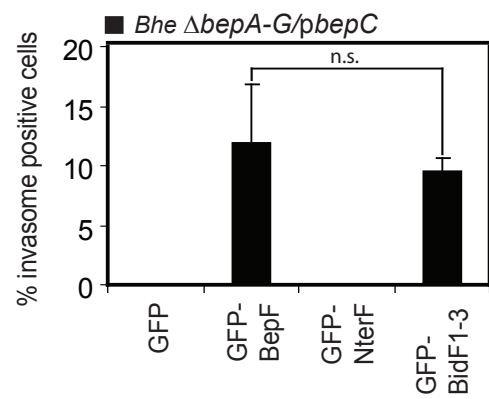
B



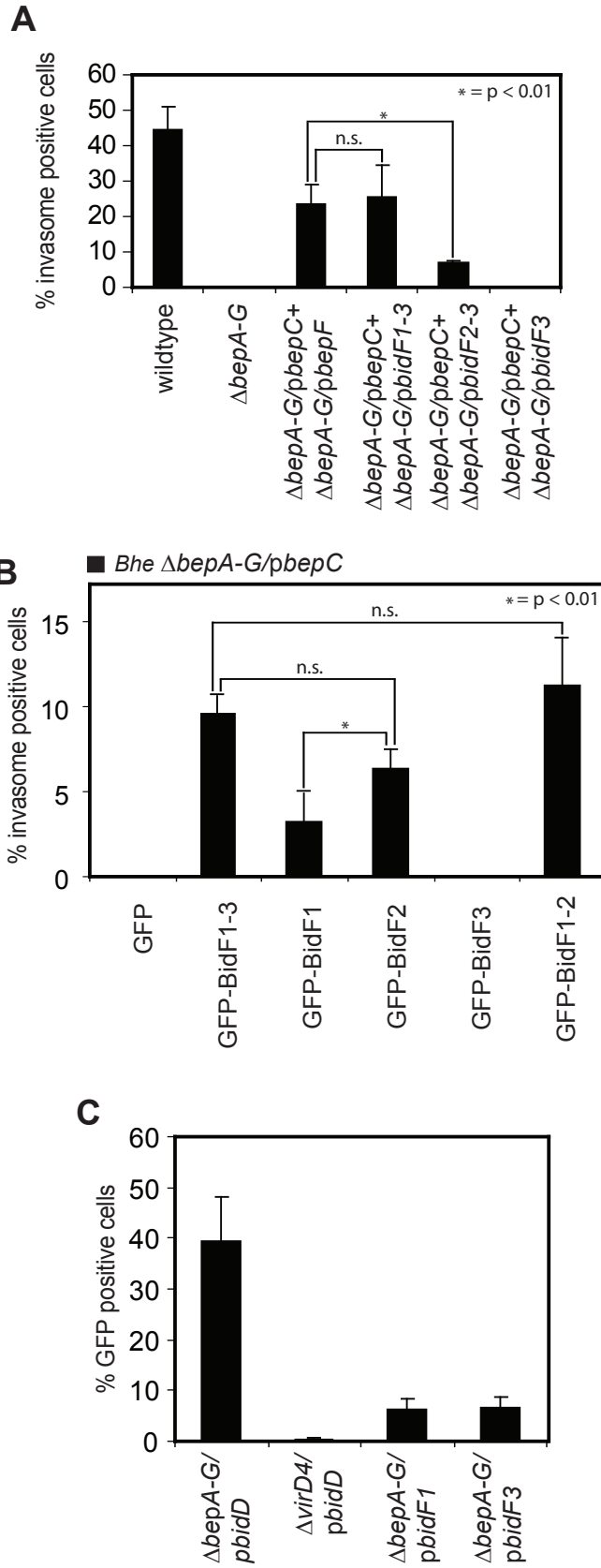
C



D



Truttmann *et al.*
Figure 1

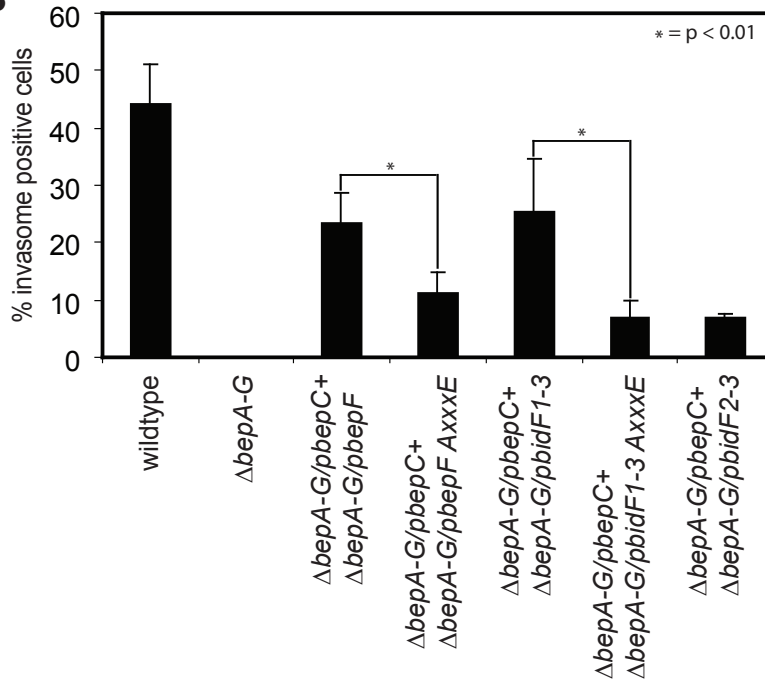


Truttmann *et al.*
Figure 2

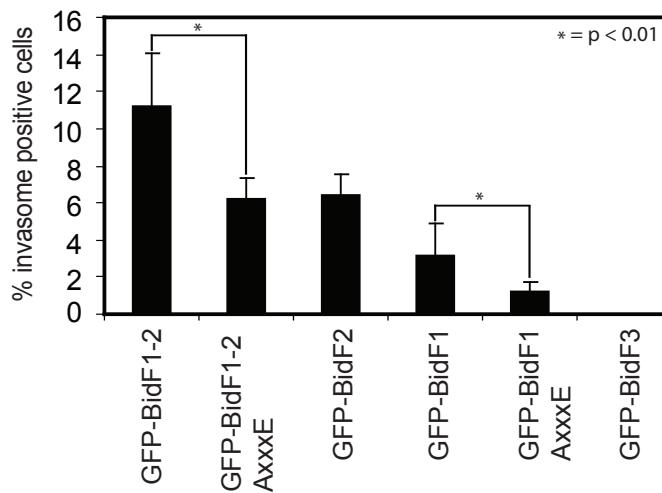
A

| | 1 | 10 | 20 | 23 |
|-----------|-------|-----------------|-----------------------------|-------|
| Consensus | L X S | W K V Q E R | I T Y I S R L I N X G | L D X |
| 1. SifA | L D E | W K A Q E K | A T Y L E A K I Q S G | L K K |
| 2. SifB | L C D | W K E O E R | K A A I S S R I S L G | L T Q |
| 3. Map | T Q Q | W F K Q E Q | I T Y I S R T V N R A | L D D |
| 4. Map 2 | T Q Q | W F Q O E Q | T T Y I S R T V N R T | L D D |
| 5. IpgB1 | L F C | W M S Q E R | T S Y V S S M I N R S | L D E |
| 6. EspM1 | I N A | W K R D E R | T V Y P S R V I N O G | L D K |
| 7. IpgB2 | I T D | W K N D E K | K V Y V S R V V N O C | L D K |
| 8. BidF2 | E F S | W Q V A N N P S | L F S P L A G K R I L G | |
| 9. BidF3 | E L S | W Q V A N F S T | I F A P L A G K O V L G | |
| 10. BidF1 | Q L S | W E V S E H | P K S I S K L A G K K M L G | |

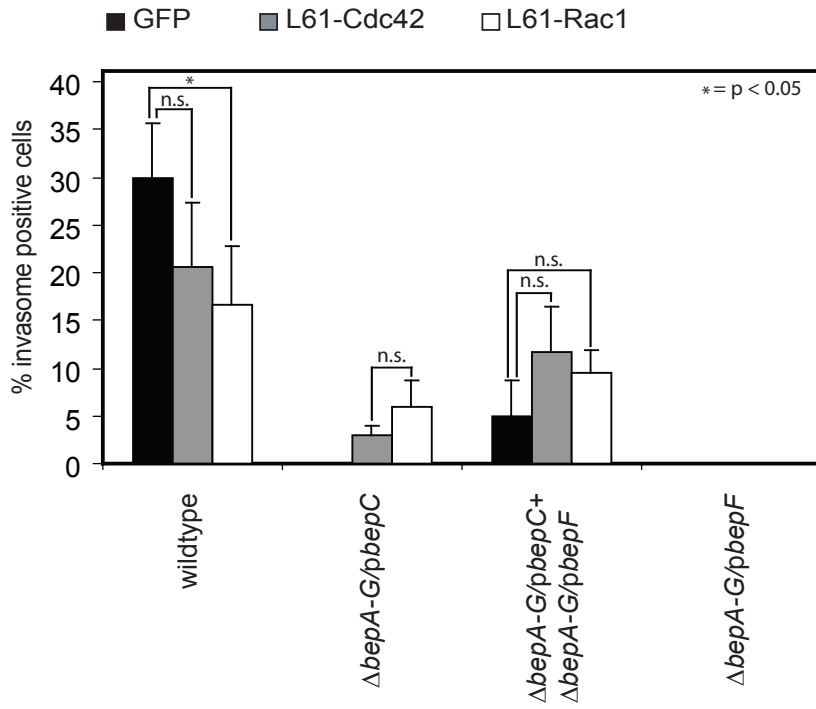
B



C

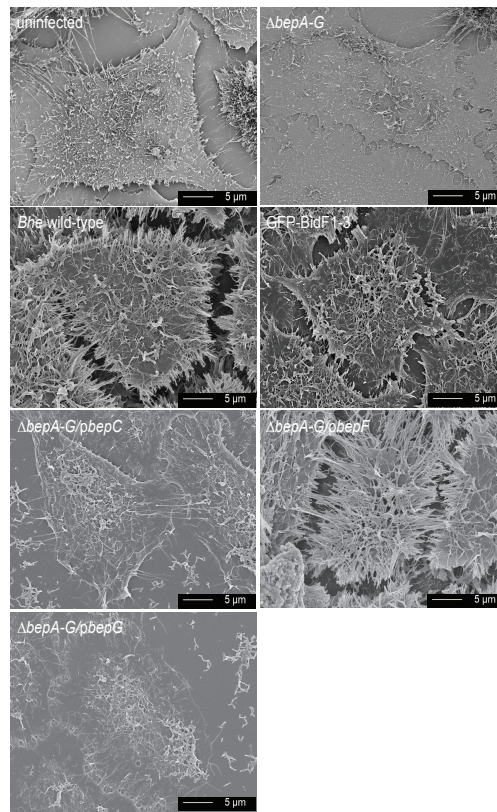


Truttmann et al.
Figure 3

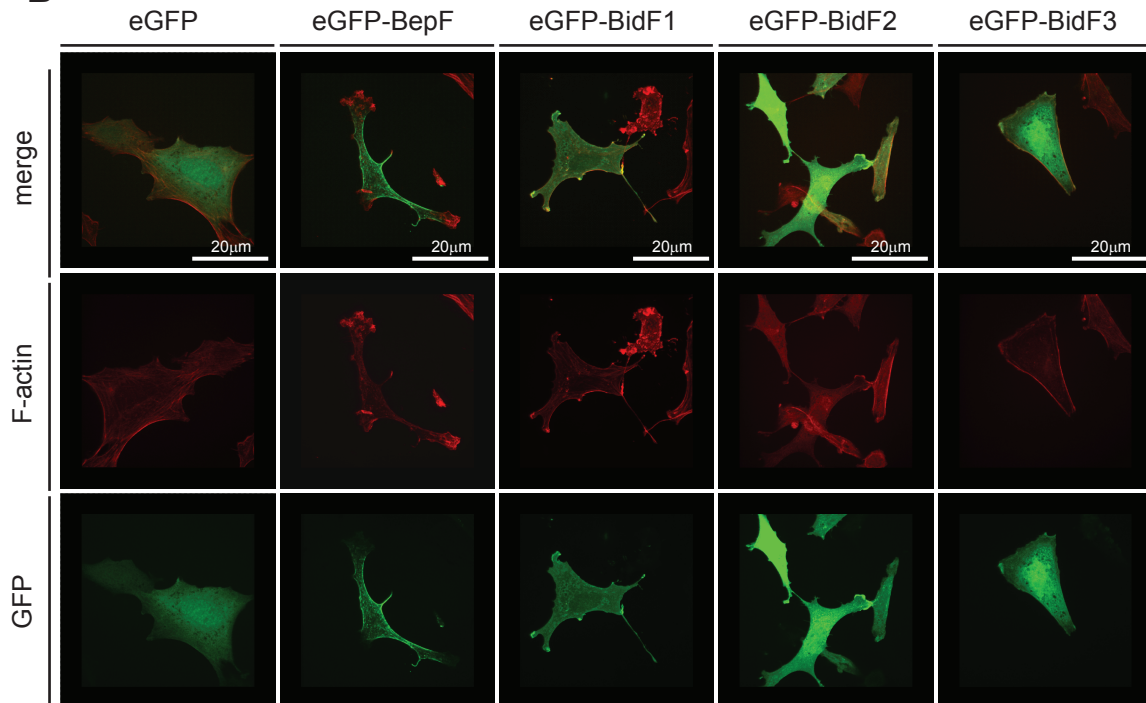


Truttmann *et al.*
Figure 4

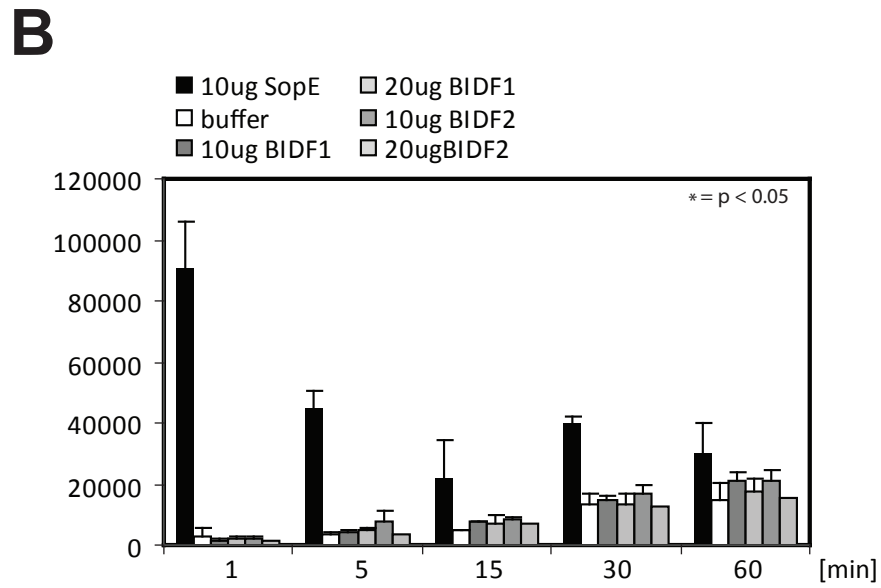
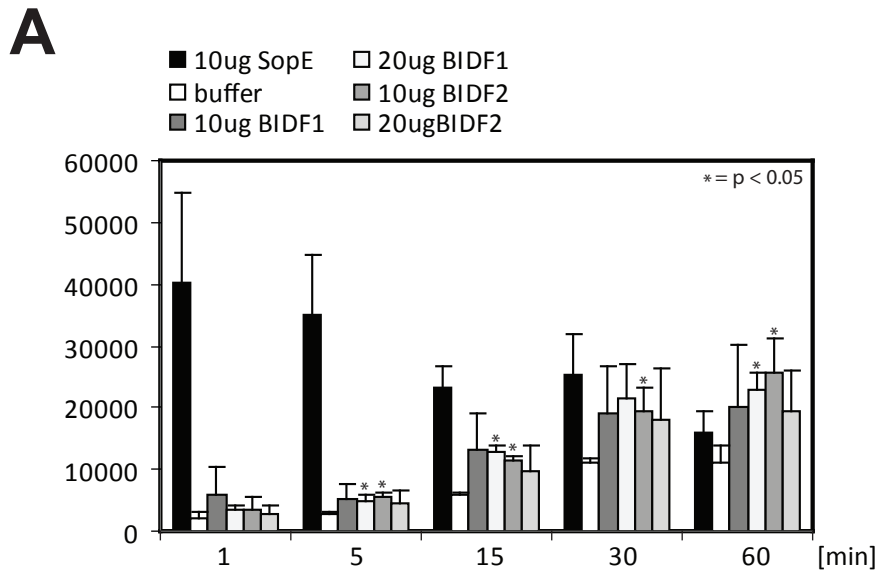
A



B



**Truttmann *et al.*
Figure 5**



Truttmann *et al.*
Figure 6

A

BepF *B. henselae*

MKKNQPSSSTSPSVKELKKRYEQTAEEASTLHQLSAGSAPKEKKQPSSRLEELRKRRYEQTASLTASQEAL
 SARGFPKEKRQPHTQQSPEQLPIHHEQQFAVTPQQSSSQT**PLYAT**PLPQQPVRTPPQRPPRAKDKELHKT
 APQDST**PLYAT**PSPQQSVQTPPQRPPRAKDKELHKAASQDST**PLYAT**PSPHKQQPMRERAQSNSSQDSE
PLYATPLPQRHQPMRERAQSNSSQDSE**PLYAT**PLPQRHQPVRRKRTQSNSSQDSE**PLYAT**PLPQRHQPV
 RKRTQSNSSQDNE**PLYATAAPSQSPRMEKSVNTMQRNLLLEAYKEEIKYWCGIVYGDRLILQKRIEEI**
QENPALGEQLSWEVSEHPKSIKLAGKKMLGVKTKARRKAEEENYLALRDTINSYVYTLKYSQQKPLHAPH
TEHTRDEQQTHRTQSAEKERAPLSNQELADRIRTEPSVLYSQTEVQYWSKIVFGNPYILQYRIEDIQKNP
DMGEEFSWQVANNPSLFSPLAGKRILGIKNDARRHAEASLSCLCSAIEGYADAVKQAKEDIVQEYQVQQS
RQELSTEPAKQLQKQQTLSKPHKLPEHSPTDAHQETTQTSMTQEWERLGARPRTVTTTHKKHTQESTLPTS
 HAEQKTTREQTENQKSLTPEKEKTPLSHKEIASRVQNDLSVQRAQIEIYNWCNIVYNNPLVLQHTTED
IKKIPMLGEELSWQVANFSTIFAPLAGKQVLGIKNNARKHAEAAIPSLCTAIDHYTEIVKQVREDIVKNH
QEQSPKKDKNVKROQSLSKPPKLPERSTEIPRHQALEASRQAQQKPSNVRSSAEKTKQKMLAL

B

Tyrosine predictions

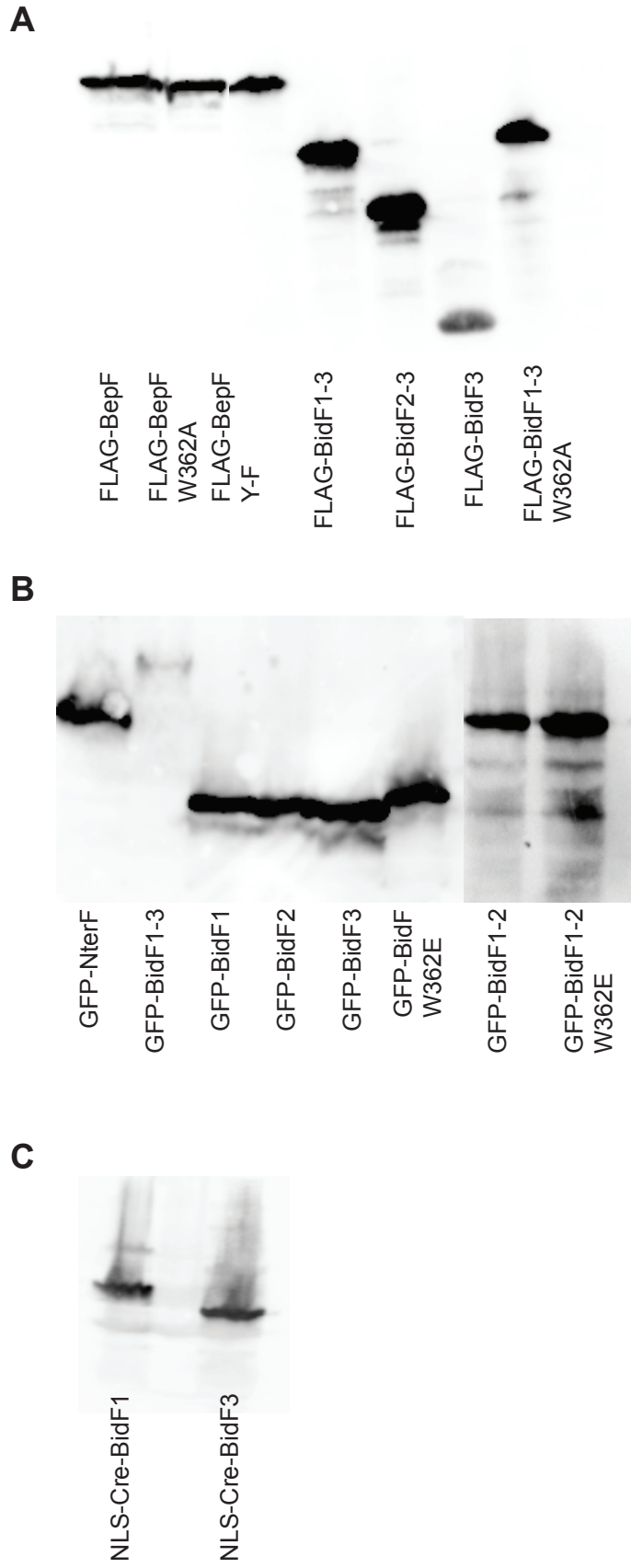
| Name | Pos | Context | Score | Pred |
|--------------------|------------|------------------|--------------|-------------|
| BepFprotein | 29 | LRKRYEQTA | 0.141 | . |
| BepFprotein | 85 | QTPLYATPL | 0.724 | *Y* |
| BepFprotein | 121 | STPLYATPS | 0.939 | **Y* |
| BepFprotein | 157 | STPLYATPS | 0.939 | **Y* |
| BepFprotein | 185 | SEPLYATPL | 0.988 | **Y* |
| BepFprotein | 213 | SEPLYATPL | 0.988 | **Y* |
| BepFprotein | 241 | SEPLYATPL | 0.988 | **Y* |
| BepFprotein | 269 | NEPLYATAA | 0.984 | **Y* |
| BepFprotein | 297 | LLEAYKEEI | 0.028 | . |
| BepFprotein | 303 | EEIKYWCGI | 0.839 | *Y* |
| BepFprotein | 309 | CGIVYGDRL | 0.106 | . |
| BepFprotein | 366 | AEENYLALR | 0.891 | *Y* |
| BepFprotein | 376 | TINSYVYTL | 0.165 | . |
| BepFprotein | 378 | NSYVYTLKY | 0.068 | . |
| BepFprotein | 382 | YTLKYSQK | 0.271 | . |
| BepFprotein | 432 | PSVLYSQTE | 0.303 | . |
| BepFprotein | 439 | TEVQYWSKI | 0.636 | *Y* |
| BepFprotein | 449 | FGNPYILQY | 0.145 | . |
| BepFprotein | 453 | YILQYRIED | 0.016 | . |
| BepFprotein | 512 | AIEGYADAV | 0.754 | *Y* |
| BepFprotein | 527 | IVQEYQVQQ | 0.018 | . |
| BepFprotein | 653 | QIEIYNWCN | 0.076 | . |
| BepFprotein | 660 | CNIVYNNPL | 0.583 | *Y* |
| BepFprotein | 727 | AIDHYTEIV | 0.484 | . |

C

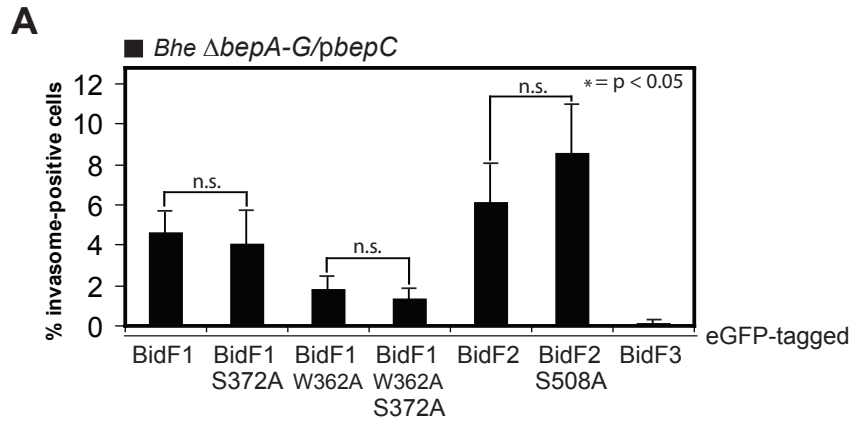
Tyrosine kinase group (Y_kin)

| Abl Kinase | | Gene Card ABL1 | | | |
|----------------------------|--------|----------------|-----------------|----|-------|
| Site | Score | Percentile | Sequence | SA | |
| Y149 | 0.2138 | 0.002 % | PQDSTPLYATPSPQQ | | 1.032 |
| Abl Kinase | | Gene Card ABL1 | | | |
| Site | Score | Percentile | Sequence | SA | |
| Y213 | 0.2366 | 0.002 % | SQDSEPLYATPLPQR | | 1.032 |
| Abl Kinase | | Gene Card ABL1 | | | |
| Site | Score | Percentile | Sequence | SA | |
| Y241 | 0.2366 | 0.002 % | NQDSEPLYATPLPQR | | 1.032 |
| Abl Kinase | | Gene Card ABL1 | | | |
| Site | Score | Percentile | Sequence | SA | |
| Y269 | 0.2366 | 0.002 % | SQDSEPLYATPLPQR | | 1.032 |
| Abl Kinase | | Gene Card ABL1 | | | |
| Site | Score | Percentile | Sequence | SA | |
| Y185 | 0.2655 | 0.003 % | SQDSTPLYATPSPHK | | 1.032 |
| Abl Kinase | | Gene Card ABL1 | | | |
| Site | Score | Percentile | Sequence | SA | |
| Y113 | 0.2925 | 0.011 % | SSSQTPLYATPLPQQ | | 1.032 |
| Src homology 2 group (SH2) | | | | | |

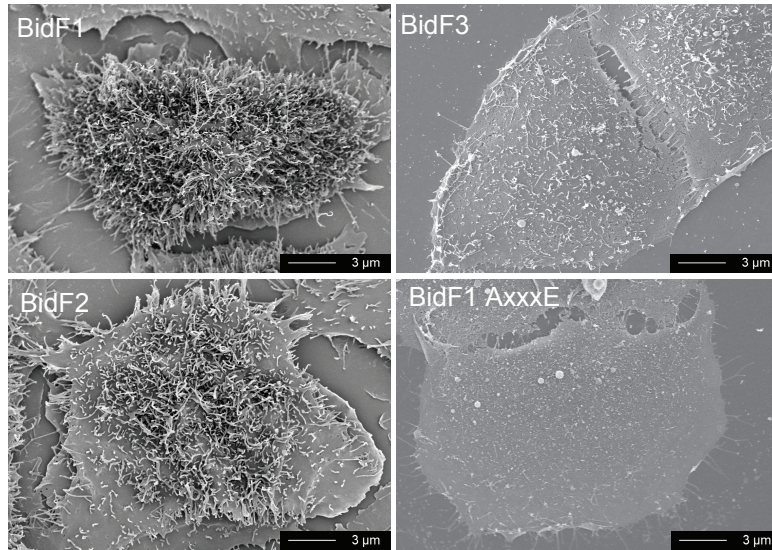
Truttmann *et al.* Figure S1



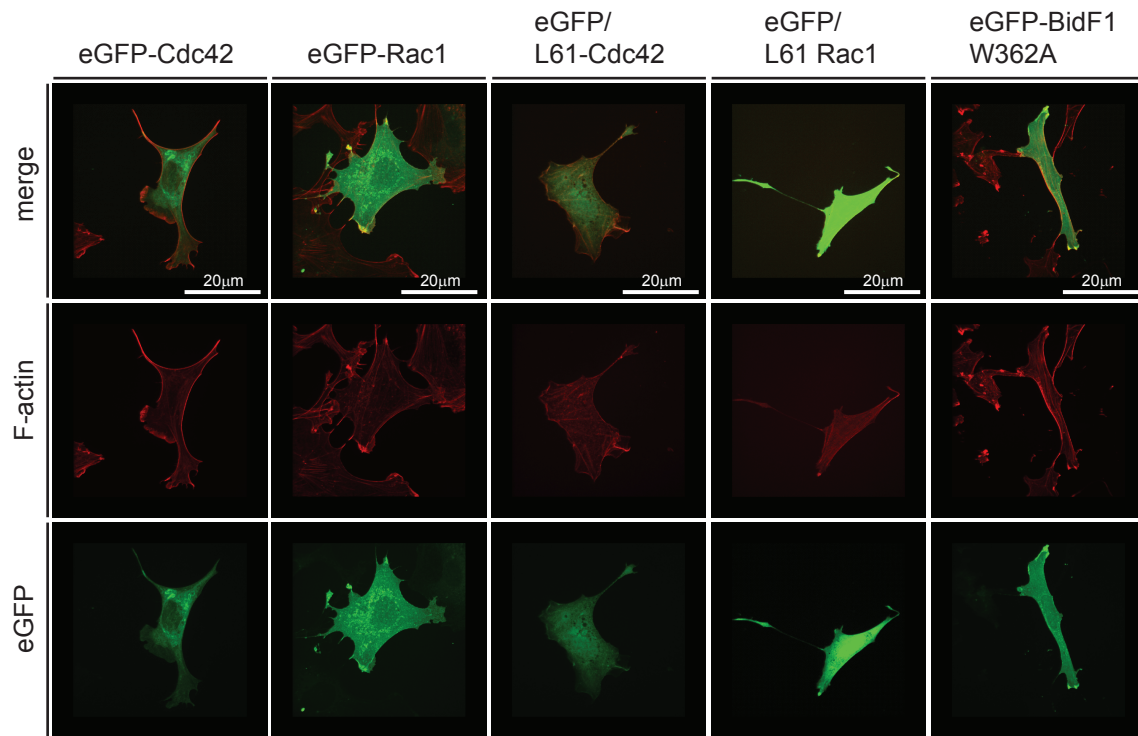
Truttmann *et al.*
Figure S2



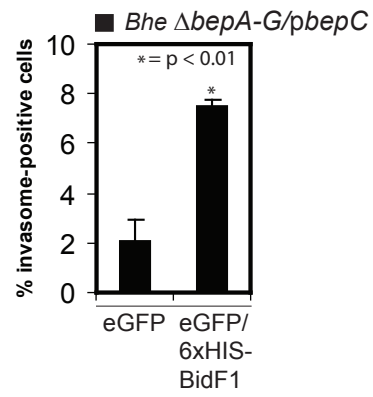
Truttmann *et al.*
Figure S3



Truttmann *et al.*
Figure S4



Truttmann *et al.*
Figure S5



Truttmann *et al.*
Figure S6

Table S1: Bacterial strains and plasmids used in this study

| Strain/Plasmid | Genotype or relevant characteristics | Reference/Source |
|-------------------------------|--|---------------------------------|
| <i>Bhe</i> strains | | |
| RSE247 | spontaneous Sm ^r strain of ATCC 49882 ^T | (Schmid <i>et al.</i> , 2004) |
| MSE150 | $\Delta bepA-G$ mutant of RSE247 | (Schulein <i>et al.</i> , 2005) |
| MSE159 | MSE150 containing pMS007 | (Schmid <i>et al.</i> , 2006) |
| TRB171 | MSE150 containing pPG106 | (Rhomberg <i>et al.</i> 2009) |
| TRB169 | MSE150 containing pPG107 | (Rhomberg <i>et al.</i> 2009) |
| MTB011 | MSE150 containing pMT001 | This study |
| MTB044 | MSE150 containing pMT004 | This study |
| MTB041 | MSE150 containing pMT005 | This study |
| MTB058 | MSE150 containing pMT030 | This study |
| MTB062 | MSE150 containing pMT031 | This study |
| MTB076 | MSE150 containing pMT052 | This study |
| MTB084 | MSE150 containing pMT041 | This study |
| MTB102 | MSE150 containing pMT043 | This study |
| <i>E. coli</i> strains | | |
| β 2150 | <i>F'</i> <i>lacZDM15 lacI^q traD36 proA+B+ thrB1004 pro thi strA hsdS lacZΔM15 ΔdapA::erm (Erm^R) pir</i> | (Schulein and Dehio, 2002) |
| NovaBlue | <i>endA1 hsdR17(r K12–m K12+) supE44 thi-1 recA1 gyrA96 relA1 lac[F' proA+B+ lacI^qZΔM15::Tn10 (Tc^R)]</i> | Novagen, Madison |
| BL21 | <i>F–, ompT, hsdSB(rB–, mB–), dcm, gal, λ(DE3)</i> | Novagen, Madison |

Plasmids

| | | |
|-------------|--|----------------------------------|
| pWay21 | Mamalian expression vector for eGFP | Molecular Motion lab, Montana |
| pCD353 | <i>Bartonella</i> spp. vector, expressing GFP | (Dehio <i>et al.</i> , 1998) |
| peGFP-Cdc42 | mammalian expression vector for eGFP-Cdc42 fusion | (del Pozo <i>et al.</i> , 1999) |
| peGFP-Rac1 | mammalian expression vector for eGFP-Rac1 fusion | (del Pozo <i>et al.</i> , 1999) |
| pET15b | <i>E.coli</i> expression vector | Novagen |
| pMS007 | derivative of pPG100, encoding FLAG-BepC | (Schmid <i>et al.</i> , 2006) |
| pMT001 | derivative of pPG100, encoding FLAG-BepF W362A | This study |
| pMT004 | derivative of pPG100, encoding FLAG-BidF1-3 | This study |
| pMT005 | derivative of pPG100, encoding FLAG-BepF-YF mutant (113, 149, 185, 213, 241, 269, 297) | This study |
| pMT030 | derivative of pPG100, encoding FLAG-BidF2-F3 | This study |
| pMT031 | derivative of pPG100, encoding FLAG-BidF3 | This study |
| pMT041 | derivative of pRS79, encoding for BidF3+C-tail BepF | This study |
| pMT043 | derivative of pRS79, encoding for BidF1+C-tail BepD | This study |
| pMT052 | derivative of pPG100, encoding FLAG-BidF1-3 W357A | This study |
| pMT573 | derivative of pET15b, encoding for C-terminal 6xHis-tagged BidF1 | This study |
| pMT575 | derivative of pET15b, encoding for C-terminal 6xHis-tagged BidF2 | This study |
| pMT560 | derivative of pWAY21, encoding eGFP-BidF1-F3 | This study |
| pMT562 | derivative of pWAY21, encoding eGFP-BidF3 | This study |
| pMT563 | derivative of pWAY21, encoding eGFP-BepF | This study |
| pMT567 | derivative of pWAY21, encoding eGFP-BidF1 | This study |

| | | |
|-----------------|--|---------------------------------|
| pMT591 | derivative of pWAY21, encoding eGFP-BidF1-F2 | This study |
| pMT592 | derivative of pWAY21, encoding eGFP-BepF aa1-298 | This study |
| pMT593 | derivative of pWAY21, encoding eGFP-BidF1 W367A | This study |
| pMT597 | derivative of pWAY21, encoding eGFP-BidF1-F2 W367A | This study |
| pMT612 | derivative of pWAY21, encoding eGFP-BepF S372A | This study |
| pMT613 | derivative of pWAY21, encoding eGFP-BepF W362A, S372A | This study |
| pMT614 | derivative of pWAY21, encoding eGFP-BepF S508A | This study |
| pRK5mycL61Cdc42 | mammalian expression vector for L61 Cdc42 | (Ridley and Hall, 1992) |
| pRK5mycL61 Rac1 | mammalian expression vector for L61 Rac1 | (Ridley and Hall, 1992) |
| pPG100 | <i>E. coli- Bartonella</i> spp. shuttle vector | (Schulein <i>et al.</i> , 2005) |
| pPG106 | derivative of pPG100, encoding FLAG-BepF | (Rhomberg <i>et al.</i> 2009) |
| pPG107 | derivative of pPG100, encoding FLAG-BepG | (Rhomberg <i>et al.</i> 2009) |
| pRS79 | Cre-vector encoding NLS::Cre::BepD (aa 352-534) | (Schulein <i>et al.</i> , 2005) |
| pRS110 | Cre-vector encoding NLS::Cre::BepF (aa 352-534) | (Schulein <i>et al.</i> , 2005) |
| pTR1769 | derivative of pWAY21, encoding eGFP-BepC | (Rhomberg <i>et al.</i> 2009) |

Table S2

| Name | Sequence ^a | Restriction site | construct |
|--------|---|------------------|-----------------------------|
| pMT109 | ATCATACCATGGCAACAGCTGCTCCATCACAATCACCACGC | NcoI | HIS-BidF1-2 |
| pMT153 | GGGAATTC <u>CATATG</u> TTAGTGATGATGATGATGATGTGCTTTAGCCGGTTCAGT AGAAAAGTTC | NdeI | HIS-BidF2 / BidF1-2 |
| pMT154 | ATCATACCATGGCAATGAGCGCTGAAAAGGAGAGACACCTCTCT | NcoI | HIS-BidF2 |
| pMT196 | ATCATACCATGGCACCCATGCTAGGAGAAGAACTCTCA | NcoI | HIS-BidF3 |
| pMT197 | GGGAATTC <u>CATATG</u> TTAGTGATGATGATGATGATGGAGTGCCAGCACCATTTT TTGTGT | NdeI | HIS-BidF3 |
| pMT109 | ATCATACCATGGCAACAGCTGCTCCATCACAATCACCACGC | NcoI | HIS-BidF1 |
| pMT110 | GGGAATTC <u>CATATG</u> TTAGTGATGATGATGATGATGTGCTTGC GTTCTGTGTGTT TGTTGTTTCAT | NdeI | HIS-BidF1 |
| pMT064 | AAAAATTC <u>CCCGGG</u> ATGACAGCTGCTCCATCACA | XmaI | GFP-BidF1 / BidF1 W362A |
| pMT104 | GGGAATTC <u>CTAGAT</u> TGCGTTCTGTGTGTTTGTGTT | XbaI | GFP-BidF1 / BidF1 W362A |
| pMT105 | ATAATAT <u>GCGGCCG</u> GATGACAGCTGCTCCATCACAATCA | NotI | HA-GFP-BidF1 |
| pMT106 | ATCTTAT <u>GGATCCT</u> TGCGTTCTGTGTGTTTGTGTT | BamHI | HA-GFP-BidF1 |
| pMT128 | AAAAATTC <u>CCCGGG</u> ATGAGCGCTGAAAAGGAGAGAG | XmaI | GFP-BidF1-2 / BidF1-2 W362A |
| pMT129 | GGGAATTC <u>CTAGAT</u> ATTATTTAGCCGGTTCAGTAGAAAAG | XbaI | GFP-BidF1-2 / BidF1-2 W362A |
| PMT64 | AAAAATTC <u>CCCGGG</u> ATGACAGCTGCTCCATCACA | XmaI | GFP-BidF2 |
| pMT130 | GGGAATTC <u>CTAGAT</u> ATTATTTAGCCGGTTCAGTAGAAAAG | XbaI | GFP-BidF2 |
| pMT20 | CGCACGCCTCCACAAAGACCACCGCGC ^a AAAAGACAAAGA | - | FLAG-BepF-YF |

| | | | |
|--------|---|------|--|
| pMT21 | GCGCGGTGGTCTTTGTGGAGGCGTGCGAACTGG | - | FLAG-BepF-YF |
| pMT32 | GGGAATTC <u>CATATG</u> ATGAAAAAAAAACCAACCATCC | NdeI | FLAG-BepF-YF / BepF W362A |
| pMT31 | GGGAATTCATATGTTAGAGTGCCAG | NdeI | FLAG-BepF-YF / BidF1-3 / BidF1-3 W362A / BidF2-3 / BidF3 |
| pMT67 | GGGAATTC <u>CTAG</u> ATTAGAGTGCCAG | XbaI | GFP-BepF / BidF1-3 |
| pMT68 | AATATAC <u>CCGGG</u> ATGAAAAAAAAACCAACCATCCT | XmaI | GFP-BepF |
| pMT64 | AAAAATTC <u>CCGGG</u> ATGACAGCTGCTCCATCACA | XmaI | GFP-BidF1-3 |
| pMT62 | GACAAACATATGATGCAACAAACACACAGAACGCAAAGCGC | NdeI | FLAG-BidF2-3 |
| pMT63 | GACAAACATATGATGCCCATGCTAGGAGAAGAAGCTC | NdeI | FLAG-BidF3 |
| pMT144 | TACCC <u>CCGGG</u> ATGAAAAAAAAACCAACCATCCT | XmaI | GFP-NterF |
| pMT145 | CTAGT <u>CTAG</u> ATTATGCGTAGAGAGGTTGTTGTC | XbaI | GFP-NterF |
| pMT114 | CATACGCGT <u>CGACA</u> AACAGCTGCTCCATCACAATCA | Sall | NLS-Cre-BIDF1 C-tail BepD |
| pMT118 | CATACGCGT <u>CGACA</u> AAGAAGCTCATGGCAAGTTGCAAA | Sall | NLS-Cre-BIDF3 C-tail BepF |
| pMT119 | TATGTCC <u>CCGGG</u> TTATTGCTGTCGTTTCACGTTTT | XmaI | NLS-Cre-BIDF3 C-tail BepF |
| pMT121 | TGATGTCTGTGTTACCGGGTTGCGTTCTGTGTGTTGTTG | | NLS-Cre-BIDF1 C-tail BepD |
| pMT122 | CAACAAACACACAGAACGCAACCCGGTGAACACAGACATCA | | NLS-Cre-BIDF1 C-tail BepD |
| pMT123 | TATGTCC <u>CCGGG</u> TACTCAGTCGAAAGACTGGGCCT | XmaI | NLS-Cre-BIDF1 C-tail BepD |

^a Restriction endonuclease cleavage sites are underlined

3.4 RESEARCH ARTICLE IV

***Bartonella henselae* engages inside-out and outside-in signaling via integrin β 1 / talin1 during invasome formation**

Matthias C. Truttmann, Benjamin Misselwitz, Wolf-Dietrich Hardt, David R. Critchley and Christoph Dehio

Submitted to the Journal of Cell Science

3.4.1 SUMMARY

Bartonella henselae (*Bhe*) Houston-1 invasion via the invasome route depends on massive rearrangements of the host actin cytoskeleton. This particular process was shown to be regulated by Cdc42- and Rac1-mediated downstream signaling that regulate actin assembly / disassembly dynamics [1].

In order to identify further host cell proteins contributing to the process of invasome formation, we performed an imaging-based high-throughput RNAi screen using invasome formation as readout. Upon initial hit scoring and re-evaluation/validation of primary hits, the transmembrane receptor subunit integrin $\beta 1$, the tyrosine kinases FAK and Src as well as the adaptor proteins paxilin, vinculin and talin1 were confirmed as essential players for invasome establishment. Re-investigation of the confirmed screening hits in additional assays implicated that integrin $\beta 1$ is important for *Bhe* effector translocation and the establishment of the F-actin invasome structure. In contrast, Cdc42, Rac1, FAK, Src, talin1, vinculin and paxilin only contributed to the later process. Additionally, *Bhe* was shown to directly bind to integrin $\beta 1$. Taken together, these results indicate that signaling through integrin $\beta 1$ may represent the major pathway hijacked by *Bhe* to enable invasome formation. Further in detail analysis of the role of integrin $\beta 1$ in that particular process showed that it is required in its extended conformation to enable effector translocation as well as promoting the F-actin rearrangements that build up the invasome. Next, by over-expressing the dominant-negative integrin $\beta 1$ isoform B, we demonstrate that outside-in signaling is crucial for invasome establishment. Investigations of the role of FAK and Src kinase during invasome formation by different means confirmed these results. In a next step, by performing knock-down/rescue experiments, we show that talin1-, but not talin2-mediated inside-out activation of integrins is required for invasome formation. Thus, we present for the first time an example of a bacterial pathogen that employs both outside-in and inside-out signaling during host cell invasion. Performing heterologous complementation experiments using talin1 knock-down Hela cells and various mouse-talin1 (mtalin1) constructs, we demonstrate that the head domain of mtalin1 is sufficient to complement talin1 knock-down and that calpain2-promoted proteolytic cleavage of mtalin1 is required for invasome establishment. Finally, we show that paxilin localizes to sites of invasome formation and identify vinculin as additional player during invasome establishment that

provides a potential direct link between integrin signaling and the regulation of actin dynamics.

3.4.2 STATEMENT OF MY OWN CONTRIBUTION

All experiments mentioned in this manuscript were performed by me. Benjamin Misselwitz significantly contributed to the establishment of a functional image analysis pipeline by programming additional modules and functionalities for CellProfiler and enhanced CellClassifier. David R. Critchley was involved in the planning of talin-related experiments. The manuscript was written by me, Dave R. Critchley and Christoph Dehio.

3.4.3 REFERENCES

1. Rhomberg TA, Truttmann MC, Guye P, Ellner Y, Dehio C (2009) A translocated protein of *Bartonella henselae* interferes with endocytic uptake of individual bacteria and triggers uptake of large bacterial aggregates via the invasome. *Cell Microbiol* 11: 927-945.

***Bartonella henselae* engages inside-out and outside-in signaling via integrin β 1 and talin1 during invasome-mediated bacterial uptake**

Matthias C. Truttmann¹, Benjamin Misselwitz², Wolf-Dietrich Hardt², David R. Critchley³ and Christoph Dehio^{1, *}

¹Focal Area Infection Biology, Biozentrum of the University of Basel, Klingelbergstrasse 70, CH-4056 Basel, Switzerland; ²Institute of Microbiology, Swiss Federal Institute of Technology Zurich, Wolfgang-Pauli-Str. 10, CH-8093 Zurich, Switzerland; ³Department of Biochemistry, University of Leicester, Lancaster Road, Leicester, LE1 9HN, UK

*Corresponding author: Prof. Christoph Dehio
Focal Area Infection Biology
Biozentrum, University of Basel
Klingelberstrasse 70
CH-4056 Basel, Switzerland
Tel. +41-61-267-2140
Fax: +41-61-267-2118
E-mail: christoph.dehio@unibas.ch

Summary

The VirB/D4 type IV secretion system (T4SS) of the bacterial pathogen *Bartonella henselae* (*Bhe*) translocates seven effector proteins (BepA-BepG) into human cells that subvert host cellular functions. Two redundant pathways dependent on BepG or the combination of BepC and BepF trigger the formation of a bacterial uptake structure termed the invasome. Invasome formation is a multi-step process consisting of bacterial adherence, effector translocation, aggregation of bacteria on the cell surface and engulfment and eventually complete internalization of the formed bacterial aggregate in an F-actin-dependent manner. In the present study, we show that *Bhe*-triggered invasome formation depends on integrin- β 1-mediated signaling cascades that eventually enable assembly of the F-actin invasome structure. We demonstrate that *Bhe* interacts with integrin β 1 in a fibronectin-independent manner and that activated integrin β 1 is essential for both effector translocation as well as the actin rearrangements leading to invasome formation. Further, we report that talin1, but not talin2, is required for inside-out activation of integrin β 1 during invasome formation. Finally, integrin- β 1-mediated outside-in signaling via FAK, Src, paxillin and vinculin is necessary for invasome formation. This is the first example of a bacterial entry process that fully exploits the bi-directional signaling capacity of integrin receptors in a talin1-specific manner.

Introduction

The zoonotic pathogen *Bartonella henselae* (*Bhe*), which is found world-wide, causes persistent asymptomatic infections in cats that serve as mammalian reservoir host. Accidental transmission of *Bhe* to humans via cat scratches or bites can manifest in a broad spectrum of clinical symptoms. While immuno-competent patients typically develop cat-scratch disease, (Florin et al., 2008), immuno-compromised patients often suffer from bacillary angiomatosis or peliosis, which is characterized by vaso-proliferative lesions in liver or skin, respectively (Dehio, 2005).

Bhe expresses a VirB/D4 type IV secretion system (T4SS) which mediates the translocation of seven *Bartonella* effector proteins, BepA to BepG, into host cells (Schmid et al., 2004; Schulein et al., 2005). The Beps trigger all known VirB/D4-associated phenotypic changes of infected endothelial cells (ECs), including (i) inhibition of apoptosis, (ii) activation of an NF- κ B-dependent pro-inflammatory response, (iii) capillary-like sprout formation of ECs embedded in a 3D-matrix and (iv) bacterial invasion of ECs as well as epithelial cells by a unique cellular structure termed the invasome (Rhomberg et al., 2009; Scheidegger et al., 2009; Schmid et al., 2006; Schmid et al., 2004; Selbach et al., 2009). Invasome formation in particular has been shown to depend on the translocation of BepG or the combination of BepC and BepF into the recipient cells (Dehio et al., 1997; Rhomberg et al., 2009; Schmid et al., 2004; Schulein and Dehio, 2002; Schulein et al., 2005; Truttmann et al., in press). *Bhe* internalization via the invasome route is a tightly controlled process, consisting of initial adherence, effector protein translocation, the formation of bacterial clusters and engulfment by plasma-membrane-derived membrane protrusions, eventually resulting in the complete internalization of the bacterial aggregates (Dehio et al., 1997; Rhomberg et al., 2009; Schmid et al., 2004). This entry process is accompanied by the inhibition of endocytic uptake of single bacteria into *Bartonella*-containing vacuoles (BCVs) (Rhomberg et al., 2009). The small GTPases Rac1 and Cdc42, their effectors WASP and SCAR/Wave as well as the downstream actin nucleation complex Arp2/3 have been shown to be essential for controlling F-actin rearrangements, leading to the establishment of the invasome structure (Rhomberg et al., 2009). In addition, recent work has indicated that BepC and BepF-dependent invasome formation requires the host cell protein cofilin1, whereas BepG-dependent invasome formation does not (Truttmann et al., in press).

Several bacterial pathogens exploit the integrin family of $\alpha\beta$ heterodimeric adhesion molecules to enable their own internalization into host cells. For example, enteropathogenic *Yersinia enterocolitica* and *Yersinia pseudotuberculosis* express the protein invasin that binds with high affinity to the integrin $\alpha5\beta1$, thereby initiating bacteria uptake in a zipper-like manner (Isberg and Barnes, 2001). In contrast, the gram-positive pathogen *Staphylococcus aureus* recruits fibronectin to its surface, a process that is mediated by a direct interaction between fibronectin and the bacterial cell-wall-attached proteins FnBP-A and FnBP-B (Jonsson et al., 1991). The interaction of the bacteria-bound fibronectin with its native receptor, integrin $\alpha5\beta1$, initiates integrin clustering and bacterial internalization into host cells (Agerer et al., 2003). In addition to the impact of integrins in mediating bacterial entry, it has recently been demonstrated that the human pathogen *Helicobacter pylori* binds via its decorated T4SS pilus to the integrin $\beta1$ subunit, resulting in the injection of the bacterial effector protein CagA and simultaneous activation of tyrosine kinases FAK and Src (Jimenez-Soto et al., 2009; Kwok et al., 2007).

Integrins are capable of promoting bi-directional signal transduction events across the cellular membrane. Talin1-mediated inside-out activation of integrins induces a conformational change that converts integrins into an active, high affinity state (Dupuy and Caron, 2008; Luo et al., 2007; Luo and Springer, 2006; Shattil et al., 2010). Activated integrin receptors can in turn interact with diverse extracellular ligands, thereby initiating outside-in signaling cascades that are generally associated with local remodeling of the actin cytoskeleton (Dupuy and Caron, 2008; Zaidel-Bar et al., 2007). Focal adhesion kinase (FAK) and Src kinase, key components of the integrin signaling core complex, as well as adaptor proteins such as Crk, paxillin and vinculin play major roles in these events (Huveneers and Danen, 2009).

Here, we show that *Bhe*-triggered invasome formation is dependent on integrin $\beta1$ -mediated signaling cascades. Further, we demonstrate that *Bhe* directly interacts with integrin $\beta1$ in a fibronectin-independent manner. Moreover, we report that integrin $\beta1$ in its active conformation is essential for *Bhe*-mediated effector translocation and the eventual F-actin rearrangements engulfing the bacterial aggregates. Finally, we demonstrate that integrin $\beta1$ -mediated outside-in signaling mediated by FAK, Src kinase, paxillin and vinculin

in combination with talin1-promoted inside-out signaling are required for invasome establishment.

Results

An RNA interference (RNAi) screen identified several components associated with integrin-mediated signaling that are essential for invasome formation. Invasome formation promoted by a spontaneous streptomycin-resistant variant of *Bartonella henselae* ATCC49882^T (Schmid et al., 2004) (further referred to as *Bhe* wild-type) has previously been shown to depend on the small Rho GTPases Rac1 and Cdc42, their downstream interaction partners WASF and Scar/WAVE as well as on the G-actin nucleation complex Arp2/3 (Rhombert et al., 2009; Truttmann et al., in press). In order to investigate which additional host cell factors may contribute to the process of *Bhe* wild-type-triggered invasome formation, we performed an immuno-fluorescence microscopy-based RNA interference (RNAi) screen in HeLa cells (FIG 1A). The short interfering RNA duplexes (siRNA) used targeted 251 different genes, including all human tyrosine kinases and integrin subunits (for detailed description of the experimental setup, image analysis, and hit selection see materials and methods). Following data processing, 41 of the 251 targeted genes were selected for validation (table S1, Fig. 1B) using three additional siRNAs per gene. Out of the 41 primary hits, only 8 genes passed the more stringent hit selection of the secondary screen, in which only hits that reduced invasome formation by more than 75% compared to controls were considered for detailed investigation (Fig. 1B, C). Among these positively validated genes of the secondary screen were the small GTPases Cdc42 and Rac1 that served as internal positive controls (Rhombert et al., 2009; Truttmann et al., in press). Further, we identified the two tyrosine kinases Src and FAK as well as the transmembrane receptor integrin β 1, and the adaptor proteins paxillin, talin1 and vinculin as novel components essential for invasome formation. Interestingly, all eight proteins identified by the RNAi screen contribute to or are regulated by integrin β 1-mediated signaling cascades that have been shown to be essential for the internalization of other bacterial pathogens such as *Y. enterocolitica* or *S. aureus* in an integrin β 1-dependent, zipper-like mechanism (Agerer et al., 2003; Isberg and Barnes, 2001).

Integrin β 1 contributes to multiple steps in invasome formation.

As invasome formation is a multi-step process, we sought to identify at which stages the validated screening hits were involved. To this end, we first tested whether *Bhe* can interact with the only transmembrane protein identified in the screen, i.e. integrin β 1. Therefore, 96 well plates were coated with various matrices including recombinant soluble heterodimeric α 5 β 1 integrin, and adhesion of wild-type *Bhe* was assessed following 60 minutes of incubation. The results showed that wild-type *Bhe* hardly adhered to gelatin- or human fibronectin-coated surfaces, while adherence to α 5 β 1 integrin coated wells was significantly increased (Fig. 2A). Next, we tested for adherence of wild-type *Bhe* to the well characterized mouse cell lines GE11/ GD25 lacking integrin β 1 (Fassler et al., 1995), and GE11 β 1A / GD25 β 1A that over-express integrin β 1 (Wennerberg et al., 1996). Therefore, cells were infected for 90 minutes with *Bhe* and the amount of adherent bacteria was determined by analysis of microscopic images. The findings demonstrated that adherence of wild-type *Bhe* was significantly increased on cells expressing β 1A compared to the corresponding integrin β 1A knock-out cells (Fig. 2B). To test if the interaction of wild-type *Bhe* with integrin β 1 was mediated by human fibronectin (hFN) recruitment to the bacterial cell surface, as shown for *S. aureus* (Agerer et al., 2003), we incubated wild-type *Bhe* for 48 hours in M199 medium containing 100 μ g/ml of hFN (Fig. S1B). Microscopic analysis showed that wild-type *Bhe* did not bind hFN. Complementary analysis of invasome formation in the presence of hFN antibodies showed that hFN depletion did not interfere with wild-type *Bhe*-triggered invasome formation (Fig. S1C).

Next, we investigated whether effector protein translocation was inhibited by knockdown of validated hits from the siRNA screen, performing a calmodulin-dependent adenylate cyclase (Cya) reporter assay for VirB/D4-dependent translocation (Schmid et al., 2006; Sory and Cornelis, 1994). Therefore, HeLa cells were transfected with the respective siRNAs and infected with *Bhe* wild-type containing pIMS404 encoding the FLAG-Cya-BidD fusion protein previously shown to be translocated into eukaryotic cells and to increase intracellular cAMP levels (Schmid et al., 2006). *Bhe* wild-type containing pIMS400 encoding for FLAG-Cya was used as a control. The results demonstrated that knockdown of integrin β 1 led to a significant reduction of effector protein translocation, while the knockdown of

FAK, talin1, Rac1, Cdc42, Src, vinculin and paxillin had no significant effect on this process (Fig. 2C).

We then analyzed whether any of the validated hits were required for processes occurring after effector translocation. Therefore, HeLa cells were first transfected with respective siRNAs and, following 24 hours incubation, transfected with a combination of plasmids pMT563 and pTR1769 encoding for eGFP-BepC and eGFP-BepG effector fusions, respectively. After incubation for another 24 hours, cells were infected with *Bhe* Δ bepA-G at an MOI = 500 for 48 hours and invasome formation was quantified thereafter. Infection of GFP-BepC/BepG-expressing cells with *Bhe* Δ bepA-G yielded approximately 8% invasome positive cells (Fig. S1C). The results showed that knockdown of any of the validated hits led to a significant decrease in BepC/BepG-triggered invasome formation except for Cdc42 (Fig. 2D), indicating that integrin β 1-mediated downstream signaling is required for the F-actin recruitment process leading to the engulfment of the bacterial aggregate that eventually results in formation of invasomes.

To test for local protein enrichment of the indicated proteins with invasome structures, we stained HeLa cells infected for 48 hours with wild-type *Bhe* using different antibodies (Ab) recognizing the activated forms of FAK (pY397), Src (pY418), paxillin (Y118) and integrin β 1 (Ab 12G10) as well as talin1 and vinculin (Fig. 2E). Cdc42 and Rac1 co-localization with invasome structures was previously reported (Rhomberg et al., 2009). Image analysis by confocal microscopy showed that FAK pY397, Src pY418, paxillin pY118 were all enriched at the edges of the characteristic F-actin rings that shape invasomes. In contrast, active integrin β 1 was only slightly enriched while no specific enrichment of talin1 or vinculin was observed in close proximity to invasomes. Thus, the observed localization patterns indicate a local involvement of FAK, Src and paxillin in the assembly of the F-actin cables shaping invasome structures. Taken together, our data demonstrate that integrin β 1 binds to *Bhe* wild-type in a fibronectin-independent manner and indicate multiple roles for integrin β 1 during the process of invasome formation.

Invasome formation requires integrin β 1 in its extended active conformation.

Integrins can exist in three different conformations. In the bent, inactive conformation integrins possess a low affinity for ligands and are found dispersed over the cell surface

(Takagi et al., 2002). In the primed conformation, integrins are in an intermediate state between the inactive, closed and the active, fully extended conformation, and display an increased binding affinity for ligands (Askari et al., 2009). Finally, in the extended, active conformation, integrins interact with high affinity with diverse single or multivalent ligands. Because our results show that integrin $\beta 1$ knockdown interferes with effector protein translocation and invasome formation (Fig. 1C, 2C, D), we wanted to investigate the consequence of Ab-mediated stabilization of the extended, active or the closed, inactive conformation on invasome formation. To address this question, we infected HeLa cells with wild-type *Bhe* in the presence of different integrin $\beta 1$ Ab and checked for invasome formation. A list of integrin $\beta 1$ Ab used and their respective binding sites can be found in the supplementary material (Fig. S2A, B). The results clearly showed that invasome formation was completely abolished in cells infected with wild-type *Bhe* and treated with the inhibitory integrin $\beta 1$ P5D2 Ab, whereas the presence of stimulating Ab had no effect on invasome formation (Fig. 3). We further performed Cya-reporter and translocation-independent invasome formation assays and the results showed that neither translocation nor translocation-independent invasome formation was affected by stimulating integrin $\beta 1$ Ab while inhibitory Ab significantly decreased effector translocation as well as the build-up of invasome structures (Fig. S3A, B). This data strongly suggest that the extended, active integrin $\beta 1$ conformation is essential for allowing *Bhe* effector translocation and subsequent invasome formation.

Active integrin $\beta 1$ clusters at sites of invasome formation

The interaction of the extended integrin conformation with its ligand is often associated with integrin clustering and stimulation of integrin-mediated downstream signaling cascades (Cluzel et al., 2005; Luo and Springer, 2006). To test for a specific recruitment of active integrin $\beta 1$ to sites of invasome formation, we first infected HeLa cells for 24 hours with wild-type *Bhe*. Polystyrene microspheres coated with either stimulating or inhibiting integrin $\beta 1$ Ab were then added to the cells, and incubated for another 24 hours. Examination and quantification of fixed and stained samples by confocal microscopy showed that approximately 92% of microspheres coated with stimulating integrin $\beta 1$ Ab clustered and localized to invasomes, whereas more than 90% of microspheres coated with inhibitory

integrin β 1 Ab neither clustered, nor localized to sites of invasome formation (Fig. 4A, B). To ensure that this was not a HeLa cell-specific finding due to the general high level of extended integrin β 1 on the HeLa cell surface (Jimenez-Soto et al., 2009), we repeated the experiments in endothelial-derived Ea.hy926 cells (Edgell et al., 1983). Infection of Ea.hy926 cells with wild-type *Bhe* for 24 hours and subsequent addition of Ab-coated microspheres for another 24 hours resulted in the same findings as seen on HeLa cells (Fig. S4A). Quantification of microspheres distribution on Ea.hy926 cells showed that approx. 75% of microspheres coated with stimulatory integrin β 1 Ab localized to invasomes, whereas only approx. 20% of beads coated with inhibitory integrin β 1 Ab co-localized with invasome structures (Fig. S4B). Uncoated microspheres showed a random distribution. These findings strongly indicate that integrin receptors containing active integrin β 1 are actively recruited to sites of invasome formation.

Integrin β 1-mediated outside-in signaling via FAK and Src is required for invasome establishment.

To test whether integrin β 1-mediated outside-in signaling contributes to invasome assembly, we transfected HeLa cells with a plasmid encoding the dominant-negative integrin β 1B isoform, which does not trigger FAK phosphorylation and is unable to affect the organization of the actin cytoskeleton (Armulik et al., 2000; Balzac et al., 1994). To date, five different integrin β 1 isoforms are characterized, which differ in their respective C-terminus. The results showed that ectopic expression of integrin β 1B reduced invasome formation by approximately 70% (Fig. 4C), strongly suggesting that integrin-dependent FAK activation is crucial for invasome formation. Next, we assessed the role of the two tyrosine kinases FAK and Src in the process of invasome assembly in more detail. FAK and Src are known to serve as phosphorylation hubs that mediate downstream signal transduction from integrins to Rho GTPases and other targets (Luo and Springer, 2006). To investigate the role of FAK in the process of invasome formation, HeLa cells were transfected with plasmids encoding the FAK mutants FAK pY397F, FAK pY861F or FAK pY925F prior to infection with wild-type *Bhe*. Tyrosine 397 is auto-phosphorylated upon FAK activation, and generates a high-affinity binding site for Src kinase (Agerer et al., 2005). Residue Y861 represents the major Src phosphorylation site in FAK and is essential for the interaction of FAK with integrin tails (Lim

et al., 2004). Phosphorylation of tyrosine 925 creates a binding site for the single SH2-domain of the adaptor protein Grb2, which links integrin activation to the Ras-MAPK pathway (Schlaepfer et al., 1994). The results showed that expression of FAK pY397F and FAK Y861F, but not FAK pY925F significantly decreased invasome formation (Fig. 4D). These findings are in line with results from the initial RNAi screen in which neither Grb2 nor any of the MAP kinases were identified as hits (table S1).

To further validate the involvement of the Src kinase in the process of invasome formation, HeLa cells were treated with specific Src kinase inhibitors prior to infection. The results showed a significant dose-dependent decrease in invasome formation in response to either of two Src kinase inhibitors (Fig. 4E, S5A). Taken together, our data suggests that outside-in signaling via integrin β 1 through FAK and Src kinase is critical for invasome formation. Further, the Ras-MAPK pathway appears not to be involved in the process of invasome establishment.

Talin1- but not talin2-mediated inside-out signaling via integrin β 1 is required for invasome formation.

In our initial screen, we identified talin1, but not talin2, as a protein contributing to invasome formation. The talin1 isoform is an adaptor protein that is essential in coupling conformational changes of integrins to downstream signaling cascades, and has been shown to initiate integrin activation (Anthis et al., 2009; Shattil et al., 2010 ; Simonson et al., 2006; Tadokoro et al., 2003). In addition, talin1 provides a link between integrins and the actin cytoskeleton (Critchley, 2009). Although talin2 is very similar (74% amino acid identity) to talin1, the relative roles of the two isoforms are not yet fully understood (Debrand et al., 2009). Since only talin1 but not talin2 was a hit in the initial RNAi screen for invasome formation, we investigated the role of the two isoforms in more detail. In a first step, we tested for the presence of both talin proteins in HeLa cells. Staining HeLa cells with specific talin1 and talin2 Ab confirmed the expression of both isoforms (Fig. S6A). Next, we tested the effects of talin1 or talin2 knockdown on invasome formation. The siRNAs used targeted a divergent region of the two proteins and were shown to result in isoform-specific knockdown (Fig. S6B, C). Infection of talin1 or talin2 knockdown cells with wild-type *Bhe* for 48 hours showed that talin1, but not talin2 knockdown decreased *Bhe*-initiated invasome

formation by more than 80% compared to mock controls (Fig. 5A). Thus, only talin1 is essential for invasome assembly.

To investigate how talin1 contributes to invasome formation, we knocked-down human talin1 (htalin1) in HeLa cells, and then transfected the cells with plasmids encoding either wild-type GFP-tagged mouse talin1 (mtalin1) or various GFP-mtalin1 mutants affecting integrin activation, actin binding and calpain cleavage. The siRNA used to knockdown human talin1 differs from the mtalin1 mRNA by a single base (Fig. S6D), and does not affect expression of mouse GFP-talin1. Expression of GFP-talin1 constructs was verified by fluorescent microscopy and only GFP-positive cells were used for phenotypic quantification. Moreover, expression of wild-type GFP-mtalin1 in htalin1-knockdown cells significantly increased invasome formation compared to cells expressing GFP alone (Fig 5B). We next tested GFP-mtalin1 containing a L325R mutation in the FERM domain that compromises the ability of talin1 to activate integrins without affecting binding to the NPxY motif in β -integrin tails (Wegener et al., 2007). The results showed that GFP-mtalin1 L325R was unable to increase invasome formation over background levels (Fig. 5B), indicating that talin1-mediated inside-out signaling via integrins is essential to the process of invasome formation. In contrast, a GFP-mtalin1 R2526G mutation that blocks talin1 dimerization and markedly reduces the activity of the C-terminal actin-binding site (Gingras et al., 2008; Kopp et al., 2010) was as effective as wild-type GFP-mtalin1 in supporting invasome formation. This result clearly establishes that invasome formation is not dependent on the ability of talin1 to link integrins to the actin cytoskeleton, and indicates that the main function of talin1 in invasome assembly is integrin activation. This conclusion is supported by the finding that the isolated GFP-mtalin1 head was almost as effective as full-length talin1 in reconstituting invasome assembly in htalin1 knockdown cells (Fig. 5C).

In previous work, it has been shown that talin1 is cleaved into the head and rod domain by the Ca^{2+} -dependent protease calpain2, and that this is required for turnover of cell-matrix junctions in cultured cells (Franco et al., 2004). Moreover, the stability of the liberated talin head is tightly regulated by the balance between cdk5-dependent phosphorylation and Smurf1-mediated ubiquitination (Huang et al., 2009). We therefore tested the ability of a GFP-mtalin1 L432G mutant that is resistant to calpain2 cleavage (Franco et al., 2004) to support invasome assembly. Interestingly, the L432G mtalin1 mutant was much less effective than wild-type talin1 in contributing to invasome formation (Fig.

5C). The importance of calpain2-mediated talin cleavage in this process was further investigated by studying invasome formation in the presence of increasing concentrations of calpeptin, a potent inhibitor of the protease calpain2. Thus, HeLa cells were infected with *Bhe* wild-type at an MOI = 300 for 48 hours in the presence of different concentrations of calpeptin, and invasome formation quantified in fixed and stained cells. The results showed a decrease in invasome formation of up to 80% in response to increasing concentrations of calpeptin (Fig. 5D). Together, these results show that liberation of the talin1 head by calpain2 cleavage is essential to invasome formation, and that the role of the talin head is to mediate inside-out activation of integrins.

Discussion

In this study, we addressed the host cell signaling mechanisms contributing to *Bhe*-triggered invasome formation. Performing and validating a fluorescence microscopy based small-scale siRNA screen, we identified six novel host cell proteins that are essential for invasome formation. Interestingly, all six identified proteins are major contributors to integrin $\beta 1$ -mediated signaling cascades. Integrin receptors are frequently implicated in the internalization of both bacteria and viruses. For example, adenovirus particles interact with integrin $\alpha V\beta 3$ promoting virus internalization into early endosomes (Nemerow, 2009; Wickham et al., 1993). Further, the bacterial pathogens *Y. enterocolitica* or *S. aureus* invade host cells in integrin $\alpha 5\beta 1$ -dependent processes (Van Nhieu and Isberg, 1991). Here, we demonstrate that the *Bhe* strain used in this study (a spontaneous streptomycin-resistant variant of *Bartonella henselae* ATCC49882^T; Schmid et al., 2004) interacts in a fibronectin-independent manner with integrin $\alpha 5\beta 1$. Previous work by Riess *et al.* (2007) showed that the *Bhe* patient isolate 'Marseille' expresses an integrin-binding adhesin termed BadA. In contrast, the *Bhe* strain used in this study only contains remnants of the *badA* gene, and although the gene is expressed, the protein is not present at the bacterial surface (Riess et al., 2007). Thus, another yet to be identified bacterial factor is required to mediate *Bhe*/integrin- $\beta 1$ -interactions.

Further, we show that integrin $\beta 1$ is required for at least two distinct steps during invasome formation, including effector translocation. *H. pylori*, a bacterial pathogen that employs the Cag-T4SS for effector translocation but does not enter the host cell, interacts

via several pili or pilus-associated proteins such as CagL, CagY or CagI directly with integrin $\beta 1$ (Jimenez-Soto et al., 2009; Kwok et al., 2007). This T4SS pilus- $\beta 1$ integrin interaction is required to enable CagA translocation into the host cell, where CagA activates FAK and Src kinases. Jimenez-Soto *et al.* (2009) suggested a model in which the conformational switch from the extended to the bent form of integrin $\beta 1$ may “pull down” the integrin-associated T4SS pilus and enable contact between the translocation system and the host cell membrane (Jimenez-Soto et al., 2009). In contrast to *H. pylori*-mediated CagA translocation, where the use of inhibiting integrin $\beta 1$ Ab did not interfere with effector translocation, our results indicate that the integrin $\beta 1$ needs to be in the extended conformation to enable *Bhe* effector translocation. Our data further suggest that the capacity of bi-directional signaling of integrins is exploited during *Bhe*-promoted invasome formation. Over-expressing integrin $\beta 1B$ in HeLa cells or siRNA-mediated knockdown of either FAK or Src significantly decreased invasome formation, indicating a major contribution of integrin $\beta 1$ -mediated outside-in signaling to the establishment of invasome structures. In addition, staining of active FAK and Src support the hypothesis of locally activated signaling cascades controlled by FAK and Src that may contribute to bacteria engulfment by F-actin leading to the establishment of invasome structures. Our results also indicate that talin1-mediated inside-out activation of integrins is required for invasome formation. Interestingly, knockdown of talin1, but not talin2, reduced invasome formation by more than 80%, indicating that talin2, although expressed in our cell system, cannot complement for loss of talin1 in this specific process. Due to the high level of conservation of talin1 and talin2, it is generally assumed that the two isoforms have overlapping functions. However, talin1 knock-out in mice is embryonic lethal, suggesting that either talin2 is not expressed in the appropriate tissue at the appropriate time or that talin1 and talin2 may have different cellular functions despite their high level of sequence similarity (Monkley et al., 2001; Monkley et al., 2000). In humans, *Bhe* infects endothelial cells which do not express talin2 (Kopp et al., 2010). Thus, the absence of talin2 in the primary target cells of *Bhe* may explain the observed specificity for talin1 in the process of invasome formation. Our finding that only talin1 but not talin2 is essential for invasome formation represents to the best of our knowledge the first example of a talin1-specific phenotype in a cell line expressing both talin isoforms.

Complementation of talin1 knockdown cells with mouse-talin1 mutants as well as results from experiments using specific protease inhibitors suggest that the calpain2-dependent proteolytic release of the talin1 head is essential for invasome formation. The talin1 head domain binds to the C-tails of β 1-integrin subunits, thereby inducing a conformational change from the bent, inactive to the extended, active state (Shattil et al., 2010). Moreover, the liberated talin1 head domain promotes β 1 integrin clustering (Cluzel et al., 2005). Our results provide evidence that in case of *Bhe*-promoted invasome formation, the talin1 head activates integrin β 1 and stabilizes it in the open conformation, thereby contributing to invasome assembly.

With respect to the data presented in this study, we propose a model in which *Bhe* interacts specifically with the extended active conformation of integrin β 1, thereby enabling effector translocation and initiating early events in outside-in signaling. *Bhe* clustering is probably a secondary event in which the membrane proteins aggregate to which *Bhe* are bound, thereby leading to the formation of *Bhe* clusters. It is tempting to speculate that integrin β 1 could be that receptor. The finding that beads coated with stimulating integrin β 1 Ab are recruited to invasome as well as the fact that integrin activation is often linked to integrin clustering (Cluzel et al., 2005) support this hypothesis. Further, our data indicate a possible link of integrin β 1 outside-in signaling via FAK / Src to paxillin and vinculin that may be involved in controlling the F-actin rearrangements leading to invasome formation.

The multi-domain protein paxillin directly binds to vinculin and is involved in the regulation of small Rho-family GTPases (Deakin and Turner, 2008). In contrast, vinculin is a major actin-binding protein containing several actin-binding domains (Ziegler et al., 2006). Recently, vinculin has been demonstrated to not only bind actin but to act as nucleation factor for *de novo* polymerization of G-actin into F-actin (Wen et al., 2009). Our data show that knockdown of either vinculin or paxillin abolished invasome formation almost completely. In addition, paxillin staining in *Bhe* wild-type infected cells showed that it co-localizes with invasome structures. Thus, our findings suggest that paxillin and vinculin, together with the kinases FAK and Src locally contribute to control the F-actin rearrangements resulting in the establishment of invasome structures. Whether or not vinculin acts as nucleation factor in this process or rather provides a link between the involved integrin β 1 subunits to F-actin remains unclear. However, published work that

demonstrated the crucial role of the Arp2/3 complex during invasome formation rather speaks against a dominant nucleation functionality of vinculin during invasome establishment (Rhomberg et al., 2009; Truttmann et al., in press).

Previous work on the role of talins in bacterial internalization demonstrated that the *Shigella* effector IpaA, involved in mediating *Shigella* uptake, interferes with talin recruitment to integrin β 1 C-tails *in vitro* (Demali et al., 2006). Further, the injected enteropathogenic *E. coli* (EPEC) protein Tir was shown to directly bind to talin, thereby contributing to EPEC-induced pedestal formation (Cantarelli et al., 2001). In case of *Bhe*-triggered invasome formation, we do not have any evidence as yet of a direct Bep-talin1 interaction. Nevertheless, our data clearly indicate that talin1-mediated inside-out activation of β 1 integrins is required for invasome formation. Moreover talin1 may contribute to invasome assembly by recruiting vinculin and thereby paxillin to the membrane, while a supportive role in linking β 1 integrins to the actin cytoskeleton (Giannone et al., 2003) can be excluded because a R2526G mutation that markedly reduce the ability of talin1 to bind actin (Gingras et al., 2008) does not affect invasome formation. However, the fact that the talin1 head domain was sufficient to rescue invasome formation indicates that the talin1-vinculin interaction is not essential, since the vinculin binding sites are all located on the talin1 rod domain (Critchley, 2009). Finally, talin1 could play a major role in controlling the formation of invasomes by preventing the recruitment of FilGAP, a negative regulator of Rac1, to the integrin β 1 C-tails (Nieves et al., 2010; Ohta et al., 2006). However, further investigations are required to define the precise role of talin1 in invasome formation.

In summary, we demonstrate that outside-in as well as inside-out signal transduction via integrins is essential for invasome formation. In addition, we demonstrate that talin1, but not talin2 is contributing to invasome formation by triggering inside-out activation of integrins. To the best of our knowledge, this is the first report that indicates active bi-directional signaling via integrins during the process of bacteria internalization in a talin1-, but not talin2-specific process.

Materials and Methods

Chemicals, siRNAs, Ab, proteins, plasmids. Src inhibitors SI5 and SU6656 were purchased from www.proteinkinase.de (Biaffin GmbH). siRNAs were purchased from Qiagen (genome-wide predesigned flexiPlate siRNAs); for all assays except screening, only experimentally verified flexiPlate siRNAs from Qiagen were used. Functionally verified siRNAs were pooled at equimolar concentrations and used for further experiments. Ab and plasmids used in this study are listed in supporting tables S2 (plasmids) and S3 (Ab). Recombinant integrin $\alpha 5\beta 1$ was purchased from RD Systems and fibronectin from Milipore.

Bacterial Strains, Growth Conditions. *B. henselae* ATCC49882^T wild-type or isogenic mutant strains were cultured following previously described procedures on solid agar plates (Columbia base agar supplemented with 5% sheep blood and appropriate antibiotics). *E. coli* strains were grown in liquid broth or solid agar plates (Luria Bertani broth) supplemented with appropriate antibiotics. Supplementary table S1 lists all bacteria strains used in this study.

Cell Lines and Cell Culture. HeLa Kyoto β cells (Snijder et al., 2009) and Ea.hy926 cells (Edgell et al., 1983) were cultured in DMEM (Gifco, invitrogen) supplemented with 10%FCS. GD25 and GD25 $\beta 1A$ (Wennerberg et al., 1996) were kindly provided by Prof. Reinhard Fässler (MPI Munich) and were cultured in DMEM supplemented with 10% FCS.

Infection and Transfection Assays. siRNA and DNA transfections and infections of HeLa cells was performed exactly as described in (Truttmann et al., in press). For RNAi screening, reverse transfection using pre-complexed siRNA was performed. Therefore, 25 μ l of 0.5 μ M siRNA stock (Qiagen flexiplate siRNA) were mixed with 100 μ l serum-free opti-mem (Diffco, Invitrogen) in a well of a 96 well plate. Next, 125 μ l Lipofectamine 2000 (Invitrogen) was added to 12.5 ml serum-free opti-mem and briefly vortexed. After 4 minutes, 125 μ l of Lipofectamine 2000-Opti-mem mix was added to each well of the 96 well plate containing the siRNA-opti-mem mix. The 96 well plate was lidded and put on an orbital shaker for 5 minutes. Following a total of 25 minutes of incubation, 50 μ l of the transfection complexes mix was added into each well of an empty, dark, flat bottom 96 well plate (Corning, Costar).

Plates were sealed and stored at -20°C until usage. The day of experiment, plates were thawed and warmed for 60 minutes at room temperature before adding cells.

For siRNA/DNA double transfections, cells were first transfected with siRNA following standard protocols and incubated for 24 hours. Afterwards, cells were washed once with DMEM/10%FCS, transfected with DNA according to manufacturer's instructions, incubated for 6 h, washed again, supplemented with fresh DMEM/10%FCS and eventually incubated for another 18 h before starting with respective assays.

Microsphere uptake assay. Microsphere uptake assays have been described previously (Rhomberg et al., 2009) In brief, Ea.hy926 or HeLa cells were pre-infected with the indicated strain of *Bhe* for 24 hours with an MOI of 100 or 300, respectively. Thereafter, cells were washed twice with M199/10% FCS and fresh M199/10% FCS containing BSA- or Ab-saturated, carboxylate-modified fluorescent (535nm/575nm) microspheres (1 µm Nile red FluoSpheres, Molecular Probes) was added to the cells (100 microspheres/cell). Following 24 hours of incubation, cells were fixed with PFA, stained for F-actin and DNA and analyzed by confocal laser scanning microscopy.

Immunoblot analysis. Protein levels were verified by analysis of total cell lysates obtained from HeLa cells. After protein separation by SDS-PAGE and transfer onto nitrocellulose, membranes were examined for the presence of the target protein specific primary Ab. Table S2 lists all primary Ab used in this study. In all experiments, secondary horseradish peroxidase-conjugated Ab (Amersham, 1:10000) was visualized by enhanced chemiluminescence (PerkinElmer).

Immunofluorescent (IF) labeling. Indirect IF labeling was performed as described (Dehio et al., 1997). Standard 96-well plate assays were stained with TRITC-phalloidin (Sigma, 100 µg/ml stock solution, final concentration 1:400), and DAPI (Roche, 0.1 mg/ml) using a Tecan Eoware freedom pipeting robot. Glass slides for confocal microscopy were stained with Cy5-phalloidin (Sigma, 100 µg/ml stock solution, final concentration 1:100), and DAPI. For specific protein stainings, various primary Ab were used (see table S2) and detected with AlexaFluor 488- or AlexaFluor 647-conjugated secondary Ab (Molecular Probes).

Adhesion assays. For *Bhe* adhesion assays, 96 well plates were coated with 35 μ l of PBS containing 0.1% gelatin, 10 μ g/ml human fibronectin or 10 μ g/ml recombinant integrin α 5 β 1 heterodimers over night. The next day, plates were washed 3 times with 100 μ l of PBS. Afterwards, 100 μ l of M199 containing 10^7 *Bhe* were added to each well for exactly 1 h without centrifugation. Next, M199 was discarded, wells were washed 3 times with 100 μ l PBS and *Bhe* were fixed with 35 μ l of 4% PFA. Bacteria were stained with DAPI and adherent *Bhe* were quantified using CellProfiler followed by visual inspection and manual curing where needed (applied CellProfiler pipeline is available online).

To investigate *Bhe* adhesion to mouse fibroblasts, we adapted a published protocol from Riess *et al.* (Riess *et al.*, 2007). In brief, 4000 GE11, GD25, GE11 β 1A or GD25 β 1A cells were seeded into each well of a 96 well plate. Following over night incubation, cells were infected with 10^7 *Bhe* in 100 μ l M199 and incubated for exactly 1 h without centrifugation. Next, M199 was discarded, wells were washed 3 times with 100 μ l PBS and *Bhe* were fixed with 35 μ l of 4% PFA. Bacteria were stained with DAPI and adherent *Bhe* were quantified using CellProfiler.

Calmodulin-dependent adenylate cyclase (Cya) reporter assay for translocation. For Cya reporter assays, 15'000 HeLa cells were seeded into wells of a 24 well plate and incubate over-night. The following day, cells were transfected according to published protocols (Truttmann *et al.*, in press) and incubated for 32 hours. Thereafter, cells were infected with *Bhe* wild-type containing pLMS404 or pLMS400 at MOI = 500 for 24 hours. Intracellular cAMP levels were determined using a cAMP Direct Biotrak EIA kit (GE Healthcare) according to manufacturer's instructions and results were normalized to protein concentrations as measured by the method of Bradford (Bradford, 1976) (Bradford Reagent, Sigma-Aldrich).

Semi-automated image analysis, invasome quantification, and screening hit selection.

Experiments performed in 96-well plates were subjected to automated high-throughput microscopy. Microscopic images were acquired using a MDC IXM automated Microscope (Molecular Devices). 10 sites per well were imaged using a 10x air-objective. Each site was acquired in three wavelengths (360nm, 488 nm, 532 nm) to visualize Cell nuclei, F-actin and bacteria. In total, one complete 96 well plate yielded in 2880 images.

For siRNA screening experiments, invasome formation was determined by an analysis pipeline consisting of CellProfiler (Carpenter et al., 2006), Enhanced CellClassifier (Misselwitz et al., 2010) and in case of screening CellHTS (Boutros et al., 2006). Images were batch-wise processed using CellProfiler (Carpenter et al., 2006) running on a Linux-cluster environment. CellProfiler was used to identify nuclei, cells as well as potential invasomes and to extract object features. For recognition of candidate invasomes a customized CellProfiler module was developed for determining places of best fit of a ring shaped template. Details of the CellProfiler and Enhanced CellClassifier pipelines and settings are available upon request

Primary CellProfiler output files (.mat) were merged, reorganized and splitted using Enhanced CellClassifier (Misselwitz et al., 2010). Data points obtained from several 96 well plates (> 10'000 cells) were used to train SVM-Models in enhanced CellClassifier that were further used to classify candidate invasomes by CellProfiler as true or false positives. The accuracy of the individual SVM-models was typically between 91-95% with a cross-validation rate of >92%. Processing of each 96 well plate by Enhanced CellClassifier resulted in a list containing the percentage of invasome positive cells in a given well. These numbers of at least three independent replica, together with well descriptions and further assay information were transferred into CellHTS (Boutros et al., 2006) to perform plate normalizations and hit scoring (median-method), where wells with a score higher than 1 were considered as potential hits. Additionally, 13 targets were picked as expert choices for validation.

Secondary validation experiments were in addition analyzed semi-automatically, using MetaExpress for nuclei detection in combination with by-eye quantification of invasomes.

Confocal Laser Scanning Microscopy. For confocal laser microscopy, the stained samples were analyzed using an IQ iXON spinning disc system from Andor in combination with an Olympus IX2-UCB microscope. Z-stacks with 20-30 focal planes with a spacing of 0.1-0.2 μm were recorded and Xz -and Yz-planes were reconstructed using Andor IQ software. Images were exported and finalized using Metamorph, ImageJ and Adobe Photoshop.

Sequence alignment. Sequence alignments of siRNA / gene sequences were performed using ClustalW (Larkin et al., 2007). JalView was used for production of alignment figures (Waterhouse et al., 2009).

Acknowledgements

We would like to thank Houchaima Ben Takaia for critical reading of the manuscript, Claudia Mistl for technical assistance and Neil Bate for the GFP-talin1 constructs. This work was supported by grant 31003A-132979 from the Swiss National Science Foundation, grant 55005501 from the Howard Hughes Medical Institute and grant 51RT-0_126008 (InfectX) from SystemsX.ch, the Swiss Initiative for Systems Biology.

References

- Agerer, F., Lux, S., Michel, A., Rohde, M., Ohlsen, K. and Hauck, C. R. (2005). Cellular invasion by *Staphylococcus aureus* reveals a functional link between focal adhesion kinase and cortactin in integrin-mediated internalisation. *J Cell Sci* 118, 2189-200.
- Agerer, F., Michel, A., Ohlsen, K. and Hauck, C. R. (2003). Integrin-mediated invasion of *Staphylococcus aureus* into human cells requires Src family protein-tyrosine kinases. *J Biol Chem* 278, 42524-31.
- Anthis, N. J., Wegener, K. L., Ye, F., Kim, C., Goult, B. T., Lowe, E. D., Vakonakis, I., Bate, N., Critchley, D. R., Ginsberg, M. H. et al. (2009). The structure of an integrin/talin complex reveals the basis of inside-out signal transduction. *EMBO J* 28, 3623-32.
- Armulik, A., Svineng, G., Wennerberg, K., Fassler, R. and Johansson, S. (2000). Expression of integrin subunit beta1B in integrin beta1-deficient GD25 cells does not interfere with alphaVbeta3 functions. *Exp Cell Res* 254, 55-63.
- Askari, J. A., Buckley, P. A., Mould, A. P. and Humphries, M. J. (2009). Linking integrin conformation to function. *J Cell Sci* 122, 165-70.
- Balzac, F., Retta, S. F., Albini, A., Melchiorri, A., Koteliansky, V. E., Geuna, M., Silengo, L. and Tarone, G. (1994). Expression of beta 1B integrin isoform in CHO cells results in a dominant negative effect on cell adhesion and motility. *J Cell Biol* 127, 557-65.
- Boutros, M., Bras, L. P. and Huber, W. (2006). Analysis of cell-based RNAi screens. *Genome Biol* 7, R66.
- Bradford, M. M. (1976). A rapid and sensitive method for the quantitation of microgram quantities of protein utilizing the principle of protein-dye binding. *Anal Biochem* 72, 248-54.
- Cantarelli, V. V., Takahashi, A., Yanagihara, I., Akeda, Y., Imura, K., Kodama, T., Kono, G., Sato, Y. and Honda, T. (2001). Talin, a host cell protein, interacts directly with the translocated intimin receptor, Tir, of enteropathogenic *Escherichia coli*, and is essential for pedestal formation. *Cell Microbiol* 3, 745-51.
- Carpenter, A. E., Jones, T. R., Lamprecht, M. R., Clarke, C., Kang, I. H., Friman, O., Guertin, D. A., Chang, J. H., Lindquist, R. A., Moffat, J. et al. (2006). CellProfiler: image analysis software for identifying and quantifying cell phenotypes. *Genome Biol* 7, R100.
- Cluzel, C., Saltel, F., Lussi, J., Paulhe, F., Imhof, B. A. and Wehrle-Haller, B. (2005). The mechanisms and dynamics of (alpha)v(beta)3 integrin clustering in living cells. *J Cell Biol* 171, 383-92.
- Critchley, D. R. (2009). Biochemical and structural properties of the integrin-associated cytoskeletal protein talin. *Annu Rev Biophys* 38, 235-54.
- Deakin, N. O. and Turner, C. E. (2008). Paxillin comes of age. *J Cell Sci* 121, 2435-44.
- Debrand, E., El Jai, Y., Spence, L., Bate, N., Praekelt, U., Pritchard, C. A., Monkley, S. J. and Critchley, D. R. (2009). Talin 2 is a large and complex gene encoding multiple transcripts and protein isoforms. *FEBS J* 276, 1610-28.
- Dehio, C. (2005). *Bartonella*-host-cell interactions and vascular tumour formation. *Nat Rev Microbiol* 3, 621-31.

Dehio, C., Meyer, M., Berger, J., Schwarz, H. and Lanz, C. (1997). Interaction of *Bartonella henselae* with endothelial cells results in bacterial aggregation on the cell surface and the subsequent engulfment and internalisation of the bacterial aggregate by a unique structure, the invasome. *J Cell Sci* 110, 2141-54.

Demali, K. A., Jue, A. L. and Burridge, K. (2006). IpaA targets beta1 integrins and rho to promote actin cytoskeleton rearrangements necessary for *Shigella* entry. *J Biol Chem* 281, 39534-41.

Dupuy, A. G. and Caron, E. (2008). Integrin-dependent phagocytosis: spreading from microadhesion to new concepts. *J Cell Sci* 121, 1773-83.

Edgell, C. J., McDonald, C. C. and Graham, J. B. (1983). Permanent cell line expressing human factor VIII-related antigen established by hybridization. *Proc Natl Acad Sci U S A* 80, 3734-7.

Fassler, R., Pfaff, M., Murphy, J., Noegel, A. A., Johansson, S., Timpl, R. and Albrecht, R. (1995). Lack of beta 1 integrin gene in embryonic stem cells affects morphology, adhesion, and migration but not integration into the inner cell mass of blastocysts. *J Cell Biol* 128, 979-88.

Florin, T. A., Zaoutis, T. E. and Zaoutis, L. B. (2008). Beyond cat scratch disease: widening spectrum of *Bartonella henselae* infection. *Pediatrics* 121, e1413-25.

Franco, S. J., Rodgers, M. A., Perrin, B. J., Han, J., Bennin, D. A., Critchley, D. R. and Huttenlocher, A. (2004). Calpain-mediated proteolysis of talin regulates adhesion dynamics. *Nat Cell Biol* 6, 977-83.

Giannone, G., Jiang, G., Sutton, D. H., Critchley, D. R. and Sheetz, M. P. (2003). Talin1 is critical for force-dependent reinforcement of initial integrin-cytoskeleton bonds but not tyrosine kinase activation. *J Cell Biol* 163, 409-19.

Gingras, A. R., Bate, N., Goult, B. T., Hazelwood, L., Canestrelli, I., Grossmann, J. G., Liu, H., Putz, N. S., Roberts, G. C., Volkman, N. et al. (2008). The structure of the C-terminal actin-binding domain of talin. *EMBO J* 27, 458-69.

Huang, C., Rajfur, Z., Yousefi, N., Chen, Z., Jacobson, K. and Ginsberg, M. H. (2009). Talin phosphorylation by Cdk5 regulates Smurf1-mediated talin head ubiquitylation and cell migration. *Nat Cell Biol* 11, 624-30.

Huveneers, S. and Danen, E. H. (2009). Adhesion signaling - crosstalk between integrins, Src and Rho. *J Cell Sci* 122, 1059-69.

Isberg, R. R. and Barnes, P. (2001). Subversion of integrins by enteropathogenic *Yersinia*. *J Cell Sci* 114, 21-28.

Jimenez-Soto, L. F., Kutter, S., Sewald, X., Ertl, C., Weiss, E., Kapp, U., Rohde, M., Pirch, T., Jung, K., Retta, S. F. et al. (2009). *Helicobacter pylori* type IV secretion apparatus exploits beta1 integrin in a novel RGD-independent manner. *PLoS Pathog* 5, e1000684.

Jonsson, K., Signas, C., Muller, H. P. and Lindberg, M. (1991). Two different genes encode fibronectin binding proteins in *Staphylococcus aureus*. The complete nucleotide sequence and characterization of the second gene. *Eur J Biochem* 202, 1041-8.

Kopp, P. M., Bate, N., Hansen, T. M., Brindle, N. P., Praekelt, U., Debrand, E., Coleman, S., Mazzeo, D., Goult, B. T., Gingras, A. R. et al. (2010). Studies on the morphology and spreading of human endothelial cells define key inter- and intramolecular interactions for talin1. *Eur J Cell Biol* 89, 661-73.

Kwok, T., Zabler, D., Urman, S., Rohde, M., Hartig, R., Wessler, S., Misselwitz, R., Berger, J., Sewald, N., Konig, W. et al. (2007). *Helicobacter* exploits integrin for type IV secretion and kinase activation. *Nature* 449, 862-6.

Larkin, M. A., Blackshields, G., Brown, N. P., Chenna, R., McGettigan, P. A., McWilliam, H., Valentin, F., Wallace, I. M., Wilm, A., Lopez, R. et al. (2007). Clustal W and Clustal X version 2.0. *Bioinformatics* 23, 2947-8.

Lim, Y., Han, I., Jeon, J., Park, H., Bahk, Y. Y. and Oh, E. S. (2004). Phosphorylation of focal adhesion kinase at tyrosine 861 is crucial for Ras transformation of fibroblasts. *J Biol Chem* 279, 29060-5.

Luo, B. H., Carman, C. V. and Springer, T. A. (2007). Structural basis of integrin regulation and signaling. *Annu Rev Immunol* 25, 619-47.

Luo, B. H. and Springer, T. A. (2006). Integrin structures and conformational signaling. *Curr Opin Cell Biol* 18, 579-86.

Misselwitz, B., Strittmatter, G., Periaswamy, B., Schlumberger, M. C., Rout, S., Horvath, P., Kozak, K. and Hardt, W. D. (2010). Enhanced CellClassifier: a multi-class classification tool for microscopy images. *BMC Bioinformatics* 11, 30.

Monkley, S. J., Pritchard, C. A. and Critchley, D. R. (2001). Analysis of the mammalian talin2 gene TLN2. *Biochem Biophys Res Commun* 286, 880-5.

Monkley, S. J., Zhou, X. H., Kinston, S. J., Giblett, S. M., Hemmings, L., Priddle, H., Brown, J. E., Pritchard, C. A., Critchley, D. R. and Fassler, R. (2000). Disruption of the talin gene arrests mouse development at the gastrulation stage. *Dev Dyn* 219, 560-74.

Nemerow, G. R. (2009). A new link between virus cell entry and inflammation: adenovirus interaction with integrins induces specific proinflammatory responses. *Mol Ther* 17, 1490-1.

Nieves, B., Jones, C. W., Ward, R., Ohta, Y., Reverte, C. G. and LaFlamme, S. E. (2010). The NPIY motif in the integrin beta1 tail dictates the requirement for talin-1 in outside-in signaling. *J Cell Sci* 123, 1216-26.

Ohta, Y., Hartwig, J. H. and Stossel, T. P. (2006). FILGAP, a Rho- and ROCK-regulated GAP for Rac binds filamin A to control actin remodelling. *Nat Cell Biol* 8, 803-14.

Rhomberg, T. A., Truttmann, M. C., Guye, P., Ellner, Y. and Dehio, C. (2009). A translocated protein of *Bartonella henselae* interferes with endocytic uptake of individual bacteria and triggers uptake of large bacterial aggregates via the invasome. *Cell Microbiol* 11, 927-45.

Riess, T., Raddatz, G., Linke, D., Schafer, A. and Kempf, V. A. (2007). Analysis of *Bartonella* adhesin A expression reveals differences between various *B. henselae* strains. *Infect Immun* 75, 35-43.

Scheidegger, F., Ellner, Y., Guye, P., Rhomberg, T. A., Weber, H., Augustin, H. G. and Dehio, C. (2009). Distinct activities of *Bartonella henselae* type IV secretion effector proteins modulate capillary-like sprout formation. *Cell Microbiol* 11, 1088-101.

Schlaepfer, D. D., Hanks, S. K., Hunter, T. and van der Geer, P. (1994). Integrin-mediated signal transduction linked to Ras pathway by GRB2 binding to focal adhesion kinase. *Nature* 372, 786-91.

Schmid, M. C., Scheidegger, F., Dehio, M., Balmelle-Devaux, N., Schulein, R., Guye, P., Chennakesava, C. S., Biedermann, B. and Dehio, C. (2006). A translocated bacterial protein protects vascular endothelial cells from apoptosis. *PLoS Pathog* 2, e115.

Schmid, M. C., Schulein, R., Dehio, M., Denecker, G., Carena, I. and Dehio, C. (2004). The VirB type IV secretion system of *Bartonella henselae* mediates invasion, proinflammatory activation and antiapoptotic protection of endothelial cells. *Mol Microbiol* 52, 81-92.

Schulein, R. and Dehio, C. (2002). The VirB/VirD4 type IV secretion system of *Bartonella* is essential for establishing intraerythrocytic infection. *Mol Microbiol* 46, 1053-67.

Schulein, R., Guye, P., Rhomberg, T. A., Schmid, M. C., Schroder, G., Vergunst, A. C., Carena, I. and Dehio, C. (2005). A bipartite signal mediates the transfer of type IV secretion substrates of *Bartonella henselae* into human cells. *Proc Natl Acad Sci U S A* 102, 856-61.

Selbach, M., Paul, F. E., Brandt, S., Guye, P., Daumke, O., Backert, S., Dehio, C. and Mann, M. (2009). Host cell interactome of tyrosine-phosphorylated bacterial proteins. *Cell Host Microbe* 5, 397-403.

Shattil, S. J., Kim, C. and Ginsberg, M. H. (2010). The final steps of integrin activation: the end game. *Nat Rev Mol Cell Biol* 11, 288-300.

Simonson, W. T., Franco, S. J. and Huttenlocher, A. (2006). Talin1 regulates TCR-mediated LFA-1 function. *J Immunol* 177, 7707-14.

Snijder, B., Sacher, R., Ramo, P., Damm, E. M., Liberali, P. and Pelkmans, L. (2009). Population context determines cell-to-cell variability in endocytosis and virus infection. *Nature* 461, 520-3.

Sory, M. P. and Cornelis, G. R. (1994). Translocation of a hybrid YopE-adenylate cyclase from *Yersinia enterocolitica* into HeLa cells. *Mol Microbiol* 14, 583-94.

Tadokoro, S., Shattil, S. J., Eto, K., Tai, V., Liddington, R. C., de Pereda, J. M., Ginsberg, M. H. and Calderwood, D. A. (2003). Talin binding to integrin beta tails: a final common step in integrin activation. *Science* 302, 103-6.

Takagi, J., Petre, B. M., Walz, T. and Springer, T. A. (2002). Global conformational rearrangements in integrin extracellular domains in outside-in and inside-out signaling. *Cell* 110, 599-11.

Truttmann, M. C., Rhomberg, T. R. and Dehio, C. Combined action of the type IV secretion effector proteins BepC and BepF promotes invasome formation of *Bartonella henselae* on endothelial and epithelial cells. *Cell Microbiol*, in press.

Van Nhieu, G. T. and Isberg, R. R. (1991). The *Yersinia pseudotuberculosis* invasin protein and human fibronectin bind to mutually exclusive sites on the alpha 5 beta 1 integrin receptor. *J Biol Chem* 266, 24367-75.

Waterhouse, A. M., Procter, J. B., Martin, D. M., Clamp, M. and Barton, G. J. (2009). Jalview Version 2--a multiple sequence alignment editor and analysis workbench. *Bioinformatics* 25, 1189-91.

Wegener, K. L., Partridge, A. W., Han, J., Pickford, A. R., Liddington, R. C., Ginsberg, M. H. and Campbell, I. D. (2007). Structural basis of integrin activation by talin. *Cell* 128, 171-82.

Wen, K. K., Rubenstein, P. A. and DeMali, K. A. (2009). Vinculin nucleates actin polymerization and modifies actin filament structure. *J Biol Chem* 284, 30463-73.

Wennerberg, K., Lohikangas, L., Gullberg, D., Pfaff, M., Johansson, S. and Fassler, R. (1996). Beta 1 integrin-dependent and -independent polymerization of fibronectin. *J Cell Biol* 132, 227-38.

Wickham, T. J., Mathias, P., Cheresch, D. A. and Nemerow, G. R. (1993). Integrins alpha v beta 3 and alpha v beta 5 promote adenovirus internalization but not virus attachment. *Cell* 73, 309-19.

Zaidel-Bar, R., Itzkovitz, S., Ma'ayan, A., Iyengar, R. and Geiger, B. (2007). Functional atlas of the integrin adhesome. *Nat Cell Biol* 9, 858-67.

Ziegler, W. H., Liddington, R. C. and Critchley, D. R. (2006). The structure and regulation of vinculin. *Trends Cell Biol* 16, 453-60.

Figure legends and tables

Figure 1. Schematic representation of RNAi screening setup and results. (A) Schematic representation of the screening setup used in this study. (B) Flowchart summarizing the procession of hits from the primary and secondary screen as well as validated hits. (C) HeLa cell infection followed by quantification of *Bhe* wild-type-triggered invasome formation upon knockdown of indicated target genes (n>1000 cells). Mock-normalized results of at least 3 independent experiments +/- s.d. are depicted. Using student's t-test the data marked by an asterisk differ statistically significantly ($p<0.01$) from mock transfected controls.

Figure 2. Integrin $\beta 1$, talin1 and FAK are engaged in multiple steps of invasome formation.

(A) Quantification of *Bhe* wild-type adherence to protein coated surfaces. Proteins used for coating are indicated. Results of three independent experiments +/- s.d. are depicted. Using student's t-test the data marked by an asterisk differ statistically significantly ($p<0.01$) from gelatin coated controls. (B) Quantification of *Bhe* wild-type adherence to mouse fibroblasts. Specific cell lines expressing / not expressing integrin $\beta 1A$ are indicated. Results of three independent experiments +/- s.d. are depicted. Using student's t-test the data marked by an asterisk differ statistically significantly ($p<0.01$) from $\beta 1A$ knock-out cells. (C) Analysis of *Bhe* effector translocation upon knockdown of indicated genes using Cya-reporter assays. Results of three independent experiments +/- s.d. are depicted. Using student's t-test the data marked by an asterisk differ statistically significantly ($p<0.01$) from controls. (D) Analysis of invasome formation on cells ectopically expressing eGFP-BepC and eGFP-BepG and infected with *Bhe* $\Delta bepA-G$ in combination with the indicated gene knockdowns. Results of four independent experiments +/- s.d. are depicted. Using student's t-test the data marked by an asterisk differ statistically significantly ($p<0.01$) from mock transfected controls. (E) Immunocytochemical localization patterns of indicated proteins upon *Bhe* wild-type-triggered invasome formation on HeLa cells. Representative images are depicted here. Co-localizing proteins are marked with an arrow. Scale bars are indicated.

Figure 3. Invasome formation in the presence of distinct integrin β 1 Ab. Quantification of *Bhe* wild-type triggered invasome formation in the presence of inhibiting (P5D2) or stimulating (12G10, B44, N29, B3B11) integrin β 1 Ab ($n > 1000$ cells). Results of at least three independent experiments \pm s.d. are depicted. Ab concentration and Ab clone name are indicated. Using student's t-test the data marked by an asterisk differ statistically significantly ($p < 0.01$) from untreated controls.

Figure 4. Integrin β 1-mediated outside-in signaling as well as integrin β 1 clustering are essential for invasome formation. **(A)** Clustering of Ab coated polystyrene beads on *Bhe* wild-type infected HeLa cells. Beads are coated with P5D2 Ab (inhibiting), 12G10 (stimulating) Ab or BSA, as indicated. **(B)** Quantification of beads distribution on *Bhe* wild-type infected Ea.hy926 cells. At least 10 randomly chosen fields of vision were quantified per condition and experiment. Results of at least three independent experiments \pm s.d. are depicted. Using student's t-test the data marked by an asterisk differ statistically significantly ($p < 0.01$) from antibody-free controls. **(C)** Quantification of invasome formation on *Bhe* wild-type infected cells over-expressing integrin β 1B *in trans*. Results of at least three independent experiments \pm s.d. are depicted. Using student's t-test the data marked by an asterisk differ statistically significantly ($p < 0.01$) from mock transfected controls. **(D)** Quantification of *Bhe* wild-type triggered invasome formation on HeLa cells expressing FAK mutants ($n > 500$ cells); results of three independent experiments \pm s.d. are depicted here. Using student's t-test the data marked by an asterisk differ statistically significantly ($p < 0.01$) from mock transfected control wells. **(E)** Quantification of invasome formation triggered by *Bhe* wild-type in the presence of Src inhibitor SU6656 ($n > 1000$ cells). Results of three independent experiments \pm s.d. are depicted. Using student's t-test the data marked by an asterisk differ statistically significantly ($p < 0.01$) from DMSO-treated controls.

Figure 5. Talin1-, but not talin2-promoted inside-out activation of integrins contributes to invasome formation. (A) Quantification of *Bhe* triggered invasome formation on HeLa cells upon talin1 knockdown ($n > 1000$ cells); results of at least three independent experiments \pm s.d. are depicted. Using student's t-test the data marked by an asterisk differ statistically significantly ($p < 0.01$) from mock-transfected control wells. **(B)** Quantification of *Bhe* triggered invasome formation on talin1 knockdown HeLa cells expressing GFP or GFP-tagged mouse-talin1, mtalin1 L325R or mtalin1 R2526G mutant *in trans* ($n > 500$ cells); experiments have been performed in independent triplicates; one representative is depicted here. Using student's t-test the data marked by an asterisk differ statistically significantly ($p < 0.01$) from GFP-talin1-expressing cells. **(C)** Quantification of *Bhe* triggered invasome formation on talin1 knockdown HeLa cells expressing GFP or GFP-tagged mouse-talin1, mtalin1 aa1-433 or mtalin1 L439G mutant *in trans* ($n > 500$ cells); experiments have been performed in independent triplicates; one representative is depicted here. Using student's t-test the data marked by an asterisk differ statistically significantly ($p < 0.01$) from GFP-talin1-expressing cells. **(D)** Quantification of *Bhe* triggered invasome formation on HeLa cells in the presence of protease inhibitor calpeptin ($n > 1000$ cells); calpeptin concentration are indicated. Results of at least three independent experiments \pm s.d. are depicted. Using student's t-test the data marked by an asterisk differ statistically significantly ($p < 0.01$) from H₂O-treated controls.

Figure S1. Bhe interacts with integrin $\beta 1$ in a fibronectin-independent manner. (A) Staining of *Bhe* wild-type and *Bhe* Δ BepA-G with human fibronectin Ab. Scale bars are indicated. **(B)** Quantification of *Bhe* wild-type-mediated invasome formation on HeLa cells in the presence of human fibronectin Ab ($n > 1000$ cells). Results of three independent experiments \pm s.d. are depicted. **(C)** Quantification of *Bhe*-mediated invasome formation on HeLa cells co-expressing GFP-BepC and GFP-BepG. Results of three independent experiments \pm s.d. are depicted.

Figure S2. Binding sites of used integrin $\beta 1$ Ab. (A) Table summarizing the described Ab target domain and the effect of inhibiting / stimulating integrin $\beta 1$ Ab on *Bhe*-mediated effector translocation into Ea.hy926 cells and invasome formation on HeLa cells. **(B)** Schematic overview of Ab binding sites occupied by the different integrin $\beta 1$ Ab used in this study.

Figure S3. Effector translocation and translocation-independent invasome formation in the presence of distinct integrin $\beta 1$ Ab. (A) Quantification of *Bhe* wild-type -mediated effector translocation into HeLa cells in the presence of indicated inhibiting or stimulating integrin $\beta 1$ Ab ($n > 1000$ cells). Results of two independent experiments \pm s.d. are depicted. Using student's t-test the data marked by an asterisk differ statistically significantly ($p < 0.01$) from controls. **(B)** Quantification of *Bhe* Δ BepA-G-triggered invasome formation on HeLa cells co-expressing eGFP-BepC and eGFP-BepG fusion in the presence of indicated inhibiting or stimulating integrin $\beta 1$ Ab ($n > 1000$ cells). Results of three independent experiments \pm s.d. are depicted. Using student's t-test the data marked by an asterisk differ statistically significantly ($p < 0.01$) from antibody-free controls.

Figure S4. Active integrin β 1 clusters at sites of invasome formation. (A) Clustering of Ab coated polystyrene beads on *Bhe* wild-type infected Ea.hy926 cells. Beads are coated with P5D2 Ab (inhibiting), 12G10 (stimulating) Ab or BSA, as indicated. **(B)** Quantification of coated beads distribution on *Bhe* wild-type infected Ea.hy926 cells. At least 10 randomly chosen fields of vision were quantified per condition and experiment. Results of at least three independent experiments +/- s.d. are depicted. Using student's t-test the data marked by an asterisk differ statistically significantly ($p < 0.01$) from antibody-free controls.

Figure S5. Invasome formation is sensitive to Src kinase inhibitor S15. Quantification of invasome formation triggered by *Bhe* wild-type in the presence of Src inhibitor 5 (S15) ($n > 1000$ cells). Results of three independent experiments +/- s.d. are depicted. Using student's t-test the data marked by an asterisk differ statistically significantly ($p < 0.01$) from DMSO treated controls.

Figure S6. Talin1 and talin2 are both expressed in HeLa cells. (A) Staining of HeLa cells infected with *Bhe* wild-type using TRITC-Phalloidin (actin), DAPI (DNA) and Ab against talin1 or talin2. **(B)** Sequence comparison of talin1 and talin2 sequences with sequence of used talin1 siRNA. **(C)** Immuno-plot of talin1 / talin2 knock-down cells to exclude cross-reactivity of used siRNAs. **(D)** Sequence comparison of htalin1, mtalin1 and htalin1 siRNA sequence used in this study.

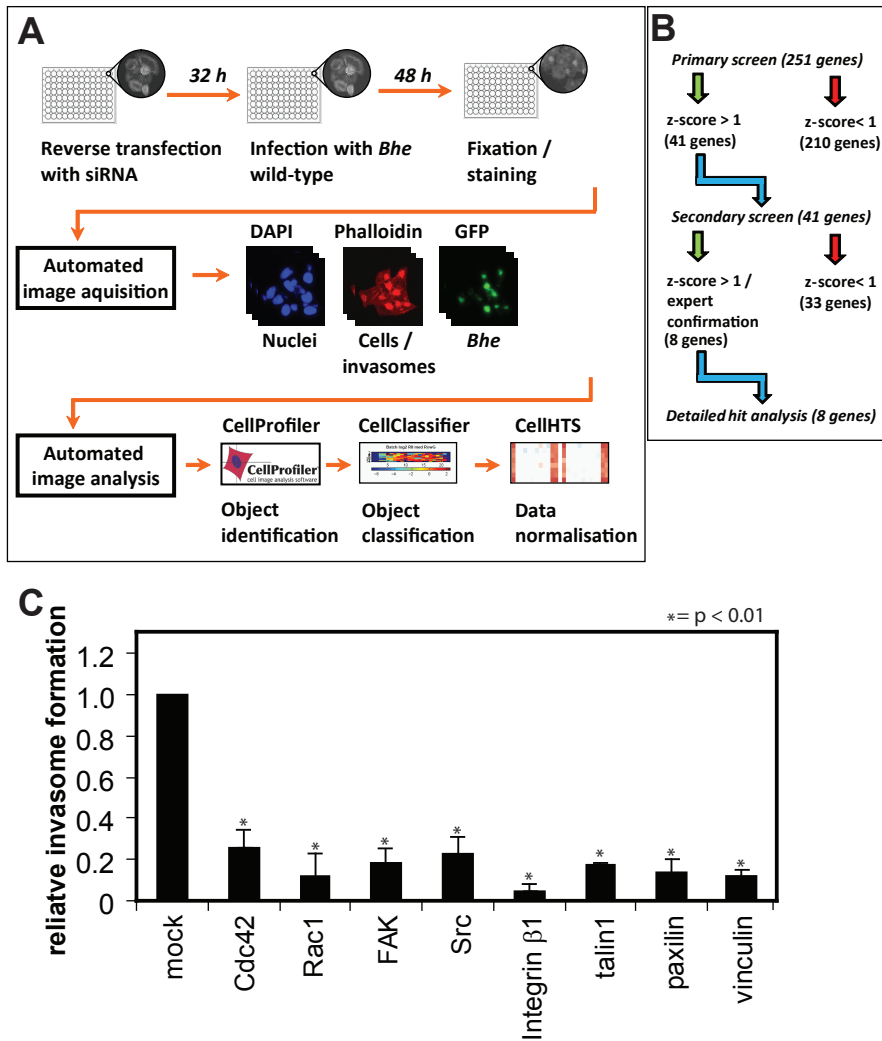


Figure 1
(Truttmann *et al.*)

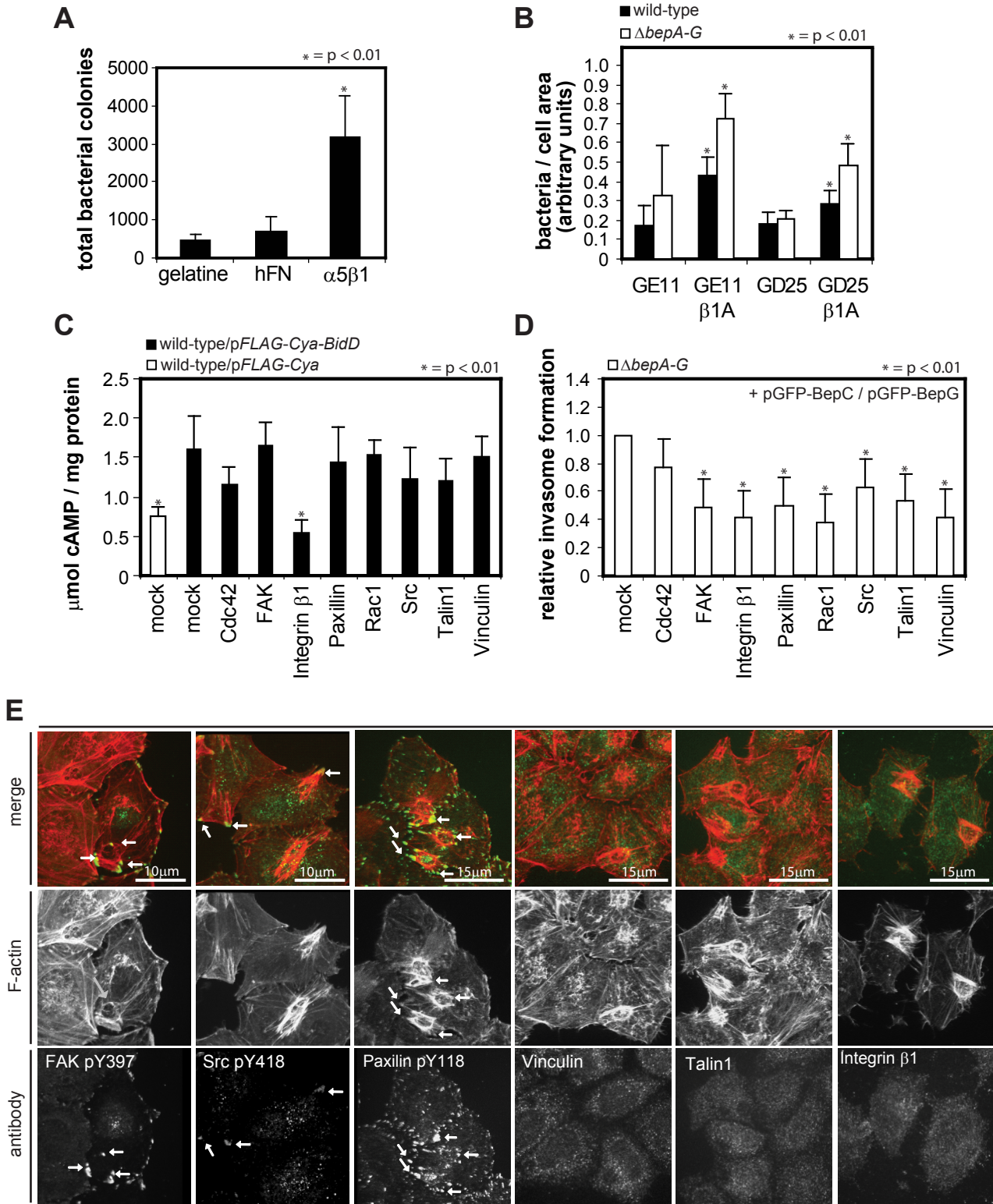


Figure 2
(Truttmann *et al.*)

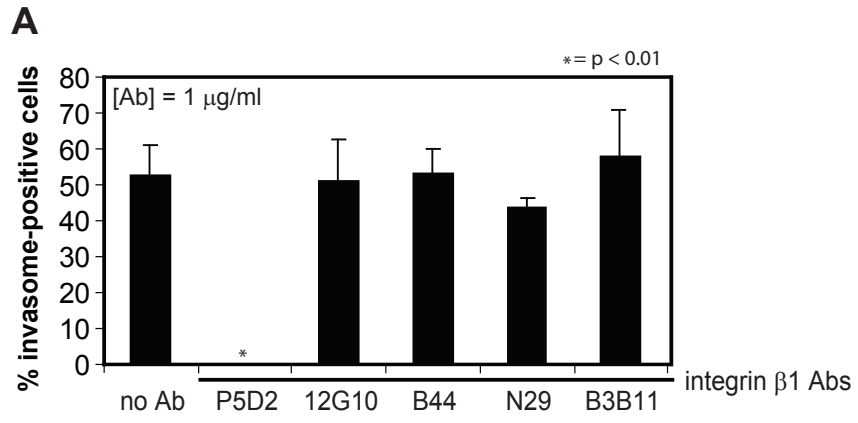


Figure 3
(Truttmann *et al.*)

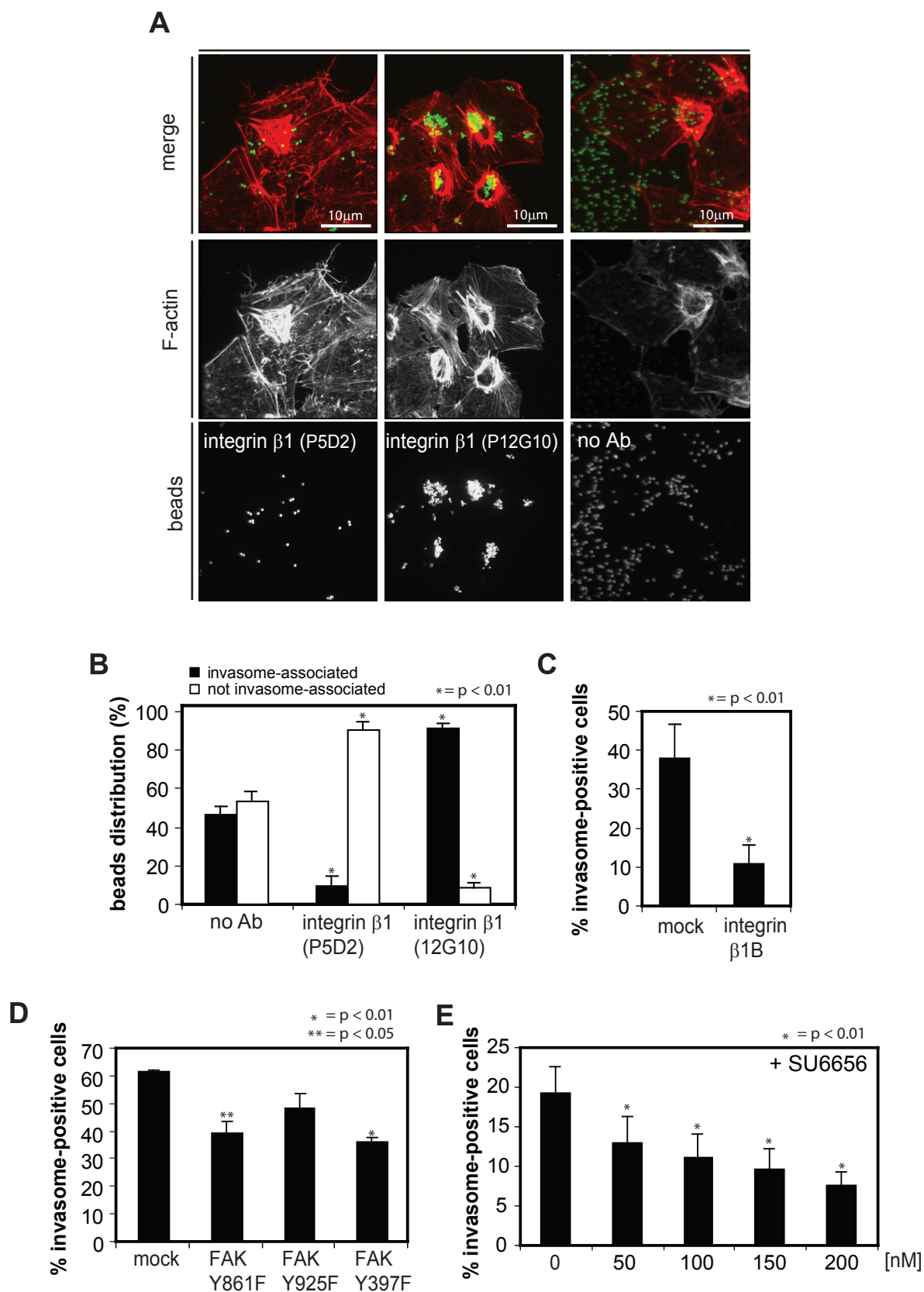


Figure 4
(Truttmann *et al.*)

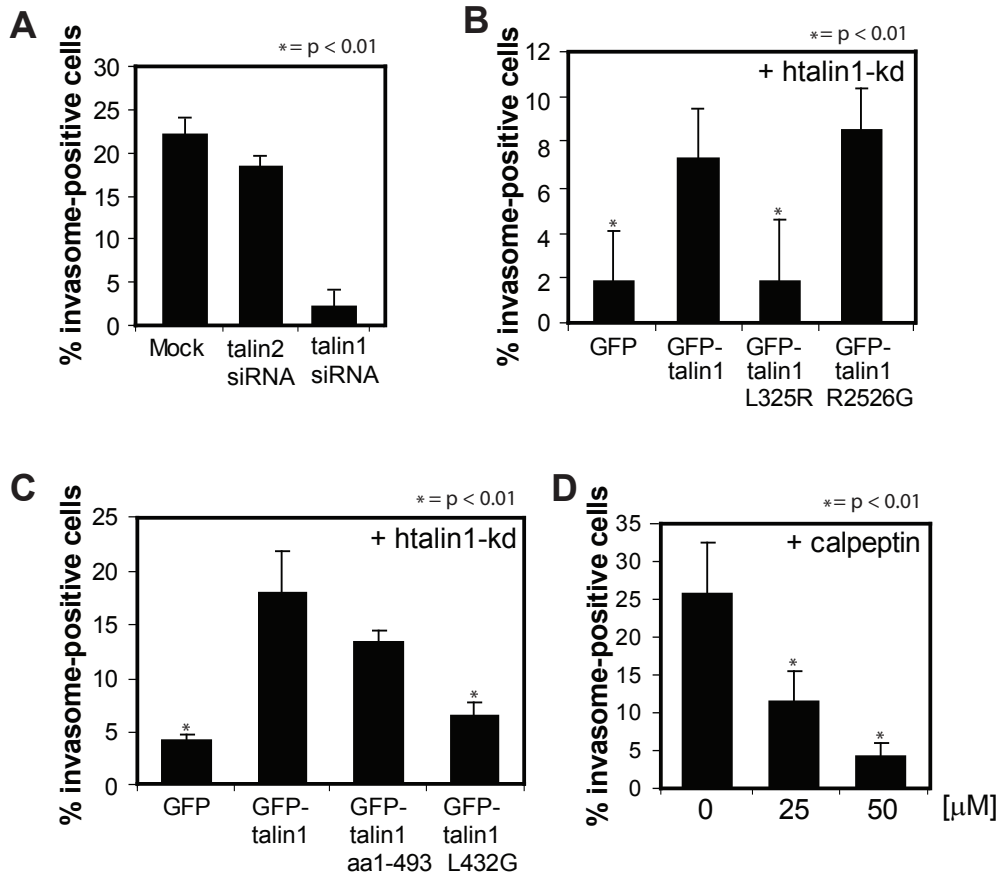


Figure 5
(Truttmann *et al.*)

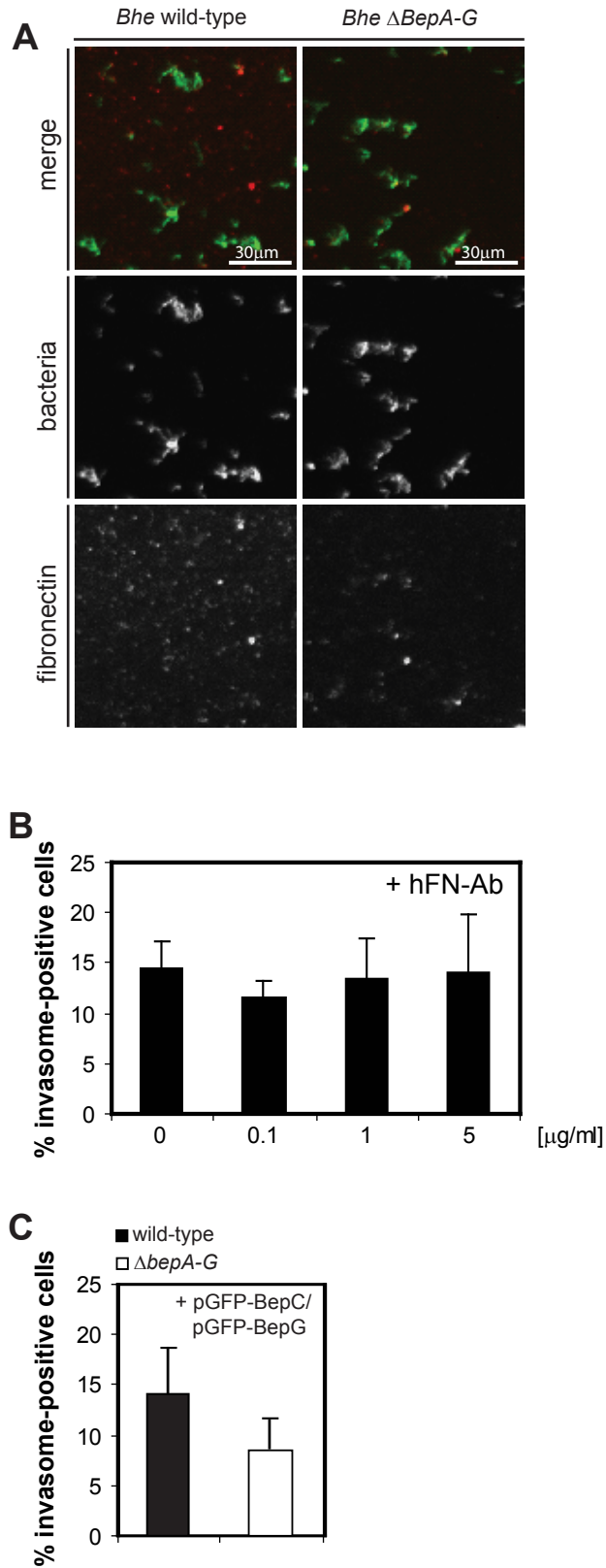


Figure S1
(Truttmann *et al.*)

A

| Treatment | Concentration | Target | Trans-location | Invasome formation |
|--|---------------|---|----------------|--------------------|
| Untreated | - | - | +++ | +++ |
| integrin β1 antibodies | | | | |
| P5D2 | 1 μ g/ml | Inhibitory mAb; suggested to interfere with ligand binding | - | - |
| N29 | 1 μ g/ml | Stimulatory mAb, binds integrin β 1 PSI domain | +++ | +++ |
| 12G10 | 1 μ g/ml | Stimulatory mAb, binds to active form of integrin β 1 | +++ | +++ |
| B44 | 1 μ g/ml | Stimulatory mAb, suggested to bind ligand-occupied, active integrin β 1 | +++ | +++ |
| B3B11 | 1 μ g/ml | Stimulatory mAb, binds to β -tail region of integrin β 1 | +++ | +++ |

B

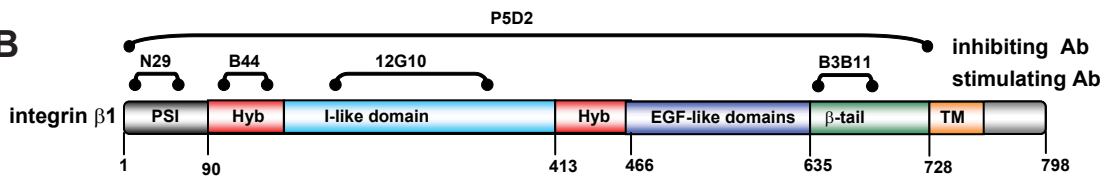


Figure S2
(Truttmann *et al.*)

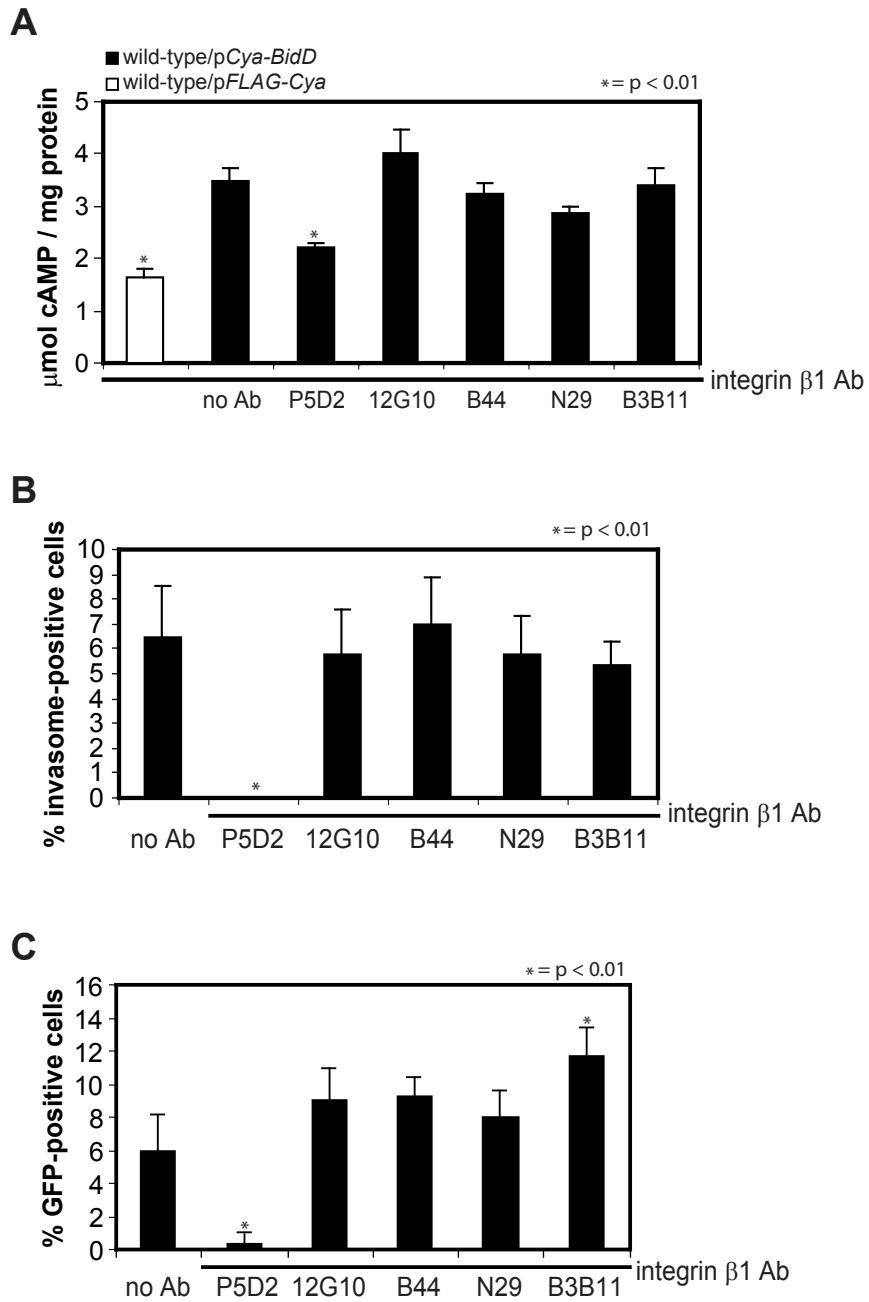
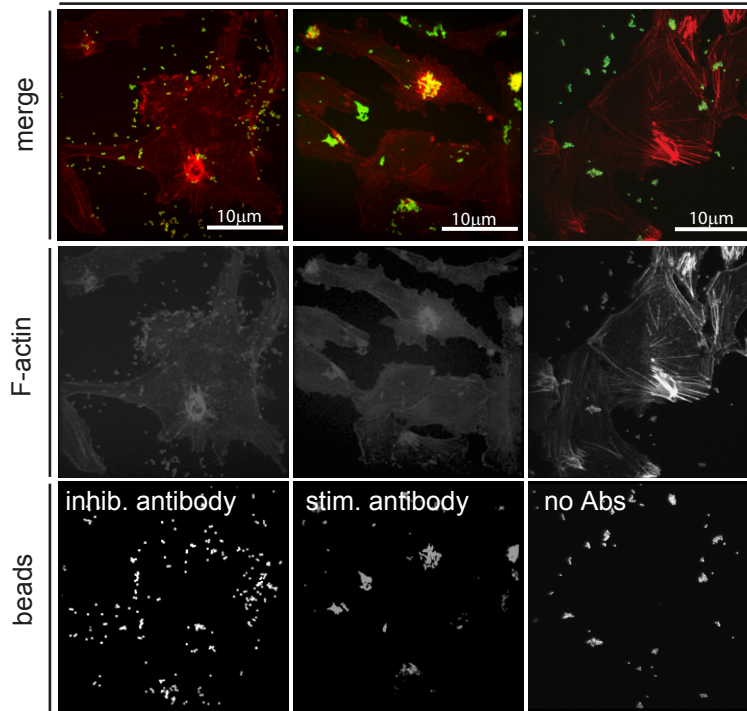


Figure S3
(Truttmann *et al.*)

A



B

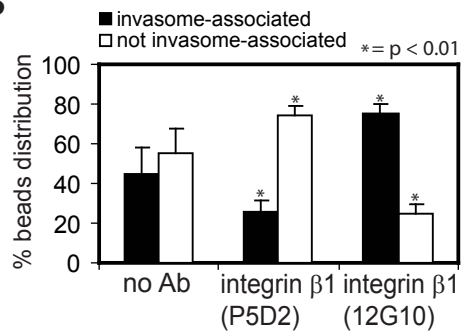


Figure S4
(Truttmann *et al.*)

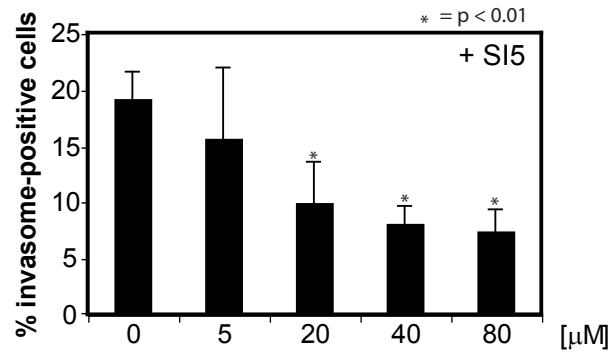
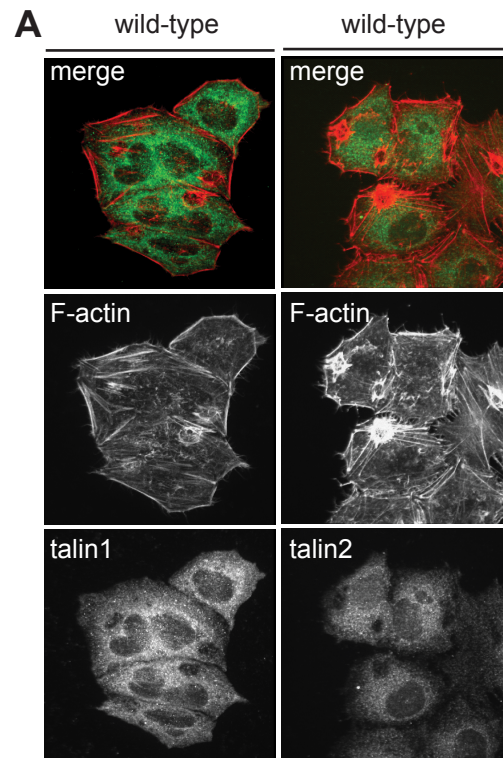


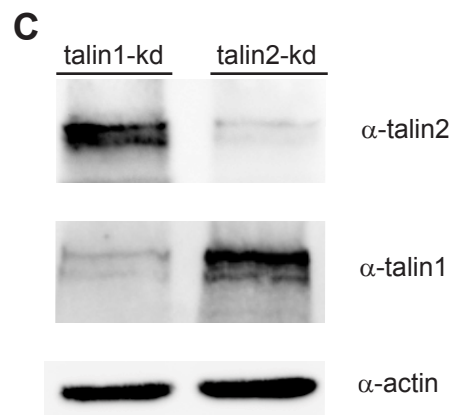
Figure S5
(Truttmann *et al.*)



B

| | |
|------------------------|-----------------------|
| <i>TLN2_siRNA/1-21</i> | CTCCTGAATAACTGCGTAAA |
| <i>TLN2_seq/1-21</i> | CTCCTGAATAACTGCGTAAA |
| <i>TLN1_seq/1-21</i> | GGCTCTGAACCGCTGTCTCAG |

10

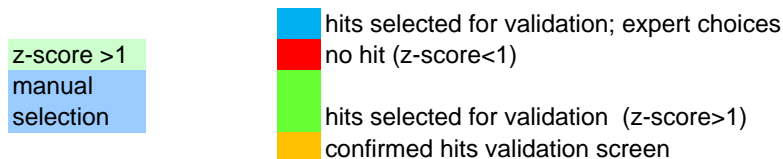


D

| | |
|------------------------|-----------------------|
| <i>hTLN1_seq/1-21</i> | AACAGAGACCCCTGAAGATCC |
| <i>TLN1_siRNA/1-21</i> | AACAGAGACCCCTGAAGATCC |
| <i>mTLN1_seq/1-21</i> | AGCAGAGACCCCTGAAGATCC |

10

Figure S6
(Truttmann *et al.*)



| Gene Symbol | primary screen | | | validation screen | | |
|-------------|----------------|-----------|--|-------------------|----------------|----------------|
| | z - score 1 | z-score 2 | | z-score oligo1 | z-score oligo2 | z-score oligo3 |
| AATK | 0.75 | -0.77 | | | | |
| ABL1 | 1.62 | 0.96 | | 0.29 | -0.64 | -0.21 |
| ABL2 | -0.96 | 0.24 | | | | |
| ACVR1 | -0.51 | -0.36 | | | | |
| ACVR1B | 0.39 | 0.33 | | | | |
| ACVR2 | 1.08 | 1.07 | | 0.95 | 0.59 | 0.06 |
| ACVRL1 | 0.5 | 0.17 | | | | |
| ANKK1 | -0.36 | -0.33 | | | | |
| ANKRD3 | 0.3 | 0.76 | | | | |
| ARAF | 0.54 | -0.36 | | | | |
| ARFIP2 | 0.39 | -0.79 | | | | |
| ARHGAP20 | 1.2 | 0.26 | | | | |
| ARHGAP21 | 0.56 | -0.17 | | | | |
| ARHGAP5 | 0.19 | -0.13 | | | | |
| ARHGAP6 | -0.11 | N/A | | | | |
| ARHGEF12 | 0.93 | 0.6 | | | | |
| ARPC3 | 0.67 | 0.17 | | | | |
| AXL | 0.87 | 0.02 | | | | |
| BAIAP2 | 0.64 | -0.12 | | | | |
| BCAR1 | 1.75 | 0.21 | | 0.99 | 0.49 | -0.08 |
| BMPR1A | 0.59 | -0.48 | | | | |
| BMPR1B | 0.48 | 0.36 | | | | |
| BMPR2 | 0.46 | 0.53 | | | | |
| BMX | -0.53 | 0.02 | | | | |
| C14orf173 | 0.96 | 0.41 | | | | |
| CDC42 | 1.68 | 1.37 | | 1.68 | 1.52 | 1.47 |
| CDC42BPA | 1.88 | 0.08 | | | | |
| CFL1 | -0.98 | 0.55 | | | | |
| CFL2 | -2.05 | | | | | |
| CHUK | 1.53 | 1.25 | | 1.04 | 1.03 | 0.72 |
| COBL | 1.34 | -0.84 | | | | |
| COL1A1 | 0 | -0.37 | | | | |
| COL1A2 | 1.4 | 0.87 | | | | |
| COL3A1 | 0.93 | 0.44 | | | | |
| COL4A4 | 0.23 | -0.96 | | | | |
| COL4A5 | 1 | -0.92 | | | | |
| COL4A6 | 0.54 | 0.47 | | | | |
| CRK | 0.15 | -0.27 | | | | |
| CSK | 1.29 | 0.2 | | 0.06 | 2 | -0.8 |
| CYTSA | 1.2 | 0.62 | | | | |
| DAAM1 | 0.01 | -1.35 | | | | |
| DAAM2 | -0.6 | -0.79 | | | | |
| DDR1 | 0.09 | 0.4 | | | | |
| DDR2 | -0.63 | -0.25 | | | | |
| DGKA | 1.44 | 1.15 | | -0.73 | -0.94 | -0.96 |
| DGKB | 0.78 | 0.36 | | | | |
| DGKD | 0.96 | -1.52 | | | | |
| DGKE | 0.99 | 0.54 | | | | |
| DGKG | 0.27 | 0.09 | | | | |
| DGKH | 0.71 | 0.54 | | | | |

| | | | | | | |
|---------|-------|-------|--|-------|-------|-------|
| DGKK | 0.39 | -1.15 | | | | |
| DGKQ | 0.11 | -0.35 | | | | |
| DGKZ | 1.78 | 0.64 | | | | |
| DIAPH1 | 0.46 | -0.32 | | | | |
| DIAPH2 | -0.18 | -0.42 | | | | |
| DIAPH3 | -0.03 | -0.33 | | | | |
| DNMBP | 1.87 | 0.33 | | | | |
| DOCK1 | 0.7 | 0.51 | | | | |
| EGFR | 0.82 | -1.6 | | | | |
| ELMO1 | 0.62 | 0.49 | | | | |
| EPHA1 | 1.45 | -0.58 | | | | |
| EPHA2 | 1.35 | -0.69 | | | | |
| EPHA3 | 0.15 | 0 | | | | |
| EPHA4 | 1.78 | 1.6 | | -1.09 | | |
| EPHA5 | 1.59 | N/A | | -0.95 | | |
| EPHA7 | 0.58 | 0.35 | | | | |
| EPHA8 | 0.65 | 0.59 | | | | |
| EPHB1 | 0.69 | -0.85 | | | | |
| EPHB2 | 0.34 | 0.69 | | | | |
| EPHB3 | 0.94 | -0.88 | | | | |
| EPHB4 | 0.41 | 0.69 | | | | |
| EPHB6 | -0.24 | 0.54 | | | | |
| ERBB2 | 1.13 | 0.83 | | -0.48 | | |
| ERBB2IP | 1.97 | 1.21 | | 1.21 | 0.63 | -0.76 |
| ERBB3 | 2.23 | 1.84 | | 0.52 | -0.33 | -0.66 |
| ERBB4 | -0.49 | 0.06 | | | | |
| FER | -0.62 | -0.1 | | | | |
| FES | 1.44 | -1.11 | | | | |
| FGFR1 | -0.14 | 0.41 | | | | |
| FGFR2 | 0.19 | 0.76 | | | | |
| FGFR3 | 0.27 | 0.75 | | | | |
| FGFR4 | 2.02 | 1.95 | | -2.73 | -0.81 | -1.07 |
| FHOD1 | 0.41 | -0.27 | | | | |
| FHOD3 | 0.4 | 0.02 | | | | |
| FLT1 | -0.89 | -0.05 | | | | |
| FLT3 | -0.32 | 0.5 | | | | |
| FLT4 | -1 | 0.08 | | | | |
| FMN1 | -0.28 | -0.41 | | | | |
| FMN2 | -1.53 | -1.76 | | | | |
| FMNL1 | -0.95 | -1.42 | | | | |
| FMNL2 | -0.61 | -1.01 | | | | |
| FMNL3 | -0.3 | -0.88 | | | | |
| FRK | 1.16 | N/A | | 0.58 | 0.33 | -0.38 |
| FYN | -0.55 | -0.86 | | | | |
| GRB2 | -0.99 | -0.51 | | | | |
| GRID2IP | -0.34 | -0.48 | | | | |
| HCK | 0.68 | -0.07 | | | | |
| ILK | 0.76 | -0.61 | | | | |
| INPP5B | -0.25 | -0.48 | | | | |
| IQGAP1 | 1 | 0.98 | | 0.98 | 0.55 | 0.35 |
| IRAK1 | 0.09 | 0.05 | | | | |
| IRAK2 | 1.62 | N/A | | 0.56 | | |
| IRAK3 | -0.97 | -0.58 | | | | |
| IRAK4 | -0.47 | -0.47 | | | | |
| ITGA1 | 0.98 | 0.28 | | | | |
| ITGA10 | 1.04 | -0.29 | | | | |
| ITGA11 | -0.07 | -0.11 | | | | |
| ITGA2 | 1.17 | -0.47 | | | | |
| ITGA2B | -0.43 | -0.89 | | | | |

| | | | | | | |
|----------|-------|-------|-------|------|-------|-------|
| ITGA3 | -0.16 | 0.47 | Red | | | |
| ITGA4 | 0.11 | -0.21 | Red | | | |
| ITGA5 | 1.39 | 0.88 | Blue | 0.05 | 0.88 | 0.45 |
| ITGA6 | 0.05 | -1.02 | Red | | | |
| ITGA7 | 0.23 | 0.22 | Red | | | |
| ITGA8 | 0.32 | -0.06 | Red | | | |
| ITGA9 | 1.28 | 0.04 | Red | | | |
| ITGAD | 0.65 | 0.48 | Red | | | |
| ITGAE | 0.88 | 0.82 | Red | | | |
| ITGAL | 0.4 | -0.16 | Red | | | |
| ITGAM | 0.01 | -0.03 | Red | | | |
| ITGAV | 0.72 | -0.18 | Red | | | |
| ITGAX | 0.94 | -0.8 | Red | | | |
| ITGB1 | 1.4 | 0.85 | Blue | 1.56 | 1.05 | 1.78 |
| ITGB1BP1 | 0.97 | 0.66 | Red | | | |
| ITGB1BP2 | 0.17 | 0.11 | Red | | | |
| ITGB1BP3 | -0.26 | -0.39 | Red | | | |
| ITGB2 | 1.03 | -0.19 | Red | | | |
| ITGB3 | 0.32 | 0.29 | Red | | | |
| ITGB3BP | 0.73 | 0.36 | Red | | | |
| ITGB4 | 0.77 | 0.13 | Red | | | |
| ITGB5 | 0.87 | -0.4 | Red | | | |
| ITGB6 | 1.01 | -0.18 | Red | | | |
| ITGB7 | 1.39 | 0.22 | Red | | | |
| ITGB8 | 1.02 | 0.61 | Red | | | |
| ITGBL1 | 0.29 | -0.16 | Red | | | |
| ITK | 0.41 | -0.02 | Red | | | |
| JAK1 | -0.32 | -0.08 | Red | | | |
| JAK2 | 0.33 | 0.44 | Red | | | |
| JAK3 | 0.21 | 0.56 | Red | | | |
| KDR | 0.04 | 0.71 | Red | | | |
| KHDRBS1 | 1.15 | -0.49 | Red | | | |
| KIAA1804 | 0.44 | -0.46 | Red | | | |
| KIT | -0.42 | 0.77 | Red | | | |
| KSR | 1.64 | 0.94 | Blue | 0.83 | | |
| KSR2 | 1.83 | 1.34 | Green | 0.25 | 0.74 | -1.04 |
| LAMA1 | 2.15 | 0.75 | Red | | | |
| LAMA5 | 1.28 | 0.47 | Red | | | |
| LAMB2L | 0.91 | -0.23 | Red | | | |
| LAMB3 | 1.04 | 0.94 | Red | | | |
| LAMC2 | 0.83 | -0.58 | Red | | | |
| LIMK1 | -0.07 | -0.2 | Red | | | |
| LIMK2 | 0.69 | 0.1 | Red | | | |
| LMTK2 | 0.19 | 0.3 | Red | | | |
| LTK | 0.38 | -0.08 | Red | | | |
| LYN | 0.14 | 0.48 | Red | | | |
| MAP3K10 | 1.61 | 1.49 | Green | 0.23 | -0.19 | -0.44 |
| MAP3K11 | 0.41 | 0.6 | Red | | | |
| MAP3K13 | 0.72 | 0.32 | Red | | | |
| MAP3K8 | 0.75 | 0.06 | Red | | | |
| MAP3K9 | -0.25 | -0.2 | Red | | | |
| MATK | -0.41 | 0.04 | Red | | | |
| MCF2L | 0.88 | 0.77 | Red | | | |
| MERTK | 0.41 | 0.05 | Red | | | |
| MET | -0.36 | -0.47 | Red | | | |
| MLKL | 0.6 | 0.3 | Red | | | |
| MST1R | 0.59 | 0.18 | Red | | | |
| NCF2 | 0.16 | -0.4 | Red | | | |
| NCKAP1 | -0.36 | N/A | Red | | | |

| | | | | | | |
|---------|-------|-------|--|-------|-------|-------|
| NTRK3 | -0.2 | 0.75 | | | | |
| P704P | 1.78 | 0.41 | | | | |
| PAK1 | 0.71 | 0.14 | | | | |
| PAK1IP1 | 0.61 | -0.13 | | | | |
| PAK2 | 1.07 | 0.19 | | | | |
| PAK3 | 0.25 | -0.33 | | | | |
| PAK4 | 1.62 | 0.36 | | | | |
| PAK6 | -0.25 | -1.32 | | | | |
| PAK7 | 0.85 | 0.45 | | | | |
| PAR6A | 0.12 | 0.09 | | | | |
| PDGFRA | 1.41 | 1.51 | | 0.22 | 0.33 | |
| PDGFRB | 0.48 | -0.2 | | | | |
| PIM1 | 1.76 | 1.59 | | 1.59 | 0.47 | -0.42 |
| PIP4K2B | 1.43 | 1.12 | | 1.12 | 0.94 | -0.56 |
| PLCB1 | 0.27 | 0.08 | | | | |
| PLCB2 | 0.96 | 0.05 | | | | |
| PLCB3 | 0.95 | -0.29 | | | | |
| PLCB4 | 0.63 | 0.63 | | | | |
| PLD1 | 0.71 | -0.29 | | | | |
| PLD2 | 0.2 | 0.03 | | | | |
| PLD3 | 1.31 | -0.17 | | | | |
| PLD4 | 0.47 | -0.38 | | | | |
| PLD5 | 0.68 | -0.43 | | | | |
| PLDN | 2.11 | 0.4 | | 0.46 | -0.15 | -0.26 |
| PRKCA | 0.81 | 0 | | | | |
| PTK2 | 2.16 | N/A | | 1.14 | 1.25 | 1.03 |
| PTK2B | 0.96 | 0.12 | | -1.81 | -2.08 | -0.12 |
| PTK7 | 1 | 0.36 | | | | |
| PXN | 2.29 | 1.31 | | 2.29 | 2.06 | 1.61 |
| RAC1 | 1.5 | 1.03 | | 1.03 | 2.51 | 1.78 |
| RAC2 | 1.15 | 1.53 | | 0.8 | -1.15 | -0.42 |
| RAC3 | 0.38 | 0.95 | | | | |
| RAF1 | -0.09 | 0.01 | | | | |
| RASA1 | 0.72 | -0.23 | | | | |
| RET | 0.54 | 0.48 | | | | |
| RHOA | 1.12 | 0.25 | | | | |
| RHOB | 0.12 | -0.18 | | | | |
| RHOBTB1 | -0.34 | -0.57 | | | | |
| RHOBTB2 | 0.08 | -0.59 | | | | |
| RHOC | 0.17 | 0 | | | | |
| RHOD | -0.19 | -0.46 | | | | |
| RHOF | -1.76 | N/A | | | | |
| RHOG | 0.3 | 0.01 | | | | |
| RHOH | 0.4 | -0.06 | | | | |
| RHOJ | -0.08 | -0.47 | | | | |
| RHOQ | 0.08 | -0.38 | | | | |
| RHOU | -0.89 | -0.93 | | | | |
| RHOV | 0.26 | -0.29 | | | | |
| RIPK1 | 0.27 | 0.33 | | | | |
| RIPK2 | -0.11 | -0.01 | | | | |
| RND1 | -0.03 | -0.38 | | | | |
| RND2 | 1.26 | 0.48 | | | | |
| RND3 | 1.17 | -1.06 | | | | |
| ROCK2 | 0.05 | N/A | | | | |
| ROR1 | -0.92 | -0.31 | | | | |
| ROR2 | -0.2 | 0.31 | | | | |
| ROS1 | -0.22 | -0.41 | | | | |
| RYK | 0 | -0.27 | | | | |
| SLC3A2 | 0.99 | 1.02 | | 0.74 | 0.66 | -0.5 |

| | | | | | | |
|--------|-------|-------|--|-------|-------|------|
| SLC7A5 | 1.24 | -0.2 | | | | |
| SOS1 | 0.06 | 0.27 | | | | |
| SPIRE1 | 0.59 | -0.1 | | | | |
| SPIRE2 | 0.48 | 0.42 | | | | |
| SRC | 1.48 | 1.32 | | 1.06 | 1.21 | 1.17 |
| SYK | 1.82 | 1.64 | | 0.1 | 0.16 | |
| TEC | 0.32 | 0.58 | | | | |
| TEK | 0.15 | -0.35 | | | | |
| TESK1 | 0 | 0.77 | | | | |
| TESK2 | 0.08 | 0.34 | | | | |
| TGFBR1 | 2.18 | 1.5 | | -0.16 | -0.05 | |
| TGFBR2 | 1.07 | 0.89 | | -0.24 | -1.15 | |
| TLN1 | 1.34 | 1.23 | | 1.34 | 1.66 | 1.8 |
| TNK1 | 1.34 | N/A | | 0.77 | | |
| TNK2 | 1.58 | -0.51 | | -1.08 | -1 | |
| TNNI3K | -0.08 | 0.14 | | | | |
| TRIP10 | 1.35 | 0.27 | | | | |
| TYK2 | -0.02 | 0.45 | | | | |
| TYRO3 | -0.25 | -0.43 | | | | |
| VAV2 | 1.45 | 1.24 | | -0.19 | 0.23 | 0.31 |
| VAV3 | -0.33 | 0.42 | | | | |
| VCL | 1.38 | 1.53 | | 1.41 | 1.66 | 1.32 |
| VTN | 0.89 | 0.83 | | | | |
| YES1 | 0.51 | -0.13 | | | | |
| ZAK | 1.48 | 1.3 | | -0.14 | -0.08 | 0.22 |

total

251 targeted genes

28 hits with $z > 1$ for both siRNAs

13 genes selected as expert choice for validation

8 hits positive in validation screen

Table S2: Bacterial strains and plasmids used in this study

| Strain/Plasmid | Genotype or relevant characteristics | Reference/Source |
|-------------------------------|---|-----------------------------------|
| <i>Bhe</i> strains | | |
| RSE247 | spontaneous Sm ^r strain of ATCC 49882 ^T | (Schmid et al., 2004) |
| MSE150 | $\Delta bepA-G$ mutant of RSE247 | (Schulein et al., 2005) |
| MTB012 | RSE247 containing pCD353 | (Truttmann et al., in press) |
| MTB013 | MSE150 containing pCD353 | (Truttmann et al., in press) |
| MSE249 | RSE247 containing pLMS400 | (Schmid et al., 2006) |
| MSE253 | RSE247 containing pLMS404 | (Schmid et al., 2006) |
| <i>E. coli</i> strains | | |
| NovaBlue | <i>endA1 hsdR17</i> (r K12–m K12+) <i>supE44 thi-1 recA1</i> <i>gyrA96 relA1 lac</i> [<i>F' proA+B+ lacI^qZΔM15::Tn10</i> (Tc ^R)] | Novagen, Madison |
| Plasmids | | |
| pWay21 | Mamalian expression vector for eGFP | Molecular Motion lab, Montana |
| pCD353 | <i>Bartonella</i> spp. vector, encoding GFP | (Dehio and Meyer, 1997) |
| pECE-integrin β 1B | pECE encoding integrin β 1 isoform B | Tarrone lab (Balzac et al., 1994) |
| pHA-FAK Y397F | pcDNA3.1 encoding for mFAK Y397F mutant | Hauck lab (Sieg et al., 1999) |
| pHA-FAK Y861F | pcDNA3.1 encoding for mFAK Y861F mutant | Hauck lab (Sieg et al., 1999) |
| pHA-FAK Y925F | pcDNA3.1 encoding for mFAK Y925F mutant | Hauck lab (Sieg et al., 1999) |
| pGFP-TLN1 | encoding GFP-mTLN1 | (Franco et al., 2004) |
| pGFP-TLN1 R2526G | encoding GFP-mtalin1 R2526G | (Gingras et al., 2008) |
| pGFP-TLN1 L325R | encoding GFP-mtalin1 L325R | (Kopp et al., 2010) |
| pGFP-TLN1 L432G | encoding GFP-mtalin1 L432G | (Franco et al., 2004) |
| pGFP-TLN1 1-433 | encoding GFP-mtalin1 aa1-433 | (Franco et al., 2004) |

Table S3: Ab used in this study

| Specificity | description | Reference/Source |
|--------------------|--|--------------------------------------|
| Talin1 | mouse talin1 Ab (97H6), recognizes talin1 root | Critchley lab (Kopp et al., 2010) |
| Talin1 | mouse talin1 Ab (TA205), recognizes talin1 head | Santa Cruz Biotech |
| Talin2 | mouse talin2 Ab (68E7) | Critchley lab (Debrand et al., 2009) |
| Integrin β 1 | mouse integrin β 1 Ab (P5D2); inhibiting | Santa Cruz Biotech |
| Integrin β 1 | mouse integrin β 1 Ab (N29); stimulating | Wlikins lab (Wilkins et al., 1996) |
| Integrin β 1 | mouse integrin β 1 Ab (B44); stimulating | Wlikins lab (Wilkins et al., 1996) |
| Integrin β 1 | mouse integrin β 1 Ab (B3B11); stimulating | Wlikins lab (Wilkins et al., 1996) |
| Integrin β 1 | mouse integrin β 1 Ab (12G10); stimulating | Humphries lab (Mould et al., 1995) |
| Src | mouse Src Ab (GD11) | Upstate |
| GFP | rabbit GFP Ab | Molecular probes |
| Paxilin | mouse Paxilin Ab (clone 349) | BD Transduction laboratories |
| Vinculin | rabbit Vinculin Ab (H-300) | Santa Cruz Biotech |
| FAK | mouse FAK Ab | BD Transduction laboratories |
| FAK pY397 | rabbit phospho-FAK (Y397) Ab | Abcam |
| Paxilin pY118 | rabbit phospho-Paxilin (Y118) Ab | Santa Cruz Biotech |
| Fibronectin | mouse human Fibronectin Ab (IST-9) | Abcam |
| Actin | mouse actin Ab (MS-X) | Milipore |

SUMMARY

4 SUMMARY

The genus *Bartonella* possesses the remarkable property to persistently infect its mammalian hosts without causing severe clinical outcomes. One particularly important feature is the ability of *Bartonella* to invade host cells for replication in a designated niche and for protection against the host immune defense. *Bartonella henselae* (*Bhe*) possesses the unique ability to promote the formation of a dedicated invasion structure, named the invasome. First, the study of this specific uptake mechanism allowed investigating the role of the VirB/D4 type 4 secretion system (T4SS) and its translocated Bep substrates in *Bhe* internalization. Moreover, invasome structures represented a suitable model system to tackle the regulatory mechanisms of F-actin assembly/disassembly in eukaryotic cells during pathogen entry. The work presented here elucidates the role of the VirB/D4-translocated Bep proteins during invasome-mediated *Bhe* uptake and assesses host cell signaling cascades required thereto.

Research article I represents a reductionistic approach to define the minimal effector set required for *Bhe*-triggered invasome formation on endothelial cells (ECs). Further, the role of the Rho family of small GTPases was assessed. We identified the effector protein BepG to be sufficient to trigger the formation of invasomes that are morphologically indistinguishable from wild-type promoted structures. Investigation of the Rho GTPases Cdc42, Rac1 and their respective downstream interaction partners signified their importance for invasome establishment; in contrast, RhoA was shown to not contribute to invasome formation. Thus, our findings suggest a dominant role for Rho GTPases in regulating F-actin rearrangements leading to the composition of invasome structures.

In **research article II**, we investigate the capacity of the deletion strain *Bhe* Δ *bepG* to promote invasome formation and demonstrate that *Bhe* encodes for a second, *bepG*-independent mechanism to promote invasome assembly. We show that the combination of BepC and BepF mediates the establishment of invasomes that are similar to BepG-promoted structures. A HeLa cell-based model system to study invasome formation in full details is introduced and characterized. Next, we outline similarities and differences in characteristics and signaling cascades promoting BepG- or BepC/BepF-dependent invasome formation. We

demonstrate that BepC/BepF in combination interfere with endocytosis-like internalization of inert microspheres and show the requirement for Cdc42 and Rac1-mediated cytoskeletal rearrangements to enable BepC/BepF-promoted invasome establishment. We also demonstrate that the ADF protein cofilin1 is only essential for BepC/BepF but not BepG-triggered invasome formation. This implies the involvement of partially different signaling cascades behind the two functionally redundant mechanisms triggering invasome establishment.

Research article III focuses on the characterization of the effector protein BepF and its specific role during the process of invasome formation. We show that, although phosphorylated in the host cell, the N-terminally situated tyrosine-rich repeat motifs are negligible for invasome formation. In contrast, the individual Bid domains BidF1 and BidF2, but not BidF3, are sufficient to promote invasome establishment together with BepC. Disruption of the WxxxE motif in BidF1 abolished BidF1 functionality, implicating a mechanistic or structural role of the motif in BidF1. TEM-assessment of morphological changes induced by BepF or BidF1 on HeLa and NIH 3T3 cells indicated that they may hyperactivate Cdc42 and Rac1. Further, over-expression of constitutive active Cdc42 or Rac1 was sufficient to substitute for BepF during the process of invasome formation. *In vitro* guanine nucleotide exchange factor (GEF) assays confirmed that BidF1 and BidF2 exhibit weak GEF activity against Cdc42. Thus, BepF was demonstrated to act as a Cdc42-GEF protein in host cells, thereby interfering with F-actin dynamics and regulation.

In **research article IV**, we focus on the host cell contribution to invasome formation. Performing an imaging-based RNAi screen, we identified five new targets essential for invasome formation and mapped their contribution to the different steps of invasome establishment. Of particular interest was the screening hit integrin β 1, which represented the only transmembrane receptor that was identified as essential component in the screen. In detail investigation of integrin β 1 revealed that it is required in its open, high affinity conformation to enable effector translocation and to promote the F-actin rearrangements leading to the invasome structure. We demonstrate that the engagement of both outside-in signaling events via integrin β 1, FAK and Src as well as inside-out signal transmission

controlled by talin1 significantly contribute to invasome formation. This is the first study demonstrating active integrin outside-in signaling and parallel inside-out activation of these receptors during bacteria invasion of the host cells.

DISCUSSION

5 DISCUSSION

In this study, I have analyzed the molecular and cellular basis of *Bartonella henselae* (*Bhe*)-triggered invasome formation. The following discussion will focus on data presented in the results chapters and discuss specific aspects to obtain a more comprehensive picture of the process of invasome assembly. The first paragraphs are dedicated to the roles of the individual effector proteins BepC, BepF and BepG, the benefit of functional redundancy and *the in vivo* relevance of invasome formation. The next paragraph is focusing on the host cell contribution and the role of integrin-mediated signaling in invasome formation. Finally, the last paragraph addresses the high-throughput screening setup developed during this work.

5.1 THE EFFECTOR PROTEINS BepC, BepF AND BepG AND THEIR ROLES IN INVASOME FORMATION

Invasome formation was first described in 1997 and since then has fascinated researchers working with *Bhe* [1]. Initial work describing this unique structure demonstrated that invasome establishment depends on F-actin but not on tubulins [1]. Further research using in-frame deletion mutants of *Bhe* highlighted that the presence of a functional VirB/D4 type 4 secretion system (T4SS) and the translocation of Bep substrates into the host cell is required for invasome assembly [2,3].

Results presented and discussed in **research articles I** and **II** show that invasome formation can be promoted by either the combined action of effectors BepC and BepF or BepG alone, thus representing a functionally redundant uptake mechanism. Comparing the domain structures of effectors BepC, BepF and BepG, it is apparent that all proteins contain at least one Bid domain and a positively charged C-tail, which together serve as translocation signal [3]. Furthermore, the three effectors BepC, BepF and BepG are composed of different additional domains (Figure 10).

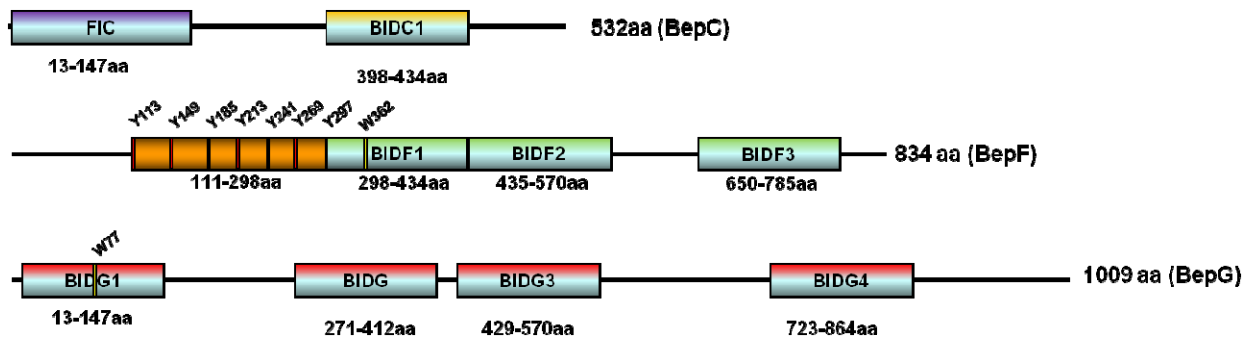


Figure 11: Schematic representation of Bhe effector proteins BepC, BepF and BepG. Indicated tryptophans mark the starting point of the WxxxE motifs. Indicated tyrosines are phosphorylated in the host cell.

Work on BepF presented and discussed in **research article III** demonstrates that the BidF1 and BidF2, but not BidF3 domains are sufficient to promote invasome formation together with BepC. Moreover, BidF1 and BidF2 domains exhibit GEF functionalities against Cdc42. Thus, it is tempting to assume that the role of BepF in invasome formation is the activation of Cdc42. In addition to the Bid domains, BepF contains an N-terminal tyrosine-rich scaffold that is phosphorylated upon translocation into the host cell, thus presenting a binding interface for the direct recruitment of proteins containing an SH2 domain [4]. The same protein domain also contains multiple PxxxP sites that are recognized by proteins harboring SH3 domains [4]. Thus, this N-terminal phospho-scaffold is likely to interfere with host cell signaling cascades in a yet unidentified manner, although shown not to contribute to invasome formation. However, further investigation is required to define the function of the N-terminal portion of BepF.

In contrast to BepF and BepG, BepC consists of a single Bid domain and an N-terminally located FIC domain (Figure 10) [3]. Work presented in **research article II** shows that BepC is essential for BepC/BepF-triggered invasome formation and also enhances BepG-mediated invasome establishment. Recent work on the FIC-domain containing bacterial effectors VopS and IbpA showed that the FIC domain is crucial for transferring an AMP residue to Rho GTPases, thereby inactivating them in a proposed reversible manner [5]. VopS, a virulence factor of the seafood-borne pathogen *V. parahaemolyticus*, is translocated by the *Vibrio* type 3 secretion system into the host cell, where it inhibits actin assembly and leads to the disruption of the cytoskeleton [6]. Further, IbpA a secreted and surface-

associated virulence factor of *H. somni*, was shown to disrupt the actin cytoskeleton in bovine respiratory epithelial cells as well as Hela cells. It is proposed that the cytotoxic effect of IbpA causes the retraction of alveolar epithelial cells due to IbpA DR2/Fic-mediated inactivation of the cellular Rho GTPases, thereby allowing *H. somni* to pass the alveolar barrier, leading to pneumonia [7]. Although there is no data available demonstrating a similar role for the FIC domain of BepC, it could explain the importance and contribution of BepC to both routes of invasome formation. Results published in **research articles I** and **III** show that the over-expression as well as the down-regulation of Cdc42 and Rac1 decreased the frequency of invasome establishment triggered by either effector sets. This strongly indicates that activated Cdc42 as well as Rac1 are dispensable or even disadvantageous at certain steps during invasome formation, although shown to be required for the process. A BepC-mediated AMPylation of Cdc42 and Rac1 could mediate this temporarily down-regulation of Rho GTPase signaling, presumably required for the retraction of the invasome structure. Alternatively, BepC could act on a GTPase regulator, thus indirectly influencing GTPase signaling by preventing or enhancing the interaction of e.g. GEF or GAP proteins with Cdc42 or Rac1. However, the molecular function of BepC remains to be studied.

BepG exclusively consists of four Bid domains that are linked by short peptide stretches [3]. Sequence analysis showed that BepG contains a WxxxE motif in its first Bid domain (BidG1). However, in contrast to BepF, exchanging tryptophane with alanine (AxxxE) in BepG did not interfere with its capacity to promote invasome assembly [8], thus indicating that BepG may not be a bacterial WxxxE GEF protein. Interestingly, results presented in **research article II** show that cofilin1 is only required for BepC/BepF- but not BepG-promoted invasome establishment. While it is not surprising that BepC/BepF-promoted invasome formation involves cofilin1, a protein that organizes actin assembly/disassembly downstream of the Rho GTPases, it is rather interesting that the BepG-dependent invasome assembly route does not [9]. This implies that BepG may substitute for or bypass cofilin1 function and therefore act downstream of the Rho GTPases. The regulation of actin dynamics downstream of Cdc42, Rac1 and RhoA by bacterial effectors is documented for several pathogens. For example, the translocated enterohaemorrhagic *E. coli* (EHEC) effector protein EspF_U targets WASP-family proteins and competitively disrupts VCA-GBD auto-regulatory interactions, thereby mediating local WASP

activation [10]. Further, the gram-negative pathogens *Vibrio cholera* and *V. parahaemolyticus* encode for VopF and VopL, respectively, which both contain three Wiskott–Aldrich homology 2 domains and harbor the capacity to act as actin nucleator similar to Arp2/3, formins or Spire [11,12].

In the case of BepG, preliminary attempts to investigate potential direct BepG-actin interactions remained inconclusive [8]. Further, the analysis of the BepG protein sequence did not identify conserved functional domains (see **research article I**). Nevertheless, the available results indicate that BepG acts downstream of the GTPases. However, further studies are required to determine the molecular function of BepG in the host cell.

Taken together, the presented work suggests that BepF and BepG may have distinct cellular targets. However, they may subvert the same signaling pathways required for invasome formation although directly modulating distinct proteins. While BepF acts as a Cdc42 GEF protein, BepG may subvert actin assembly/disassembly downstream or even independent of the Rho GTPases. In contrast, BepC contributes to both invasome formation pathways, indicating a modulator function e.g. by the tempo-spatial down-regulation of Cdc42 and Rac1. Future work on BepC and BepG may allow to define their concert role in the process of invasome formation.

5.2 BEPG VS. BEPC/BEPF TRIGGERED INVASOME FORMATION: THE BENEFIT OF DEGENERACY

Degeneracy, also referred to as functional redundancy, is a general biological principle that contributes to an increase in robustness of relevant circuits [13]. Redundant systems relay in general on one of four principles: i) the expression of several well-conserved, ancestrally related and functionally equivalent proteins, ii) the expression of ancestrally unrelated proteins that modulate a shared target in a similar manner, iii) the expression of ancestrally unrelated proteins that modulate a shared target by distinct alterations or iv) the expression of ancestrally unrelated proteins, which have distinct targets but affect the same cellular processes. The effector set of the bacterial pathogen *Salmonella enterica* represents an illustrative case to exemplify at least three of the four different principles of functional

redundancy: First, the two homologue effector proteins SopE and SopE2, which share 69% identity, are both guanine nucleotide exchange factors (GEFs) targeting Cdc42 among other GTPases [14]. Next, the structurally unrelated effector proteins SipA and SipC both bind to actin and influence the modulation of the actin cytoskeleton [15]. Moreover, *S. enterica* effectors SopB and SopE/SopE2 activate Cdc42 by two completely different mechanisms: SopB acts as a specific phosphatase affecting the fluxing of phosphoinositides whereas SopE/SopE2 exhibits GEF activity against Cdc42 [15,16]. Finally, SipA, SopE/SopE2 all have actin regulation activities and trigger membrane ruffling, although at different frequencies [17]. Indication for functional redundancy of bacterial effectors is also given for *Legionella pneumophila* and the plant pathogen *Pseudomonas syringae*, which express more than 30 effector substrates for their respective secretion apparatus [18,19]. Single effector deletions in either of the two species have little or no effect on *Legionella* or *Pseudomonas* virulence, suggesting the involvement of redundant pathogenesis mechanisms controlled by different effectors [20].

The existence of a functionally redundant mechanism to trigger invasome formation indicates a prominent role of invasome structures for *Bhe* pathogenicity. Work presented in **research articles I** and **II** demonstrated that the invasome formation is coupled to the inhibition of individual *Bhe* uptake. Furthermore, stainings of infected cells for the lysosomal marker protein LAMP1 showed that individual *Bhe* internalizing the cell independently of the invasome route co-localize with LAMP1 while *Bhe* invading via the invasome route did not. Thus, invasome-mediated cell invasion could represent a mechanism to bypass cellular degradation pathways and therefore be of benefit for the bacteria. However, the redundant mechanisms behind invasome formation should be put into a broader context since *Bhe* only accidentally infects humans while cats serve as their reservoir hosts. Transmission from cat to cat occurs via arthropod vectors, while cat to human transmission is caused by cat scratches or bites [21]. Thus, *Bhe* experiences various host environments; however, there is no report about invasome formation on cat or arthropod cells. To date, the effector expression profile in tempo-spatial resolution as well as the translocation pattern/hierarchy into the various host cells remains to be elucidated. While the two component system BatR/BatS controls the expression of the VirB/D4 T4SS and effectors BepA-E and BepG, there is some indication that BepF is regulated by other means [22]. Therefore, it is possible

that BepF is not expressed and translocated in the same host / tissue environment as the other Bep proteins or displays a different tempo-spatial regulation pattern. Concluding, the encoded functional redundancy to trigger invasome formation could also represent a mechanism to guarantee host adaptability and tissue specificity rather than increased systems robustness.

5.3 THE *IN VIVO* RELEVANCE OF INVASOME FORMATION

To date, no human *ex vivo* sample was described to show invasome structures on ECs. Histopathology of samples from bacillary angiomatosis patients only displayed bacterial aggregates within or closeby proliferating endothelial cells, but no invasomes [23]. However, various clinical *Bhe* isolates were shown to trigger invasome formation *in vitro* in a VirB/D4-dependent manner (additional work by Marco Faustmann and Matthias Truttmann; data not shown). Moreover, findings presented in **research article II** demonstrate that invasome formation is not limited to ECs but can also occur on epithelial cells. However, the current data do not allow to conclusively answer the question about the *in vivo* role of invasomes. The lack of an appropriate animal model to study invasome formation further complicates the situation. Nevertheless, independent of its *in vivo* relevance, invasome structures remain a remarkable phenotype to study the re-organization of F-actin networks triggered by *Bhe*-translocated effector proteins.

5.4 INTEGRIN β 1-MEDIATED TRANSMEMBRANE SIGNALING DURING INVASOME FORMATION

In **research article IV**, we identified integrin β 1 as key molecule important to enable VirB/D4-dependent effector translocation into the host cell, to control the F-actin rearrangements that lead to the assembly of the invasome structure and to contribute to *Bhe* adherence. Integrin receptors and in particular integrin α 5 β 1 are frequently targeted by pathogenic bacteria. Heterodimeric integrin receptors show a broad but specific expression pattern in human cells. For example, integrin α 2 β 1 and α V β 3 are predominantly expressed in endothelial cells whereas the α 4-subunit containing heterodimers α 4 β 1 and α 4 β 7 are restricted to lymphocytes, monocytes and eosinophiles [24,25]. Thus, binding to a specific heterodimeric integrin receptor allows the pathogen to specifically target its dedicated host cell. In contrast, binding to integrin β 1, a high abundant β subunit that forms receptors with the α subunits α 1- α 10 and α V guarantees the ability to adhere to various cell types [26].

Bhe invades endothelial cells in humans, its accidental host [21]. Human ECs express α 2 β 1 as well as α 5 β 1 integrins among other receptors. Knock-down of either integrin α subunit did not affect effector translocation or invasome assembly. In contrast, knock-down of integrin β 1 abolished invasome formation on infected cells (see **research article IV**), indicating that *Bhe* recognizes the β 1 subunit independently of the respective α subunit. This may offer *Bhe* the opportunity to bind to various endo- and epithelial cell types. Whether or not this chance is exploited during infection remains unclear.

Besides providing docking sites for pathogenic bacteria, integrin receptors also play an essential role in activating cellular signaling cascades that enable pathogen internalization in an actin-dependent manner (see chapter 1.2). The signal transduction network from integrins to actin modulators is dense and heavily interlinked (see chapter 1.2.4, Figure 4). Most integrin-mediated signaling cascades start with the recruitment and activation of FAK and Src kinase, which, upon auto- and cross-phosphorylation, offer binding scaffolds for adaptor proteins that are themselves - once recruited - phosphorylated by the two kinases [26]. A rather direct link from FAK/Src to the control of actin dynamics is offered via the proteins talin, paxilin and vinculin. Talin recruits paxilin and vinculin to the cytoplasmic C-tails of integrin receptors [27,28]. Paxilin is phosphorylated at multiple sites by FAK/Src and thereafter interacts with additional actin-binding proteins that in turn affect

actin dynamics [29]. Moreover, paxilin and vinculin both possess the ability to directly bind to actin, thereby linking the integrin receptors to the actin cytoskeleton. Finally, vinculin modifies F-actin filaments directly and serves as a *de-novo* actin nucleator [30]. Incoming signals can also be transmitted from integrins to Rho GTPases that eventually mediate actin rearrangements. For example, signal transduction from FAK to p130CAS, CrkII and down to the Dock180-ELMO complex regulates Rho GTPases [31]. Furthermore, integrin-mediated activation of phosphatidylinositol-4,5-bisphosphate 3-kinase (PI3K) leads to the production of PIP₃ and the subsequent activation of the Rho GEFs Vav and Tiam, which act on Rac1 [32]. Another important branch of signal perception from integrins to actin modulators that bypasses FAK and Src kinases is given by the integrin-dependent activation of the integrin-linked kinase (ILK), which recruits PINCH and parvin to the membrane. Together, the three proteins form a complex that regulates Rho GTPase activation status [33].

Work presented in **research article IV** shows that besides integrin β 1 and the Rho GTPases Cdc42 and Rac1, the two kinases FAK and Src and the adaptors talin1, vinculin and paxilin are all essential for invasome formation. In contrast knock-down of ILK, PINCH or parvin did not affect invasome formation at all, while the knock-down of PI3K had only moderate effects. Further, the subsequent analysis of the roles of Dock180, Crk, p130CAS and the Vav/Tiam-family GEFs did not lead to the identification of a GEF protein essential for invasome formation. Thus, the findings presented in **research article IV** allow to propose a preliminary model in which outside-in signaling via FAK/Src to paxilin plays a major role in invasome formation. Once phosphorylated by FAK/Src, paxillin can increase vinculin recruitment to the membrane, which in turn could directly affect the actin cytoskeleton and promote *Bhe* engulfment. Talin1 may contribute to the process i) by increasing the possible outside-in signal flow through inside-out activation of integrins [34] ii) by contributing to the recruitment of paxilin and vinculin to the membrane [29] or iii) by inducing integrin β 1 clustering [35]. Current data support the first and third hypothesis while the second one cannot be excluded. However, this simplified model does not yet include the actin reorganization events controlled by Cdc42 and Rac1, both shown to be essential for invasome assembly (see **research articles I and II**). Two extensions of the preliminary model could be proposed to include the role of Cdc42 and Rac1: First, integrin activation by *Bhe* may not only activate vinculin-mediated changes of the actin cytoskeleton but could also

involve the activation of Cdc42 and Rac1. Single knock-downs of RhoGEFs and RhoGAPs, which transfer the incoming signaling from the membrane-level to the GTPase-level, did not yield a significant reduction in invasome formation (see **research article IV**). However, this may rather indicate the involvement of redundant mechanisms than the absence of such downstream signaling events. Alternatively, the GTPases could be activated independently of integrin signaling cascades by the Bep effectors. BepF has been demonstrated to activate Cdc42 (see **research article III**) while the role of BepC and BepG remain elusive. Thus, additional work is required to obtain a comprehensive picture of cellular signaling in invasome formation.

5.5 AN AUTOMATED SETUP TO STUDY INVASOME FORMATION: TOWARDS GENOME-WIDE SCREENING

Molecular systems biology of host-pathogen interactions is a topic of increasing scientific importance (see chapter 1.1.2). In **research article IV**, *Bhe*-promoted invasome formation was assessed using systems biology-related approaches. This included microscopy-based high-throughput RNAi screening, automated liquid handling as well as automated image acquisition and analysis. Although this massive automation of various experimental steps was elementary for project progression, it also generated diverse problems: The automated liquid handlers were a major source of biological contaminations. While these contaminants are of limited severity for short-term infection studies (< 1 hour) or virus infection experiments in the presence of antibiotics / anti-fungals [36], they have an enormous impact on the outcome on long-lasting bacterial infection experiments. Further, the down-scaling of experimental setups from 96 to 384 well plates required work-intensive readjustments of protocols and automation procedures.

Besides these technical issues, software-based automated invasome detection on microscopic images using CellProfiler [37] was a major issue to solve. Invasomes are not uniform in appearance and can be round, elliptic, stretched, open or closed, of diverse size and flanked by actin cables of different length / thickness [8,38]. As a result, standard pattern matching algorithm designed to specifically detect objects of a defined size and

shape did not work properly. To solve that problem, support vector machine (SVM) learning tools (CellClassifier [39]) were implemented in the analysis pipeline. Diverse object properties such as cell and bacterial number, shape, size and neighborhood were extracted in a quantitative manner and used to define SVM-models. Using these user-trained models, the SVM machine allowed to group CellProfiler-predicted invasomes into true and false positives. However, also the SVM-based secondary invasome detection was error-prone due to unevenly illuminated images, distinct absolute intensity rates that varied in a per well or per plate fashion or out-of-focus images. Nevertheless, the final automated image analysis setup enabled invasome identification and quantification at an acceptable accuracy of about 92% (see **research article IV**). Concluding, the establishment of an automated RNAi screening setup suitable to screen for *Bhe*-triggered invasome formation was time- and resource-intensive process because of hardware problems and the complexity of the screening phenotype. However, such a functional system is a prerequisite for large-scale screening approaches.

One of the major advantages of systems biology-related experimental setups is that they allow to investigate a given process in an unbiased manner. Many genome-wide RNAi screens to analyze phenotypic penetrance upon gene knock-down have been performed and lead to the identification of specifically engaged signaling patterns [40,41,42]. In contrast, the RNAi screen presented in **research article IV** targeted only ~250 genes in total. The selected targets included all human tyrosine kinases, Rho GTPases, integrins and formins; thus, only a small part of the human genome was tested in a biased manner. In addition, the siRNA library was enriched by several targets that were proposed by the web-based service STRING [43,44]. STRING arranges user input (genes, proteins) into signaling networks based on database knowledge. In addition, the service adds additional interaction partners to the input-based signaling circuits that i) increase the interconnectivity of the input proteins or ii) fill existing gaps in signaling patterns. This network extension(s) occur in an user-controlled, iterative manner (Figure 11).

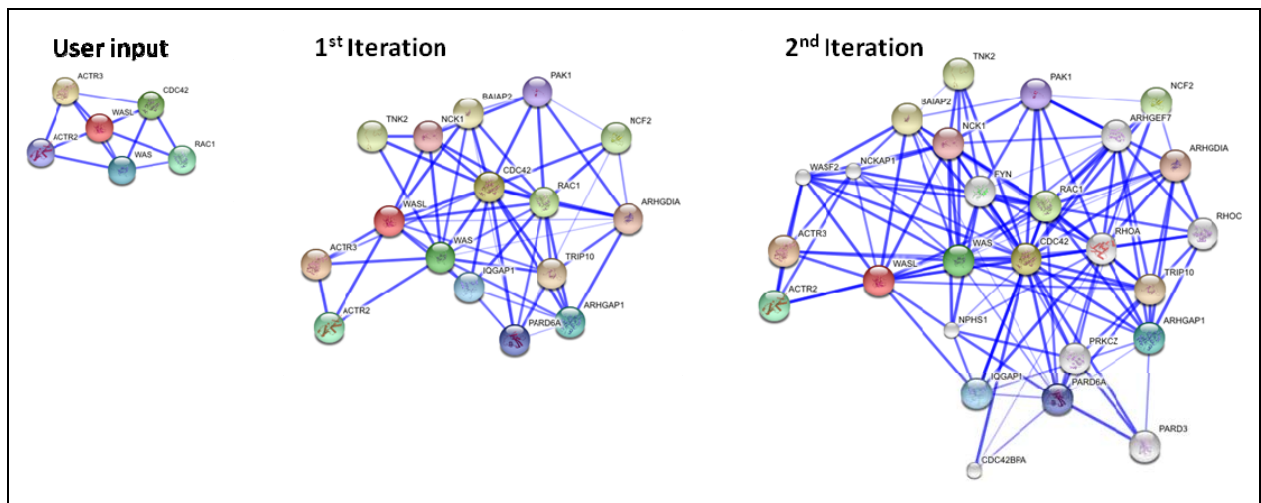


Figure 12: Iterative network expansion using STRING. String-predicted interaction network based on user input of Cdc42, Rac1, Actr2 (Arp2), Actr3 (Arp3), WASL (Scar/WAVE) and WASp. Network was expanded by two iterations at maximal stringency (0.8).

Testing this siRNA library allowed to identify the role of integrin β 1-mediated signaling in *Bhe*-triggered invasome formation (see **research article IV**). While the validated hits integrin β 1, FAK and Src were parts of the integrin and the tyrosine kinase libraries, respectively, talin1, vinculin and paxillin were screening targets proposed by STRING. Thus, the positive validation rate of STRING-proposed targets was overproportional, demonstrating the potential of *in silico* library design. Nevertheless, STRING-based predictions are of limited use as they do not allow to identify new signaling networks and circuits. However, the approach chosen in **research article IV** was suitable to test the fully automated screening platform and allowed to indentify six new players essential for invasome formation.

Large-scale screening approaches generate vast amounts of data that needs to be analyzed and properly stored. In the case of the established invasome formation screening assay, a genome-wide RNAi screen in which each transcript is targeted only once will yield in a total of approximately 66'000 images, which is, following lossless image compression, equivalent to approximately 0.9TB of server space. However, despite the cost-intensive storage of images form large-scale screens, long-time storage of primary data offers several advantages: First, upon improvement of analysis pipelines, the original data can be reprocessed and the result quality can thereby be improved. Further, the original images

can be reanalyzed in a different context to approach another biological question. E.g. in the case of the *Bhe*-triggered invasome formation screen, invasome quantification is taken as the primary readout. However, the same image set could be used to quantify the total bacterial load per cell or the *Bhe* clustering and localization behavior on knock-down cells. Finally, original images from different research groups can be pooled and re-analyzed in a standardized manner. The advantage hereby is that a single analysis pipeline always extracts the same features of the same quality for all image sets. Thus, software-based variability and analysis artifacts can be excluded, thereby increasing the comparability and reproducibility of the results.

Taken together, the high level of assay standardization and automation implemented during the work presented in this thesis builds a solid fundament for future genome-wide screens approaching *Bhe*-triggered invasome formation.

5.6 REFERENCES

1. Dehio C, Meyer M, Berger J, Schwarz H, Lanz C (1997) Interaction of *Bartonella henselae* with endothelial cells results in bacterial aggregation on the cell surface and the subsequent engulfment and internalisation of the bacterial aggregate by a unique structure, the invasome. *J Cell Sci* 110 (Pt 18): 2141-2154.
2. Schmid MC, Schulein R, Dehio M, Denecker G, Carena I, et al. (2004) The VirB type IV secretion system of *Bartonella henselae* mediates invasion, proinflammatory activation and antiapoptotic protection of endothelial cells. *Mol Microbiol* 52: 81-92.
3. Schulein R, Guye P, Rhomberg TA, Schmid MC, Schroder G, et al. (2005) A bipartite signal mediates the transfer of type IV secretion substrates of *Bartonella henselae* into human cells. *Proc Natl Acad Sci U S A* 102: 856-861.
4. Koch CA, Anderson D, Moran MF, Ellis C, Pawson T (1991) SH2 and SH3 domains: elements that control interactions of cytoplasmic signaling proteins. *Science* 252: 668-674.
5. Roy CR, Mukherjee S (2009) Bacterial FIC Proteins AMP Up Infection. *Sci Signal* 2: pe14.
6. Casselli T, Lynch T, Southward CM, Jones BW, DeVinney R (2008) *Vibrio parahaemolyticus* inhibition of Rho family GTPase activation requires a functional chromosome I type III secretion system. *Infect Immun* 76: 2202-2211.
7. Zekarias B, Mattoo S, Worby C, Lehmann J, Rosenbusch RF, et al. (2010) *Histophilus somni* IbpA DR2/Fic in virulence and immunoprotection at the natural host alveolar epithelial barrier. *Infect Immun* 78: 1850-1858.
8. Rhomberg TA (2007) Molecular and Cellular Basis of the Internlization of *Bartonella henselae* by Human Endothelial Cells. Basel: University of Basel. 152 p.
9. Carlier MF, Ressad F, Pantaloni D (1999) Control of actin dynamics in cell motility. Role of ADF/cofilin. *J Biol Chem* 274: 33827-33830.
10. Campellone KG, Robbins D, Leong JM (2004) EspFU is a translocated *EHEC* effector that interacts with Tir and N-WASP and promotes Nck-independent actin assembly. *Dev Cell* 7: 217-228.
11. Liverman AD, Cheng HC, Trosky JE, Leung DW, Yarbrough ML, et al. (2007) Arp2/3-independent assembly of actin by *Vibrio* type III effector VopL. *Proc Natl Acad Sci U S A* 104: 17117-17122.
12. Tam VC, Serruto D, Dziejman M, Briehner W, Mekalanos JJ (2007) A type III secretion system in *Vibrio cholerae* translocates a formin/spire hybrid-like actin nucleator to promote intestinal colonization. *Cell Host Microbe* 1: 95-107.
13. Edelman GM, Gally JA (2001) Degeneracy and complexity in biological systems. *Proc Natl Acad Sci U S A* 98: 13763-13768.
14. Friebel A, Ilchmann H, Aepfelbacher M, Ehrbar K, Machleidt W, et al. (2001) SopE and SopE2 from *Salmonella typhimurium* activate different sets of RhoGTPases of the host cell. *J Biol Chem* 276: 34035-34040.

15. Zhou D, Galan J (2001) *Salmonella* entry into host cells: the work in concert of type III secreted effector proteins. *Microbes Infect* 3: 1293-1298.
16. Zhou D, Chen LM, Hernandez L, Shears SB, Galan JE (2001) A *Salmonella* inositol polyphosphatase acts in conjunction with other bacterial effectors to promote host cell actin cytoskeleton rearrangements and bacterial internalization. *Mol Microbiol* 39: 248-259.
17. Perrett CA, Jepson MA (2009) Regulation of *Salmonella*-induced membrane ruffling by SipA differs in strains lacking other effectors. *Cell Microbiol* 11: 475-487.
18. Burstein D, Zusman T, Degtyar E, Viner R, Segal G, et al. (2009) Genome-scale identification of *Legionella pneumophila* effectors using a machine learning approach. *PLoS Pathog* 5: e1000508.
19. Schechter LM, Roberts KA, Jamir Y, Alfano JR, Collmer A (2004) *Pseudomonas syringae* type III secretion system targeting signals and novel effectors studied with a Cya translocation reporter. *J Bacteriol* 186: 543-555.
20. Ninio S, Roy CR (2007) Effector proteins translocated by *Legionella pneumophila*: strength in numbers. *Trends Microbiol* 15: 372-380.
21. Dehio C (2005) *Bartonella*-host-cell interactions and vascular tumour formation. *Nat Rev Microbiol* 3: 621-631.
22. Quebatte M, Dehio M, Tropel D, Basler A, Toller I, et al. (2010) The BatR/BatS two-component regulatory system controls the adaptive response of *Bartonella henselae* during human endothelial cell infection. *J Bacteriol* 192: 3352-3367.
23. Manders SM (1996) Bacillary angiomatosis. *Clin Dermatol* 14: 295-299.
24. Kassner PD, Alon R, Springer TA, Hemler ME (1995) Specialized functional properties of the integrin alpha 4 cytoplasmic domain. *Mol Biol Cell* 6: 661-674.
25. Leavesley DI, Schwartz MA, Rosenfeld M, Cheresh DA (1993) Integrin beta 1- and beta 3-mediated endothelial cell migration is triggered through distinct signaling mechanisms. *J Cell Biol* 121: 163-170.
26. Harburger DS, Calderwood DA (2009) Integrin signalling at a glance. *J Cell Sci* 122: 159-163.
27. Ginsberg MH, Partridge A, Shattil SJ (2005) Integrin regulation. *Curr Opin Cell Biol* 17: 509-516.
28. Moser M, Legate KR, Zent R, Fassler R (2009) The tail of integrins, talin, and kindlins. *Science* 324: 895-899.
29. Deakin NO, Turner CE (2008) Paxillin comes of age. *J Cell Sci* 121: 2435-2444.
30. Wen KK, Rubenstein PA, DeMali KA (2009) Vinculin nucleates actin polymerization and modifies actin filament structure. *J Biol Chem* 284: 30463-30473.
31. Iwahara T, Akagi T, Fujitsuka Y, Hanafusa H (2004) CrkII regulates focal adhesion kinase activation by making a complex with Crk-associated substrate, p130Cas. *Proc Natl Acad Sci U S A* 101: 17693-17698.
32. Rossman KL, Der CJ, Sondek J (2005) GEF means go: turning on RHO GTPases with guanine nucleotide-exchange factors. *Nat Rev Mol Cell Biol* 6: 167-180.
33. Wu C (2004) The PINCH-ILK-parvin complexes: assembly, functions and regulation. *Biochim Biophys Acta* 1692: 55-62.
34. Calderwood DA (2004) Integrin activation. *J Cell Sci* 117: 657-666.

35. Cluzel C, Saltel F, Lussi J, Paulhe F, Imhof BA, et al. (2005) The mechanisms and dynamics of (alpha)v(beta)3 integrin clustering in living cells. *J Cell Biol* 171: 383-392.
36. Snijder B, Sacher R, Ramo P, Damm EM, Liberali P, et al. (2009) Population context determines cell-to-cell variability in endocytosis and virus infection. *Nature* 461: 520-523.
37. Carpenter AE, Jones TR, Lamprecht MR, Clarke C, Kang IH, et al. (2006) CellProfiler: image analysis software for identifying and quantifying cell phenotypes. *Genome Biol* 7: R100.
38. Rhomberg TA, Truttmann MC, Guye P, Ellner Y, Dehio C (2009) A translocated protein of *Bartonella henselae* interferes with endocytic uptake of individual bacteria and triggers uptake of large bacterial aggregates via the invasome. *Cell Microbiol* 11: 927-945.
39. Misselwitz B, Strittmatter G, Periaswamy B, Schlumberger MC, Rout S, et al. (2010) Enhanced CellClassifier: a multi-class classification tool for microscopy images. *BMC Bioinformatics* 11: 30.
40. Agaisse H, Burrack LS, Philips JA, Rubin EJ, Perrimon N, et al. (2005) Genome-wide RNAi screen for host factors required for intracellular bacterial infection. *Science* 309: 1248-1251.
41. Pielage JF, Powell KR, Kalman D, Engel JN (2008) RNAi screen reveals an Abl kinase-dependent host cell pathway involved in *Pseudomonas aeruginosa* internalization. *PLoS Pathog* 4: e1000031.
42. Zhou H, Xu M, Huang Q, Gates AT, Zhang XD, et al. (2008) Genome-scale RNAi screen for host factors required for HIV replication. *Cell Host Microbe* 4: 495-504.
43. Snel B, Lehmann G, Bork P, Huynen MA (2000) STRING: a web-server to retrieve and display the repeatedly occurring neighbourhood of a gene. *Nucleic Acids Res* 28: 3442-3444.
44. Jensen LJ, Kuhn M, Stark M, Chaffron S, Creevey C, et al. (2009) STRING 8--a global view on proteins and their functional interactions in 630 organisms. *Nucleic Acids Res* 37: D412-416.

OUTLOOK

6 OUTLOOK

In this chapter I will highlight remaining open questions regarding *B. henselae* (*Bhe*)-triggered invasome formation and provide suggestions of experimental setups that allow to approach the open points. Finally, I will emphasize how certain advances in *Bhe* research may generate impact by providing new insights on more general microbiological and cell biological problems.

6.1 BEPC/BEPF AND BEPG-PROMOTED INVASOME FORMATION

The work presented in **research articles I and II** demonstrate that *Bhe* encodes for two functional redundant effector sets (BepC/BepF and BepG) that trigger invasome formation. In order to generate a comprehensive picture of the distinct invasome formation mechanisms, there are several aspects that remain to be clarified.

It is yet unclear whether there is a **tempo-spatial regulation of effector translocation**. Further, the potential **translocation hierarchy** is not studied and it is unknown if effector translocation occurs in the reservoir as well as the incidental host. To assess the general capacity of *Bhe* to translocate BepC, BepF and BepG into various cell types, Cya or TEM β -lactamase reporter assays for translocation could be performed using different cell types such as HUVECs, Ea.hy926 or cat endothelial cells [1,2]. The potential translocation hierarchy and the tempo-spatial translocation regulation could be approached by methods that allow detecting effector protein translocation in real-time, such as a combination of split-GFP / RFP, each coupled to different BID domains of BepG or BepC/BepF [3]. Alternatively, a combination of SNAP / FIASH-tagged BID domains could be used in effector translocation assays into substrate-loaded eukaryotic cells as described elsewhere for *Shigella* effectors [3,4].

Next, the **molecular functions of effectors BepC and BepG** should be addressed. BepC is essential for BepC/BepF-promoted invasome formation and enhances BepG-mediated invasome establishment [5]. As BepC contains a FIC domain, the capacity of BepC to AMPylate host cell proteins should be tested with a special emphasis on Rho GTPases and RhoGEF and RhoGAP proteins. **BepG** was demonstrated to be sufficient to trigger invasome

formation on endothelial cells [6]. To define the minimal domain(s) required for the BepG-associated function in invasome formation, experiments analogue to work performed with BepF should be considered (see **research article III**). Further, to find the cellular interaction partner(s) of BepG, MS/MS analysis of immuno-precipitated, tagged BidG fusions may lead to the identification of direct as well as indirect interaction partners. In case of evidence for BepG exhibiting regulatory functions on cellular enzymes, over-expression and purification of the demonstrated functional portion of BepG may be an option to consider. The purified protein(s) could be used for *in vitro* enzymatic assays as well as for crystallization and subsequent structure determination. Of particular interest is the fact that BepG-promoted invasome formation does not require cofilin1 [5]. This may indicate that BepG somehow substitutes for cofilin1 function in the regulation of actin dynamics. In a first step, actin co-sedimentation assays aiming to analyze the ability of BepG to bind actin could be performed. Next, assuming that BepG or at least certain domains of it can be purified, *in vitro* actin polymerization / depolymerisation assays as well as actin nucleation experiments could be considered.

To obtain a comprehensive picture of invasome formation, the **signaling in invasome formation** needs to be understood. The small GTPases Cdc42 and Rac1 and their downstream interaction partners represent key players for general invasome formation, while cofilin1 is only required for BepC/BepF-mediated invasome establishment [5]. To identify further host cell proteins that are required for either both or only one invasome formation pathway, systematic genome-wide RNAi screens using i) BepC/BepF- or ii) BepG-triggered invasome formation as readout should be performed and identified hits further validated. The obtained results should allow to define a signaling core complex generally required for invasome formation (e.g. Rac1, integrin β 1, FAK, etc.). In addition, associated components essential for only BepC/BepF- or BepG-mediated invasome formation may be identified (e.g. cofilin1).

In summary, performing the above discussed approaches may explain why *Bhe*-promoted invasome formation is encoded in a redundant manner. Further, the knowledge of the molecular function of BepC, BepF and BepG and the distinct protein domains may influence the current view of evolutionary relationships between the individual effector proteins on an intra- as well as inter-species level.

6.2 THE *IN VIVO* RELEVANCE AND FUNCTION OF *BHE*-MEDIATED INVASOME FORMATION

As of now, there is no report demonstrating the *in vivo* existence of invasome structures on e.g. *ex vivo* tissue samples. Thus, the relevance and function of *Bhe*-triggered invasome formation remains unclear.

Although there is an established mouse model to study *Bhe* infections of the immunocompetent, incidental host [7], there is no available **animal model to study invasome formation**. A potential solution could be the infection of severe combined immunodeficiency (SCID) [8] or cyclophosphamide-treated immuno-compromised mice [9] with *Bhe* to simulate the infection of immune-compromised humans. To enhance the affinity of *Bhe* to mouse cells, *Bhe virB* mutant strains could be complemented with the homologue *Bgr* or *Bbi virB* genes. Alternatively, *Bhe* effector proteins BepC, BepF and BepG could be expressed in *B. grahamii* (*Bgr*) or *B. birtlesii* (*Bbi*), as defined mouse models are established for these two *Bartonella spp.* [10]. In order to guarantee the translocation of the *in trans* expressed *Bhe* Bep proteins, it may be required to extend their C-terminal effector portion by a defined translocation signal of *Bgr* or *Bbi* Bep proteins. However, *in vitro* infections of mouse endothelial cells should be performed in any case for prove-of-principle experiments before infecting animals.

Published work discusses invasome formation exclusively in the context of *Bhe* internalization into host cells [5,6,11]. However, a completely new hypothesis worth investigating suggests that invasome formation could represent a ***Bhe* transcytosis mechanism** rather than *Bhe* internalization strategy. Transcytosis is defined as the movement of macromolecules from one side of a cell to the other and can occur by a variety of mechanisms [12]. In contrast to transmigration, where the macromolecules pass the cell layer at sites of cell-cell contacts, transcytosis is characterized by the transport of macromolecules through an intact cell [13]. Interestingly, the size of invasome structures on endothelial cells is comparable to the size of leukocytes, which perform transcytosis to reach inflamed epithelial tissue layers (personal communication of Ann Ridley to Christoph Dehio). Further, assuming that invasomes would mediate *Bhe* transcytosis, this could provide potential explanations to various observations: First, the absence of invasome structures and the existence of large *Bhe* clusters within and onto endothelial cells in *ex vivo* samples could be rationalized. Next, a possible explanation for the characteristic four days

absence of *Bhe* from the blood stream during infections of the mammalian reservoir host could be explained by *Bhe* invading deeper tissue layers to reside and replicate. Finally, as the ability to promote transcytosis would represent a major host adaptability factor, this could clarify the importance of invasome formation and therefore explain why this process is encoded in a redundant manner.

To explore the potential of invasomes to mediate *Bhe* transcytosis, standard transcytosis/transmigration assays using trans-well setups should be performed. Further, another rather simple experiment would be the infection of endothelial cells in the presence of *N-ethylmaleimide* (NEM), an alkylating agent that inhibits the docking and fusion of plasmalemmal vesicles with their target membranes, thus blocking trans-vascular transport of macromolecules [14]. In case initial results support the transcytosis hypothesis, more sophisticated experiments should be performed, such as *in vitro* infections of multi-layer cell cultures or flow-chamber experiments to check for *Bhe* adherence/transcytosis under physical stresses that mimic *in vivo* situations.

Taken together, investigating the *in vivo* role of invasome formation in the context of transcytosis may completely change the current view on what invasome structures represent and eventually remove them from the list of potential *in vitro* artifacts.

6.3 ESTABLISHMENT OF INITIAL CONTACT BETWEEN BHE AND THE HOST CELL

Results presented in **research article IV** show that *Bhe* interacts with integrin $\alpha 5\beta 1$. However, it is not known whether i) $\beta 1$ integrin is the only surface-exposed host cell protein bound by *Bhe* and ii) which *Bhe* protein acts as adhesin.

Interestingly, $\beta 1$ integrin knock-down cells are still colonized by *Bhe*, indicating an additional **host adhesion factor(s)** recognized by *Bhe*. To identify these surface-exposed proteins bound by *Bhe*, validated hits from genome-wide RNAi screens for invasome formation may be retested in adherence assays. Further, potential target proteins may be re-investigated in combined *Bhe* infection / antibody blocking assays, using adherence as readout.

To screen for potential ***Bhe* adhesins**, transposon mutagenesis of *Bhe* wild-type and the subsequent testing of a saturating number of *Bhe* mutants in adhesion assays may lead to the identification of prime candidates for adherence factors. Alternatively, defined host cell proteins such as integrin $\beta 1$ could be immobilized on agarose beads and used to “fish” in a solubilized *Bhe* membrane fraction for binding proteins. Comparing the results of gel-free MS/MS analysis of control conditions (e.g. agarose beads only) versus test condition (e.g. integrin $\beta 1$ coupled to agarose beads) may indicate interacting *Bhe* proteins.

Of particular interest in terms of *Bhe* adhesion is the *Bartonella* adhesin **BadA** [15,16]. *Bhe* Houston-1 used in this work only contains remnants of the BadA gene [15]. However, recent mass spectrometry analysis indicated that this remnant BadA fragment is expressed, although anti-BadA antibodies do not recognize any BadA at the cell surface of *Bhe* Houston-1 (*personal communication from Maxime Quebatte to Matthias Truttmann*) [15]. To investigate for the role of BadA in *Bhe* Houston-1, clean of the BadA knock-outs should be performed in a *Bhe* wild-type background and the capacity of the knock-out strain to adhere to cells and to trigger invasome formation should be addressed.

Concluding, the determination of the *Bhe*-host cell binding interface would allow putting *Bhe* internalization into a broader context and comparing it to invasion strategies of e.g. *Yersinia*, *Salmonella* or *Shigella*. Further, the characterization of the *Bhe* protein required for host cell attachment could provide indications about the in-detail composition of the VirB/D4 T4SS and the existence of a secretion pilus thereof.

6.4 *BHE* AGGREGATION ON THE HOST CELL SURFACE

Bhe clustering on the cell surface is a pre-requisite for invasome formation [11]. Current results suggest that *Bhe* aggregation may be a passive event resulting of transmembrane receptor clustering to which *Bhe* may be bound. However, solid data on *Bhe* aggregation is not available yet.

To approach the **kinetics of *Bhe* clustering**, life-cell microscopy may be the method of choice that allows to follow *Bhe* clustering in a time-resolved manner. Further to that, the contribution of on-side replication of adherent *Bhe* should be assessed, e.g. by quantitative analysis of images resulting from life-cell microscopy. Finally, similar experiments should be performed in a flow-chamber setup to investigate *Bhe* clustering under physical stresses.

With respect to *Bhe* aggregation, the **role of integrin β 1** in this particular process is of specific interest. To assess the function of integrin β 1 in *Bhe* clustering, life-cell microscopy of *Bhe* infections using fluorescent *Bhe* (e.g. dsRed-expressing strains) and cells expressing GFP-tagged integrin β 1 should be performed and the co-localization of *Bhe* and integrin β 1 could be described qualitatively as well as quantitatively. A similar setup could be used to study the co-localization of *Bhe* with other cellular receptors such as CD98 or laminins.

In summary, investigating *Bhe* clustering may contribute to understand the kinetic restrictions of invasome formation and could increase the knowledge about the plausible *in vivo* role of invasome structures.

6.5 THE IMPACT OF *BHE* RESEARCH ON GENERAL MICROBIOLOGY AND CELL BIOLOGY

Although the above proposed approaches primarily aim to increase knowledge about *Bhe*-triggered invasome formation, certain aspects may influence other related fields of biology.

Understanding how *Bhe* binds to integrins and presumably co-clusters with them may allow answering some of the still open, general questions of integrin-related cell biology, such as how integrin clustering works, whether clustering or integrin activation comes first, how integrin engagement changes integrin conformations, etc. As integrins are increasingly implicated in playing a crucial role in breast cancer malignancy and were found to be potential prognostic markers for cancer [17,18], these results would have a broad impact on understanding general aspects of cancer- and cell biology.

Next, results from genome-wide RNAi screens using *Bhe*-triggered invasome formation as readout and the thereby obtained signaling networks may help to close gaps in the general actin assembly / disassembly signaling networks. As the invasome represents a huge F-actin structure, it is a well pronounced phenotype that is perfectly suited to study actin dynamics. Thus, a considerably big part of validated screening hits essential for invasome establishment may be part of F-actin regulation circuits. Therefore, the results from *Bhe* research may influence general cell biology and provide new clues about the regulation of actin dynamics that represents a major theme in the biology of e.g. cell migration or cancer metastasis.

Finally, assuming that invasomes would represent transcytosis structures, understanding invasome formation would provide general knowledge about signaling behind transcytosis. Further, invasome formation assays may represent an easy-to-perform experiment to further investigate transcytosis *in vitro*. As transcytosis is a common mechanism used by e.g. leukocytes to cross the endothelial barrier [19] or abused by e.g. HIV to cross tight endothelial as well as epithelial layers [20,21], new insights into the regulation of transcytosis may stimulate general research on pathogen transcytosis as well as immunology.

Taken together, the investigation of *Bhe*-triggered invasome formation may not only result in new insights of *Bhe* biology but could also positively influence the general understanding of the cell- and microbiology.

6.6 REFERENCES

1. Schmid MC, Scheidegger F, Dehio M, Balmelle-Devaux N, Schulein R, et al. (2006) A translocated bacterial protein protects vascular endothelial cells from apoptosis. *PLoS Pathog* 2: e115.
2. Mills E, Baruch K, Charpentier X, Kobi S, Rosenshine I (2008) Real-time analysis of effector translocation by the type III secretion system of enteropathogenic *Escherichia coli*. *Cell Host Microbe* 3: 104-113.
3. Rodrigues CD, Enninga J (2010) The 'when and whereabouts' of injected pathogen effectors. *Nat Methods* 7: 267-269.
4. Enninga J, Mounier J, Sansonetti P, Tran Van Nhieu G (2005) Secretion of type III effectors into host cells in real time. *Nat Methods* 2: 959-965.
5. Truttmann MC, Rhomberg, T.R., Dehio, C. (In Press) Combined action of the type IV secretion effector proteins BepC and BepF promotes invasome formation of *Bartonella henselae* on endothelial and epithelial cells. *Cell Microbiol* in press.
6. Rhomberg TA, Truttmann MC, Guye P, Ellner Y, Dehio C (2009) A translocated protein of *Bartonella henselae* interferes with endocytic uptake of individual bacteria and triggers uptake of large bacterial aggregates via the invasome. *Cell Microbiol* 11: 927-945.
7. Regnath T, Mielke ME, Arvand M, Hahn H (1998) Murine model of *Bartonella henselae* infection in the immunocompetent host. *Infect Immun* 66: 5534-5536.
8. Bosma GC, Custer RP, Bosma MJ (1983) A severe combined immunodeficiency mutation in the mouse. *Nature* 301: 527-530.
9. Kawamura I, Mitsuyama M, Nomoto K (1990) Enhanced protection of cyclophosphamide-treated mice against infection with *Pseudomonas aeruginosa* after treatment with Z-100, a polysaccharide-rich extract from *Mycobacterium tuberculosis* Aoyama B. *Immunopharmacol Immunotoxicol* 12: 331-343.
10. Vayssier-Taussat M, Le Rhun D, Deng HK, Biville F, Cescau S, et al. (2010) The Trw type IV secretion system of *Bartonella* mediates host-specific adhesion to erythrocytes. *PLoS Pathog* 6: e1000946.
11. Dehio C, Meyer M, Berger J, Schwarz H, Lanz C (1997) Interaction of *Bartonella henselae* with endothelial cells results in bacterial aggregation on the cell surface and the subsequent engulfment and internalisation of the bacterial aggregate by a unique structure, the invasome. *J Cell Sci* 110 (Pt 18): 2141-2154.
12. Tuma PL, Hubbard AL (2003) Transcytosis: crossing cellular barriers. *Physiol Rev* 83: 871-932.
13. Liu Y, Shaw SK, Ma S, Yang L, Luscinskas FW, et al. (2004) Regulation of leukocyte transmigration: cell surface interactions and signaling events. *J Immunol* 172: 7-13.
14. Jackson RC, Modern PA (1990) N-ethylmaleimide-sensitive protein(s) involved in cortical exocytosis in the sea urchin egg: localization to both cortical vesicles and plasma membrane. *J Cell Sci* 96 (Pt 2): 313-321.
15. Riess T, Raddatz G, Linke D, Schafer A, Kempf VA (2007) Analysis of *Bartonella* adhesin A expression reveals differences between various *B. henselae* strains. *Infect Immun* 75: 35-43.

16. Szczesny P, Linke D, Ursinus A, Bar K, Schwarz H, et al. (2008) Structure of the head of the *Bartonella* adhesin BadA. PLoS Pathog 4: e1000119.
17. Dingemans AM, van den Boogaart V, Vosse BA, van Suylen RJ, Griffioen AW, et al. (2010) Integrin expression profiling identifies integrin alpha5 and beta1 as prognostic factors in early stage non-small cell lung cancer. Mol Cancer 9: 152.
18. Shimizu H, Seiki T, Asada M, Yoshimatsu K, Koyama N (2003) Alpha6beta1 integrin induces proteasome-mediated cleavage of erbB2 in breast cancer cells. Oncogene 22: 831-839.
19. Middleton J, Patterson AM, Gardner L, Schmutz C, Ashton BA (2002) Leukocyte extravasation: chemokine transport and presentation by the endothelium. Blood 100: 3853-3860.
20. Bomsel M (1997) Transcytosis of infectious human immunodeficiency virus across a tight human epithelial cell line barrier. Nat Med 3: 42-47.
21. Gujuluva C, Burns AR, Pushkarsky T, Popik W, Berger O, et al. (2001) HIV-1 penetrates coronary artery endothelial cells by transcytosis. Mol Med 7: 169-176.

ACKNOWLEDGMENTS

7 ACKNOWLEDGMENTS

This work was performed in the group of Prof. Christoph Dehio in the Focal area infections biology at the Biozentrum of the University of Basel, Switzerland.

First and foremost, I am grateful to my supervisor Prof. Christoph Dehio for giving me the opportunity to work on my PhD thesis in his lab and under his supervision. I enjoyed the productive discussions we had and appreciated all the helpful comments, guidance and positive criticism.

Next, I would like to thank Prof. Cécile Arrieumerlou and Prof. Dirk Bumann for their constructive inputs during my PhD committee meetings and for their help by providing solutions to emerging problems.

Dave Critchley is acknowledged for his spontaneous joining of the integrin/talin project. His thoughtful input was of enormous value and has massively influenced the progression of my work.

Furthermore, I would like to express my gratitude to former and current members of the Dehio lab: Raquel Conde, Shyan Low, Phillipp Engel, Jérémie Gay-Fraret, Patrick Guye, Arnaud Goepfert, Alexander Harms, Barabara Hauert, Sonja Huser, Marius Liesch, Rusudan Okojava, Kathrin Piles, Arto Pulliainen, Maxime Quebatte, Florine Scheidegger, Houchaima Ben Takaia and David Tropel. I enjoyed working in an inspiring and friendly atmosphere with you.

A special thank goes to Claudia Mistl, Simone Muntwiler and Yvonne Ellner for their technical assistance and constant supply with cultured cells.

I am grateful to Thomas Rhomberg who has worked on *B. henselae* invasion into human cells and build a solid fundament for me to start with my research.

I was pleased to work with Mario Emenlauer. His IT support and optimism were invaluable for proceeding with PC-related work tasks. Further, I appreciated our good discussions we had about various topics.

Acknowledgments

Further, I would like to acknowledge Florian Geier for all the great discussion we had and for help with statistics and computing.

In the past four years, I experienced a friendly and joyful atmosphere on the 4th floor, thus thanks to all the colleagues from the different labs that were part of that inspiring group. Special thanks go to the members of the Arrieumerlou lab, with which I have spent countless hours in the S2-labs up- and downstairs.

I am especially grateful to Roger Sauder, Marina Kuhn, Roli, the cleaning ladies and the BC2 crew headed by Michel Podvinec; they were all elementary pieces that allowed me to concentrate on my own work without spending too much time on setting up PCs, preparing media, cleaning lab-ware or ordering consumables. It meant a lot to me!

Florine Scheidegger and Javier Pizzaro-Cerda are acknowledged for critical reading of my thesis.

Ein herzliches Dankeschön geht an meine Eltern Andrea & Jakob Truttman und meinen Bruder Daniel. Ohne eure konsequente Unterstützung über die letzten acht Jahre wäre ich nie hier angekommen wo ich jetzt bin. Ich werde die erholsamen Wochenenden zu Hause im schönen Urnerland in bester Erinnerung behalten.

My greatest thanks go to Corinne; you have been with me throughout my entire PhD, never complained when I had to work long hours, and motivated me when I was feed up. My heart belongs to you.

In loving memory, I would like to thank my grandfather Hans Zraggen and my dear friend Marco Faustmann for the time we spent together. Although too short, I was grateful having you around me. Hope, you have found your peace; you only deserve the best!

CURRICULUM VITAE

8 CURRICULUM VITAE

| | | |
|---|---|----------------|
| NAME / SURNAME | Matthias Truttmann | |
| ADDRESS | Ringstrasse 46c, 6467 Schattdorf Uri | |
| DATE OF BIRTH | 2 nd Sept. 1983 | |
| HOMETOWN | Seelisberg UR | |
| CITIZENSHIP | CH-Switzerland | |
| MARTIAL STATUS | unmarried | |
| E-MAIL | M.Truttmann@stud.unibas.ch | |
| PHONE | 078 614 02 46 | |
| EDUCATION | | |
| Focal Area Infection Biology, Biozentrum, University of Basel, CH | PHD THESIS PhD project: "A systematic approach to the molecular and cellular basis of <i>B. henselae</i> -triggered invasome formation" supervisor: Prof. Christoph Dehio Thesis committee: Prof. Christoph Dehio (PI), Prof. Dirk Bumann, Prof. Cecile Arrieumerlou | 2006 - present |
| Biozentrum, University of Basel, CH / Basilea Pharmaceutical AG, Basel, CH | MASTER IN MOLECULAR BIOLOGY Major in Biochemistry Master project: "Inhibition kinetics of class A TEM β -lactamases" supervisor: Prof. Malcolm Page Thesis committee: Prof. Urs Jenal (PI), Prof. Malcolm Page | 2005 - 2006 |
| Biozentrum, University of Basel, CH | BACHELOR IN MOLECULAR BIOLOGY | 2002 - 2005 |
| Kollegium Karl Borromäus, Altdorf, CH | KANTONALE MATURA (major in mathematics and physics) | 1997 - 2002 |

Curriculum vitae

| | | |
|---|--|----------------------------|
| WORK EXPERIANCE | | |
| Focal Area Infection Biology, Biozentrum, University of Basel, CH | ASSISTANT Group of Prof. Christoph Dehio | 11.2006-present |
| | PhD projects: - RNAi screen to study <i>Bartonella henselae</i> host cell entry - Molecular characterization of <i>Bartonella</i> effector proteins involved in invasome formation | |
| Basilea Pharmaceutical AG, Basel, CH | RESEARCH ASSISTENT | 07.2005 – 10.2005 |
| TEACHING Biozentrum, University of Basel, CH | Tutorage of first-year students (general biology) | 2005 - 2006 2007 - 2008 |
| | Tutorage of third-year students "Blockcourse microbiology" | 2007 - 2010 |
| | Co-supervision of Masterstudents | 2008 - present |
| Kollegium Karl Borromäus, Altdorf, CH | Temporary Teacher (physics, biology and chemistry; college-level) | 09.2004 |
| PRESENTATIONS / AWARDS | | |
| Gordon research conference (GRC) on „signaling by adhesion receptors, Maine, US | Selected speaker and Poster: " <i>Integrin β1-mediated signaling via talin1 promotes B.henselae-triggered invasome formation</i> " | 07.2010 |
| Biozentrum Symposium, Basel, CH | Poster: " <i>Integrin β1 mediated signaling is essential for at least two distinct processes involved in B. henselae-triggered invasome formation</i> " | 01.2010 |
| Biozentrum Symposium, Basel, CH | Poster: " <i>Identification of eukaryotic core signaling pathways involved in invasome formation by imaging-based RNAi screens</i> " | 01.2009 |
| All SystemX.ch day, Basel, CH | Posterprize: " <i>Identification of eukaryotic core signaling pathways involved in invasome formation by imaging-based RNAi screens</i> " | 10.2008 |
| ESF congress on Systems biology, Sant Feliu de Guixoles, Spain | Poster: " <i>Development of an imaging-based RNAi screen to study actin-dependent bacterial uptake into host cells</i> " | 09.2008 |

Curriculum vitae

| | |
|--------------------|---|
| LANGUAGES | <p>German Mother tongue</p> <p>English fluent</p> <ul style="list-style-type: none"> - Cambridge First Certificate 2002 - TOFL preparation course, 02.2005 – 03.2005 Ontario language School, Toronto (CA) <p>French advanced</p> |
| SWISS ARMY | <p>Special officer (captain) ABC defense laboratory; Advisor bacteriology</p> |
| PERSONAL INTERESTS | <p>Playing the violin Inline-and ice-hockey Cross-Country mountainbiking</p> |
| PUBLICATIONS | <p>Rhomberg TA, <u>Truttmann MC</u>, Guye P, Ellner Y, Dehio C. A translocated protein of <i>Bartonella henselae</i> interferes with endocytic uptake of individual bacteria and triggers uptake of large bacterial aggregates via the invasome. <i>Cell Microbiol.</i> 2009 Jun;11(6):927-45.</p> <p><u>Matthias C. Truttmann</u>, Thomas A. Rhomberg and Christoph Dehio Combined action of the type IV secretion effector proteins BepC and BepF promotes invasome formation of <i>Bartonella henselae</i> on endothelial and epithelial cells. <i>Cell Microbiol.</i> <i>In Press</i></p> <p><u>Matthias C. Truttmann</u>, Benjamin Misselwitz, Wolf-Dietrich Hardt, David R. Critchley and Christoph Dehio. <i>Bartonella henselae</i> engages inside-out and outside-in signaling via talin1 / integrin β1 during invasome formation. Submitted to the <i>Journal of Cell Science</i></p> <p><u>Matthias C. Truttmann</u>, Arnaud Goepfert, Shyan H. Low and Christoph Dehio <i>Bartonella henselae</i> effector protein BepF exhibits guanine nucleotide exchange factor functionalities on Cdc42. In preparation for <i>Cell. Microbiol.</i></p> |